

**About the Book :**

The International Conference on Smart Innovations in Electrical Engineering (ICSIEE) is a prestigious platform that brings together researchers, practitioners, and industry experts to explore and discuss cutting-edge advancements in the field of electrical engineering. The conference aims to foster collaboration, share knowledge, and address critical challenges faced by the industry. Let's delve into the key areas of focus for ICSIEE: Electric Vehicles (EVs), Smart Grids, Power, Control, and Instrumentation, Artificial Intelligence-Based Applications, Industrial Automation, Energy Storage Systems, Sustainability and Green Systems, Energy Management Systems, Sensor Networks and Security and Fault Detection & Diagnosis. In summary, ICSIEE serves as a catalyst for innovation, collaboration, and sustainable solutions in electrical engineering. We look forward to engaging discussions and impactful outcomes during this enlightening conference.



₹ Rs.350 /-



Research Culture Society and Publication  
An International ISBN Books Publisher  
[www.researchculturesociety.org](http://www.researchculturesociety.org)



# International Conference on Smart Innovations in Electrical Engineering



(ICSIEE- 2024)

Date: 09 - 10 May, 2024

*Conference Proceedings*

**Dr. Honey Baby**

*Organized by :*

Department of Electrical and Electronics Engineering  
Mangalam College of Engineering, Mangalam Hills, Ettumanoor  
Kottayam, Kerala, India

Research Culture Society and Publication  
[www.researchculturesociety.org](http://www.researchculturesociety.org)



International Conference on Smart Innovations in Electrical Engineering

# International Conference on Smart Innovations in Electrical Engineering

(ICSIEE- 2024)

Date: 09 - 10 May, 2024

*Conference Proceedings*

ISBN: 978-93-92504-58-7

*Edited by:*

*Dr. Honey Baby*

*Associate Professor/ HOD, Electrical and Electronics Engineering*

*( Mangalam College Of Engineering )*

*Organized by :*

*Department of Electrical and Electronics Engineering  
Mangalam College of Engineering, Kottayam, Kerala, India*



*Published by :*

**Research Culture Society and Publication**

[www.researchculturesociety.org](http://www.researchculturesociety.org)



\*\*\*

**International Conference on Smart Innovations in Electrical Engineering****- Dr. Honey Baby**

**Copyright:** © The research work, information compiled as a theory with other contents are subject to copyright taken by author(s) / editor(s) / contributors of this book. The author(s) / editor(s) / contributors has/have transferred rights to publish book(s) to ‘Research Culture Society and Publication’.

**Imprint:**

Any product name, brand name or other such mark name in this book are subjected to trademark or brand, or patent protection or registered trademark of their respective holder. The use of product name, brand name, trademark name, common name and product details and distractions etc., even without a particular marking in this work is no way to be constructed to mean that such names may be regarded as unrestricted in respect of trademark and brand protection legislation and could thus be used by anyone.

**Disclaimer:**

The author (s), contributors and editor(s) are solely responsible for the content, images, theory, and datasets of the papers compiled in this book. The opinions expressed in our published works are those of the author(s)/contributors and do not reflect our publication house, publishers and editors, the publisher does not take responsibility for any copyright claim and/or damage of property and/or any third parties claim in any matter. The publication house and/or publisher is not responsible for any kind of typo-error, errors, omissions, or claims for damages, including exemplary damages, arising out of use, inability to use, or with regard to the accuracy or sufficiency of the information in the published work.

**Published and Printed at : ( First Edition – May, 2024 )**

**Research Culture Society and Publication / Research Culture Society**

(Reg. International ISBN Books and ISSN Journals Publisher)



India : C – 1, Radha Raman Soc, At & Po - Padra, Dis - Vadodara, Gujarat, India – 391440.

USA : 7886, Delrosa Avenue, Sanbernardino, CA 92410.

Canada : Loutit Road, Fort McMurray, Alberta, T9k0a2.

Greece : Mourkoussi Str, Zografou, Athens, 15773

Email: RCSPBOOKS@gmail.com / editor@ijrcs.org

www.researchculturesociety.org / www.ijrcs.org

MRP : Rs. 350 /-

ISBN: 978-93-92504-58-7





# Research Culture Society and Publication

(Reg. International ISBN Books and ISSN Journals Publisher)

Email: [RCSPBOOKS@gmail.com](mailto:RCSPBOOKS@gmail.com) / [editor@ijrcs.org](mailto:editor@ijrcs.org)

[WWW.RESEARCHCULTURESOCIETY.ORG](http://WWW.RESEARCHCULTURESOCIETY.ORG) / [WWW.IJRCS.ORG](http://WWW.IJRCS.ORG)

Conference, Seminar, Symposium organization in association/collaboration with different Institutions.

Conference, Seminar, Symposium Publication with ISSN Journals and ISBN Books (Print / Online).

## Conference Publications

International Journals and Books Publisher

Publish your Conference, Seminar, Congress, Symposium  
with a trusted International Publisher



ISSN  
Journals

ISBN  
Books

SPECIAL ISSUE

PROCEEDINGS

ABSTRACT BOOK

DOIs - Indexing

Nominal Processing Charge

Research Culture Society and Publication



[www.ijrcs.org](http://www.ijrcs.org)

[www.ijirmf.com](http://www.ijirmf.com)



[editor@ijrcs.org](mailto:editor@ijrcs.org)

[editor@ijirmf.com](mailto:editor@ijirmf.com)

# CALL FOR PAPERS



International Peer-Reviewed Refereed Indexed ISSN Approved High Impact Factor Journals with Quality Publication

Research Culture Society Journals

IJIRMF, IJRCS, JSHE, IJEDI, Shikshan Sanshodhan

Research Study Fields

Research Publication in all subjects / topics of the following study fields :

Science, Engineering, Healthcare Sciences, Agriculture, Pharmacy, Medicine, Nursing Commerce, Management, Social Sciences, Law, Humanities, Education, Life Skills

Free e-Certificates  
Digital Object Identification  
Nominal Processing Fee

Submit papers to

editor@ijrcs.org

Or

editor@ijirmf.com

<http://jshe.researchculturesociety.org/>

<http://shikshansanshodhan.researchculturesociety.org/>

<http://ijedi.researchculturesociety.org/>

WWW.IJRCS.ORG

WWW.IJIRMF.COM

## About the organizing Institutions:

**Mangalam College of Engineering (MLMCE)** stands supreme in technical education with excellence and quality in education. In keeping with MLM's goal of excellence, the academic programs are supported by well-experienced and dedicated faculty, committed to equipping the student with the knowledge and skills needed for succeeding in today's rapidly changing world. Approved by the All India Council for Technical Education (AICTE) and affiliated to the APJ Abdul Kalam University, Thiruvananthapuram. Mangalam College of Engineering is accredited by the National Assessment and Accreditation Council (NAAC) with an 'A' Grade on a point scale of 3.24 out of 4 in the 2nd Cycle in 2023. Also, four departments of Mangalam namely CE, CSE, ECE, and ME are accredited by the National Board of Accreditation (NBA). MLM is promoted by the Mangalam Educational Society, with a mission to bring out leaders for a technology-driven environment.

**Objectives of the International Conference:** The International Conference on Smart Innovations in Electrical Engineering (ICSIEE) is a prestigious platform that brings together researchers, practitioners, and industry experts to explore and discuss cutting-edge advancements in the field of electrical engineering. The conference aims to foster collaboration, share knowledge, and address critical challenges faced by the industry. Let's delve into the key areas of focus for ICSIEE:

- Electric Vehicles
- Smart Grid
- Power, Control and Instrumentation
- Artificial Intelligence Based Applications
- Industrial Automation
- Energy Storage Systems
- Sustainability and Green Systems
- Electrical Drives Power Converters & Inverters
- Energy Management Systems
- Sensor Networks and Security
- Fault Detection & Diagnosis



## Conference Committee

### Organizers – Conference Chair Members:

**Dr. Honey Baby**, Head of the Department, Electrical and Electronics Engineering,  
Mangalam College of Engineering, Kottayam, Kerala

**Dr. Reshma Gopi R**, Associate Professor, Electrical and Electronics Engineering, Mangalam  
College of Engineering, Kottayam, Kerala

### Advisory Member and Committee Members:

**Sreekala V M**, Assistant Professor, Electrical and Electronics Engineering,  
Mangalam College of Engineering, Kottayam, Kerala

**Anupama M**, Assistant Professor, Electrical and Electronics Engineering,  
Mangalam College of Engineering, Kottayam, Kerala

**Arun Chandrakumar K**, Assistant Professor, Electrical and Electronics Engineering,  
Mangalam College of Engineering, Kottayam, Kerala

**Jolly George**, Assistant Professor, Electrical and Electronics Engineering, Mangalam  
College of Engineering, Kottayam, Kerala

**Aiswarya Chandran**, Assistant Professor, Electrical and Electronics Engineering, Mangalam  
College of Engineering, Kottayam, Kerala

**Vineesh T V**, Lab Instructor, Electrical and Electronics Engineering, Mangalam College of  
Engineering, Kottayam, Kerala

### Keynote Speakers and Committee Members:

**Dr. Ramesh Unnikrishnan**, Advisor (Grade II) All India Council for Technical Education,  
Ministry of Education, Government of India

**Dr. Nallapaneni Manoj Kumar**, School of Energy and Environment, City University of  
Hong Kong, Swiss School of Business and Management Geneva, Switzerland

**Dr. Abhilash T Vijayan**, Associate Professor, Rajeev Gandhi Institute of Technology,  
Kottayam

**Dr. Palanisamy K**, Professor, School of Engineering, Vellore Institute of Technology

**Dr. Sreejith S**, Associate Professor(Grade 1), NIT, Silchar

### Session Chair and Committee Members:

**Dr. Nallapaneni Manoj Kumar**, School of Energy and Environment, City University of  
Hong Kong, Swiss School of Business and Management Geneva, Switzerland

**Dr. Abhilash T Vijayan**, Associate Professor, Rajeev Gandhi Institute of Technology,  
Kottayam

**Preethi Sebastian**, Associate Professor, Electrical and Electronics Engineering,  
Mangalam College of Engineering, Kottayam, Kerala

**Dr. Honey Baby**  
ICSIEE-2024 Conference Chair  
Head of the Department  
Department of Electrical and Electronics Engineering  
Mangalam College of Engineering, Mangalam Hills, Ettumanoor  
Kottayam, Kerala

---

Dear Colleagues!

I am delighted that our organization is jointly conducting the International Conference on Smart Innovations in Electrical Engineering, in association with 'Research Culture Society on 09 – 10 May, 2024.

Greetings from the Department of Electrical and Electronics Engineering at Mangalam College of Engineering, Kerala, for the International Conference on Smart Innovations in Electrical Engineering (ICSIEE 2024). It gives me great pleasure and pride to extend a warm welcome to every one of you.

This conference represents a confluence of common objectives and aspirations towards sustainable development in our field, as well as a meeting of bright minds. It gives us a forum to discuss ideas, encourage creativity, and take on upcoming challenges.

I would like to extend my sincere gratitude to the hardworking members of the organizing committee, under the direction of the Department of Electrical and Electronics Engineering, whose continuous commitment has made this happening. Because of their dedication, this conference offers a valuable platform for faculty, students, engineers, and researchers to participate in thought-provoking conversations and cooperative projects.

ICSIEE 2024 offers an excellent opportunity for all of us to investigate state-of-the-art developments, gain knowledge from one another, and collaborate in the development of sustainable solutions that will influence the direction of civil engineering. I urge everyone to get involved, contribute their knowledge, and establish enduring relationships with other attendees.

I would like extend my best wishes for a successful and fulfilling conference experience as we set out on this joint voyage of exploration and discovery. Thank you for your contributions. May they help us move our field closer to revolutionary advancement and help us realize our long-term objectives.

ICSIEE'24 welcomes you. Together, let us motivate and be motivated.

Warm regards,

Thank you!

**Dr. Honey Baby**  
ICSIEE-2024 Conference Chair  
Head of the Department  
Department of Electrical and Electronics Engineering  
Mangalam College of Engineering, Mangalam Hills, Ettumanoor

---



## Chairman Message



Greetings to all of you for the International Conference on Smart Innovations in Electrical Engineering (ICSIEE'24), which has been organized by the privilege of institution's Department of Electrical and Electronics Engineering. It is a pleasure and honour to be here. I am excited to see how bright minds from all over the world are coming together to advance knowledge and create meaningful partnerships.

This conference acts as a hub for intellectual exchange, presenting cutting-edge research and exchanging creative ideas. It is a forum where professionals from various fields come together to discuss the urgent issues facing the modern world.

I urge you to fully participate in the conversations, arguments, and presentations as we set out on this journey together. Your contributions and insights are extremely valuable in guiding the conversation and setting the path for a more promising future. I am sure there will be plenty of thought-provoking discussions, educational workshops, and beneficial networking opportunities at the conference. Now is the time to create new alliances, strengthen existing ones, and encourage one another to pursue greater things in life. I would like to express my gratitude to all the lecturers, patrons, volunteer, and attendees on behalf of the organizing committee for their amazing efforts in making this conference a reality. It is truly admirable how committed and dedicated you are.

Join us in creating an experience that endures on in this conference, one that advances knowledge for the good of society and leaves a lasting impact on our respective fields. I hope our time together is inspiring, illuminating, and enriching.

Sincerely,

**Dr. Biju Varghese**  
Chairman,  
Mangalam College of Engineering

## Principal Message



Greetings and salutations to all of you on behalf of the Department of Electrical and Electronics Engineering at Mangalam College of Engineering, Kerala, which is hosting the International Conference on Smart Innovations in Electrical Engineering (ICSIEE-2024).

I am excited to see bright minds from all over the world come together to learn about the newest developments and trends in electrical engineering as the principal of MLMCE. Our dedication to advancing innovation, exchanging knowledge, and tackling the issues confronting our industry is demonstrated by this conference.

My sincere gratitude is extended to the Department of Electrical and Electronics Engineering's organizing committee for their tireless efforts in making this conference a reality. Their commitment and diligence have made sure that engineers, researchers, educators, and students will have a forum to participate in thought-provoking conversations and cooperative efforts.

All participants possess an ideal chance to share their knowledge, gain from one another, and investigate long-term solutions that will influence electrical engineering in the future at ICSIEE 2024. I urge you to take full advantage of this enlightening opportunity and establish enduring relationships with your peers.

I hope this conference is advantageous and executing for each of you as you set out on this path of exploration and discovery. I hope your work opens doors for revolutionary breakthroughs in our area.

Greetings once more from ICSIEE'24. Let us motivate and uplift one another together.

Warm regards,

**Dr. Vinodh P Vijayan**  
Principal  
Mangalam College of Engineering

## Table of Contents

<b>INDEX</b>		
Sr.No	Contents	Page No.
a)	About the organizing Institutions: Objectives of the International Conference : About the Conference	<b>5</b>
b)	Conference Committee	6
c)	Message from Head of the Department & Conference Chair	7
d)	Message from Chairman	8
e)	Message from Principal	9
	Table of Contents	10-11
Paper ID	Title & Author(s) Name	-
<b>ICSIEE2401</b>	Drone-Based Plant Disease Detection and Alert System Using GSM Module -- <i>Jinas Haidharali P, Jazil Jahafar P, Nabeela K P, Amen Mubarack K, Muhammed Aslam E U</i>	<b>13</b>
<b>ICSIEE2402</b>	Electrical Estimation and Design Of High-Rise Building In Middle East -- <i>Mohammed Shamil C P, Mohammed Jasim C P, Mohammed Faizal, Ajmal M S, Mohammed Shabas KP</i>	<b>19</b>
<b>ICSIEE2403</b>	Vortex Generators for Passive Cooling Of Rooftop Photovoltaic Systems Under Free Convection With Smart Concentric System -- <i>Aslam Farooq K H, Ryan Titus, Gibson Antony, Joyal Jomon., Renu Mary George</i>	<b>26</b>
<b>ICSIEE2404</b>	An Adaptive Control System In Plug-In-Ev -- <i>Adil N, Cyril Shaji John, Edwin Biju Mathai, Pranav P Pillai, Juna John Daniel, Dr Vinod V.P</i>	<b>35</b>
<b>ICSIEE2405</b>	Smart Garbage Segregation Bins Powered By Solar Energy With Sms Notifications And Machine Learning Image Processing -- <i>Annmary C.A. Sona Elsa Abraham, Nivetha , Vinayak T.S, Dr. Leena T Timothy</i>	<b>40</b>
<b>ICSIEE2406</b>	IoT Based Hybrid Charging Station -- <i>Ajmal Sudhir, Deepak Devassy, Anupama K M, Sidharth K A, Dr Annie Bincy C A</i>	<b>48</b>
<b>ICSIEE2407</b>	Energy Harvesting Using Vertical Axis Wind Turbine from Highway Traffic Vehicles Movement -- <i>Sandra Satheesh, Gautham Krishna K S, Nelson E S, Dr. Reshma Gopi R</i>	<b>54</b>

<b>ICSIEE2408</b>	A Hybrid Bidirectional Dc-Dc Converter Based on A Sepic/Zeta Converter with Modified Switched Capacitor Cell - - <i>Adithyan M Unnithan, Aditya Raj, Aditya P Nair, Rithika Dileep, Atheena A, Dr. Vinod V.P</i>	<b>60</b>
<b>ICSIEE2409</b>	Comparative Analysis of Open Loop and Closed Loop Control Systems for Switched Reluctance Motors in Plug-In Hybrid Electric Vehicles -- <i>Chama R Chandran, Amay Krishnan, Akash Krishnan, Chaithra A, Krishna Prasad V, Dr. Vinod V P</i>	<b>66</b>
<b>ICSIEE2410</b>	Application Of Nature-Inspired Search Algorithms to Enhance Multi-Layer Thickness Optimization in Solar Cells -- <i>Okram James singh, Chingakham Foren, Soibam Milan Singh, Sm Nawaj Sarif, Laishram Arun Singh,</i>	<b>71</b>
<b>ICSIEE2411</b>	Automatic Solar Cleansifier -- <i>Abdul Hadi C, Adeeb T, Muhammed Harshad C, Ansif Mohammed T, Jithin Mohan</i>	<b>77</b>
<b>ICSIEE2412</b>	Dual Powered Smart Street Light with Fault Recognition -- <i>Adarsh Joseph, Rojin Manuel, Traies Rose Thomas Kurian, Noyal Thomas, Assoc. Prof. Kanaka Xavier</i>	<b>81</b>
<b>ICSIEE2413</b>	Failure Modes And Effects Analysis Of Power Transformers -- <i>Abhijith A, Prof. Valsa Basil</i>	<b>91</b>
<b>ICSIEE2414</b>	Efficient Dual Motor Power Train for Two-Wheeled Electric-Cycle -- <i>Likhitha S Shenoj, Salim C Shajahan, Shoma Mani</i>	<b>97</b>
<b>ICSIEE2415</b>	An Intelligent Vacuum Based Grass Cutter For Agricultural Application -- <i>Aswin Aji, Albin Thomas, Jolly George, Aiswarya Chandran</i>	<b>104</b>
<b>ICSIEE2416</b>	Efficiency Analysis of Gear Change Control Strategy Of Clutchless Automatic Manual Transmission Of An Electric Vehicle -- <i>Alsufiyan Nazim P N, Lekshmi Nair J, Assoc. Prof. Preethi Sebastian</i>	<b>109</b>
<b>ICSIEE2417</b>	Maximizing Voltage Gain And Efficiency In Bldc Motor-Driven Electric Vehicle Through Sepic Converter Integration -- <i>Anu Lal B, Shwetha Saji, Ojes O, Althaf Hassan</i>	<b>114</b>
<b>ICSIEE2418</b>	Novel Single Phase Cuk Derived Bridgeless Pfc Converter For On Board Ev Charger With Alternate Dc Source And Reduced Number Of Components -- <i>Kavyasree A, Dr Reshma Gopi R.</i>	<b>124</b>
<b>ICSIEE2419</b>	Dc-Dc Converter with Single Input And Dual Output For Electric Vehicle -- <i>Aadhiya Majeed, Aparna Pradeep, Dr. Honey Baby, Arun Chandrakumar K</i>	<b>134</b>

<b>ICSIEE2420</b>	A Comparative Study of The Recent High Gain Boost Converters Topology For Renewable Energy Applications -- <i>Nivya P S, Aiswarya Chandran</i>	<b>135</b>
<b>ICSIEE2421</b>	Ai Based Pll for Grid Synchronization -- <i>Dilshad P, Faheem Irshad M T, Mr. Gaisoon Jafer, Murshid K P, Riyas P, Jithin Raj V</i>	<b>136</b>
<b>ICSIEE2422</b>	Grid - Tied Solar Panel Companion Inverter -- <i>Nivedh Johnson, Manu M Venu, Jolly George</i>	<b>137</b>
<b>ICSIEE2423</b>	Power Quality Enhancement In Electrical System By Incorporating Renewable Energy Resources With UPQC -- <i>Aparna Pradeep, Ms. Aadhiya Majeed, Dr. Honey Baby</i>	<b>138</b>
<b>ICSIEE2424</b>	Third Eye for Blind -- <i>Mohamad sha K, Anandeshwer E R, Justin Peter, Alishya Philip, Dr. Reshma Gopi R</i>	<b>139</b>
<b>Inter – Disciplinary Paper</b>		
<b>ICSIEE2425</b>	A Study on The Enhancement Of Electrochemical Performance Of Copper Tin Sulphide (Cu <sub>3</sub> Sns <sub>4</sub> ) Annealed At Different Temperatures -- <i>Anju Sebastian, Deepthi V, Anandhan A Saj, B Vidhya, V Maheskuma</i>	<b>141</b>



# Drone-Based Plant Disease Detection and Alert System Using GSM Module

<sup>1</sup>Jinas Haidharali P, <sup>2</sup>Jazil Jahafar P, <sup>3</sup>Nabeela K P, <sup>4</sup>Amen Mubarak K, <sup>5</sup>Muhammed Aslam E U,  
<sup>1,2,3,4</sup>UG student, dept. of EEE, MEA Engineering College, Perinthalmanna, Kerala, India  
<sup>5</sup>Assistant Professor, dept. of EEE, MEA Engineering College, Perinthalmanna, Kerala, India  
Emails, <sup>1</sup>[20gee05@meaec.edu.in](mailto:20gee05@meaec.edu.in), <sup>2</sup>[20nee02@meaec.edu.in](mailto:20nee02@meaec.edu.in), <sup>3</sup>[20nee04@meaec.edu.in](mailto:20nee04@meaec.edu.in),  
<sup>4</sup>[20nee05@meaec.edu.in](mailto:20nee05@meaec.edu.in), : <sup>5</sup>[muhammedaslam@meaec.edu.in](mailto:muhammedaslam@meaec.edu.in)

**Abstract:** *In recent years, there has been a growing interest in the development of autonomous drone systems for various applications. One such application is plant disease detection in agriculture. This research paper aims to develop an autonomous drone system equipped with a Raspberry Pi and a GSM module for efficient plant disease monitoring. To achieve this, the drone will be programmed to autonomously navigate a field, analyze plants using Convolutional Neural Networks, and send SMS alerts containing the location coordinate and type of leaf disease to a specified number upon detection. The integration of drones, CNN, and GSM technology offers a promising solution for real-time disease detection and alerting. The motivation for this research comes from the need for early detection of plant diseases in agriculture to minimize crop losses and improve overall yield.*

## Introduction:

Early detection of plant diseases plays a crucial role in ensuring the health and productivity of crops in agriculture. Traditional methods of disease detection involve the manual inspection of plants, which can be time-consuming and labor-intensive. Moreover, these methods are often subjective and prone to human errors. There is a need for a more efficient and reliable approach to disease detection to minimize crop loss and increase food production. Drones have been used for diverse application purposes in precision agriculture and new ways of using them are being explored [1].

The emergence of autonomous drones equipped with advanced technologies presents a promising solution to address the limitations of traditional methods. These drones, integrated with computer vision and machine learning algorithms, can scan vast agricultural fields and capture high-resolution images of plants. These images can then be analyzed using Convolutional Neural Networks, a deep learning technique known for its effectiveness in image classification and object detection tasks. Previous studies have shown the successful implementation of image recognition techniques for plant disease detection in various crops, including wheat, apples, and mango trees [2].

The objective of this research paper is to further explore the potential of autonomous drone systems in plant disease detection and develop a system that can accurately identify and classify disease-infected plants in real-time. By integrating computer vision and deep convolutional neural networks, the autonomous drone system will be able to analyze the captured images of plants and identify the presence of diseases.

The scope of this research paper includes designing and programming the autonomous drone system to navigate fields and capture images of plants using high-resolution drone cameras. The captured images will then be processed and analyzed using deep learning algorithms to detect and classify plant diseases. Furthermore, the integration of a GSM module into the system will enable real-time communication and alerting. Additionally, GPS integration will provide accurate location tracking capabilities. This research paper aims to address the challenges of accurately segmenting disease regions in plant images and differentiating between similar symptoms caused by different diseases [3]. The primary goal for this research paper is to develop a cost-effective and efficient solution for plant disease detection in agriculture using autonomous drones equipped with computer vision and deep learning algorithms [4]. The paper will focus on the integration of an autonomous drone with a Raspberry Pi and GSM module for plant disease detection and alerting.

The design and implementation of the autonomous drone system for plant disease detection involve several key components and processes. The hardware components include the Raspberry Pi, GPS module, GSM module, and high-resolution drone cameras. The software components encompass the programming of the drone for autonomous navigation, image capture, and analysis using Convolutional Neural Networks [5].

#### Understanding the Role of Drones in Agriculture :

In recent years, drones have been increasingly employed in the field of agriculture due to their versatility and efficiency in data collection. These unmanned aerial vehicles can quickly and easily access remote or large-scale agricultural areas, providing valuable insights and data for farmers and researchers to make informed decisions. They can be equipped with various sensors and cameras to capture images, thermal data, and other relevant information about the crops.

#### Utilizing Convolutional Neural Networks for Plant Disease Detection :

Convolutional Neural Networks have significantly transformed the realm of computer vision and have demonstrated remarkable efficacy in tasks related to image classification and object detection [6]. They can learn and extract meaningful features from images, making them suitable for plant disease detection [7]. Previous studies have shown the successful use of CNNs in detecting and classifying plant diseases based on leaf images. These studies have demonstrated the ability of CNNs to accurately identify various leaf diseases, including fungal infections, viral infections, and nutrient deficiencies. One of the key advantages of integrating CNNs with drone technology is the ability to perform real-time disease detection in agricultural fields. As the drone captures high-resolution images of the plants, it can quickly process and analyze the images using the CNN algorithm. The CNN is trained using a large dataset of healthy and diseased plant images, enabling it to identify patterns and features associated with different plant diseases.

#### Integrating GSM Technology for Real-Time Alerting :

To enhance the effectiveness of the autonomous drone system in plant disease detection, the integration of GSM technology is crucial. The GSM module will allow the drone to send real-time alerts and notifications to farmers or relevant stakeholders upon detecting a disease in the plants. This will enable prompt action to be taken, such as implementing control measures or applying targeted treatments. Additionally, the use of GSM technology will enable farmers to receive regular updates on the health of their crops, even when they are not physically present in the field. This real-time communication will provide farmers with valuable insights into the overall condition of their plants and allow them to make timely decisions regarding irrigation, fertilization, and pest control. Furthermore, the integration of GSM technology will enable the drone to send not only alerts about the presence of diseases in the plants but also the location coordinates and the type of disease detected [8]. This information can be sent as an SMS to the farmers' mobile phones, ensuring that they are notified immediately. The process of integrating GSM technology involves several steps. Firstly, the drone captures images of the plants using its on-board cameras. The images undergo pre-processing to improve their quality and eliminate any noise or undesired elements. Next, the images are segmented to isolate the regions of interest, namely the areas affected by diseases. After segmentation, the CNN is employed to extract features from the segmented images. These features are then used for the recognition and classification of plant diseases.

Once the plant diseases are classified, the drone utilizes the integrated GSM module to send an SMS alert containing relevant information. This includes the location coordinates of the affected area, allowing farmers to pinpoint the exact location of the disease outbreak. The SMS alert will also specify the type of disease detected, providing farmers with critical information for appropriate management and treatment strategies. The integration of GSM technology in the autonomous drone system for plant disease

detection not only enhances the efficiency and effectiveness of disease monitoring but also enables timely decision-making for farmers.

#### Integrating GPS for Accurate Location Tracking :

In addition to the integration of GSM technology, incorporating GPS into the autonomous drone system plays a crucial role in enabling accurate location tracking capabilities [8]. By utilizing GPS, the drone can precisely determine the geographic coordinates of the disease-affected areas within the agricultural fields.

The integration of GPS technology allows for the creation of detailed maps indicating the specific locations where diseased plants have been identified. This information is valuable for farmers as it facilitates targeted intervention and management strategies, such as selective pesticide application or focused monitoring of specific areas within the fields. Furthermore, the utilization of GPS enables the autonomous drone system to generate comprehensive reports that include the geographic distribution of plant diseases. These reports can provide farmers and agricultural experts with insights into the spatial patterns of disease prevalence, aiding in the development of tailored crop management plans and mitigation measures.

Integrating GPS technology into the autonomous drone system enhances the overall effectiveness of disease detection and monitoring by providing precise and reliable spatial information. This capability empowers farmers to make informed decisions and take proactive measures to safeguard crop health and maximize agricultural productivity.

#### Programming Automatic Drone Navigation :

To achieve autonomous drone navigation, several programming steps are required. The first step is to define the target field location and set it as the destination for the drone. The drone's navigation system will use GPS coordinates to determine its current location and calculate the most efficient path to reach the target field location. Once the path is calculated, the drone's programming should include obstacle avoidance mechanisms to ensure safe navigation. The drone's programming should also include the ability to adjust its flight altitude if necessary, to capture images of the plants from different angles and perspectives. This can be done by integrating altitude control algorithms into the drone's programming.

Furthermore, it is crucial to implement a mechanism for the drone to ensure its safe return to the starting point after completing its mission of capturing images and detecting plant diseases. This can be achieved by incorporating advanced navigation algorithms and techniques. One approach is to use simultaneous localization and mapping algorithms, which allow the drone to create a map of its environment in real-time and simultaneously determine its position within that map. By continuously updating its location and the map, the drone can navigate back to the starting point with precision [9]. Another important aspect is the inclusion of failsafe mechanisms in the drone's programming. These mechanisms can include emergency landing procedures in case of technical issues or low battery levels, as well as communication channels to receive commands or instructions from the user or operator if needed.

#### **Method :**

The autonomous drone system for plant disease detection integrates various technologies and functionalities to achieve its objectives. A block diagram can be formulated to illustrate the components and their interactions within the system.

#### Block Diagram :

The block diagram of the autonomous drone system comprises the following key components:

**Raspberry Pi:** The central processing unit of the drone system, responsible for running the necessary algorithms and coordinating the functionalities of other components.

**Camera :** The camera captures images of the plants, which are then processed for disease detection using convolutional neural networks.

**GSM Module :** The GSM module enables the drone to send SMS alerts containing the location coordinates and type of leaf disease upon detection.

**GPS Module :** The GPS module provides real-time location information of the drone, which is essential for autonomous navigation and returning to the starting point.

**Drone :** The drone itself is equipped with propellers for flight, motors for movement, and sensors for detecting obstacles and maintaining stability.

**Altitude Control Algorithms:** These algorithms ensure that the drone maintains a desired altitude during its flight.

**Obstacle Detection and Avoidance:** This component uses sensors or computer vision techniques to detect obstacles in the drone's path and a collision avoidance algorithm to navigate around them.

**Battery :** The battery provides the necessary power to all the components of the drone system, allowing it to fly and perform its functions.

**User/Operator Interface :** This component allows the user or operator to interact with the drone system, providing commands or instructions if needed.

The autonomous drone system works as follows:

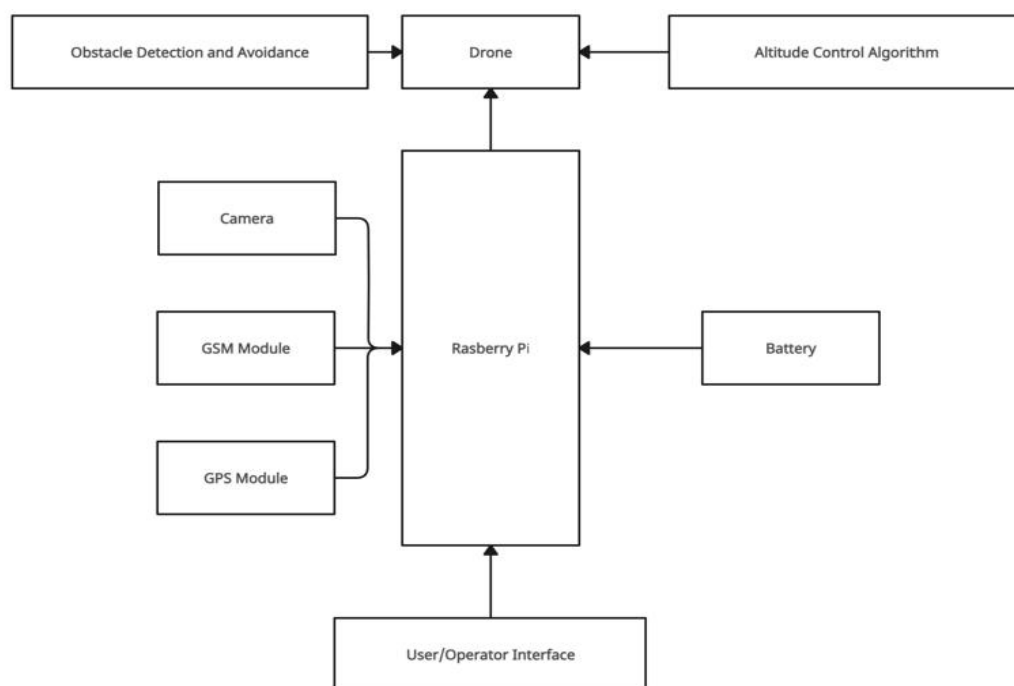


Figure 1: Block Diagram of the Autonomous Drone System

The drone's flight path and destination are pre-programmed using the Raspberry Pi, GPS module, and flight controller. The drone takes off and autonomously navigates to the specified field location using the GPS module for guidance. Once the drone reaches the field location, it starts capturing images of the plants using the camera. These images are then processed and analyzed using convolutional neural networks to detect any signs of plant diseases. If a disease is detected, the drone uses the GSM module to send an SMS alert containing the location coordinates and the type of leaf disease to a designated recipient. The recipient can then take appropriate action based on the information received. After completing its task, the drone autonomously returns to the starting point using the GPS module. The drone uses altitude control

algorithms to maintain a desired altitude during its flight and avoids obstacles using obstacle detection and avoidance techniques. The integration of these components and functionalities in the autonomous drone system for plant disease detection facilitates real-time monitoring, accurate disease identification, and timely alerting to farmers, ultimately enhancing crop management and productivity.

**Maintenance and Troubleshooting of the Autonomous Drone :**

System, regular maintenance and troubleshooting procedures should be implemented. Regular maintenance includes checking the condition of the drone's hardware components, such as propellers, motors, and batteries. Additionally, software updates should be performed to keep the drone's programming and navigation algorithms up-to-date with the latest advancements. Troubleshooting procedures should be in place to address any technical issues that may arise during the operation of the autonomous drone. These procedures should include diagnostic tests to identify the cause of the issue and appropriate steps to resolve it. Another essential aspect of maintaining and troubleshooting the autonomous drone is ensuring data integrity. This can be achieved by implementing data backup and storage protocols, as well as regular checks for data corruption or loss.

**Findings:**

**Impacts and Benefits of Autonomous Disease Detection Drones in Agriculture :**The integration of autonomous disease detection drones in agriculture can have numerous impacts and benefits.

**Improved early detection of plant diseases:** By using autonomous drones equipped with specialized sensors, farmers can quickly identify and diagnose plant diseases before they spread.

**Cost and time savings:** Autonomously operated drones can cover large areas of farmland in a shorter time compared to manual inspections. This saves farmers valuable time and reduces labor costs associated with disease detection and monitoring.

**Enhanced efficiency and accuracy:** Autonomous drones can analyze plant health data with high precision and accuracy, enabling farmers to make informed decisions regarding pest control measures and disease management.

**Remote monitoring and real-time data analysis:** With autonomous drones, farmers can remotely monitor their fields and receive real-time data on plant health conditions. This allows for immediate action to be taken in response to any detected diseases or abnormalities, leading to more timely and effective interventions.

**Increased crop productivity and yield:** By detecting diseases early on and implementing appropriate interventions, farmers can prevent or reduce crop loss, leading to higher yields and ultimately, increased profitability.

**Environmental sustainability:** By using autonomous disease detection drones, farmers can minimize the need for chemical treatments on their crops. This reduces the environmental impact of agriculture and promotes sustainable farming practices.

**Improved decision-making and resource allocation:** Autonomous disease detection drones provide farmers with accurate and detailed information about the health status of their crops. This enables farmers to make more informed decisions about resource allocation, such as optimizing fertilizer and pesticide usage, ensuring that treatments are targeted and effective.



**Conclusion:**

In conclusion, the integration of autonomous drones, Convolutional Neural Networks, and GSM technology holds great potential for revolutionizing disease detection in agriculture. This technology can provide farmers with real-time, accurate information about the health of their crops, allowing for early intervention and targeted treatment. However, additional research and advancements are necessary to overcome the existing constraints and challenges in implementing this technology on a larger scale. Future studies could focus on refining the CNN algorithms to improve disease detection accuracy, as well as expanding the range of plant diseases that can be detected. Additionally, efforts should be made to enhance the autonomous capabilities of the drones, allowing for seamless navigation and data collection in different field environments. Furthermore, it is crucial to establish protocols and guidelines for the integration of autonomous drones in agricultural practices to ensure their safe and responsible use. This includes addressing concerns such as privacy, airspace regulations, and potential risks associated with drone operations.

Advancements in artificial intelligence and machine learning algorithms have the potential to enhance the capabilities of autonomous disease-detection drones in the future. By continuously training and refining these algorithms, we can improve the accuracy and efficiency of disease detection, making it easier for farmers to identify and manage plant diseases effectively. GSM and GPS technology can also be further integrated to enable real-time tracking and remote monitoring of the drones, allowing farmers to receive instant alerts and updates on the health status of their crops [8]. Moreover, on-going research should focus on developing more robust and cost-effective sensors and imaging technologies specifically designed for drone-based disease detection. This will further improve the accuracy and reliability of disease detection, allowing for earlier intervention and prevention of crop losses [10]. Additionally, collaborations between researchers, farmers, and agricultural organizations will be crucial for the successful implementation and adoption of this technology.

**References:**

1. Chin, R., Catal, C. & Kassahun, A. Plant disease detection using drones in precision agriculture. *Precision Agric* 24, 1663–1682 (2023). <https://doi.org/10.1007/s11119-023-10014-y>.
2. Deep Learning for Image Based Mango Leaf Disease Detection. Dec. 2019.
3. H. S. Malik et al., Disease Recognition in Sugarcane Crop Using Deep Learning. 2021
4. R. Thangaraj, S. Anandamurugan and V. K. Kaliappan, Automated tomato leaf disease classification using transfer learning-based deep convolution neural network, 2021.
5. Abbas et al. Drones in Plant Disease Assessment, Efficient Monitoring, and Detection: A Way Forward to Smart Agriculture. *Agronomy*. vol. 13. no. 6. pp. 1524-1524. May 2021. [10.3390/agronomy13061524](https://doi.org/10.3390/agronomy13061524).
6. J. F. Tusubira, B. Akera, S. Nsumba, J. Nakatumba-Nabende and E. Mwebaze. "Scoring Root Necrosis in Cassava Using Semantic Segmentation". Jan. 2020.
7. X. Liu, H. Liu, S. Yu and Z. Zhong. "A control system for fine farming of apple trees". Aug. 2023.
8. B. P. S. S. A. S. Rath. "Integrating GPS, GSM and Cellular Phone for Location Tracking and Monitoring". [10.48550/arXiv.1307.3147](https://arxiv.org/abs/10.48550/arXiv.1307.3147).
9. Li, Z., Zhang, Y., & Zhang, J. (2019). Simple vision-based navigation and control strategy for autonomous drones. *IEEE Access*, 7, 109117-109127. <https://doi.org/10.1109/ACCESS.2019.2933440>.
10. L. Jia, J. Wang, Q. Liu and Q. Yan, Application Research of Artificial Intelligence Technology in Intelligent Agriculture

# Electrical Estimation and Design of High - Rise Building In Middle East

Mohammed Shamil C P<sup>1</sup>, Mohammed Jasim C P<sup>2</sup>, Mohammed Faizal<sup>3</sup>, Ajmal M S<sup>4</sup>

<sup>5</sup>Mohammed Shabas KP

<sup>1,2,3,4</sup> UG Student, Dept. Of EEE, MEA Engineering College, Perinthanna, Kerala, India.

<sup>5</sup>Assistant Professor, Dept .Of EEE, MEA Engineering College, Perinthanna, Kerala, India.

Email, <sup>1</sup>20nee03@meaec.edu.in, <sup>2</sup>20gee04@meaec.edu.in, <sup>3</sup>20gee06@meaec.edu.in, <sup>4</sup>20gee12@meaec.edu.in, -

<sup>5</sup>ajmalms@meaec.edu.in

**Abstract:** This project delves into the intricate realm of electrical estimation and design tailored for high-rise buildings in the Middle East. The focal points include meticulous wiring configurations, circuit breaker selections, and the strategic installation of step-down transformers, all crucial for sustaining optimal voltage levels. Additionally, the project explores the integration Power Factor Improvement (PFI) panels for achieving near unity power factor, and robust fire security systems. In adherence to established codes, this research recognizes the contemporary significance of precise electrical protection and installation practices in both residential and commercial high-rise structures. As high-rise buildings redefine skylines in the Middle East, the project aims to present a comprehensive framework that balances innovation with regional nuances, contributing to the development of resilient, energy-efficient, and safe structures in this dynamic and evolving landscape.

**Key Words:** PowerFactorImportant(PFI)

## Introduction

Ensuring a secure electrical connection for high-rise buildings involves a multifaceted approach with critical parameters at its core. This includes meticulous attention to proper wiring, aligning wire assortments with rated currents, and the selection of circuit breakers to prevent short circuits and overcurrent faults. The installation of a suitable step- down transformer to maintain the required voltage level, adds layers of resilience to the electrical infrastructure. Integrating a Power Factor Improvement (PFI) panel to achieve nearly unity power factor and a robust fire security system further contribute to a comprehensive safety net. All these elements and equipment installations adhere rigorously to standard codes, emphasizing the contemporary significance of precise electrical protection and installation practices in both residential and commercial high-rise buildings. Embarking on the realm of electrical engineering, this project is dedicated to crafting an integrated and robust electrical infrastructure for high-rise buildings in the Middle East. From load calculations to ensuring electrical safety, our objective is to deliver cutting-edge design solutions that seamlessly blend efficiency, security, and cost- effectiveness.

- Civil Structure
- Load Calculation
- Distribution System
- Power Supply
- Electrical safety
- Communication And Security
- Cost Effective Solution

In conclusion, this project unfolds as a testament to the fusion of innovation and precision in the electrical design of high-rise buildings in the dynamic landscape of the Middle East. Through meticulous load calculations, strategic distribution systems, and a focus on safety and efficiency, the

result is a comprehensive blueprint that not only meets but exceeds the demands of modern architecture. As we deliver high-quality design solutions, this endeavor not only illuminates the future of electrical engineering but also contributes to the evolution of sustainable, secure, and seamlessly integrated high-rise structures in the region.

### **Literature Review:**

The survey on load calculation methodologies for high-rise buildings delves into diverse approaches utilized in estimating and distributing electrical loads within vertical structures. Exploring scholarly articles, industry reports, and case studies, the survey aims to provide insights into challenges unique to high-rise construction and evaluate the effectiveness of existing load calculation methods. Additionally, it investigates recent innovations in load management technologies, such as smart grids and energy storage solutions, to identify advancements that could enhance precision and efficiency in load calculations. Furthermore, the survey addresses challenges specific to load balancing in high-rise buildings.

#### Types of Wiring Cleat Wiring:

This system of wiring comprise of ordinary VIR or PVC insulated wires (occasionally, sheathed and weather proof cable) braided and compounded held on walls or ceilings by means of porcelain cleats, Plastic or wood. Cleat wiring system is a temporary wiring system therefore it is not suitable for domestic premises. The use of cleat wiring system is over nowadays.

#### Casing and Capping wiring:

Casing and Capping wiring system was famous wiring system in the past but, it is considered obsolete this days because of Conduit and sheathed wiring system. The cables used in this kind of wiring were either VIR or PVC or any other approved insulated cables. The cables were carried through the wooden casing enclosures. The casing is made up of a strip of wood with parallel grooves cut length wise so as to accommodate VIR cables. The grooves were made to separate opposite polarity. the capping (also made of wood) used to cover the wires and cables installed and fitted in the casing.

#### Batten Wiring (CTS or TRS):

Single core or double core or three core TRS cables with a circular oval shape cables are used in this kind of wiring. Mostly, single core cables are preferred. TRS cables are chemical proof, water proof, Steam proof, but are slightly affected by lubricating oil. The TRS cables are run on well seasoned and Straight teak wood batten with at least a thickness of 10mm. The cables are held on the wooden batten by means of tinned brass link clips (buckle clip) already fixed on the batten with brass pins and spaced at an interval of 10cm for horizontal runs and 15cm for vertical runs.

#### Conduit Wiring:

There are two additional types of conduit wiring according to pipe installation

##### 1) Surface Conduit Wiring

If conduits installed on roof or wall, It is known as surface conduit wiring. in this wiring method, they make holes on the surface of wall on equal distances and conduit is installed then with the help of rawal plugs

##### 2) Concealed Conduit wiring

If the conduits is hidden inside the wall slots with the help of plastering, it is called concealed conduit wiring. In other words, the electrical wiring system inside wall, roof or floor with the help of plastic or metallic piping is called concealed conduit wiring. obviously, It is the most popular, beautiful, stronger and common electrical wiring system nowadays.

### **Case Study:**

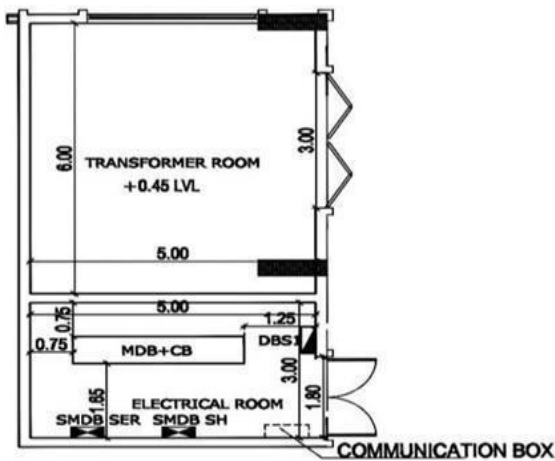
Selected Structure nestled in the vibrant landscape of Fujairah, UAE, our project centers on a G+5 residential/commercial building crowned with a luxurious penthouse. This architectural gem symbolizes

the intersection of modern living and commercial spaces, embodying the essence of dynamic urban development in the heart of Fujairah.

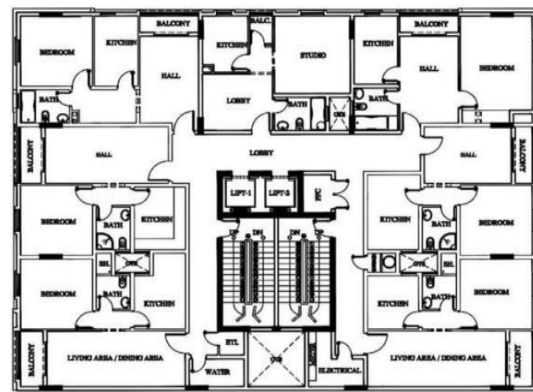
Target Designing

- Complete wiring design for the building
- Power distribution design
- Load selection and calculation
- Lift load and motor selection
- Transformer selection
- Capacitor bank selection
- Civil Plan

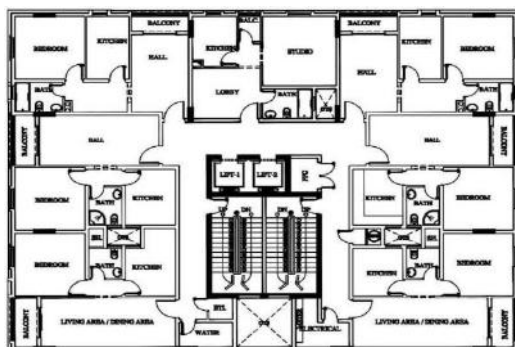
Unveiling the blueprint of our G+5 residential/commercial building with a penthouse in Fujairah, this civil plan encapsulates the meticulous design, spatial organization, and structural intricacies shaping this architectural marvel.



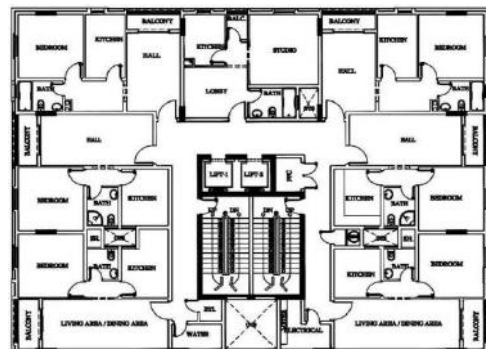
Transformer Room



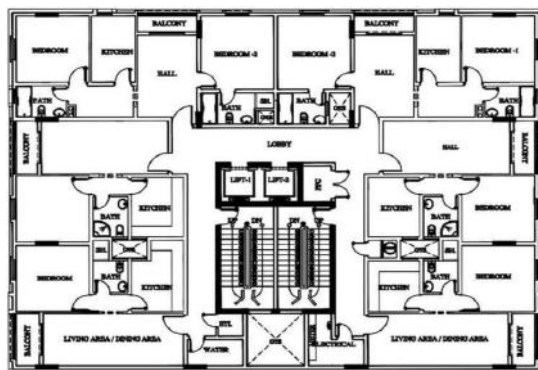
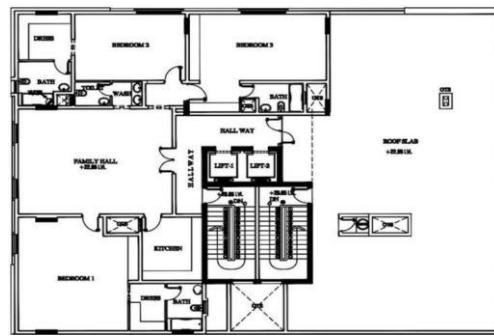
2<sup>nd</sup>, 3<sup>rd</sup> and 4<sup>th</sup> floors



First Floor



Ground Floor

5<sup>th</sup> Floor

Penthouse

The presented civil diagram serves as the foundational map that breathes life into our architectural vision for the G+5 residential/commercial building with a penthouse in Fujairah. This detailed representation encompasses the structural framework, spatial configurations, and intricate elements crucial to the construction's integrity. As we unveil this blueprint, it becomes the guiding cornerstone, illustrating the harmonious blend of design and engineering precision essential for the realization of our vision in the vibrant landscape of Fujairah, UAE.

#### Electrical Schematics Planning

In tandem with the intricacies depicted in the civil diagram, our electrical schematics for the G+5 residential/commercial building with a penthouse in Fujairah encapsulate a comprehensive vision that extends beyond conventional wiring. Thorough load calculations anticipate the diverse energy needs of both residential and commercial spaces, informing a nuanced power distribution strategy that aligns seamlessly with the architectural layout. The meticulous alignment of distribution boards ensures an efficient and organized electricity flow throughout the structure. Transformer selection is strategically orchestrated to maintain optimal voltage levels, guaranteeing a safe and reliable power supply. In integrating load calculation, power distribution, distribution board alignment, and transformer selection, our electrical schematics become a vital blueprint, illuminating not only spaces but also the path to a resilient, efficient, and seamlessly integrated electrical infrastructure.

#### Electricity Wiring Rules According to ADDC:

##### Electricity Parameters

The parameters for electricity supplies provided in the Emirate of Abu Dhabi are defined in the Electricity Supply Regulations, issued by the DoE.

- The nominal Voltage at LV shall be 230V single-phase or 400V three-phase.
- The permissible variation from the nominal Voltage shall be kept within + 10% and - 6%
- The nominal frequency shall be 50Hz.
- The power factor at the Connection Point between the Distribution Company and the Owner's Electrical
- Installation shall be maintained between 0.9 lagging and unity.
- Power factor correction equipment must be used where required to achieve this value.

##### Isolation and Switching

All Electrical Installations must be provided with a means of safe isolation at the Electricity Intake, which must be lockable or otherwise provided with a means of preventing interference. An Electrical Installation must be further sectionalized by means of isolation at the origin of each Circuit, in order to provide ease of access for safe working. All mechanical equipment should be provided with a means of isolation close to the equipment which can be locked and kept under the control of the person performing



maintenance. This isolation must be effective on all phases and neutral of the supply, must be clearly marked and must be located in an easily accessible position.

#### Overload and short-circuit protection

All Electrical Installations and individual Circuits therein must be provided with devices that protect against thermal, electromagnetic and other detrimental effects caused by overload and short-circuits. Such devices must be located at suitable sections and Circuits so as to give effective automatic disconnection in such conditions. The main circuit-breaker at the Connection Point must be of MCCB or ACB type and adequately rated for the maximum Prospective Fault Current. All Circuits must be individually protected against overloads and short-circuits by suitable devices. Replaceable or re-wireable fuse links are not permitted for this purpose. To ensure protection against overload, Circuit conductors must be sized taking into account the time-current characteristic of the Protective Device. Protective Devices at the Main Distribution Board must have a Prospective Fault Current withstand and interruption rating above the maximum Prospective Fault Current declared by the Distribution Company for the relevant Connection Point.

#### Insulation

All Electrical Installations must be sufficiently insulated to protect against electric shock from Direct Contact by any person. Such insulation must be capable of withstanding wear and tear during normal use of the equipment. Supplementary insulation or 'double insulation' may be used where additional robustness is required. Live conductors are required to be inaccessible without the use of a special key or tool, available only to authorized persons and only for the purpose of testing, using special equipment and procedures. Uninsulated equipment may be used at voltages not exceeding 12V AC or 30V DC and only where supplied by a SELV source.

#### Earthing

Earthing of Exposed-Conductive-Parts of an Electrical Installation and of Appliances in a Premises is required and must provide the following functions of safety:

- a) allow the passage of fault current in the event of a live conductor touching an Exposed Conductive-Part.
- b) ensure that the magnitude of fault current is sufficient to operate Protective Devices within 0.4 Sec for all parts of an Electrical Installation; and
- c) ensure that, in association with Protective Devices, a 'high resistance' fault to Earth does not persist so as to cause overheating or fire.

#### Selection of Components:

##### Cable Selection

For fixed wiring within Premises, PVC, rubber or XLPE insulated cables with stranded copper conductors must be used, Solid core copper or aluminum conductor cables are not permitted. For locations subject to a higher than normal risk of interference or damage, armoured cables are recommended. For locations with higher than normal fire risk, either cables must be installed in metal conduit or mineral-insulated- copper-clad (MICC) complying with BS EN 60702 or enhanced fire resistance cables must be used. In addition, safety Circuits such as fire alarms, emergency lighting and control Circuits, which are required to remain operational in the event of a fire, must be installed in metal conduits or supplied by MICC cables. The location and selection of cables must take into consideration any special requirements for the prevention of spread of fire. Fire barriers, low smoke insulation or other measures may be required (relevant building regulations should be referenced).

##### Distribution Board

All Distribution Boards must be factory assembled, type- tested and comply with BS EN 61439. Distribution Boards must be of robust construction, capable of withstanding expected electrical, thermal,

and environmental stresses in normal service and during faults. Apparatus forming part of the assembly of Distribution Boards shall have electrical isolation clearances sufficient to withstand normal Voltages, surge Voltages and creepages as defined in BS EN 61439-1. Each Distribution Board must have a neutral bar which is mounted on insulators and which has a sufficient number of terminal points of adequate size for the largest cable expected to be used. Each Distribution Board must have an Earth bar which has a means of connection to the incoming Earth Conductor and cable gland of the incoming cable.

**Circuit Rating for PVC Single-Core Cables (non-armoured) Installed in Conduit or Trunking:**

No.	PHASE & NEUTRAL CABLE SIZES (mm <sup>2</sup> )	EARTH CABLE SIZES (mm <sup>2</sup> )	CABLE KW RATING (30°C)	CABLE AMPERE RATING (30°C)	CABLE KW RATING (40°C)	CABLE AMPERE RATING (40°C)	CIRCUIT BREAKER RATING	ADDC ALLOWED KW RATING	CIRCUIT TYPE
1	2.5	2.5	4.7KW	24	4.1KW	20.9A	10A	<3KW	Lighting Only
2	2.5	2.5	4.7KW	24	4.1KW	20.9A	16A	1KW-1.8KW	Lighting Only
3	4	4	6.3KW	32	5.4KW	27.8A	20A	200-600W	Radial Circuit to Sockets
4	4	4	6.3KW	32	5.4KW	27.8A	20A	<=2.8KW	Radial Circuit for Appliances
5	2x4	2x4	9.3KW	48	8.1KW	41.7A	32A	0.8-2.8KW	Ring Circuit to Sockets
6	6	6	8KW	41	7KW	35.7A	32A	<=6KW	Radial Circuit to Large Appliances
7	10	10	11.1KW	57	9.7KW	49.6A	40A	6.1-8KW	Radial Circuit to Machinery
8	16	16	14.8KW	76	12.9KW	66.1A	63A	9-12KW	Radial Circuit
9	25	16	19.7KW	101	17.2KW	87.9A	80A	<=15KW	Radial Circuit
10	35	25	24.4KW	125	21.2KW	108.7A	100A	<=18KW	Radial Circuit
11	50	25	29.5KW	151	25.7KW	131.4A	125A	<=23KW	Radial Circuit
12	70	35	37.5KW	192	32.6KW	167A	160A	<=30KW	Radial Circuit

**Circuit Rating for XLPE Multi-Core Cables (armoured) Installed on Perforated Cable Tray:**

No.	PHASE & NEUTRAL CABLE SIZES (mm <sup>2</sup> )	EARTH CABLE SIZES (mm <sup>2</sup> )	CABLE KW RATING (30°C)	CABLE AMPERE RATING (30°C)	CABLE KW RATING (40°C)	CABLE AMPERE RATING (40°C)	CIRCUIT BREAKER RATING	ADDC ALLOWED KW RATING	CIRCUIT TYPE
1	4C4	1C4		44A	20.7KW	35.2A	20A	<8KW	Power Circuit
2	4C6	1C6		56A	26.4KW	44.8A	32A	8-9.9KW	Power Circuit
3	4C10	1C10		78A	36.7KW	62.4A	40A	10-17KW	Power Circuit
4	4C16	1C16		99A	46.6KW	79.2A	63A	18-31KW	Power Circuit
5	4C25	1C16		131A	61.7KW	104.8A	100A	32-49.5KW	Power Circuit
6	4C35	1C25		162A	76.3KW	129.6A	125A	51-62KW	Power Circuit
7	4C50	1C25		197A	92.8KW	157.6A	160A	63-70KW	Power Circuit
8	4C70	1C35		251A	118.2KW	200.8A	160A	71-80KW	Power Circuit
9	4C95	1C50		304A	143.2KW	243.2A	200A	81-100KW	Power Circuit
10	4C120	1C70		353A	166.3KW	282.4A	250A	101-125KW	Power Circuit
11	4C150	1C95		406A	191.3KW	324.8A	300A	126-150KW	Power Circuit
12	4C185	1C95		463A	218.1KW	370.4A	350A	151-175KW	Power Circuit
13	4C240	1C120		546A	257.2KW	436.8A	400A	200KW	Power Circuit
14	4C300	1C150		628A	295.8KW	502.4A	400A	200KW	Power Circuit
15	2x4C150	2x1C95			382.6KW	649.8A	630A	250-300KW	Power Circuit
16	2x4C240	2x1C120			514.4KW	873.6A	800A	350-400KW	Power Circuit
17	3x4C185	3x1C95			654.4KW	1111.2A	1000A	450-500KW	Power Circuit

**Capacitor Bank**

- The Voltage rating of capacitor units shall be 480V as a minimum.
- Capacitor units shall be temperature class D.
- Capacitor units shall be metal encapsulated.
- Capacitor units shall be capable of continuous operation in accordance with the over-voltage and overcurrent requirements of IEC 60831.
- Built-in discharge resistors for capacitors shall be sized to ensure safe discharge of the capacitor to less than 50V in one minute after a switch off.
- Capacitors shall have provision for effective Earth connection of the case to the capacitor mounting frame and to the Circuit Earth Conductor.

- Each capacitor shall be provided with a permanent nameplate, which includes the following information;
  - (a) Name of manufacturer;
  - (b) Serial number;
  - (c) year of manufacturer;
  - (d) rated reactive power;
  - (e) rated Voltage(rms);
  - (f) number of phases;
  - (g) rated frequency;
  - (h) statement of discharge device;
  - (i) short circuit current;
  - (j) statement of liquid fill;
- Capacitor Bank = 40% Total Load

**Conclusion:**

In conclusion, our project for the G+5 residential/commercial building with a penthouse in Fujairah underscores a meticulous approach to meet diverse power requirements. Through a comprehensive analysis encompassing the intended use, occupant numbers, and electrical equipment specifications, we have laid the groundwork for an informed electrical system design. The thorough estimation of electrical loads serves as the cornerstone for crafting an effective and tailored system that prioritizes safety, reliability, and energy efficiency. Our commitment extends to ensuring strict compliance with Abu Dhabi Distribution Company (ADDC) codes and regulations, thus upholding the highest standards of electrical safety. This culmination of a comprehensive understanding of power requirements, unwavering adherence to safety regulations, and a pronounced emphasis on energy efficiency defines our blueprint, poised to illuminate and empower high-rise structures in the dynamic landscape of the Middle East.

**Reference:**

1. Cahier Technique no. 172 – Earthing Systems in LV B Lacroix, R Calvas, Schneider Electric.
2. Cahier Technique no. 173 – Earthing Systems Worldwide B Lacroix, R Calvas, Schneider Electric.
3. Neutral Earthing in LV Networks A Robert, J Hoeffelman, CIRED Conference June 2001.
4. Plugs and Sockets Around the World Conrad H. McGregor, World Standards.
5. The Distribution Code – Annex 1 – E/R 1 – Limits for Harmonics in the Electricity Supply System approved by the Regulation and Supervision Bureau.
6. The Distribution Code – Annex 1 – E/R 7 – Limits for Voltage Fluctuations in the Electricity Supply System Approved by the Regulation and Supervision Bureau.
7. The Distribution Code – Annex 1 – E/R 10 – Limits for Voltage Unbalance in the Electricity Supply System Approved by the Regulation and Supervision Bureau.
8. Designing for Low Resistance Grounding Lightning Eliminators & Consultants, Inc.
9. Guide to the Installation of Photovoltaic Systems Microgeneration Certification Scheme ('MCS').

# Vortex Generators for Passive Cooling of Rooftop Photovoltaic Systems Under Free Convection With Smart Concentric System

<sup>1</sup>Aslam Farooq K H, <sup>2</sup>Ryan Titus, <sup>3</sup>Gibson Antony, <sup>4</sup>Joyal Jomon, <sup>5</sup>Ms.Renu Mary George  
<sup>1,2,3,4</sup>UG Student, Dept. of EEE, Albertian Institute of Science and Technology, Kochi, Kerala  
<sup>5</sup>Assistant Professor, Dept. of EEE, Albertian Institute of Science and Technology, Kochi, Kerala  
Email: <sup>1</sup>farooqaslam170@gmail.com, <sup>2</sup>ryantitus2255@gmail.com, <sup>3</sup>antonygibson41@gmail.com,  
<sup>4</sup>joyaljomon05@gmail.com, <sup>5</sup>renumary@aisat.ac.in

**Abstract:** *Decreasing the operating temperature of a photovoltaic (PV) module can increase its electrical output and longevity. This can be achieved by increasing the radiative and convective heat losses on the front or the rear module surface. In this report, we have proposed, a passive cooling method for the rooftop PV system, which enhances convection heat flux on the module's rear surface. As the vortex generators (VGs) are attached on the surface of the roof without physical contact to the module back sheet, this technique would not void the module warranty and can be easily retrofitted on an existing rooftop system. In the absence of wind (free convection), the module is subjected to the highest temperatures, and our VG design specifically targets this worst-case scenario. The previous results reveal a temperature reduction of more than 4 °C using VGs in the configuration studied. This can be translated to a significant increase in module lifespan by around 30% to 40%, thus reducing the levelized cost of electricity also by using a smart concentric system we can utilize the sunlight more efficiently.*

**Key Words:** *Photovoltaic, Vortex Generators*

## Introduction:

Reducing photovoltaic (PV) module operating temperature potentially brings system-level economic benefits and positively impacts the environment. Despite the newly adapted cell technologies (tunnel oxide passivated contacts and hetero-junction solar cells) having a lower temperature dependency for the output power, a module would still have a loss of around 8%–9% of the electrical generation if operated 30°C above the standard test condition. A technique that could reduce the module operating temperature reduces this loss and also the material degradation rate within the PV module. It was estimated that even just 1 °C of temperature reduction could increase the longevity of the module by 7%, while 5°C of cooling could lead to a 50% increase in lifespan. With a cost-effective cooling approach, the module lifespan can be extended, consequently reducing the need for recycling.

With these potential benefits in sight, several PV cooling technologies have been investigated in the last decade. However, most of these are yet to demonstrate on a large scale in a cost-effective manner. For example, although passive air cooling using aluminum fins on the module's rear surface has the potential to deliver a positive economic impact, it comes with a few drawbacks. The most crucial concern is the high electrical insulation requirement needed for such a conductive metal back sheet. The exposed metal part (in this case, the aluminum heat sink) needs to be grounded, causing a high potential difference across the module packaging material between the cells and the grounded metal part. Hence, some module manufacturers are not confident about using aluminum as part of the back sheet solution. The incompatibility with the bifacial concept, the extra risk, and the cost outweigh the benefit this type of cooling solution can provide, thus no large-scale adaptation has been seen. To alleviate these issues with the existing passive cooling methods, the previously studied the use of vortex generators (VGs) on the PV module under free convection. A 2 °C to 3 °C of temperature reduction has been achieved in a controlled environment. However, some of the limitations with the aluminum-based method still apply (voiding of the module warranty, incompatibility with bifacial operation). It will narrow the scope to the

residential or commercial and industrial (CI) rooftop PV setup, where a roof surface is situated behind and parallel to the PV module thus creating a channel for air to propagate in between the module and roof. In such a configuration, air circulation in these systems on the rear side of PV modules is limited and needs enhancement to prevent a higher operational temperature. VGs have been used for enhancing heat transfer performance in a channel flow, especially for heat exchangers. In the field of renewable energy, VGs are commonly used in solar water or air heaters, including a few studies on the free convection passive VG (span wise vortexes). Delta-wing VGs have also been used in parallel vertical panel radiators driven by buoyancy force. To date, there has been no study so far on VG design for passive cooling in a top-surface-heated free convection tilted channel flow setup. Hence, we utilized what was learned in the previous article to design a novel system with rectangular wing (RW) VGs aimed at increasing the convective cooling for the rooftop PV module. Instead of VGs being directly attached to the heated module rear surface, they have developed a VG design that attaches to the roof surface, where the VGs have no physical contact with the PV module. This arrangement bypasses the IEC testing requirement that would apply for VGs attached on the module surfaces and therefore allows a broader choice of material and a more feasible retrofitting solution. The module and the roof form a tilted channel (module-roof channel) where the airflow is driven by buoyancy force in the absence of wind. The designed VG array can interact with the free convection channel flow and produce longitudinal vortexes. For this article, the size of the VG and the corresponding blockage ratio needs to be much larger than its counterpart found in a vertical buoyancy-driven Channel, or a bottom-plate-heated channel. Therefore, this article explores the key parameters related to VG geometry and arrangement that govern the free convection flow characteristics in a tilted channel. We now that the availability of the sunlight is not constant throughout the day its depends on many factors such as weather ,humidity and environmental conditions and also there is particular time where the availability of sunlight is maximum and also there is time when it is minimum. To overcome this, a smart concentric system is proposed. It uses a special lenses to intensify the sunlight to the PV module during the non-peak hours of the sunlight availability. This results in the increase in the efficiency of the PV system. In their research published in the journal Renewable Energy, Zhou, Zibo, Tkachenko, Svetlana, Bahl, Prateek, Tavener,

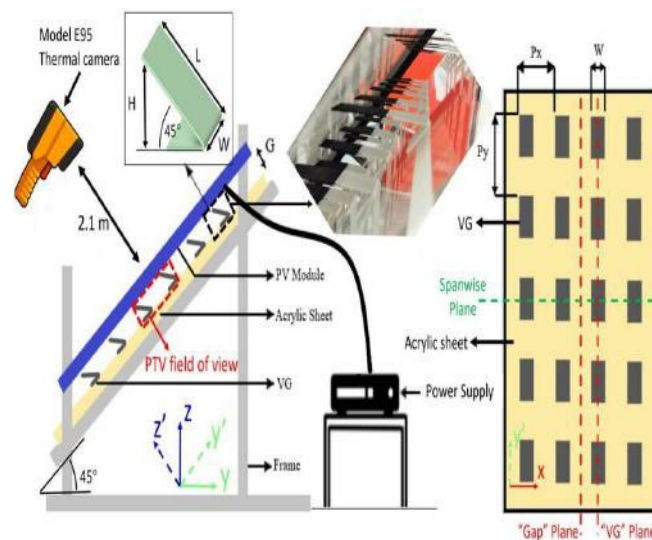


Fig. 1. Schematic demonstrating the model roof setup for the infrared thermographic (Left) and all the parameters defining the VG design. The inserted Photo shows the array of VGs from the side of the channel; (right) top view of The acrylic roof with VGs attached. The “gap” and “VG” planes and a span wise.

Dana, de Silva, Charitha, Timchenko, Victoria, Jiang, Jessica Yajie, Keevers, Mark, and Green, Martin (2022) investigated a potentially cost-effective passive cooling method for photovoltaic (PV) modules. The study focuses on using vortex generators (VGs) optimized for free convection conditions (in the

absence of wind). These VGs are attached to the rear surface of the module and arranged in an array. This research contributes to improving PV module performance by addressing temperature-related challenges. By implementing VGs, we can enhance energy yield and prolong the lifespan of commercial crystalline silicon modules. The paper titled “TOP Con—Technology Options for Cost-Efficient Industrial Manufacturing” was published in the journal *Solar Energy Materials and Solar Cells*, volume 227 in 2021. In this study, the authors explore strategies for industrial manufacturing of TOP Conbased solar cells. They assess various process routes based on currently production-ready and upcoming alternative process technologies.

## Method:

### A. Designing Of VG

1) Infrared Thermography: As can be seen in Fig. 1, a model roof setup was configured to represent the airflow in the vicinity of a PV module on a roof of a building. A thermal camera was mounted on a tripod for the surface temperature measurement. A 60-cell PV module with a size of  $1 \times 1.65$  m is mounted on an aluminium mounting structure and inclined at  $45^\circ$ . The distance between the camera and the module is 2.1 m. To simulate the solar heating in the PV module was plugged into the power supply unit model which pumped 20 A. This can produce around  $520 \text{ W/m}^2$  of heat generation in the PV module. The module temperature in our setup can still be elevated by around  $30^\circ \text{C}$  above the ambient owing to the different radiation conditions between indoor and outdoor testing at  $800 \text{ W/m}^2$ . The x, y, and z refer to the coordinate system defined in Figs. 1 and 3.2 with x and y along the ground. With the module tilted at  $45^\circ$  to the “wall-normal” direction, we also use the coordinate system  $y'$  and  $z'$  denoted on the same figures. The model roof is made from a 6 mm thick acrylic sheet which has low thermal conductivity. The temperature difference across its thickness is measured to be around  $10^\circ \text{C}$  during the experiment. An RW VGs are the only shape that was used because it has shown effectiveness in the experiments conducted in the literature we took as reference. The length L and the width W of the RW VGs vary as defined in Fig. 3.1. The height H can be derived from the length L, as we keep the angle of the VG constant at  $45^\circ$  in the article we referred. The distance between the acrylic roof and the module is defined as parameter G, along with the horizontal pitch  $P_x$  and vertical pitch  $P_y$  between the VGs demonstrated in Fig. 1, where  $P_y$  is fixed at 10 cm for this article. G is set to be 10 or 15 cm (designated as G10 and G15), which is common for residential rooftop PV systems. The VG is attached on the top surface of the roof with a double-sided tape which is 150 m thick. Note that the  $45^\circ$  module and roof tilt angle are chosen here as this inclination angle closely resembles what is required in IEC testing conditions. A lower tilt angle would result in a lower free convection flow rate thus a lower cooling potential for VG. The optimal shape and arrangement for VGs could be different too at a lower tilt angle. The height of VGs over the parameter G gives the ratio  $H/G$ , which must be lower than one as the VGs need to fit in the roof-module channel. Consequently, the ratio  $H/G$  controls how much of the channel is occupied in the vertical  $z'$  direction (defined in Fig. 3.1) and thus can be regarded as the vertical filling ratio. In the other direction, the horizontal filling ratio  $W/P_x$  measures how much the VG is occupying the channel in the horizontal (spanwise) direction. Thus, a wider VG and smaller  $P_x$  (less space between VG spanwise) would lead to a smaller  $W/P_x$  ratio leaving less space for the airflow. Unlike the VGs directly attached to the module which can act as a heat sink, here the VGs achieve cooling purely by encouraging the mixing of the flow in the module-roof channel. The VGs were three-dimensional (3-D) printed at a thickness of 1.5 mm using polylactic acid material. To reduce the amount of 3-D printing required, we have designed a set of modular VG pieces which can be assembled into VGs with different lengths [up to 14 cm (L14)] and widths.



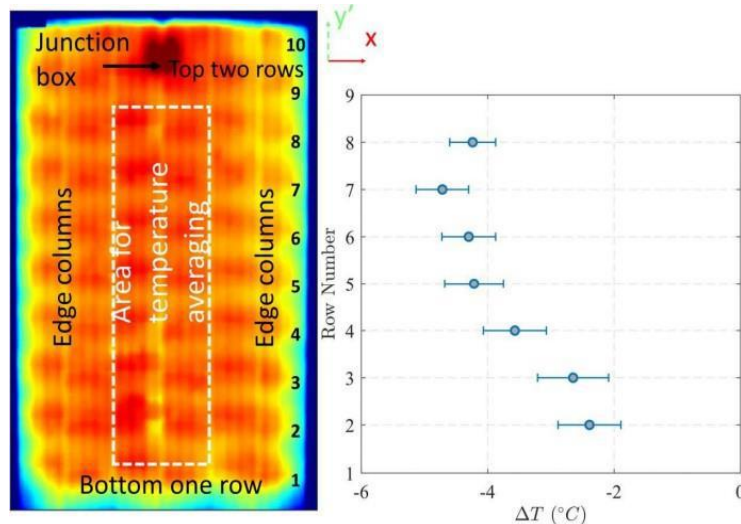


Fig. 2. Thermal images captured during the experiment from the article we referred the white dashed boxes indicate the region used for evaluating the average temperature of the module; (right) the measured  $\Delta T$  (temperature difference between VG case and baseline case)

The cooling ability of the roof VG has been evaluated by comparing the module temperature to that of a separated baseline case without any VGs attached. As the ambient air temperature varies day-to-day, the baseline cases were repeated at different ambient air temperatures,

A linear equation is fitted to describe the relationship between the baseline module temperature and the ambient air temperature with a heat input of 520 W/m<sup>2</sup>. The difference between the module temperatures measured for a given VG design and the corresponding baseline temperature at the same ambient temperature (evaluated from the fitted linear relationship) has been defined as Delta-T (T), where a negative T implies a cooling effect from that given VG design. Flow visualization is a technique used to observe and analyze the behavior of fluid flow in various systems, such as air, water, or other liquids. It involves making the flow patterns visible through different methods to better understand the dynamics of the fluid motion. By visually representing the flow, researchers and engineers can gain insights into the characteristics of the flow field, identify areas of turbulence, separation, or recirculation, and optimize the design of systems for improved performance. In the context of the study on Vortex Generators for Passive Cooling of Rooftop Photovoltaic Systems, flow visualization was employed to investigate the flow between the PV module and the roof surfaces. A setup with a pulsed LED-based light source and a helium-filled soap bubble generator was used to illuminate and seed the flow, allowing researchers to observe and analyze the flow patterns in the channel between the PV module and the roof. This visualization technique provided valuable insights into how the vortex generators influenced the flow dynamics and heat transfer processes, ultimately contributing to the understanding of how to enhance the cooling efficiency of rooftop PV systems under free convection conditions. Flow visualization plays a crucial role in fluid dynamics research and engineering applications by providing a qualitative understanding of complex flow phenomena, which can guide the development of more efficient and optimized designs for various systems and applications. This provides information on the material properties of the photovoltaic (PV) module and vortex generator (VG) used in the study on passive cooling of rooftop PV systems under free convection. The table presents key properties of the materials involved, which are essential for numerical simulations and analysis conducted in the research.



Material	Thickness [m]	Thermal conductivity[W/m/K]	Density[kg/m <sup>3</sup> ]	Heat capacity[J/kg]
Glass	3*10 <sup>-3</sup>	1.8	3000	500
EVA	500*10 <sup>-6</sup>	0.35	960	2090
Silicon	175*10 <sup>-6</sup>	130	2329	700
Tedlar	100*10 <sup>-6</sup>	0.2	1200	1250
PLA VG	1.5*10 <sup>-3</sup>	0.18	1190	1470
Roof	0.01	0.08	700	2310

Fig. 3. PV and VG Material Properties

Here is a breakdown of the information typically found in Table 3:

**Material Properties:** This section lists the properties of the materials used in the study, such as the type of material (PV module and VG), density, specific heat capacity, thermal conductivity, and other relevant properties.

**PV Module Properties:** This subsection details the specific properties of the PV module material, which is crucial for understanding how heat is transferred within the module and between the module and its surroundings.

**VG Properties:** This subsection outlines the properties of the vortex generator material, which is designed to enhance convective heat transfer on the rear surface of the PV module. Understanding the properties of the VG material is essential for evaluating its effectiveness in improving cooling efficiency.

**Numerical Simulation:** The material properties listed in Table I are likely used as input parameters in the numerical simulations conducted using software like ANSYS Fluent. These properties help model the heat transfer and fluid dynamics within the system accurately.

In summary, Table 3 serves as a reference for the material properties of the PV module and VG, providing essential data for the numerical simulations and analysis carried out in the study on passive cooling of rooftop PV systems. From Fig 4 we can assume that the optimal value for W/Px is around 0.6. For a VG design with high H/G (the right side of the plot), a high W/Px would lead to high “blockage” and thus “suffocate” the free convection channel flow (corresponding to the top right corner Fig. 4). On the other hand, a narrow VG with a less-than-ideal W/Px would result in insufficient mixing in the channel.

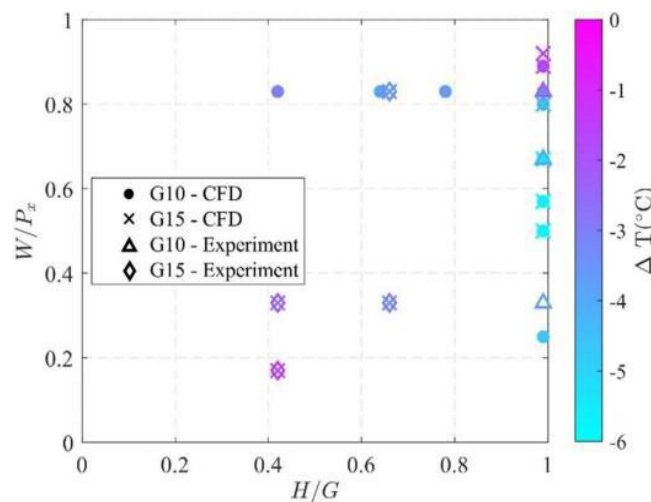


Fig. 4. 2-D plot showing the combined effect of ratios H/G and W/Px on  $\Delta T$ , the cooling ability of each VG design (from literature referred)

A W/Px of around 0.6 allows an adequate level of flow mixing while maintaining a high flow rate in the roof-module channel, consequently, a high cooling potential. The figure suggests that an optimal VG design should balance the H/G and W/Px ratios to maximize cooling performance without impeding flow circulation. In summary, Figure 4 provides valuable insights into the relationship between the H/G and W/Px ratios and the cooling ability of VG designs, guiding the optimization of VG configurations for enhanced passive cooling of rooftop photovoltaic systems.

### **Design Of Smart Concentric System**

#### **A. Data Collection And Analysis Of Site**

The data of the site where the PV system is going to place should be collected by various means. The geographical data can be collected through internet and also through physical means. The data should contain availability of the sunlight, weather condition during various seasons, environmental conditions such as atmospheric humidity, temperature and moisture contents of the air etc. By physical means analyze the availability of the sunlight and intensity of the sunlight through out the day. By this data we can obtain the duration for concentrating the light on PV for an optimum period.

#### **B. Design Of The Frame**

We need to design a frame to carry the lens used for concentrating the light on PV module. It should be designed in a manner of easily controllable i.e. can be moved smoothly using a stepper or servo motor. The frame should be designed in a manner to reduce the load on the motor as much as possible. It should also bring the lens to the position of concentration with least movement so that we can achieve the desired output.

#### **C. Load Calculation**

The load on the motor should be calculated using simulation software and also calculate the power consumption by the system using a simulation software and also through practical working and data collection.

### **System Components:**

#### **A. Fresnel Lens**

Fresnel lenses are flat on one side, with the other side made up of a number of concentric grooves acting as individual prisms, bending parallel light rays to a common focal length. There are various types of Fresnel lens, each suited to different types of application. For concentric PV (CPV) application, large, hardwearing acrylic Fresnel lenses are designed so that the flat side faces the sun, and the grooved side faces the photovoltaic cell in order to focus the light. They take a large area of scattered sunlight and focus them on the cell, much like using a magnifying glass to focus the rays of the sun onto kindling to start a fire. The CPV is made up of many solar cells each of it has its own Fresnel lens.

#### **B. Stepper Motor/ Servo Motor**

A servo motor is a rotary or linear actuator that allows for precise control of angular or linear position, velocity, and acceleration in a mechanical system. It constitutes part of a servomechanism, and consists of a suitable motor coupled to a sensor for position feedback. It also requires a relatively sophisticated controller, often dedicated module designed specifically for use with servomotors. It is not a specific class of motor, although the term servomotor is often used to refer to a motor suitable for use in a closed-loop control system. Servomotors are used in applications such as robotics.

### **C.Bh 1750 Ambient Light Sensors**

BH1750 ambient light sensors are electronic components designed to measure the intensity of ambient light in their surroundings. These sensors utilize a photodetector to convert light energy into electrical signals, which are then processed to provide accurate light level readings. BH1750 sensors are commonly used in applications such as automatic lighting control, backlight adjustment for displays, and energy-saving systems. They offer high sensitivity and accuracy across a wide range of light levels, making them suitable for various indoor and outdoor lighting environments. BH1750 ambient light sensors contribute to energy efficiency and improved user experience in electronic devices and smart systems.

### **D.Metal Plates**

Metal plates are flat, thin pieces of metal typically manufactured through processes such as rolling, forging, or machining. They are commonly made from materials like steel, aluminum, copper, and various alloys. Metal plates find extensive use in construction, manufacturing, automotive, aerospace, and other industries due to their strength, durability, and versatility. They serve various purposes including structural support, reinforcement, heat dissipation, and electrical conductivity.

Metal plates come in different sizes, thicknesses, and finishes to suit specific applications, and they can be further processed through cutting, bending, welding, or surface treatment to meet particular requirements.

### **E.EVA Material**

EVA (Ethylene-Vinyl Acetate) is a versatile copolymer widely used in various industries. It offers flexibility, softness, and lightweight properties, making it ideal for applications such as footwear, padding materials, and sports equipment. EVA provides excellent shock absorption, durability against environmental factors, and moldability for diverse shapes and sizes. It also offers insulation against temperature and sound, along with the ability to be easily colored, enabling vibrant designs in finished products.

### **F.Solar Panel**

PV module is a pack of photovoltaic cell which is arranged in an orderly manner. As we know the PV cell absorbs the sunlight and converts it to electricity. In this project the PV module is the main test subject our objective of the project is to improve the efficiency of the module and also increase the life span of the module. For that here we use a 60-cell PV module with a size of  $1 \times 1.65$  m (poly crystalline type). The maximum output power is 270 w at an optimum voltage of 31V, the optimum operating current is 9A. It weights around 19kg, the front cover is made up of tempered glass with anti reflective coating and the frame is of anodized aluminum alloy. The operating temperature ranges from -45 degree Celsius to +85 degree Celsius. Its maximum system voltage is around 1000V and maximum series fuse rating is 15A, the maximum front and back load are of about 5400Pa and 2400Pa

### **G.Lithium- Ion Battery**

A lithium-ion or Li-ion battery is a type of rechargeable battery that uses the reversible intercalation of Li<sup>+</sup> ions into electronically conducting solids to store energy. In comparison with other commercial rechargeable batteries, Li-ion batteries are characterized by higher specific energy, higher energy density, higher energy efficiency, a longer cycle life, and a longer calendar life. Generally, the negative electrode of a conventional lithium-ion cell is graphite made from carbon. The positive electrode is typically a metal oxide or phosphate. The electrolyte is a lithium salt in an organic solvent. The negative electrode (which is the anode when the cell is discharging) and the positive electrode (which is the cathode

when discharging) are prevented from shorting by a separator. The electrodes are separated from external electronics with a piece of metal called a current collector.

### **H.Weather Proof Cable**

Weatherproof cables are specially designed cables that are resistant to environmental elements such as moisture, extreme temperatures, UV radiation, and mechanical stress. These cables are commonly used in outdoor applications where they may be exposed to harsh weather conditions including outdoor lighting, security cameras, and outdoor electrical wiring. Weatherproof cables are typically insulated and jacketed with materials such as PVC (polyvinyl chloride) or polyethylene, providing protection against water ingress and physical damage. They ensure reliable performance and durability in challenging outdoor environments, making them essential for outdoor electrical and communication systems.

### **I.Screws, Nuts Bolts**

Screws, nuts, and bolts are essential fasteners used in construction, manufacturing, and various other applications. They are threaded mechanical devices designed to join two or more components together securely. Screws feature a threaded shaft with a pointed end, while nuts are internally threaded and designed to mate with screws. Bolts are similar to screws but typically have a head on one end and a threaded shaft on the other, requiring a nut for assembly. Together, they provide a reliable means of fastening materials, allowing for easy disassembly and reassembly when necessary. Screws, nuts, and bolts come in various sizes, shapes, and materials to suit different applications and requirements.

### **J.Pulley Wheel**

Pulley wheels are circular mechanical devices with a grooved rim designed to support and guide a rope, belt, or cable. They are commonly used in systems to transmit motion and lift loads by redirecting the direction of force. Pulleys can be fixed, movable, or compound, depending on their configuration and application. They are essential components in various machines and systems such as cranes, elevators, and conveyor belts, enabling efficient transfer of force and motion. Pulley wheels come in different sizes and materials to accommodate specific load requirements and environmental conditions.

### **K.Microcontroller Unit**

A microcontroller unit (MCU) is a compact integrated circuit that contains a processor core, memory, and input/output peripherals. It is designed to execute specific tasks within electronic devices, such as controlling sensors, motors, and other hardware components. MCUs are widely used in embedded systems, consumer electronics, automotive systems, and industrial automation due to their small size, low power consumption, and cost-effectiveness. They are programmed to perform predetermined functions and can be reprogrammed to adapt to changing requirements. MCUs play a crucial role in the operation of a wide range of electronic devices and systems, providing computational capabilities in a compact and efficient package.

### **L.Electronic Components**

Electronic components are fundamental units used in electronic circuits to manipulate electric signals or flow of electrons. They include resistors, capacitors, inductors, diodes, transistors, and integrated circuits, among others. Each component serves a specific purpose, such as regulating voltage, storing charge, amplifying signals, or switching currents. These components are assembled together to create circuits that perform various functions, from simple tasks like turning on a light to complex operations in computers and communication systems. Electronic components are essential building blocks of modern technology, enabling the creation of a wide range of electronic devices and systems.

**Conclusion:**

The utilization of vortex generators in conjunction with a smart concentric system for passive cooling of rooftop photovoltaic (PV) systems under free convection offers a promising avenue for enhancing energy generation efficiency and prolonging the lifespan of PV installations. Through experimental and computational analyses, it has been demonstrated that the integration of vortex generators can effectively mitigate the thermal stresses experienced by rooftop PV panels by promoting airflow and heat dissipation. The vortex generators induce vortices that disrupt the boundary layer, thus enhancing convective heat transfer and reducing the temperature differentials across the PV surface. Moreover, the incorporation of a smart concentric system further optimizes the cooling process by dynamically adjusting airflow rates based on environmental conditions and system requirements. This intelligent control mechanism ensures efficient operation while minimizing energy consumption and maximizing the overall performance of the PV system. In conclusion, the combination of vortex generators and a smart concentric system presents a viable and cost-effective solution for passive cooling of rooftop PV systems, offering benefits such as improved energy output, increased durability, and reduced maintenance costs. As renewable energy technologies continue to evolve, integrating innovative cooling strategies like this will play a crucial role in maximizing the efficiency and sustainability of solar power generation.

**References:**

1. B. Kafle et al., "TOPCon—Technology options for cost efficient industrial manufacturing," *Sol. Energy Mater. Sol. Cells*, vol. 227, 2021, Art. no. 111100.
2. J. Haschke, O. Dupre', M. Boccard, and C. Ballif, "Silicon heterojunction solar cells: Recent technological development and practical aspects-from lab to industry," *Sol. Energy Mater. Sol. Cells*, vol. 187, pp. 140–153, 2018.
3. O. Dupre', R. Vaillon, and M. A. Green, "Thermal behavior of photo-voltaic devices," *Phys. Eng.*, vol. 10, pp. 973–978, 2017.
4. M. Hasanuzzaman, A. Malek, M. M. Islam, A. K. Pandey, and N. A. Rahim, "Global advancement of cooling technologies for PV systems: A review," *Sol. Energy*, vol. 137, pp. 25–45, 2016.
5. J. Siecker, K. Kusakana, and B. P. Numbi, "A review of solar photo-voltaic systems cooling technologies," *Renewable Sustain. Energy Rev.*, vol. 79, pp. 192–203, 2017.
6. Z. Zhou, Y. Jiang, N. Ekins-Daukes, M. Keevers, and M. A. Green, "Optical and thermal emission benefits of differently textured glass for photovoltaic modules," *IEEE J. Photovolt.*, vol. 11, no. 1, pp. 131–137, Jan. 2021.
7. "COOLBACK," 2020, Accessed: Jun. 22, 2021. [Online]. Available: <https://www.coolback.com/>
8. T. M. Walsh, Z. Xiong, Y. S. Khoo, A. A. O. Tay, and A. G. Aberle, "Singapore modules-optimised PV modules for the tropics," *Energy Procedia*, vol. 15, pp. 388–395, 2012.
9. Z. Zhou et al., "Passive PV module cooling under free convection through vortex generators," *Renewable Energy*, vol. 190, pp. 319–329, 2022.
10. P. Bahl, C. M. de Silva, A. A. Chughtai, C. R. MacIntyre, and C. Doolan, "An experimental framework to capture the flow dynamics of droplets expelled by a sneeze," *Exp. Fluids*, vol. 61, no. 8, pp. 1–9, 2020.
11. L. Garelli, G. R. Rodriguez, J. J. Dorella, and M. A. Storti, "Heat transfer enhancement in panel type radiators using delta-wing vortex generators," *Int. J. Thermal Sci.*, vol. 137, pp. 64–74, 2019.
12. S. A. G. Nassab, Y. Sheikhejad, and M. F. Nia, "Novel design of natural solar air heat for higher thermal performance utilizing porous vortex generator," *Thermal Sci. Eng. Prog.*, vol. 33, 2022, Art. no. 101385.

# An Adaptive Control System In Plug-In-EV

Adil N <sup>1</sup>, Cyril Shaji John<sup>2</sup>, Edwin Biju Mathai <sup>3</sup>, Pranav P Pillai <sup>4</sup>,  
Juna John Daniel<sup>5</sup>, Dr Vinod V.P <sup>6</sup>

<sup>1,2,3,4</sup> UG student, Dept. of EEE, Sree Buddha College of Engineering, Pattoor,

<sup>5</sup> Assistant Professor, Dept. of EEE, Sree Buddha College of Engineering, Pattoor

<sup>6</sup> Professor, Dept. of EEE, Sree Buddha College of Engineering, Pattoor

**Abstract:** *The energy management technique in plug-in electric vehicles (PEVs) is done by sliding mode control (SMC). SMC is applied to adjust the motor's torque while ensuring the motor speed remains constant. This strategy is crucial for enhancing the vehicle's battery life by improving energy utilization and efficiency. The SMC allows for more accurate control over the motor's torque, significantly benefiting the vehicle's energy management system. The goal of PEV energy management systems is to get the most mileage out of a single battery charge for the car. In order to maximize Plug-in Electric Vehicle performance, efficiency, and driving range while maintaining dependable and safe operation, energy management is essential.*

**Keywords:** *Plug-in electric vehicles, SMC Controller.*

## Introduction:

During past decades' electric vehicles (EVs) have been gradually gaining popularity in the vehicle industry due to the various benefits they offer compared to their conventional counterparts. The vast majority of the vehicle manufacturers and many research organizations recommend the replacement of the conventional internal combustion engine (ICE) vehicles with EVs. Pure EVs that run solely on electricity eliminate the fossil fuel usage and consequently reduce the associated gas emissions. Additionally, their operation at low noise levels can highly reduce noise pollution, that adversely affect the life in urban areas. Therefore, it is evident that as the number of EVs entering the circulation increases, the overall transportation environmental footprint will be mitigated. The main environmental concern related to the difficulties in recycling the EV batteries seems to be overcome lately; there exist industries capable of fully recycling Lithium-ion (Li-ion) batteries, the type of batteries that the recent EVs make use [1]. Plug-in Electric Vehicles (PEVs) have emerged as a promising solution for sustainable transportation. Central to the operation of these vehicles is the concept of energy management, which refers to the process of maximizing the amount of electrical energy stored in the vehicle's battery to power different components. This energy, stored in the form of electricity, is the driving force that propels the vehicle, powers the onboard systems, and ensures the vehicle's performance.

The management of this stored energy is crucial to the effective operation of the PEV. This is where energy management systems come into play. Energy management systems are developed to a high degree of complexity technologies that monitor and regulate the charging process of the battery. They keep a constant eye on the battery's state of charge (SOC), which is a measure of the current energy level in the battery as a percentage of its capacity. By regulating the SOC, the energy management system ensures that the battery is neither overcharged nor undercharged. One of the key functions of the energy management system is to control the charging speed. This involves adjusting the rate at which electricity is fed into the battery during charging, to ensure that the battery is charged as efficiently and safely as possible. Too fast, and the battery could overheat or degrade; too slow, and the charging process becomes impractically long. Another important function of the energy management system is cell balancing. A battery pack is made up of multiple individual cells, each of which needs to be kept at a similar state of charge to the others to ensure optimal performance and longevity. The energy management system also protects the battery from deep discharging or overcharging. Deep discharging can cause the battery to deplete its charge to a level that could damage its internal components, while overcharging can lead to overheating and potential safety risks. It involves a range of technologies and processes, all working together to ensure that the vehicle's

stored electrical energy is used as efficiently and safely as possible. As the technology continues to evolve, so too will the sophistication and effectiveness of these energy management systems, paving the way for a future of sustainable, electric-powered transportation

### Methodology:

The Battery serves as the primary power source for the electric vehicle (EV). It stores electrical energy in chemical form and supplies it to the rest of the EV system as needed, and convert one level of DC Current to Another level of DC Current. The DC/DC converter is responsible for converting the high-voltage DC power from the battery into a lower voltage that is suitable for the rest of the EV's electrical systems. It ensures efficient power transfer and voltage regulation. The VSI is an essential component in the EV's powertrain. It converts the DC power from the battery into three-phase AC power required to drive the Permanent Magnet Synchronous Motor (PMSM) efficiently. The PMSM motor is the main propulsion system of the EV. It receives the three-phase AC power from the VSI and converts it into mechanical energy to drive the vehicle's wheels. PMSM motors are known for their high efficiency and torque density. The SMC is a sophisticated control algorithm used to regulate the operation of the PMSM motor. It continuously monitors the motor's performance and adjusts its parameters to ensure optimal operation. By dynamically adjusting the motor's torque and speed, the SMC helps improve efficiency and performance while ensuring stability. The SMC is depicted as a closed-loop system connected to the VSI, indicating that it receives feedback from the motor and adjusts the output (Torque) of the VSI accordingly. This closed-loop control allows the SMC to continuously optimize the motor's operation based on real-time feedback, ensuring precise control and efficient energy management.

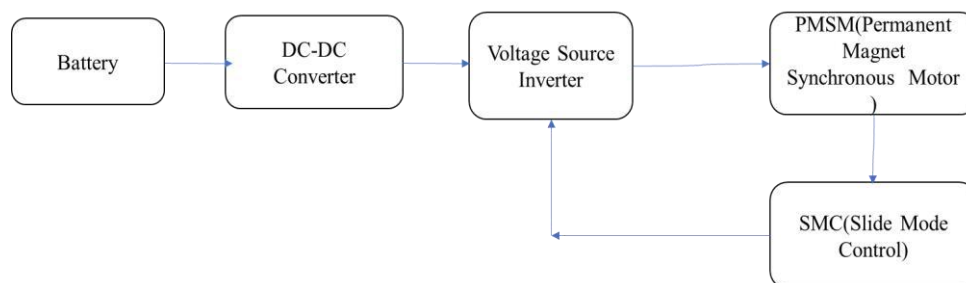


Fig1. Block Diagram

The energy management system focuses on optimizing the operation of plug-in electric vehicles (PEVs) by adjusting motor torque while maintaining a constant motor speed, set at a specific RPM. This technique is designed to enhance energy efficiency and extend the operational range of the vehicle's battery. It operates by continuously monitoring the vehicle's energy demand and dynamically adjusting the torque produced by the motor to match this demand without altering the motor speed. This ensures that the vehicle can efficiently respond to varying energy requirements while avoiding excessive or wasteful energy consumption. The increased battery range, achieved through this method, allows the vehicle to operate effectively over a broader spectrum of conditions. Overall, this strategy aims to maximize energy utilization within the system, promoting a balance between performance and energy



conservation by tailoring motor output to the precise needs of the vehicle at any given time. The combination of SMC and load angle control could be considered in a broader control strategy that involves both torque and flux control, especially in applications where precise control under varying load conditions is essential.

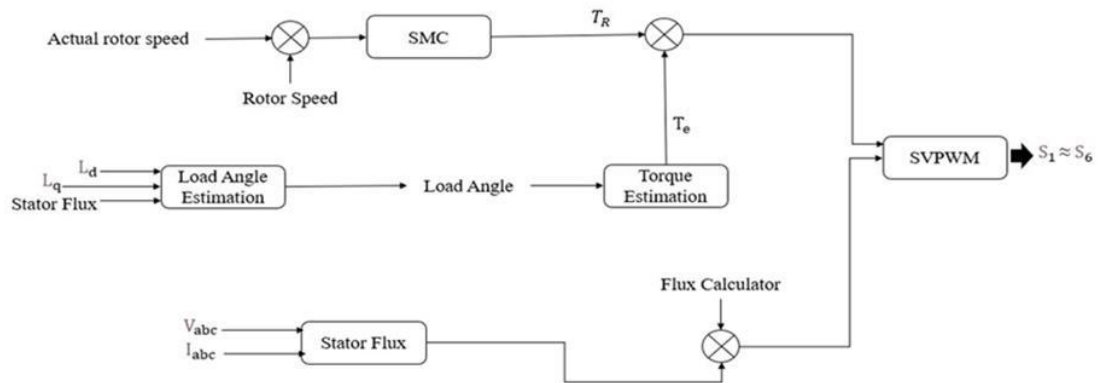


Fig 2: Control System Methodology

The load angle represents the relative position between the stator magnetic flux and the rotor position. The load angle plays a pivotal role in determining the switching sequence and duration of voltage space vectors. The integrates SMC cascade and controllers to optimize the performance and stability of the PEV system, with a specific emphasis on the unique characteristics and benefits of the sliding mode controller and Load angle control contributes to precise timing of switching events, influencing the torque production. DTC, known for its swift and direct torque and flux control, is implemented for efficient motor control without a separate current control loop. Maintaining the motor's rated speed as constant, the system adapts torque based on Load Angle and DTC. This dynamic and adaptive control strategy ensures stability and efficiency, contributing to optimal performance in the PEV system. The combined approach of SMC cascade, Load Angle, and DTC controllers provides a comprehensive solution for enhanced system control and stability, ultimately advancing sustainable and efficient electric transportation.

The combination of renewable energy sources (RES) and electric vehicles (EVs) with the power grid marks a significant move toward sustainable energy practices. This integration supports the use of clean energy and enables complex interactions within the energy system, promoting a shift to a greener and more efficient infrastructure. It involves advanced mechanisms to handle the two-way power flow and interactions within the grid, enhancing stability and reducing energy wastage. This setup not only addresses environmental concerns but also adapts to practical limitations like battery wear and user needs, ensuring the solution is economically and socially sustainable. Adjusting motor torque to maintain constant RPM optimizes energy use and increases battery range, demonstrating the critical role of adaptive control in maximizing efficiency and supporting sustainable energy transition

### Result:

At initially the motor is began to rotate in Constant speed by varying torque by SMC Controller. From 0-2 sec the motor will operate and rotate in 1500 RPM and settle downs to settled rpm. At that time the torque will have some fluctuations of +/- 50 and it began to stable in a linear way by SMC Controller.

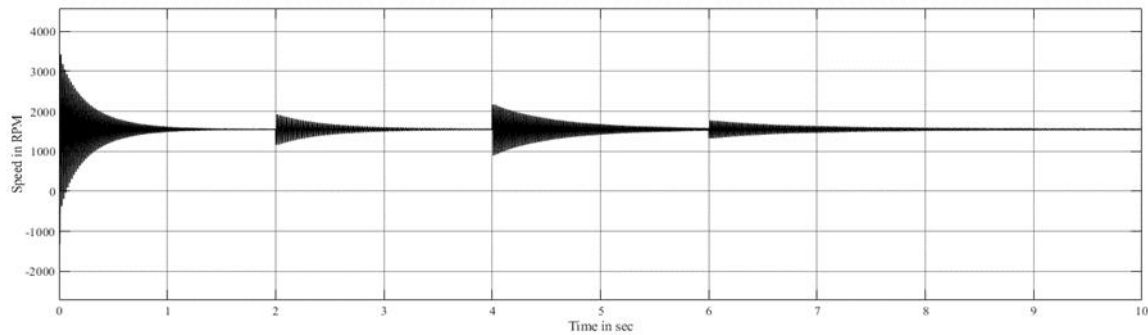


Fig. 3. Speed changes with respect to time

At time 2-4 we decelerate the vehicle and torque will increase to 50 Nm i.e.; torque is inversely proportional to speed.

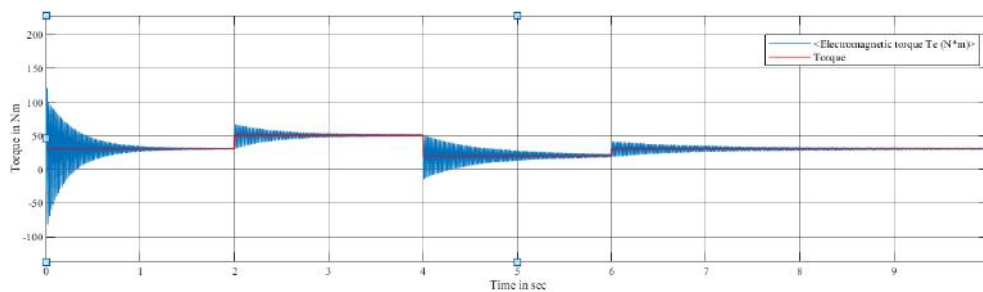


Fig. 4. Torque changes with respect to time

At that time the SMC will control the system parameters and stabilises the motor rpm. When the vehicle speed is increased then the torque will reduce then the SMC will control the motor parameters and settles the motor rpm in linear way without any changes.

### Conclusion:

The combination of renewable energy sources (RES) and electric vehicles (EVs) with the power grid marks a significant move toward sustainable energy practices. This integration supports the use of clean energy and enables complex interactions within the energy system, promoting a shift to a greener and more efficient infrastructure. It involves advanced mechanisms to handle the two-way power flow and interactions within the grid, enhancing stability and reducing energy wastage. This setup not only addresses environmental concerns but also adapts to practical limitations like battery wear and user needs, ensuring the solution is economically and socially sustainable. Adjusting motor torque to maintain constant RPM optimizes energy use and increases battery range, demonstrating the critical role of adaptive control in maximizing efficiency and supporting sustainable energy transitions.

### References:

1. Jemma J., Makrygiorgou Antonio & T. Alexandridis “Unified Modeling, Control and Stability for a Vehicle to grid and Plug-in EV System” IEEE Journal of Emerging and Selected Topics in Power Electronics, Department of Electrical and Computer Engineering, University of Patras, Rion, Greece.
2. V. Nirmal Kannan M. RamachandranA. Mariya Chithra Mary G.Prabhakar, “Microgrid Energy Optimization and Realization by Means of Plug-in Electric Vehicles in both V2G - G2V

- Environment” IEEE, 2023 8th International Conference on Communication and Electronics Systems (ICCES).
3. Kumari Suman; Abraham T. Mathew “Speed Control of Permanent Magnet Synchronous Motor Drive System Using PI, PID, SMC and SMC plus PID Controller” IEEE Conference, 2018 International Conference on Advances in Computing, Communications and Informatics (ICACCI).
  4. Jajna Prasad Sahoo, S. Sivasubramani “A Charging Coordination Strategy for Seamless Integration of Plug-In Electric Vehicles into a Distribution Network” IEEE Conferences 2023 IEEE IAS Global Conference on Renewable Energy and Hydrogen Technologies (GlobConHT), Dept. of Electrical Engineering, Indian Institute of Technology Patna, Patna, India Alan, M. (2013). Leadership Styles.
  5. S. Sakunthala, Dr. P. Nagaraju Mandadi, Dr. R. Kiranmayi “A Study on Industrial Motor Drives Comparison and Applications of PMSM and BLDC Motor Drives” 2017 IEEE Conference, International Conference on Energy, Communication, Data Analytics and Soft Computing (ICECDS-2017) Armstrong, M. (2003). A Handbook of Human Resource Management Practice. London: Kogan Page.
  6. Jajna Prasad Sahoo Divya Rashmi S. Sivasubraman “Intelligent Coordinated Charging of Plug in Electric Vehicles for G2V and V2G Transactions” IEEE Conferences, 2022 IEEE IAS Global Conference on Emerging Technologies (GlobConET) Department of Electrical Engineering, Indian Institute of Technology, Patna.
  7. Subhasish Deb; Arup Kumar Goswami; Rahul Lamichane Chetri; Rajesh Roy "Impact of Plug-in Electric Vehicle Integration in Distribution System Congestion Management" 2021 IEEE Conference Paper 2020 3rd International Conference on Energy Babatunde, O., & Emem, I. (2015). The Impact of Leadership Style on Employee’s Performance in an Organization, Journal of International Knowledge sharing Platform 5(1), 2224-5731.

# Smart Garbage Segregation Bins Powered by Solar Energy with SMS Notifications and Machine Learning Image Processing

Annmary C.A<sup>1</sup>, Sona Elsa Abraham<sup>2</sup>, Nivetha<sup>3</sup>, Vinayak T.S<sup>4</sup>, Dr. Leena T Timothy<sup>5</sup>  
<sup>1,2,3,4</sup> UG Student, EEE, Albertian Institute of Science & Technology, Kalamassery India  
<sup>5</sup> Associate Professor, EEE, Albertian Institute of Science & Technology, Kalamassery India,

**Abstract:** *Our project focuses on creating a smart waste bin that sorts solid waste into separate compartments to enhance user engagement in waste management. The smart bin is designed to alert staff when it requires emptying and is powered by renewable solar energy. The study employed an Agile Development methodology consisting of six main stages: planning, design, development, testing, release, and feedback. Quality assessment based on ISO/IEC 25010 standards resulted in an impressive average rating of 4.55. The innovative smart bin streamlines waste disposal processes, prevents overflow through SMS notifications, and functions autonomously using solar power. Suggestions for further improvement include incorporating a compressor and algorithm for more efficient waste management, as well as implementing a solar tracker to boost energy generation. Integration of this technology is expected to enhance waste management efficiency, particularly in institutions grappling with escalating waste disposal issues due to population growth.*

**Keywords:** *Waste management, Waste segregation, IoT, AI, Sustainable energy*

## Introduction:

Solid waste management is a pressing global issue, with billions of metric tons of waste generated annually and inadequate management practices contributing to environmental threats. Waste segregation is crucial for addressing this challenge, yet effective implementation remains a significant hurdle, particularly in developing countries like the Philippines. Inefficient waste management practices lead to overflowing bins, attracting pests and creating unsanitary conditions. To address these environmental concerns, our project focuses on developing a smart waste segregator system powered by solar energy. This innovative system will use real-time object recognition to sort garbage into biodegradable, non-biodegradable, and recyclable categories. It will also feature alerts for users when bins are full and interactive disposal methods to promote efficient and sustainable waste management practices. By leveraging technology and renewable energy sources, this smart waste segregator system aims to enhance waste management efficiency and promote environmental awareness among academic institutions and beyond. Through collaborative efforts and innovative solutions, we can work towards a cleaner and more sustainable future for our planet.

## Problem Statement:

Traditional waste management systems often face challenges in efficiently segregating and managing waste, leading to environmental pollution and health hazards. Manual segregation of waste is time-consuming and often prone to errors. Additionally, the lack of real-time monitoring and tracking mechanisms hinders effective waste management practices. To address these challenges, the proposed project aims to develop smart garbage segregation bins equipped with sensors for waste detection and sorting, powered by solar energy to ensure sustainable operation. The bins will be integrated with machine learning image processing technology to automate the segregation process based on the type of waste detected. Furthermore, the system will send SMS notifications to waste management authorities and users

to facilitate timely collection and disposal of segregated waste. By implementing this innovative solution, we aim to enhance waste management efficiency, promote sustainable practices, and reduce environmental pollution

### Methodology:

The Agile Development methodology, as depicted in Figure 1, to steer the hardware and software development of the device. This approach enabled efficient work management and guaranteed the production of a top-notch product while adhering to budget limitations. The methodology comprised six essential phases: requirements analysis, planning, design, coding, unit testing, and client acceptance..



Fig1. Agile Methodology

### Planning Phase:

In the Planning Phase, a comprehensive Gantt chart was meticulously crafted to delineate the sequential flow of activities throughout the project's development. This phase kicked off with a meticulous information-gathering process, a pivotal step aimed at unequivocally defining the project's objectives and anticipated benefits. It culminated in the submission of the final hardbound manuscript. Prior to the formal initiation of proposal work, the project's prerequisites were succinctly outlined in the preliminary materials prepared by the proponents. This phase entailed a meticulous review and analysis of these requirements, encompassing the core variables of the study, facilitated through in-depth discussions to garner a diverse array of ideas and concepts pertaining to the project's workflow.

### Design Phase:

During the Design Phase, the development of the GULP smart bin involved the utilization of two distinct approaches: visual design and architectural structure. The project leader spearheaded an iterative process wherein the team extensively deliberated on the requirements set forth in the preceding phase. Through collaborative discussions, they strategized on how best to fulfil these objectives and suggested tools that could facilitate the attainment of optimal results. Key tools such as System Design Architecture, Block Diagram, and Use Case Diagram were instrumental in guiding the developers towards conceptualizing and implementing the project's architectural framework. Furthermore, a preliminary prototype of the user interface was crafted by the project designer to provide a tangible representation of the envisioned end-user experience.

The Block Diagram in Figure 2 showcases the integration of a solar panel as the primary power source for the Smart Bin system. The operational flow begins with depositing garbage into the temporary storage box, where a Pi camera, under the control of Raspberry Pi 4, performs garbage classification. Each garbage receptacle is color-coded (green for biodegradable, red for non-biodegradable, and yellow for recyclable) for efficient segregation and features corresponding light indicators. Stepper and servo motors

are employed to transport garbage to the designated bins, while a Dot Matrix LED module displays an emoticon post-disposal. Ultrasonic sensors within each bin assess bin status, with the data relayed back to the Raspberry Pi for initiating SMS alerts to school maintenance staff for timely garbage clearance.

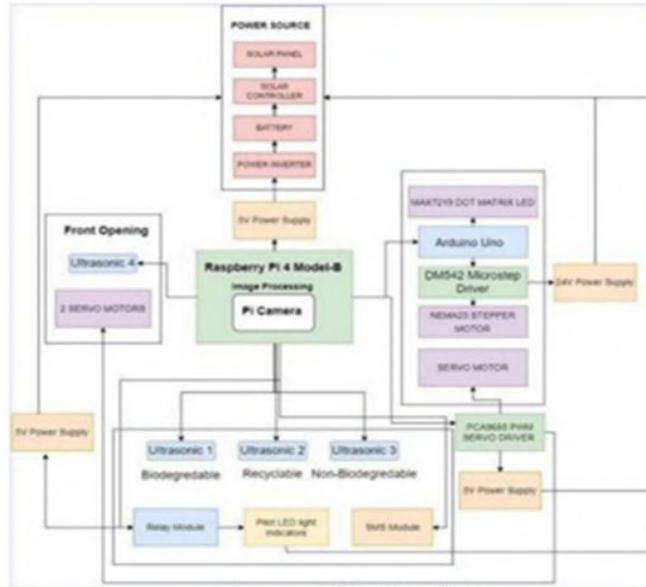


Fig2; GULP Block Diagram

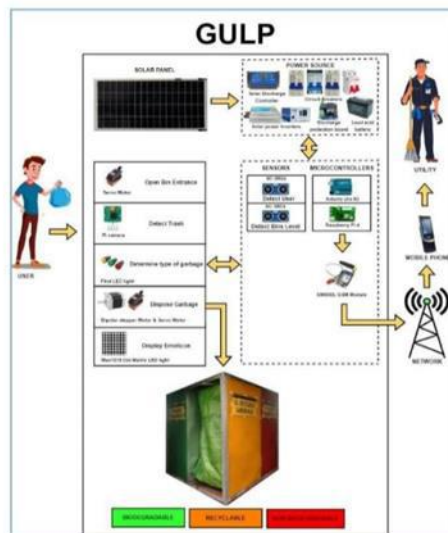


Fig3.GULP Systems architecture

The evaluation and feedback from end-users, as shown in Figure 6, highlighted their appreciation for the system's features, such as its garbage classification mechanism, notification In Figure 3, the system architecture is organized to showcase the main components required for application implementation and operational processes. The physical machine integrates various hardware components for specific functions, which are divided into Front End (user interface) and Back End (operational components

inaccessible to regular users). When garbage is brought near the device, the bin lid automatically opens. We presented the system to the organization for approval through a combination of a PowerPoint presentation for an overview and a live system demonstration for a more in-depth understanding. Before the training and briefing session, an appointment schedule was set up for the presentation and demonstration, which included training and briefing on the application. During the presentation, we conducted training and briefing to familiarize the users with the system for utility staff, and the display of emoticons. The utility staff were impressed by how the system made garbage disposal interactive and engaging for users.

In this phase we implemented the designed prototype by utilizing a combination of Thonny Python IDE and Arduino IDE, along with programming languages such as Python and Arduino. Various hardware components were employed in the coding and development process, including the Raspberry Pi 4 Model B Starter Kit, Raspberry Pi 3 Model B+ Camera Module, Ultrasonic Sensor Distance Measuring Module HC-SR04, SIM800L V2 5V Wireless GSM GPRS Module, Tower Pro Digital Robot Servo Motor (180 Rotation) – MG996R, Solar Panel Monocrystalline 200 Watt with MC4 Photovoltaic Connector, 30A PWM 12V Solar Panel Regulator Charge Controller Solar Battery Charger LCD Display USB (COD), 105D31L Battery, 12V DC to 220-230V AC Car Home Solar Power Inverter with Buzzer, Stepper Motor Nema 23 Wantai, MAX7219 Dot Matrix Module, 4 Channel 5V Relay Module with Optocoupler, Fiber Switch Adaptor 5V 2A Heavy Duty, and XH-M609 DC 12V 24V Voltage Charge Discharge Protection Board. Furthermore, the UNO R3 Development Board ATmega328P CH340G was specifically utilized to control the stepper driver/motor and MAX7219 Dot Matrix Module within the system architecture.

Table 1 Types of garbage tested using GULP

Table 1. Types of Garbage Tested using GULP	
Garbage	Garbage Identification Result
Cardboard	Biodegradable
Yellow Paper	Biodegradable
Paper Meal Box	Biodegradable
Paper Bag	Biodegradable
Office Paper	Biodegradable
Newspaper	Biodegradable
Burger Paper Wrapper	Biodegradable
Milk tea Cup	Non-biodegradable
Instant Noodles Plastic Wrapper	Non-biodegradable
Cheese Snack Plastic Wrapper	Non-biodegradable
Ice Water Plastic Wrapper	Non-biodegradable
Juice Plastic Wrapper	Non-biodegradable
Coffee Stick Plastic Wrapper	Non-biodegradable
Chocolate Powder Plastic Wrapper	Non-biodegradable
Disposable Cups	Non-biodegradable
Candy Plastic Wrapper	Non-biodegradable
Corn Snack Plastic Wrapper	Non-biodegradable
Chocolate Bar Plastic Wrapper	Non-biodegradable
Biscuit Plastic Wrapper	Non-biodegradable
Black Plastic Trash Bag	Non-biodegradable
Instant Noodles Seasoning Plastic	Non-biodegradable
Juice Plastic Bottle	Recyclable
Water Plastic Bottle	Recyclable
Canned Goods Can	Recyclable

### Test:

During the testing phase, we conducted iterative development to ensure the functionality of the product, checking for errors until none were found. A subset of waste samples was tested, as shown in Table 1, to validate accurate sorting of various waste types. The training dataset, depicted in Figure 4, was utilized by researchers via Lobe.ai machine-learning image classification with the Resnet50-V2 model. A total of 1151 garbage images were employed, achieving a 98% accuracy rate in predictions. Image processing was carried out using the Python programming language. The application's adherence to ISO/IEC 25010 Standards was evaluated by twenty-two regular users, seven utility personnel, and the Head of Health and Sanitation, totaling thirty individuals. To quantitatively analyze the results, researchers utilized a Likert scale, a common tool for measuring changes in behavior, attitudes, knowledge, beliefs, and values. The



Likert scale, presented in Table 2, provided respondents with a range of statements to evaluate their average assessment of ISO/IEC 25010 compliance.

Table1 Likert Scale

Table 2. Likert Scale

Scale	Parameters	Verbal Interpretation
5	4.20 - 5.00	Excellent (E)
4	3.40 - 4.19	Very Good (VG)
3	2.60 - 3.39	Good (G)
2	1.80 - 2.59	Fair (F)
1	1.00 - 1.79	Poor (P)

Table 3 ISO/IEC 25010 Evaluation Results

Table 3. ISO/IEC 25010 Evaluation Result

Characteristic	Mean	Verbal Interpretation
Functionality/ Suitability	4.41	Excellent (E)
Performance Efficiency	4.61	Excellent (E)
Compatibility	4.53	Excellent (E)
Usability	4.65	Excellent (E)
Reliability	4.52	Excellent (E)
Security	4.50	Excellent (E)
Maintainability	4.58	Excellent (E)
Portability	4.57	Excellent (E)
<b>Overall Weighted Mean</b>	<b>4.55</b>	<b>Excellent (E)</b>

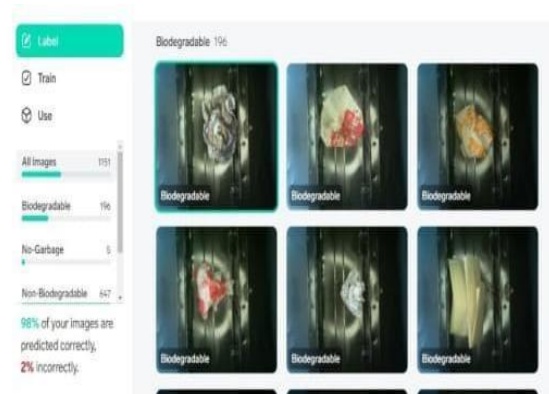


Fig .4. Garbage Data Set Training

We successfully presented the system to the organization for approval by combining a PowerPoint presentation with a live demonstration. The PowerPoint offered a concise overview, while the live demo provided hands-on experience. To ensure broad participation, the researchers scheduled a session with all key stakeholders present. The training focused on familiarizing participants with the application and its features. Figure 5 shows the valuable feedback from end-users, indicating their high satisfaction with the

system's functionality, especially its ability to identify garbage types, alert staff when bins are full, and display emoticons. Utility staff were impressed by how the system enhanced user engagement in garbage disposal.

**Discussion:**

The study addressed gaps in the field by developing an intelligent waste management system that utilizes a Convolutional Neural Network (CNN) deep learning algorithm for effective garbage identification and sorting. By employing machine learning image classification with Lobe.ai's Resnet50-V2 model, the system significantly enhanced the accuracy of garbage categorization. The system's functionalities were implemented using Python for image processing, C++ for Arduino interface management, and SMS notifications for alerting staff about full bins. Favorable user feedback regarding the system's functionality and user-friendly interface confirms its successful implementation. The system optimizes waste disposal processes, starting from lid opening triggered by motion detection to recognizing and discarding garbage into designated bins equipped with LED indicators and emoticon displays. Users commended the engaging and pleasant experience offered by the system during waste disposal activities.

**Novelty of the Concept:**

Our project "Smart garbage segregation bins powered by solar energy with SMS notifications and machine learning image processing" offers several novel features and advancements in waste management technology includes;

1. **Integration of Solar Energy:** The use of solar energy to power the smart garbage segregation bins makes the system more sustainable and environmentally friendly. This reduces the reliance on traditional energy sources and contributes to the promotion of renewable energy solutions.
2. **Machine Learning Image Processing:** The incorporation of machine learning technology for image processing enables automated waste segregation based on the type of waste detected. This advanced feature enhances the efficiency and accuracy of waste sorting, minimizing human error and improving overall waste management processes.
3. **Real-time SMS Notifications:** The system's capability to send real-time SMS notifications to waste management authorities and users enhances communication and coordination for timely collection and disposal of segregated waste. This feature promotes proactive waste management practices and ensures efficient handling of waste.
4. **Smart Sensor Technology:** The smart garbage segregation bins are equipped with sensors for waste detection and sorting, allowing for automated segregation based on predefined criteria. This technology streamlines the waste segregation process, making it more efficient and effective compared to traditional manual methods.

Overall, the combination of solar energy utilization, machine learning image processing, real-time SMS notifications, and smart sensor technology in the smart garbage segregation bins represents a significant advancement in waste management technology, offering a comprehensive and innovative solution for sustainable waste management practices

**Conclusion:**

The GULP (Great User-oriented Litter Placer) system, a Solar-Powered Smart Garbage Segregation Bins with SMS Notification and Machine Learning Image Processing, was well-received by users at Northern Bukidnon State College. The system was highly rated by the ISO 25010 evaluation tool, highlighting its significance, accessibility, and convenience for waste disposal on campus. To further enhance the system, the inclusion of compressors and a solar tracker with solar panels is recommended.

Compressors can aid in maximizing trash compression, creating additional space for disposal and reducing the frequency of immediate waste collection. An algorithm capable of detecting multiple types of garbage simultaneously is also suggested for improved efficiency. Furthermore, integrating a solar tracker with solar panels can optimize renewable energy production for the smart bin by maximizing solar radiation intake throughout the day.

### References:

1. Abdel-Shafy, H. I., & Mansour, M. S. M. (2018). Solid waste issue: Sources, composition, disposal, recycling, and valorization. *Egyptian Journal of Petroleum*, 27(4), 1275–1290. <https://doi.org/10.1016/j.ejpe.2018.07.00>.
2. Castro, R. C. C., Magsakay, E. D. R., Geronimo, A. J. S., Conato, C., Denise Cruz, J., Alva ran, J. R., & Oblanca, V. J. (2020). Development of Waste Management System using the Concept of “Basura Advantage Points” through Artificial Neural Network. 2020 IEEE 12th International Conference on Humanoid, Nanotechnology, Information Technology, Communication and Control, Environment, and Management, HNICEM 2020, 3–7. <https://doi.org/10.1109/HNICEM51456.2020.9400123>.
3. Chaturvedi, V., Yadav, M., & Tiwari, N. (2021). Smart Waste Management System using Internet of Things and RFID Technology. *New Frontiers in Communication and Intelligent Systems*, 63– 68. <https://doi.org/10.52458/978-81-95502-00-4-8>
4. S.Sakunthala, Dr. P.Nagaraju Mandadi ,Dr. R.Kiranmayi “A Study on Industrial Motor Drives Comparison and Applications of PMSM and BLDC Motor Drives” 2017 IEEE Conference, International Conference on Energy, Communication, Data Analytics and Soft Computing (ICECDS-2017)Armstrong, M. (2003). *A Handbook of Human Resource Management Practice*. London: Kogan Page.
5. Fadel, F. (2017). The Design and Implementation of Smart Trash Bin. *Academic Journal of Nawroz University*, 6(3), 141–148. <https://doi.org/10.25007/ajnu.v6n3a103>.
6. Gangwani, M., Pandey, M., Punjabi, N., Sahu, S., & Khatwani, P. (2019).A Comprehensive Study on Waste Segregation Techniques. *International Journal of Engineering Research & Technology*, 8(4), 689–693. <https://recycle.epa.gov.tw/en/NAV06Content.ht>
7. Hondo, D., Arthur, L & Gamaralalage, P. J. D. (2020). Solid Waste Management in Developing Asia: Prioritizing Waste Separation. *ADB Policy Brief*, 7(2020), <https://www.adb.org/sites/default/files/publication/652121/adb-pb2020-7.pdf>
8. Kaza, S., Yao, L., Bhada-tata, P & Woerden, F. Van. (2018). What a waste 2.0. Kihila, J. M., Wernsted, K., & Kaseva, M. (2021). Waste segregation and potential for recycling -A case study in Dar es Salaam City, Tanzania. *Sustainable Environment*, . <https://doi.org/10.1080/27658511.2021.1935532>
9. Kulkarni, D. N., Mahendrakar, A., Molak, O., Kumar, S., & Chitnis, P. (2020). Smart Waste Bin. *SSRN Electronic Journal*. <https://doi.org/10.2139/ssrn.3645414>
10. Kumari, P. K. S., Jeewananda, L., Supunya, R., & Karunanayake, V. (2019). Iot Based Smart Waste Bin Model To Optimize the Waste. *University of Moratuwa*, January 2018, 359– 363.
11. Lam, K. N., Huynh, N. H., Ngoc, N. B., Nhu, T. T. H. T. H., Thao, N. T., Hao, P. H., Kiet, V. Van, Huynh, B. X., & Kalita, J. (2021). Using Artificial Intelligence and IoT for Constructing a Smart Trash Bin. In *Communications in Computer and Information Science: Vol. 1500 CCIS (Issue November 2021)*. Springer Singapore. [https://doi.org/10.1007/978-981-16-8062-5\\_29](https://doi.org/10.1007/978-981-16-8062-5_29)
12. Madrigal, D. V, & Oracion, E. G. (2011). Solid Waste Management Awareness , Attitude , and Practices in a Philippine Catholic Higher Education. *Mapari, R., Narkhede, S., Navale, A., & Babrah, J. (2020)*.
13. Automatic waste segregator and monitoring system. *International Journal of Advanced Computer Research*, 10(49),172–181. <https://doi.org/10.19101/ijacr.2020.1048053>
14. Mustafa, M. R., & Ku Azir, K. N. F. (2017). Smart Bin: Internet-of-Things Garbage Monitoring System. *MATEC Web of Conferences*, 140, 1–4. [https://doi.org/10.1051/mateconf/20171400103\\_0](https://doi.org/10.1051/mateconf/20171400103_0)

15. Padal Jr, C. M., May L. Salado, M. J., & P. Sobejana, N. (2019). SPAMAST Smart Garbage Bin Monitoring System Using Wireless Sensor Network. *Journal of Engineering Research and Reports*, August, 1–16. <https://doi.org/10.9734/jerr/2019/v6i316953>
16. Paul, J., Endaya, S., Mabitasan, F. S., Cyvel, J., & Gonzales, M. (2020). Design and Implementation of Automated Waste Segregator with Smart Compression. *Journal of Engineering and Computer Studies*, 4(3), 50–56Philippine News Agency. (2022).
17. Solid waste segregation remains major challenge in PH: DENR chief. *Philippine News Agency*. <https://www.pna.gov.ph/articles/1175460>

# IOT Based Hybrid Charging Station

Ajmal Sudhir <sup>1</sup>, Deepak Devassy <sup>2</sup>, Anupama K M <sup>3</sup>, Sidharth K A <sup>4</sup>, Dr Annie Bincy C A <sup>5</sup>

<sup>1,2,3,4</sup> Student, Electrical and Electronics Engineering, Albertian Institute of Science and Technology, Kalamassery,

<sup>5</sup> Professor, Electrical and Electronics Engineering, Albertian Institute of Science and Technology, Kalamassery

**Abstract:** *The global shift towards sustainable transportation has been underscored by the emergence of electric vehicles (EVs), including electric two-wheelers, heralding a new era in mobility. Yet, the realization of this transformative potential hinges significantly on the establishment of a robust charging infrastructure tailored to the needs of these vehicles. Specifically, the provision of electric charging stations designed to accommodate two-wheelers is deemed indispensable to facilitate the widespread adoption of such vehicles and propel the transition towards greener modes of transportation. In response to the imperative of sustainability, there has been a growing emphasis on the integration of renewable energy sources within the realm of electric mobility. Hybrid power generation, which combines solar energy with grid electricity, offers a promising avenue for ensuring continuous and sustainable charging operations. This approach not only mitigates environmental concerns associated with reliance solely on grid electricity but also contributes to greater resilience in the face of fluctuating energy demands. Crucially, the advent of the Internet of Things (IoT) has revolutionized the management of charging infrastructure, enabling real-time monitoring and remote administration of charging stations. Such capabilities empower users to access vital information regarding charging slot availability and exert greater control over the charging process, thereby enhancing convenience and optimizing resource utilization.*

**Keywords:** *electric vehicles, IoT*

## Introduction:

Electric mobility is transforming the global transportation sector, with electric two-wheelers, such as scooters and motorcycles, emerging as a popular and environmentally friendly alternative to conventional vehicles. To support their widespread adoption, a robust and specialized charging infrastructure is crucial. Dedicated charging stations for electric two-wheelers, equipped with hybrid power generation systems that combine solar energy and grid electricity, can provide riders with convenient and sustainable charging options. By strategically locating these charging stations in urban areas and along major commuting routes, we can address range anxiety and accelerate the transition to cleaner and greener transportation solutions. Crucially, the advent of the Internet of Things (IoT) has revolutionized the management of charging infrastructure, enabling real-time monitoring and remote administration of charging stations.

The dynamic load management algorithms have emerged as a pivotal tool for optimizing energy distribution within charging networks, thereby enhancing efficiency and cost-effectiveness. Amidst these advancements, it becomes increasingly apparent that understanding the evolution and significance of electric charging stations is paramount for shaping the future of modern transportation and fostering a greener world. The burgeoning adoption of EVs represents a pivotal opportunity for mitigating carbon emissions and advancing sustainability objectives. However, the realization of this potential is contingent upon addressing the prevailing challenges surrounding charging infrastructure adequacy and efficiency. Indeed, the lack of robust charging infrastructure constitutes a notable impediment to the widespread adoption of EVs. Existing charging stations, often reliant solely on grid electricity, raise concerns regarding environmental impact and grid strain, particularly during peak usage periods. Moreover, the

absence of real-time monitoring and management capabilities results in suboptimal utilization of available resources, culminating in inconvenience for EV users and inefficiencies within the charging network.

**Method:**

Two methods has been used in this paper. The first method is SOLAR and the second method is KSEB. The main priority here is SOLAR. If there is no production, we will use KSEB as the second option. The priority here is SOLAR panel. If we use KSEB, we will use AC to DC converter. These two sources will sense the voltage-by-voltage sensor. Through this voltage sensor, we can know which source has enough voltage. The next stage is going to a relay. it's a SOLAR - KSEB relay, after sensing the voltage, we will cut off the relay. This is connected to the voltage sensor. The relay is going to a 12V battery.

**BLOCK DIAGRAM**

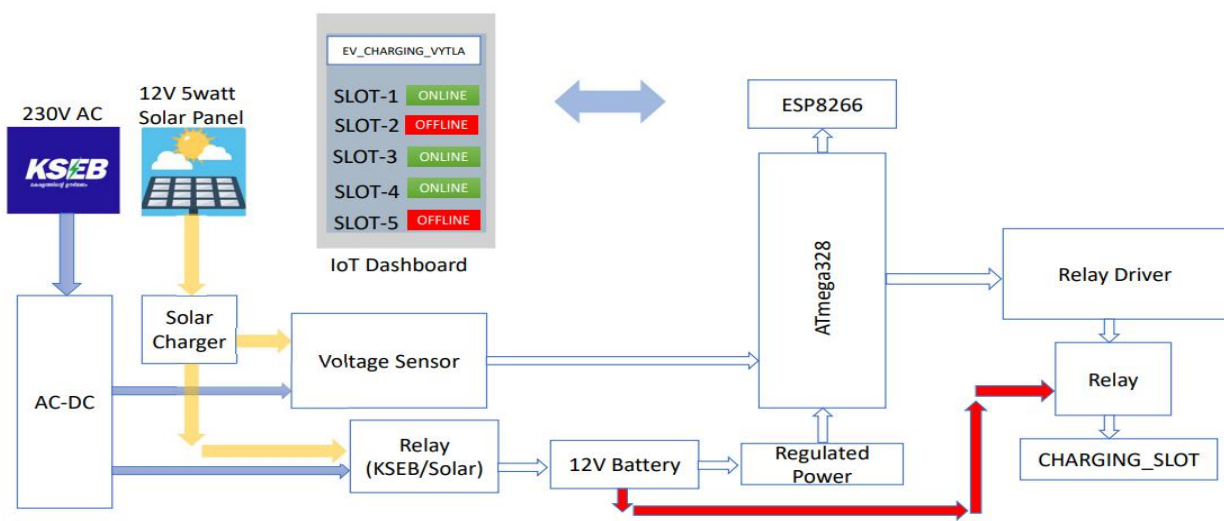


Fig. 1. block diagram

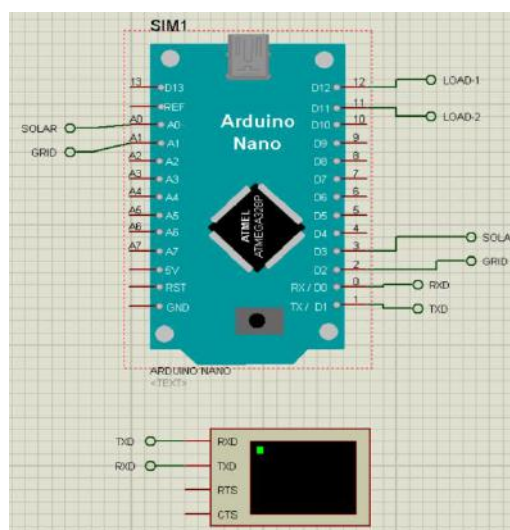


Fig. 2. Circuit diagram Arduino nano and dashboard in proteus

A power is regulated to the charging battery. The power is sent to the control unit. The power is sent from the voltage sensor to the control unit. We will use ATMEGA328 controller to control the relay. The relay is connected to the relay driver., for controlling relay we use relay driver, you have to control the relay. So, in some case a person is charging or the charging is over the relay is automatically cutoff, to control a there is relay driver., the relay driver controls by an controlling unit, That is ATMEGA328. The output will show in the display via ESP8266. The ESP8266 is connected with nearby WI-FI hotspot and it is automatically shows nearby devices. It is an IoT dashboard. Iot dashboard shows how many charging slots are available for charging and which power source is used.

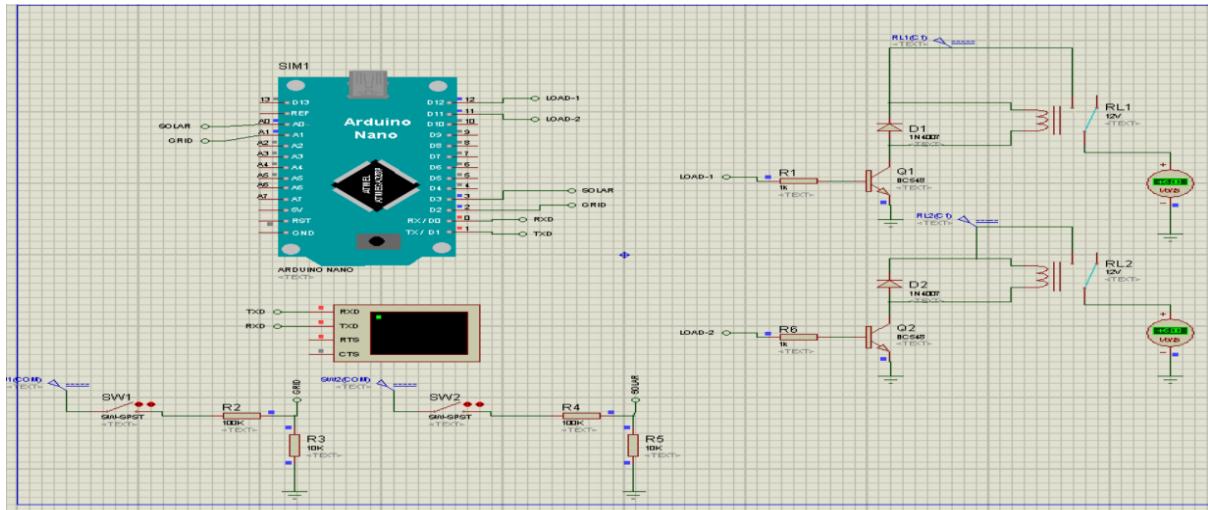


Fig. 3.Circuit diagram of slot relay

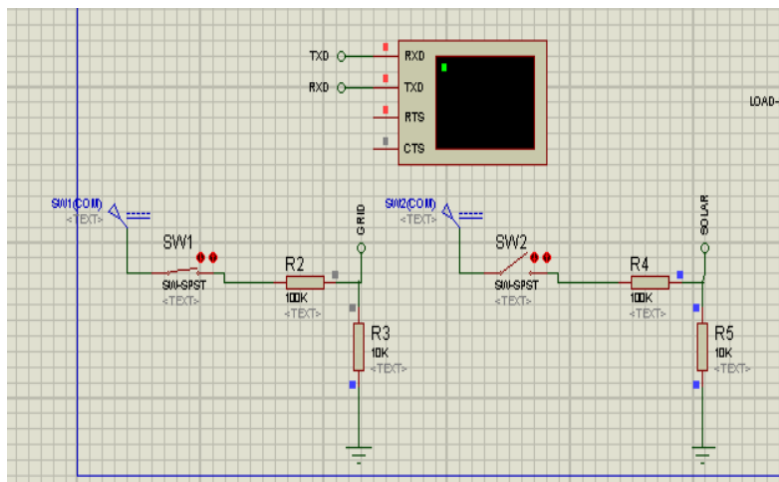


Fig. 4. Circuit diagram of power source relay

**Simulation Results:**

For simulation, we are using in the Proteus software. The components we have taken are, Arduino Nano and IoT Dashboard. We have provided an IOOT Dashboard to show the display. In the normal case, the IOT Dashboard shows, the voltage source and the availability of charging slots L1 or L2. if L1 is online the charging slot L1 is available, if L2 is online the charging slot is available. In case, if the source of power taken from the solar is less it automatically switch to grid. that is the how to grid power is ON in



IOT dashboard. That is what the grid power on is showing. Then automatically, the grid power on will show the voltage there.in case the charging slot 1 is occupied or out of power it will automatically cutoff the relay and it shows the slot 1 is offline. After it regain the power in charging slot it will automatically turn ON the relay and it shows the charging slot is online. These are the simulations provided.

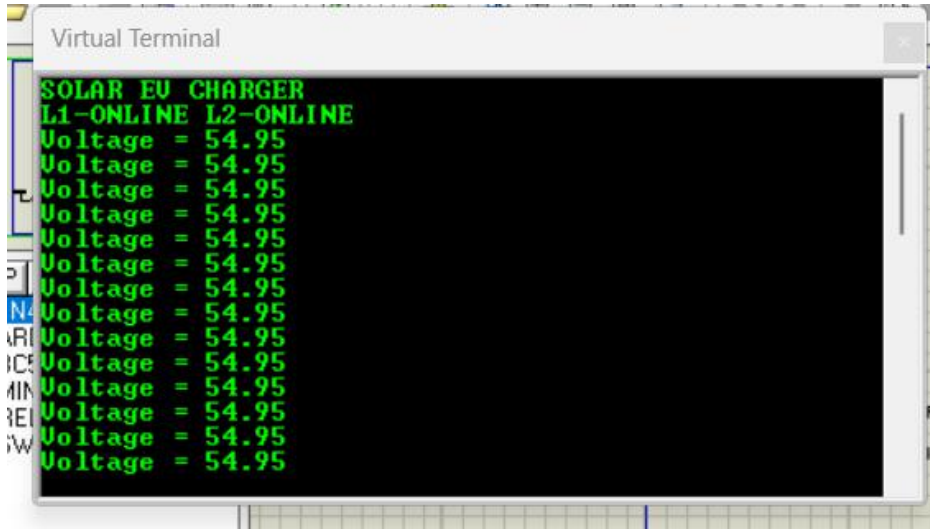


Fig.5.simulation analysis of normal readings

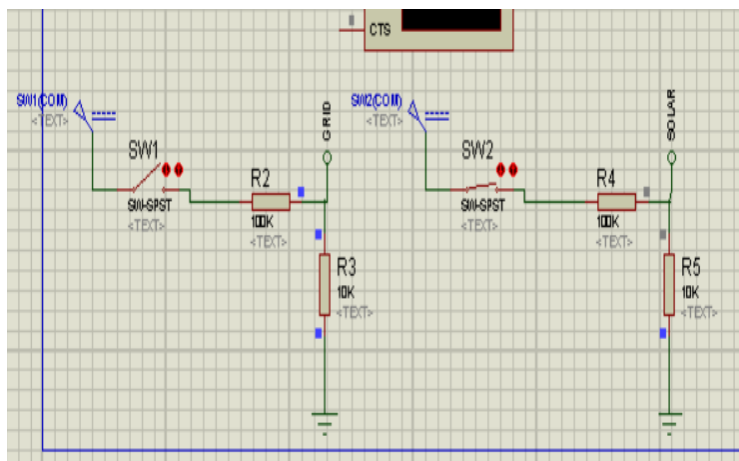


Fig. 6. Circuit diagram when grid connection is cut-off

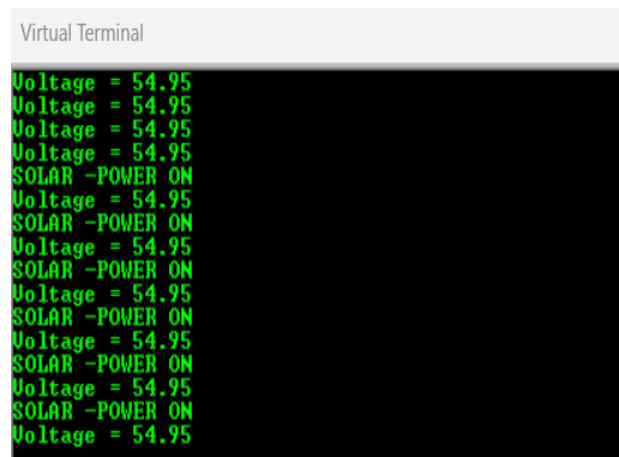


Fig. 7. Simulation analysis of when grid connection is cutoff

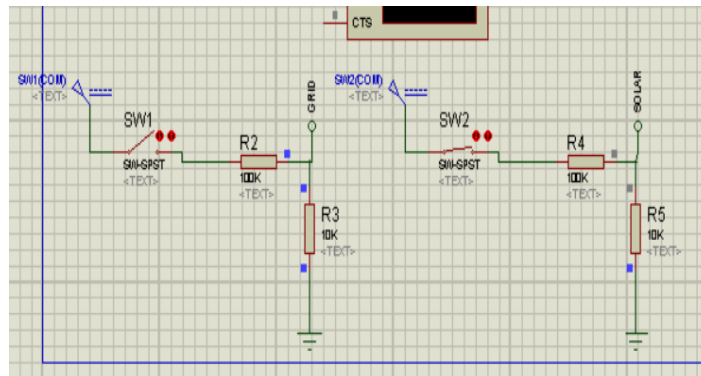


Fig. 8. Circuit diagram when solar connection is cut-off

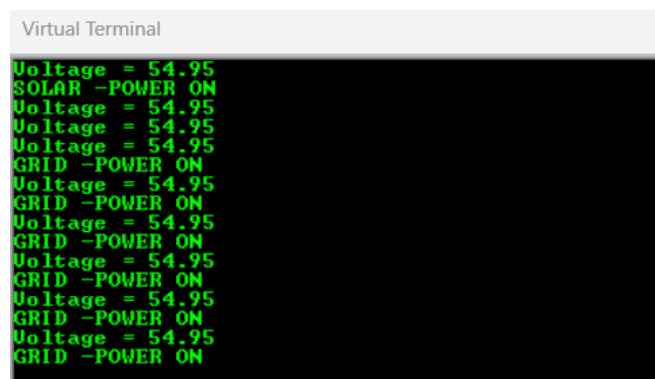


Fig. 9. Simulation analysis of when solar connection is cutoff

### Conclusion:

Following advantages are present on establishing an IOT based charging station.

- **Sustainability:** Integration of renewable energy sources such as solar power reduces carbon emissions and environmental impact.
  - **Efficiency:** Real-time monitoring and dynamic load management optimize energy distribution, enhancing operational efficiency. Cost savings are achieved through reduced reliance on grid electricity and improved resource utilization.
- **Call to Action:** Embrace the transition towards sustainable mobility solutions by supporting initiatives like IoT-based Hybrid EV Charging Stations. Together, we can drive positive environmental change and shape a cleaner, greener future for generations to come.
- **Long-Term Impact:** Ensures high efficiency, reliability, and adaptability

### References:

1. D. Lyu, T. B. Soeiro, and P. Bauer, "Design and implementation of a re-configurable phase-shift full-bridge converter for wide voltage range EV charging application," *IEEE Trans. Transp. Electric.*, early access, May 20, 2022, doi: 10.1109/TTE.2022.3176826.
2. L Gong, X Jin, J Xu, Z Deng, H Li, "A dynamic ZVS-guaranteed and seamless-mode-transition modulation scheme for the dab converter that maximizes the ZVS range and lowers the inductor RMS-L.," *IEEE Trans. Power Electron.*, vol. 37, no. 11, pp. 13119–13134, Nov. 2022

3. Sebastian Rivera, Samir Kouro, Sergio Vazquez, Stefan M. GOETZ, RICARDO LIZANA, And ENRIQUE ROMERO-CADAVAL, “Electric vehicle charging infrastructure”, IEEE , 9 February 2021, Digital Object Identifier 10.1109/MIE.2020.3039039.
4. C. Gonçalves, P. Pinson, and R. J. Bessa, “Towards data markets in renewable energy forecasting,” IEEE Trans. Sustain. Energy, vol. 12, no. 1, pp. 533–542, Jan. 2021
5. X. Yang, Y. Zhang, F. Zhang, C. Xu, and B. Yi, “Enhancing utilization of PV energy in building microgrids via autonomous demand response,” IEEE Access, vol. 9, pp. 23554–23564, 2021.
6. Jajna Prasad Sahoo Divya Rashmi S. Sivasubraman “Intelligent Coordinated Charging of Plug in Electric Vehicles for G2V and V2G Transactions” IEEEConferences, 2022 IEEE IAS Global Conference on Emerging Technologies (GlobConET) Department of Electrical Engineering, Indian Institute of Technology, Patna.
7. T. Schubert, “Real challenges and solutions for validating system-on-chip high level formal verification of nextgeneration microprocessors,” in Proc. 40th Design Automation Conf. (DAC’03), Jun. 2–6, 2021. [Online]. Available: <http://www.computer.org/csdl/proceedings/dac/2021/2394/00/2394001-abs.html>
8. R. L. Myer, “Parametric oscillators and nonlinear materials,” in Nonlinear Optics, vol. 4, P. G. Harper and B. S. Wherret, Eds. San Francisco, CA, USA: Academic, 2021, pp. 47–160
9. R. L. Myer, “Parametric oscillators and nonlinear materials,” in Nonlinear Optics, vol. 4, P. G. Harper and B. S. Wherret, Eds. San Francisco, CA, USA: Academic, 2020, pp. 47–160
10. M. Gorkii, “Optimal design,” Dokl. Akad. Nauk SSSR, vol. 12, pp. 111-122, 1961 (Transl.: in L. Pontryagin, Ed., The Mathematical Theory of Optimal Processes. New York, NY, USA: Interscience, 2020, ch. 2, sec. 3, pp. 127–135).

# Energy Harvesting Using Vertical Axis Wind Turbine from Highway Traffic Vehicles Movement

<sup>1</sup>Sandra Satheesh, <sup>2</sup>Gautham Krishna K S, <sup>3</sup>Nelson E S, <sup>4</sup>DrReshma Gopi R

<sup>1,2,3</sup>UG student, dept of EEE, Mangalam College of Engineering, Ettumanoor

<sup>4</sup>Associate Professor, dept of EEE, Mangalam College of Engineering, Ettumanoor

**Abstract:** *This paper describes the electric energy harvesting method using Vertical Axis Wind Turbines to harness the wind energy generated by the turbulence created by the movement of automobiles along our National Highways. The electric power generated from the wind is presumed to supply power to the National Highway streetlights and electric car charging. There are several alternative renewable sources that we may employ in place of existing non-renewable sources. Further testing with diverse sources, is required to ensure that the alternatives chosen have no problems in the long term. Wind energy is effective and renewable. Electricity production can be facilitated through the aerodynamic losses incurred by vehicles in motion on highways. This energy would be beneficial in a variety of applications, including ship power systems, hybrid electric vehicles, the telecommunications industry, rural electrification, etc. The escalating expenses of traditional energy sources have led to a growing interest in the environmental advantages of these technologies, which may contribute to their broad adoption and approval.*

**Keywords:** *Wind Turbines, wind energy harvesting, hybrid electric vehicles, Energy management*

## Introduction:

Renewable energy is regarded as a sustainable and environmentally friendly source of power. Currently, it stands as one of the most crucial subjects. The depletion of fossil fuel reserves is occurring at a rapid pace, with no new reserves being discovered [1]. Furthermore, the production of energy through the utilisation of fossil fuels has the potential to give rise to a plethora of environmental issues, such as the discharge of greenhouse gases, the escalation of global temperatures, and the occurrence of acid precipitation. Renewable energy sources are significant contributors in such circumstances. Renewable sources of energy encompass a variety of natural resources such as wind, solar radiation, geothermal heat, hydro power, tidal energy, biomass, and other similar sources. The conversion of energy from various sources, regardless of whether they are depletable or non-depletable, into a usable form, results in environmental consequences. The utilisation of analytical techniques to evaluate sustainability with regards to energy and environmental aspects, followed by a comparative analysis of various alternatives, can provide guidance for future energy strategies and governmental regulations.

Wind energy (or wind power) describes the process by which wind is used to generate electricity. The process of converting the kinetic energy present in the wind into mechanical power is accomplished by wind turbines. The transformation of mechanical power into electrical power can be accomplished using a generator. Direct utilisation of mechanical power can be employed for particular purposes, such as water pumping. The phenomenon of wind can be attributed to the non-uniform heating of the atmosphere by solar radiation, irregularities in the topography of the earth's surface, and the rotational motion of the planet. The patterns of wind flow are influenced by various natural elements such as mountains, bodies of water, and vegetation. The process of generating electricity from wind involves the utilisation of wind turbines, which operate by rotating rotor blades in a propeller-like manner to harness the kinetic energy of wind. The rotational motion of the rotor is responsible for driving the drive shaft, which in turn drives an electric generator. The amount of energy that a turbine can harness from the wind is influenced by three primary factors, namely wind speed, air density, and swept area.

## Method:

### Harnessing Wind Energy

The significant progress in wind turbine technology has led to a substantial surge in wind energy harvesting over the last few decades. In the realm of wind energy harvesting, wind turbines are typically categorised as either Vertical Axis Wind Turbines (VAWTs) or Horizontal Axis Wind Turbines (HAWTs), based on the location of their respective rotation axes. The classification of VAWT can be broadly categorised into two distinct groups, namely, those that employ aerodynamic drag for the purpose of harnessing wind power and those that utilise lift. One of the benefits of vertical axis wind turbines (VAWTs) is their ability to harness wind energy from multiple directions. This simplifies their design and eliminates the problem posed by gyroscopic forces exerted on the rotor of a conventional machine as the turbine follows the wind [2]. The proposed model is as in Fig. 1.

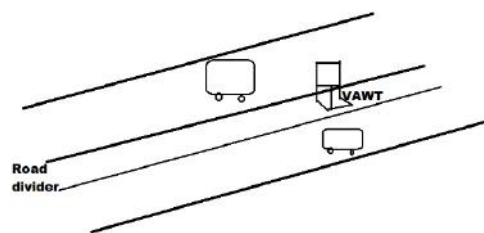


Figure 1. Wind energy extraction model

### Vertical Axis Wind Turbine

Along with the increasing number of wind farms containing Along with the growing number of wind farms comprising huge HAWTs, there has also been an increase in small-scale wind turbines such as vertical axis wind turbines in recent years. Small VAWTs are suitable for energy harvesting in urban and suburban areas due to their capability to function efficiently in the presence of turbulent and fluctuating flow [3]. This is particularly advantageous in areas where wind patterns are typically unsteady and gusty. In addition, because the generator and electrical components are mounted at the base, VAWTs provide a more suitable design solution, compared to the traditional HAWT, for small-scale urban installations such as on the rooftops of residential/commercial buildings. It is possible for a VAWT system that is designed with optimal efficiency to be economically competitive with power plants that rely on fossil fuels.

In a study conducted by Gideon Quartey et al. [4] a proposal was made for the installation of a wind turbine on the roof of a vehicle to produce electricity for the purpose of charging batteries while the vehicle is in motion. Theoretical calculations indicate that the batteries can be recharged with a substantial amount of electrical power, approximately 3.26 kW, while the vehicle is being driven at a speed of 120 km/h. Awal et al. [5] conducted a study on the structural configuration of wind turbines and suggested an innovative approach for installation. This approach involves placing the generator on the roof of a vehicle and connecting it to the turbine shaft using a belt. The implementation of the installed method has the potential to substantially enhance the power of electricity generation. Nevertheless, the utilisation of Horizontal Axis Wind Turbines has brought to light several deficiencies. During operation, Horizontal Axis Wind Turbines (HAWTs) generate significant noise due to the blade's interaction with the surrounding airflows. This noise emission poses a potential hazard to avian species and contributes to environmental noise pollution.

In contrast to the HAWT, the VAWT successfully addresses these aforementioned obstacles. The VAWT comprises two distinct categories, namely Savonius and Darrieus, which are classified based on the pressure differential of the blades. The Savonius turbine exhibits several advantages over the Darrieus turbine, including its capacity for self-starting in low-speed winds, operational versatility, omnidirectional

wind-catching ability, and noiseless operation. The Savonius Vertical Axis Wind Turbine (SVAWT) has been widely employed in urban areas for wind energy harvesting owing to its numerous benefits [6].

### Analysis:

#### Power From Wind

The energy transferred to the rotor by the wind depends on the air density, the swept area of the rotor and wind speed [7]. A wind flow, can be understood as a set of moving particles, which develops an energy flow (flow of air through a turbine) or wind power (power available in the air) stream through the area A, defined by the square-cube law:

$$\text{Power, } P = 0.5 * \rho * v^3 * A \quad (1)$$

#### Power Coefficient

When a wind turbine is crossed by a flow of air, it can get the energy of the mass flow and convert it in rotating energy [8]. This conversion presents some limits, due to the Betz' law,  $C_p = 0.59$ . Power coefficient  $C_p$  is given by

$$C_p = P / (0.5 * \rho * A * v^3) \quad (2)$$

#### Blade Diameter And Swept Area

For the swept area for Savonius Wind Turbine blade is given below, the swept area for Savonius blade is obtained by multiplication of rotor diameter, D and the rotor height, H. The power output of blade is improved with the swept area.

$$A = D * H \quad (3)$$

The Savonius rotor's design places the rotor height twice as high as the rotor diameter, which improves stability and efficiency. The two-bladed Savonius rotor is as shown in Fig. 2. The summary of rotor blade design is as in Table 1.

#### Effect Of End Plates

To study the effect of end plates, rotors with and without end plates are tested at constant values of other considered parameters. Rotors with end plates give higher mechanical power than rotors without end plates. This is because the existence of endplates increases the amount of air which strikes the blades of Savonius rotor.

#### Tip Speed Ratio

The tip speed ratio is defined as the ratio of the tangential velocity of the rotor blade tip to the speed of the wind. Enhancing the rotational rate of the rotor leads to an improvement in wind turbine performance through the achievement of a high tip speed ratio. The tip speed ratio is given by

$$\lambda = \omega R / v \quad (4)$$

where,  $\omega$  is angular velocity, R is radius revolving part of the turbine, and v is undisturbed wind speed. The coefficient of power is directly proportional to the ratio between the energy components from the rotating motion and the air flow motion. Consequently, it depends on the tip speed ratio. Based on the tip speed ratio, the power coefficient which is the amount of energy taken from the wind can be calculated by

$$C_p(\lambda) = 0.00044\lambda^4 - 0.012\lambda^3 + 0.097\lambda^2 - 0.2\lambda + 0.11 \quad (5)$$

### Result:

The main challenge in using wind energy is to create a wind turbine with a straightforward layout, a low working speed, and independent wind directions. The Savonius rotor seems promising in these circumstances, but it has two significant flaws: low efficiency and strong negative torque. Many scientific experts are currently working to enhance the Savonius turbine's capabilities by maximising the effects of

various geometric aspects and by creating novel designs.

The simulated mathematical model of wind turbine is as shown in Fig. 3.

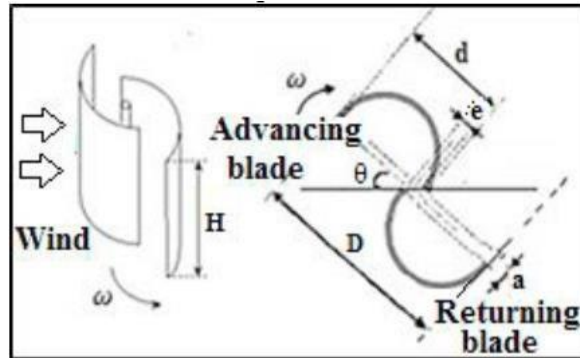


Fig. 2. Two-bladed Savonius Rotor

Table 1 Summary of rotor blade design

Parameter	Value
Power Generated	50 watts
Rated wind speed	8 m/s
Aspect ratio	1.2
Number of blade	2
Diameter	0.4 m
Height	0.5 m

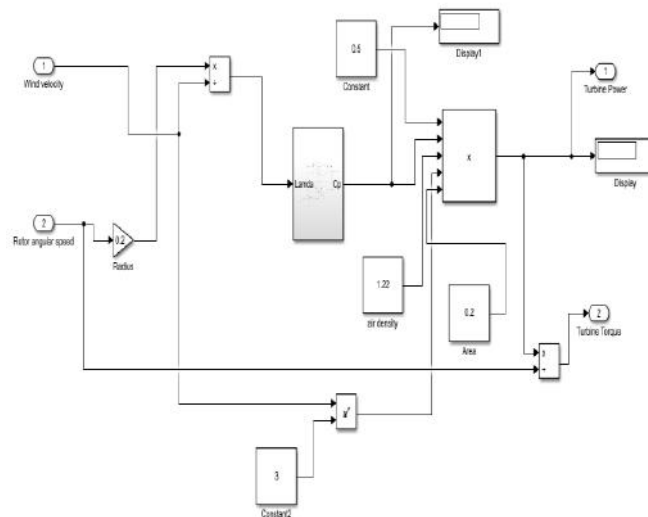


Fig. 3. Turbine SIMULINK model

The analysis is conducted with respect to a specified power output of 50 watts. The air density is taken as 1.22 kg/m<sup>3</sup> and pitch angle as 0.



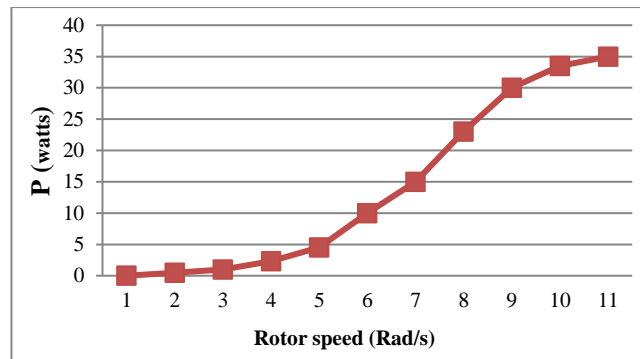


Fig. 4. Turbine power output vs. rotor speed

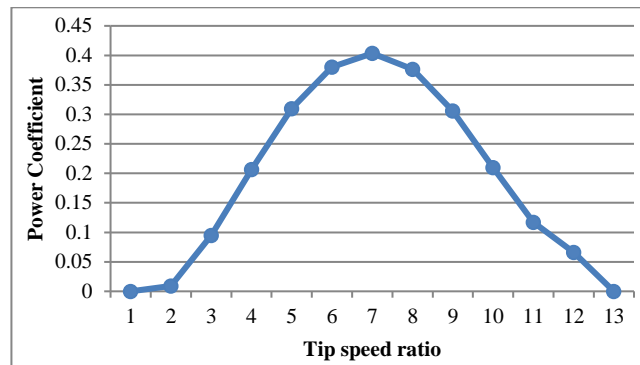


Fig. 5. Power coefficient vs. tip speed ratio

The Fig. 4 demonstrates that power increases with increasing rotor speed. The Fig. 5 indicates the power coefficient first rises with an increase in tip speed ratio. However, after a certain point, the power coefficient decreases as the ratio of tip speed increases. The maximum power coefficient was observed at 0.403.

#### Final System:

The prototype made as per design is as in Fig. 6.



Fig. 6. Hardware architecture- Prototype of VAWT

#### Conclusion:

Numerous studies have been conducted over the years to improve the Savonius rotor's design in order to achieve better performance. In this work, the characteristics of turbine model has been analysed. In order to enhance the performance of the rotor, the development of the Savonius rotor blade's shape continues to be a particularly promising study area. It is believed that further study on parameters like overlap ratio, and number of blades is necessary to get a reasonable level of performance, while Savonius'

performance is improved by the addition of additional sets like obstacle shielding, curtains, or conveyor deflectors.

**References:**

1. Sayais SY, Salunkhe GP, Patil PG. and Khatik MF. Power generation on highway by using vertical axis wind turbine & solar system. *International Research Journal of Engineering and Technology (IRJET)*, 2018;5(03).
2. Zemamou M, Aggour M, and Toumi A. Review of savonius wind turbine design and performance. *Energy Procedia*.2017; 141:383-388.
3. Kumar PS, Chandrasena RPS, Ramu V, Srinivas GN and Babu KVSM. Energy management system for small scale hybrid wind solar battery based microgrid. *IEEE Access*.2020; 8:8336-8345.
4. Khandagale MR. and Marlapalle MB. Design & Analysis of Savonius VAWT for 50W Rated Power output. *Int J Eng Res Gen Sci*.2017;5:189-200.
5. Quartey G and Adzimah SK. Generation of electrical power by a wind turbine for charging moving electric cars. *J. Energy Technol. Policy*.2014;4:19.
6. Awal, M.R., Jusoh, M., Sakib, M.N., Hossain, F.S., Beson, M.R.C. and Aljunid, S.A. Design and implementation of vehicle mounted wind turbine. *ARN J Eng Appl Sci*,2015; 10:8699-8860.
7. Energy Management System for Small Scale Hybrid Wind Solar Battery Based Microgrid ; P. Satish Kumar, R.P.S. Chandrasena, V. Ramu, G.N. Sreenivas and K. Victor Sam Moses Babu (2017)
8. Gopi, RR. and Annamalai, C. Day Ahead Energy Consumption Forecasting Through Time-Series Neural Network. *Indonesian Journal of Electrical Engineering and Informatics (IJEEI)*.2023; 11(1):164-179.
9. Kavade, R.K. and Ghanegaonkar, P.M., 2017. Design and analysis of vertical axis wind turbine for household application. *Journal of Clean Energy Technologies*. 2017; 5(5):353-358.

# A Hybrid Bidirectional Dc-Dc Converter Based on a Sepic / Zeta Converter with a Modified Switched Capacitor Cell

<sup>1</sup>Adithyan M Unnithan ,<sup>2</sup>Aditya Raj ,<sup>3</sup>Aditya P Nair ,<sup>4</sup>Rithika Dileep, <sup>5</sup>Atheena A, <sup>6</sup>Dr.Vinod V.P

<sup>1 2 3 4</sup>UG student, Dept. of EEE, Sree Buddha College of Engineering, Pattoor

<sup>5</sup>Assistant Professor, Dept. of EEE, Sree Buddha College of Engineering, Pattoor

<sup>6</sup>Professor, Dept. of EEE, Sree Buddha College of Engineering, Pattoor

**Abstract:** *The DC-DC converter, which is bidirectional, merges a SEPIC/Zeta converter with a tailor-made switched capacitor cell. This combination offers a wide range of applications in DC microgrids and renewable energy systems. The converter is adept at managing both charging and discharging processes, thereby improving voltage stability and the overall performance of the system. It integrates an MPPT using a P&O algorithm to optimize energy harvesting, while FUZZY logic is employed to reduce circuit stresses, ensuring the system's robustness. With an input of 240V and an output of 813V, this converter exhibits extraordinary capabilities that surpass current energy storage needs. Its bidirectional power flow and MPPT optimization highlight its potential to transform the integration of battery energy storage in sustainable energy applications.*

**Keywords:** *MPPT, SEPIC/Zeta, DC-DC converter, Fuzzy Logic controller.*

## Introduction:

The electricity grid is experiencing a transformation. Renewable energy sources like solar and wind are playing a growing role, introducing new concepts like distributed generation (DG) and DC microgrids. However, these renewables are inherently intermittent, meaning their power output fluctuates. To address this and ensure stable operation in DC microgrids, Battery Energy Storage Systems (BESS) are being integrated. BESS act as a buffer, storing excess energy and releasing it during periods of low generation. In grid-tied applications, BESS can also smooth out the power delivered to the grid, increasing system stability and independence from the main grid. The increasing use of BESS has led to a surge in research on bidirectional DC-DC converters. These converters are essential for interfacing BESS with the DC microgrid. They allow for two-way power flow: charging the BESS when there's excess power and drawing power from the BESS when needed. BESS voltage can vary significantly. For some applications, converter topologies that can both step-up and step-down voltage are ideal. This is where Buck-Boost converters come in. However, Buck-Boost converters have a drawback - they subject their switches to higher voltage stress compared to simpler Buck and Boost converters. This necessitates using active switches with a breakdown voltage exceeding 650V, which can lead to a decrease in overall efficiency due to the higher on-resistance of these high voltage switches.

The new hybrid converter for 800V BESS integration in EV charging in this research proposes a new hybrid bidirectional DC-DC converter for integrating Battery Energy Storage Systems (BESS). It combines a SEPIC/Zeta converter with a switched capacitor cell. This design reduces voltage stress on switches but increases component count and peak current. Despite the current increase, the capacitor cell allows lower resistance switches, potentially offsetting some losses. The converter operates as a current source, enabling a smaller filter for the battery pack. Simulations validate the design for a 1kW converter with 240V input, 800V output, and 50kHz switching frequency. Crucially, the 800V output aligns perfectly with the voltage requirements of new and upcoming electric vehicles, enabling efficient and

faster charging. This is a significant advantage for the fast-growing electric vehicle charging segment.

### Problem Identification:

Addressing the issue of high voltage stress on semiconductors in conventional SEPIC/Zeta converters, the study sheds light on challenges associated with increased component count and peak current in active switches within the proposed hybrid bidirectional converter. This recognition underscores the potential impact on overall efficiency and design complexity. Moreover, the research identifies another critical concern related to the need for a larger capacitive filter when interfacing with battery energy storage systems (BESS) due to high current ripple. The proposed converter offers solutions to these challenges by specifically aiming to mitigate current ripple, thereby allowing for the use of a smaller capacitive filter. This strategic approach not only addresses the identified issues but also contributes to enhancing the overall efficiency and compactness of the converter when integrated with battery energy storage systems, presenting a promising advancement in converter technology.

Bidirectional DC-DC converters are essential for managing power flow in both directions within electronic systems. They efficiently convert voltage levels up or down, enabling applications like energy storage, electric vehicles, and renewable energy integration. By controlling the switching of semiconductors, these converters regulate energy flow and maintain stable output voltage. This flexibility is crucial in modern power systems, allowing for efficient bidirectional energy transfer between sources and storage, like the grid and batteries. As renewable energy and storage gain traction, bidirectional DC-DC converters play a key role in building a more sustainable and adaptable future for power electronics.

### Methodology:

A Bi-Directional DC-DC converter serves as a pivotal component in energy management systems, seamlessly transferring energy between two distinct sources to optimize power utilization. In the context of a standard photovoltaic (PV) system, bidirectional SEPIC/Zeta converters play a crucial role in enhancing energy efficiency and overall system performance. This integration is particularly significant when considering the dynamic nature of solar power generation. In the typical configuration, a PV system is equipped with a bi-directional converter that allows for the bidirectional flow of energy. During periods of ample sunlight, the photovoltaic modules harness solar energy, and the bi-directional SEPIC/Zeta converter efficiently manages the power flow. Notably, the converter ensures that the energy generated by the PV modules is optimally utilized by employing the Perturb and Observe method for Maximum Power Point Tracking (MPPT). The MPPT algorithm, in this scenario, employs the Perturb and Observe method, a widely used technique that continuously adjusts the operating point of the PV system to maximize power output. By dynamically tuning the system parameters based on real-time conditions, the MPPT algorithm ensures that the PV modules operate at their peak efficiency, thereby extracting the maximum available power from the solar irradiance.

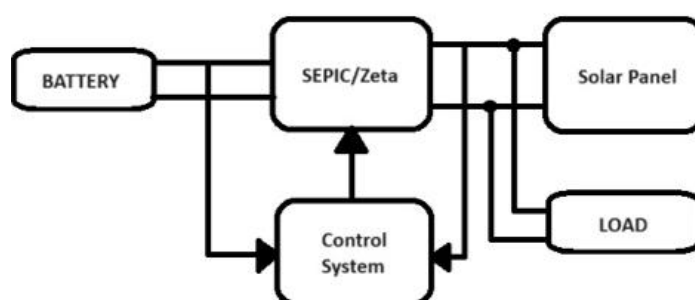


Fig 1. Block Diagram

A noteworthy feature of this system is its ability to seamlessly transition between power sources.

Initially, when solar irradiance is abundant, the solar panels supply power to the bi-directional SEPIC/Zeta converter. Concurrently, the converter efficiently charges the battery, acting as an energy reservoir. As solar conditions change and irradiance diminishes, the battery seamlessly takes on the role of the energy source, entering the Zeta mode for charging. This transition between SEPIC and Zeta modes ensures continuous power supply, optimizing energy utilization and enhancing the overall reliability of the PV system. In summary, the integration of a bi-directional SEPIC/Zeta converter, coupled with an intelligent MPPT algorithm, represents a sophisticated solution for standard PV systems. This approach not only maximizes power extraction from solar modules but also provides a seamless energy transition mechanism, ensuring efficient and continuous power supply under varying environmental conditions.

In conclusion, the integration of a novel bidirectional DC-DC converter, combining a SEPIC/Zeta PWM converter with a modified switched capacitor cell, represents a significant breakthrough in advancing the efficiency and reliability of Battery Energy Storage Systems (BESS) connected to DC microgrids and renewable energy solutions. The research successfully addresses the challenge of minimizing voltage stress on semiconductors during the charging and discharging cycles of the BESS, achieving this through a carefully designed modification in the switched capacitor cell. The selection of specific converter design parameters, such as the input voltage of 240V, output voltage of 400V, rated power of 1000W, and a switching frequency of 50kHz, underscores the practical applicability and scalability of the proposed solution in real-world scenarios. The numerical simulation results provide compelling evidence of the converter's effectiveness in reducing voltage stress on switches, establishing its suitability for integration into DC microgrids and renewable energy systems. This research not only contributes to the growing body of knowledge in power electronics but also marks a significant step forward in the development of sustainable energy technologies. The innovative approach showcased in this study holds promise for enhancing the overall performance and resilience of energy storage systems, playing a vital role

The SEPIC input receives charging both from the solar panel and the battery. The level of irradiance plays a crucial role in determining the power flow, dictating whether current from the solar panel is directed towards the load or the battery. Particularly during the morning hours when sunlight is abundant, solar power is primarily utilized to supply the load, thereby reducing the reliance on the battery. It's important to note that the SEPIC input operates at 240V, while its output voltage reaches 813V.

## Results And Discussion:

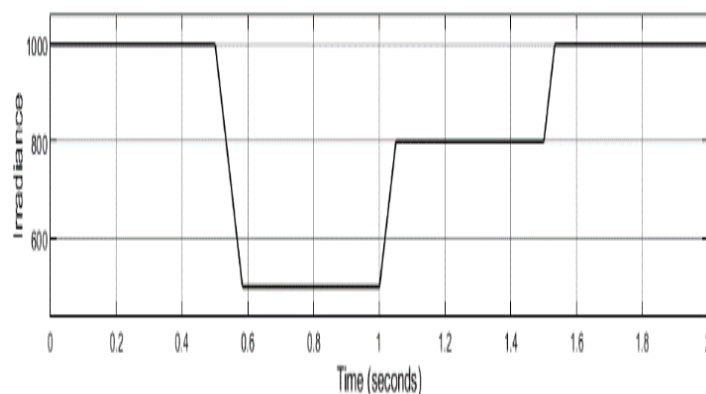


Fig 2. Irradiance

This graph represents Irradiance (energy per unit area), starting with an initial input of 1000, from 0 to 0.58 second the solar is giving power to the SEPIC converter and it also charges the battery at the same time and then decreasing to 500 and fluctuating thereafter. Between 0.58 and 1 second, the battery

is utilized. From 1 to 1.5 seconds, both the battery and solar power are employed, while from 1.5 to 2 seconds, solar power alone is utilized. During solar operation, the load is supplied with power while simultaneously recharging the battery. Continuous power supply is ensured for the load without interruptions. In this scenario, one of the primary objectives outlined is achieved. Specifically, between 0.58 and 1 second, power is drawn from the battery. From 1 to 1.5 seconds, both the battery and solar energy sources are utilized, while between 1.5 and 2 seconds, only solar energy is utilized. This approach ensures uninterrupted power delivery to the load, showcasing the effectiveness of the proposed system.

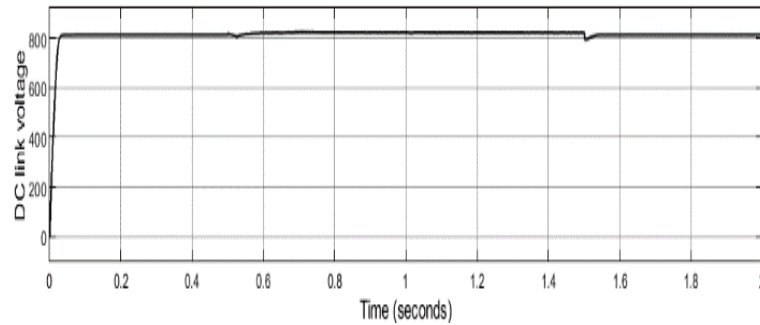


Fig 3. DC Link Voltage

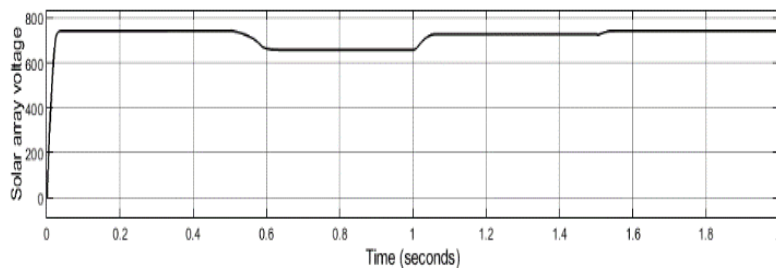


Fig 4. Solar Panel Voltage

In the graph provided, the fluctuation in irradiance levels directly influences the output of the solar panel, as evidenced by the variation observed between 0.6 seconds and 1 second. This dynamic relationship highlights how changes in irradiance levels affect the performance of the solar panel, resulting in corresponding fluctuations in its output.

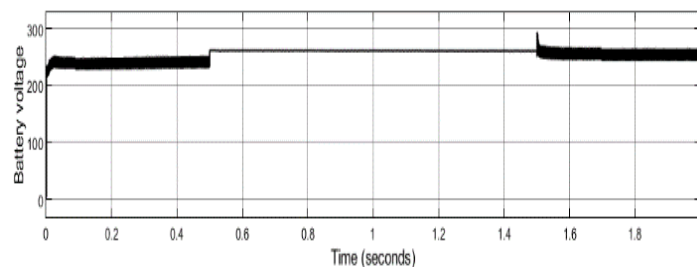


Fig 5. Battery Voltage

Between 0.5 and 1.5 seconds on the graph, the battery serves as the primary energy source. The outcomes depicted above are derived from this period of battery utilization. This timeframe showcases the performance and behaviour of the system during battery operation.

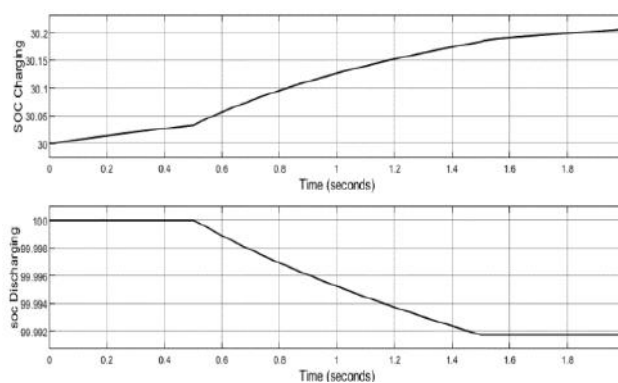


Fig 6. Charging and Discharging with Separate Battery Pack

In this scenario, two states of charge (SOC) for the battery are considered: 30% and 100%. Initially, the charging process of the battery from 0 to 2 seconds is illustrated when the battery is at 30% SOC. Subsequently, in the second graph, the discharge phase of the battery is depicted, lasting until 1.5 seconds. This cycle of charging and discharging repeats, demonstrating the dynamic behavior of the system under different SOC conditions.

### Conclusion:

The integration of a novel bidirectional DC-DC converter, which combines a SEPIC/Zeta converter with a modified switched capacitor cell, signifies a notable breakthrough in advancing the efficiency and reliability of Battery Energy Storage Systems (BESS) interfaced with DC microgrids and renewable energy solutions. This research effectively tackles the challenge of minimizing voltage stress on semiconductors during BESS charging and discharging cycles by intricately modifying the switched capacitor cell. The selection of specific converter design parameters, such as an input voltage of 240V, output voltage of 813V, rated power of 1000W, and a switching frequency of 50kHz, underscores the practical applicability and scalability of the proposed solution in real-world scenarios. Numerical simulation results compellingly demonstrate the converter's efficacy in reducing voltage stress on switches, validating its suitability for integration into DC microgrids and renewable energy systems. This study not only contributes to the expanding field of power electronics but also signifies a significant advancement in sustainable energy technology development. The innovative approach presented in this research holds promise for enhancing the overall performance and resilience of energy storage systems, playing a pivotal role in the transition towards cleaner energy solutions.'

### References:

1. C.-M. Lai, C.-T. Pan, and M.-C. Cheng, "High efficiency modular high step-up interleaved boost converter for DC-microgrid applications," *IEEE Trans. Ind. Appl.*, vol. 48, no. 1, pp. 161–171, Jan./Feb. 2012.
2. J. W. Kolar, F. Krismer, Y. Lobsiger, J. Muhlethaler, T. Nussbaumer, and J. Minibock, "Extreme efficiency power electronics," in *Proc. 7th Int. Conf. Integer. Power Electron. Syst. (CIPS)*, 2012, pp. 1–22.
3. H. Chen, K. Sabi, H. Kim, T. Harada, R. Erickson, and D. Maksimovic, "A 98.7% efficient composite converter architecture with application-tailored efficiency characteristic," *IEEE Trans. Power Electron.*, vol. 31, no. 1, pp. 101–110, Jan. 2016.
4. S. Choi, V. G. Agelidis, J. Yang, D. Coutellier, and P. Marabeas, "Analysis, design and experimental results of a floating-output interleaved-input boost-derived DC–DC high-gain transformer-less converter," *IET Power Electron.*, vol. 4, no. 1, pp. 168–180, 2011.
5. C.-M. Lai, Y.-H. Cheng, J. Teh, and Y.-C. Lin, "A new combined boost converter with improved voltage gain as a battery-powered front-end interface for automotive audio amplifiers," *Energies*, vol. 10, no. 8, p. 1128, Aug. 2017.
6. F. S. Garcia, J. A. Pomilio, and G. Spiazzi, "Modeling and control design of the interleaved double dual



- boost converter*,” IEEE Trans. Ind. Electron., vol. 60, no. 8, pp. 3283–3290, Aug. 2013
7. M. Pavlovsky, G. Guidi, and A. Kawamura, “Assessment of coupled and independent phase designs of interleaved multiphase buck/boost DC–DC converter for EV power train,” IEEE Trans. Power Electron., vol. 29, no. 6, pp. 2693–2704, Jun. 2014
  8. Rodriguez, A. Vazquez, M. R. Rogina, and F. Briz, “Synchronous boost converter with high efficiency at light load using QSW-ZVS and SiC MOSFETs,” IEEE Trans. Ind. Electron., vol. 65, no. 1, pp. 386–393, Jan. 2018.
  9. T. Schoenen, M. S. Kunter, M. D. Hennen, and R. W. De Doncker, “Advantages of a variable DC-link voltage by using a DC–DC converter in hybrid-electric vehicles,” in Proc. IEEE Vehicle Power Propuls. Conf., Sep. 2010, pp. 1–5.
  10. A. B. de Almeida and C. H. I. Font, “DC-DC bidirectional 4-switch Cúk converter with voltage-doubler concept for interfacing batteries in microgrids,” 13th IEEE International Conference on Industry Applications (INDUSCON), pp. 263-268, 2018.
  11. G. Tibola and J. L. Duarte, “Isolated bidirectional DC-DC converter for interfacing local storage in two-phase DC grids,” in Proc. of IEEE 8th International Symposium on Power Electronics for Distributed Generation Systems (PEDG), pp. 1-8, 2017.
  12. D. E. Soman, K. Vikram, R. Krishna, M. Gabrysch, S. K. Kottayil, and M. Leijon, “Analysis of three-level Buck-Boost converter operation for improved renewable energy conversion and smart grid integration,” in Proc. of IEEE International Energy Conference (ENERGYCON), pp. 76-81, 2014.
  13. C. Pham, T. Kerekes and R. Teodorescu, “High efficient bidirectional battery converter for residential PV systems,” in Proc. of 3rd IEEE International Symposium on Power Electronics for Distributed Generation Systems (PEDG), pp. 890-894, 2012.
  14. K. Uddin, A. D. Moore, A. Barai, and J. Marco, “The effects of high frequency current ripple on electric vehicle battery performance,” Applied Energy, vol. 178, pp. 142-154, September 2016.

# Comparative Analysis of Open Loop and Closed Loop Control Systems for Switched Reluctance Motors in Plug-in Hybrid Electric Vehicles

<sup>1</sup>Chama R Chandran, <sup>2</sup>Amay Krishnan, <sup>3</sup>Akash Krishnan, <sup>4</sup>Chaithra A, <sup>5</sup>Krishna Prasad V, <sup>6</sup>Dr. Vinod V P

<sup>1,2,3,4</sup> UG student, Dept. of EEE, Sree Buddha College of Engineering, Pattoor

<sup>5</sup> Assistant Professor, Dept. of EEE, Sree Buddha College of Engineering, Pattoor

<sup>6</sup> Professor, Dept. of EEE, Sree Buddha College of Engineering, Pattoor

**Abstract:** *This study aims to investigate the performance of open-loop and closed-loop control strategies in switched reluctance motors (SRMs) for Plug-in Hybrid Electric Vehicles (PHEVs). The study compares and analyzes the effectiveness of each control method based on various parameters, including torque response, speed control, efficiency, torque ripple, and noise generation. Switched reluctance motors have been gaining attention as a viable option for PHEVs due to their simplicity, high efficiency, and cost-effectiveness. The control strategy employed for SRMs plays a crucial role in achieving optimal performance and efficiency. Open-loop control is a simple and cost-effective approach, but it lacks accuracy and efficiency in varying operating conditions. In contrast, closed-loop control provides improved precision and robustness by utilizing feedback from sensors and control elements. The findings of this study contribute to a better understanding of the performance characteristics and control strategies of SRMs in PHEV applications. The results obtained can aid the development of efficient and reliable control systems for SRMs, thereby improving their overall performance and energy efficiency in hybrid electric vehicles. The selection of the control strategy depends on factors such as motor specifications, desired system performance, and specific application requirements. Ultimately, the study aims to enhance the performance and efficiency of SRMs in PHEVs with the use of the most optimal control strategy.*

**Keywords:** *Switched Reluctance Motor, Plug-in Hybrid Electric Vehicles, Closed loop control, Proportional-Integral control*

## Introduction:

The growing population and increased usage of vehicles is a common trend that is being seen. As fossil fuel is commonly used in vehicles, there arises several environmental challenges too. In order to combat these environmental issues Electric Vehicles were introduced. There are mainly four types of Electric Vehicles that are being used namely: 1. Battery Electric Vehicle (BEV) 2. Hybrid Electric Vehicle (HEV) 3. Plug-In Hybrid Electric Vehicle (PHEV) 4. Fuel Cell Electric Vehicle (FCEV) There are different driving modes used. This include SRG alone mode, battery alone mode, SRG and battery hybrid mode, SRG driving and battery charging, regenerative braking[1] Further the different propulsion systems of the vehicles are analyses in order to get an idea of which topology is better and efficient for the propulsion system[2]. The most commonly used motors in electric vehicles are DC series motor, BLDC motor, PMSM, three phase AC induction motor and SRM. Here, an SRM is used. SRM have several advantage over other motors. They have simple structure, low cost and high dependability. One main disadvantage in SRM is the torque ripple torque ripple[3]. There are several torque ripple reduction methods available[4]. Here, we are analyzing the torque ripple and power factor of SRM in electric vehicle by comparing an open loop system and closed loop system. A three phase 12/8 poles SRG and SRM platform is selected[5,6]. The control system for controlling SRM is PI-based[7]. Here SEPIC converter

is incorporated for the boosting of the signal from the SRG[8]. DC/DC converter is an important component in the electric vehicle[9,10]. This provides an efficient conversion. Also certain strategies to increase efficiency of SRM is analysed. This approach offers robust performance across a wide range of operating conditions and can compensate for variations in motor parameters or external disturbances

### Method:

The main objective is to reduce the torque ripple in the SRM. For this an open loop system and closed loop system is considered.

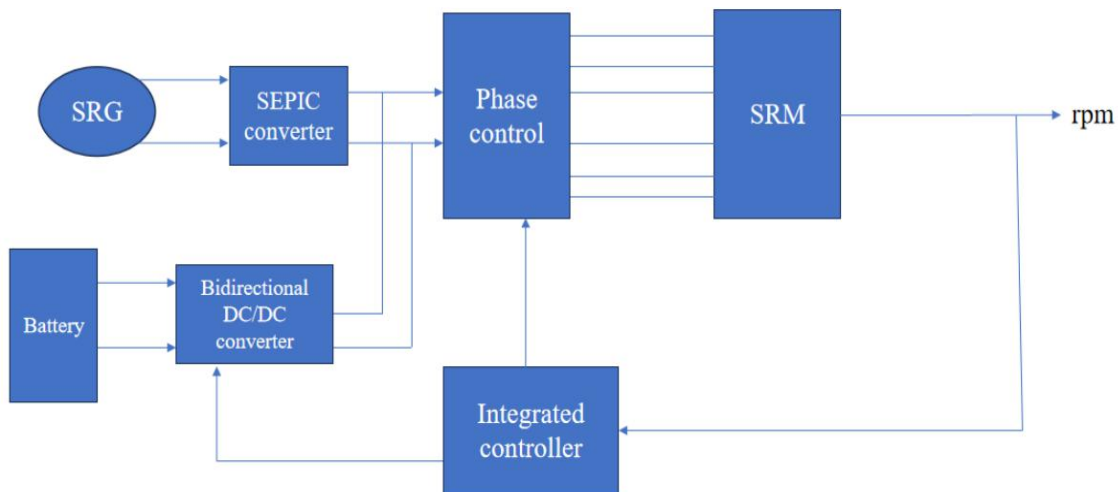


Figure 1. Block Diagram of Proposed System

Here an SRG is used to generate a signal. Before entering the SEPIC converter, the AC output from the SRG is converted by a rectifier. The SEPIC converter is used to boost the signal. The phase controller controls the phases of the SRM by energizing the poles. The output from the SRM is taken as an error signal and fed to the integrated controller. The controller used here is the integrated PI controller. A 36V battery is used here. Also there is the bidirectional DC/DC converter.

### Open Loop System:

In the open loop system, the switching of the poles for the working of SRM is in a linear manner. Here the torque phase is controlled by frequent switching of the reluctance path. This switching causes torque ripple in the output produced. This has an adverse effect on the efficiency of the system output. The switching of poles are done at a turn-on angle of  $40^\circ$  and a turn-off angle of  $75^\circ$ .

### Closed Loop System:

In the closed loop system, the rpm of the switched reluctance motor is taken from the output and fed to the control system. At the control system, the reference value of turn-on angle is kept at  $40^\circ$  and turn-off angle is at  $75^\circ$ . There, in the control system is the position sensor. In a Switched Reluctance Motor, the position sensor plays a major role in determining the rotor position. Unlike other types of motors such as Permanent Magnet Synchronous Motors (PMSM) or Induction Motors (IM), SRMs do not inherently produce a magnetic field, instead, they rely on the alignment of rotor and stator poles to generate torque. Hence, the precise control of the rotor position is essential for efficient operation. Then the error caused in the switching is corrected by giving the proper switching signals to the phase controller. Also the switching of different modes are controlled by the switches.

Here an SRG is used to generate a signal. Before entering the SEPIC converter, the AC output from the SRG is converted by a rectifier. The SEPIC converter is used to boost the signal. The phase controller controls the phases of the SRM by energizing the poles. The output from the SRM is taken as an error signal and fed to the integrated controller. The controller used here is the integrated PI controller. A 36V battery is used here. Also there is the bidirectional DC/DC converter.

### Open Loop System:

In the open loop system, the switching of the poles for the working of SRM is in a linear manner. Here the torque phase is controlled by frequent switching of the reluctance path. This switching causes torque ripple in the output produced. This has an adverse effect on the efficiency of the system output. The switching of poles is done at a turn-on angle of  $40^\circ$  and a turn-off angle of  $75^\circ$ .

### Closed Loop System:

In the closed loop system, the rpm of the switched reluctance motor is taken from the output and fed to the control system. At the control system, the reference value of turn-on angle is kept at  $40^\circ$  and turn-off angle is at  $75^\circ$ . There, in the control system is the position sensor. In a Switched Reluctance Motor, the position sensor plays a major role in determining the rotor position. Unlike other types of motors such as Permanent Magnet Synchronous Motors (PMSM) or Induction Motors (IM), SRMs do not inherently produce a magnetic field, instead, they rely on the alignment of rotor and stator poles to generate torque. Hence, the precise control of the rotor position is essential for efficient operation. Then the error caused in the switching is corrected by giving the proper switching signals to the phase controller. Also the switching of different modes are controlled by the switches.

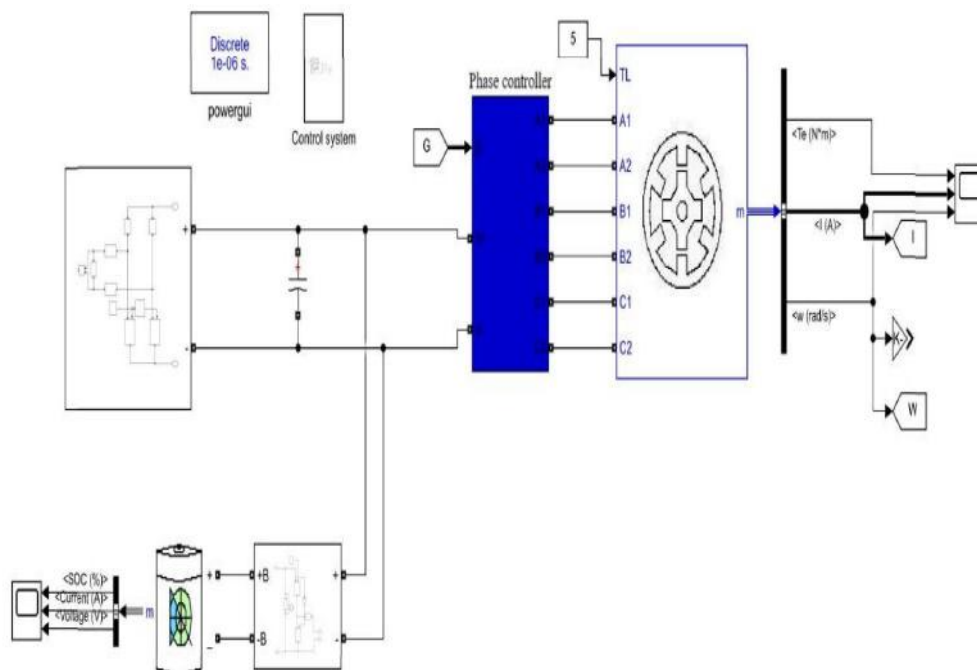


Figure 2. Open loop system simulation.

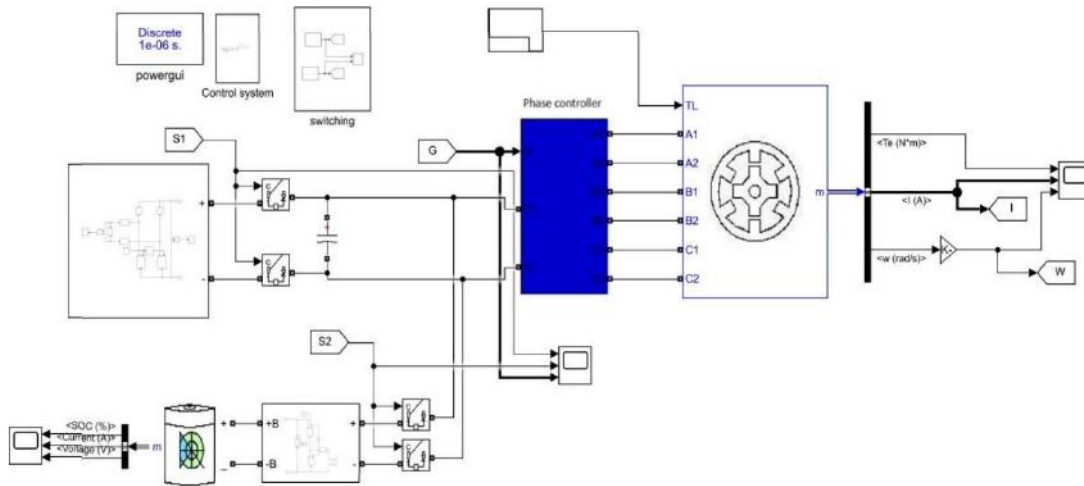


Figure 3. Closed loop system simulation.

**Subsystem: Control System**

The SRM’s rpm is fed to the position sensor, where it is compared with ideal turn-on and turn-off angles. From there the error is detected and the corrected angle is given. This corrected output is given as input to the phase controller. The phase controller chooses the next pole in the switched reluctance motor which is needed to be energized. The driving modes are also controlled in the control system. The switching is changed according to the load of the vehicle.

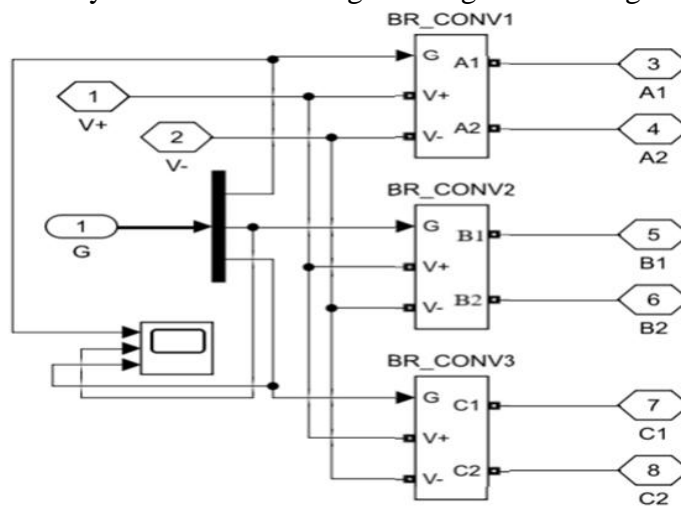


Figure 4. Control system

**Subsystem: Phase Controller**

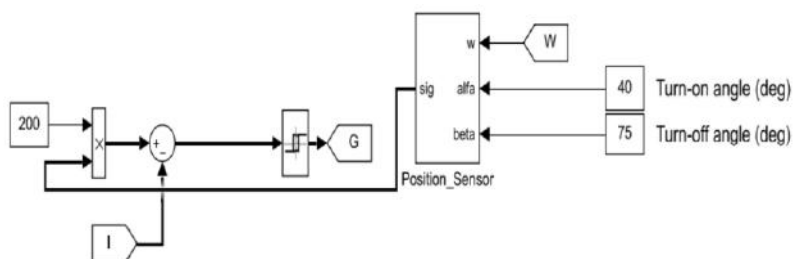


Figure 5. Phase controller

Phase controller is a device which is critical in determining the alignment of stator and rotor poles. Closed-loop phase control is incorporated here. The output from the control system is the input in the

phase controller. This signal energizes the windings of the SRM. This approach offers robust performance across a wide range of operating conditions and can compensate for variations in motor parameters or external disturbances

### **Conclusion:**

By analyzing the open loop and closed loop systems for phase controlling in a switched reluctance motor, it can be seen that the closed loop system reduces the torque ripple in an SRM. In conclusion, this research paper has successfully addressed the critical issue of torque ripple reduction in Switched Reluctance Motors (SRMs). Through the implementation of closed-loop phase control strategy and experimental validation, significant advancements have been achieved in mitigating torque fluctuations during motor operation. By leveraging sophisticated control algorithms and innovative techniques, including sensor-based feedback and optimized phase control, the study has demonstrated remarkable reductions in torque ripple across various operating conditions. These findings not only contribute to the advancement of SRM technology but also hold substantial implications for enhancing the efficiency, reliability, and performance in an electric vehicle. Moving forward, continued research in this domain is crucial for further refining control methodologies and unlocking the full potential of SRMs.

### **References:**

1. Kiyota, Kyohei; Sugimoto, Hiroya; Chiba, Akira (2014). Comparing Electric Motors: An Analysis Using Four Standard Driving Schedules , IEEE Industry Applications Magazine.
2. Bilatiu, Cristina-Adina, Cosman, Sorin Iulian; Martis, Radu-Andrei; Martis, Claudia Steluta; Morariu, Silvan (2019) ,Identification and Evaluation of Electric and Hybrid Vehicles Propulsion Systems.
3. Takahiro Kamagai, Daisuke Sato, Jun-ichi Itoh, Torque ripple reduction method for SRM based on mathematical model considering voltage limitation.
4. heng, He, Chen, Hao, Wang, Qing (2019),An Integrated Drive Power Converter Topology for Plugin Hybrid Electric Vehicle with G2V, V2G and V2H Functions, 22nd International Conference on Electrical Machines and Systems (ICEMS).
5. He Cheng, Lunjun Wang, Lei Xu, Xudong Ge and Shiyang Yang, An Integrated Electrified Powertrain Topology with SRG and SRM for Plug-In Hybrid Electrical Vehicle.
6. Yukun Ding, Kexun Yu, Ning Tao, Jiasong Wang, Patrick J Palanas, Xianfei Xie, Operation Control Strategies for Switched Reluctance Motor Driven Flywheel Energy Storage System With Switching Angle Optimazation.
7. Iiham Akbar, Nanang Ismail, Eki Ahmad Zaki Hamidi, Diky Zakaria PI based SRM speed control system.
8. R Nithya, R Sundaramoorthi. Design and implementation of SEPIC converter with low ripple battery current for electric vehicle applications.
9. Rahul Kumar Pandey, Prashant Tirkey, Sunil Kumar, Jitendra Nath Mahto. A Review on DC-DC Converters Used in Electric Vehicles.
10. P Bhavani Sree, N P G Bhavani. Efficiency Improvement of Electrical Vehicles Using Novel Switched Reluctance Motor and Compared with Permanent Magnet Motor by Reducing Power Loss.

# Application of Nature-Inspired Search Algorithms to Enhance Multi-Layer Thickness Optimization in Solar Cells

<sup>1</sup>Okram James singh, <sup>2</sup>Chingakham Foren, <sup>3</sup> Soibam Milan Singh, <sup>4</sup>Sm Nawaj Sarif, <sup>5</sup> Laishram Arun Singh, <sup>6</sup>Sailesh Irungbam, <sup>7</sup>Romesh Laishram

<sup>1,2,3,4,5,6</sup>Department of Electrical Engineering, Manipur Institute of Technology, Manipur University campus, Canchipur, Manipur- 795003, India

<sup>7</sup>Department of Electronics & Communication Engineering, Manipur Institute of Technology, Manipur University campus, Canchipur, Manipur- 795003, India

*Abstract: Thin-film solar cells typically follow a stacked structure in their design. It's vital to optimize the thickness of each layer in this stack to maximize the solar cell's efficiency. While the brute-force method can determine the optimal thickness of each layer, it requires a high computational time to compute in a multi-layer solar cell. Therefore, in this paper, we propose the application of nature-inspired search algorithms to find the optimal thickness of each layer. The simulation study carried out using a P3HT-based solar cell structure shows that the proposed strategy takes less time to find the optimal thickness compared to the brute-force method*

**Keywords:** Plug-in electric vehicles, SMC Controller

## Introduction:

Solar cells play a crucial role in modern society as a source of renewable energy. Solar power utilizes the sun's radiant heat and light for electricity generation, supporting solar architecture and thermal energy production [1]. The optimized architecture of solar cells is of paramount importance as it affects the conversion of solar energy to electrical energy. From the design of solar cell device perspective, it is generally available as dual junction or multi-junction solar cell. In recent years researchers have focused on the design of multilayer solar cell. The study in [2] explores the efficiency of perovskite-silicon tandem solar cells and investigates the impact of surface roughness and perovskite layer thickness on their performance. A design and analysis of multi-layer silicon nanoparticle solar cells is provided in [3], where range of silicon nano-particles are investigated for improved electrical performance. A multi-layer InGaAs/GaAs quantum dot solar cell is proposed in [4], where the impact of spacer layer thickness on photocurrent density is investigated. In [5], a multilayer dye-sensitized solar cells based on TiO<sub>2</sub> and ZnO is proposed which is able to produce high current density resulting in high efficiency. Recently, organic solar cells (OSC) have gained popularity which can generate large scale power and less expensive as compared to conventional solar cells [6]. A multilayer OSC is proposed in [7], aiming to maximize light absorption by optimizing the total number of excitons created within the multilayer structure as a function of layer thickness.

The main objective of designing multilayer solar cells is to optimize power output under specific solar spectra. These cells are constructed by stacking individual layers sequentially. A crucial factor in multilayer solar cell design is the thickness of each layer, which produces an optimum output power. Simulations of optoelectronic devices have contributed to comprehending and developing more finely tuned structures, approaching the theoretical maximum efficiencies. A simulation study of c-Si solar cells has been carried by the authors in [8] to discover optimized device structures. Nevertheless, the parameter sweep method remains the predominant approach for obtaining results across a wide range



of parameter values. However, this brute-force method which takes large computation time is often inefficient when the user seeks only the final optimized device structure. To alleviate this issue, nature-inspired search algorithms can be deployed to find the optimal multi-layer solar cell structure. An optimization of a multi-layer OSC is proposed in [9], in which genetic algorithm (GA) is employed for finding the thickness of the optical layers. It was shown in this experiment that GA found the optimal thickness much faster than brute force method. The proposed method took less time to search for the optimal thickness values as compared to brute force method. In another approach [10], Artificial Rabbits Optimization (ARO)–based optimization technique was proposed for the optimization of a multi-layer perovskite solar cell.

In this paper, we investigate the application of popular nature-inspired search algorithms to find the thickness of the optical spacer layers in a multi-layer OSC. This article seeks to empirically validate the hypothesis that nature-inspired algorithms outperform brute-force method in tasks like optimizing optoelectronic device structures.

### Methodology:

In this section methodology for finding thickness of the optical spacer layer is presented. The methodology is depicted in Figure 1. It consists of two important sub-blocks for simulation. First the organic solar cell is constructed in Lumerical, finite difference time domain (FDTD) solutions. The second module is the optimizer where the thickness of solar cell is generated and supplied to FDTD system to find the current density. Iteratively, the optimized block finds the best thickness values that generate maximum current density. The sub-modules are described below.

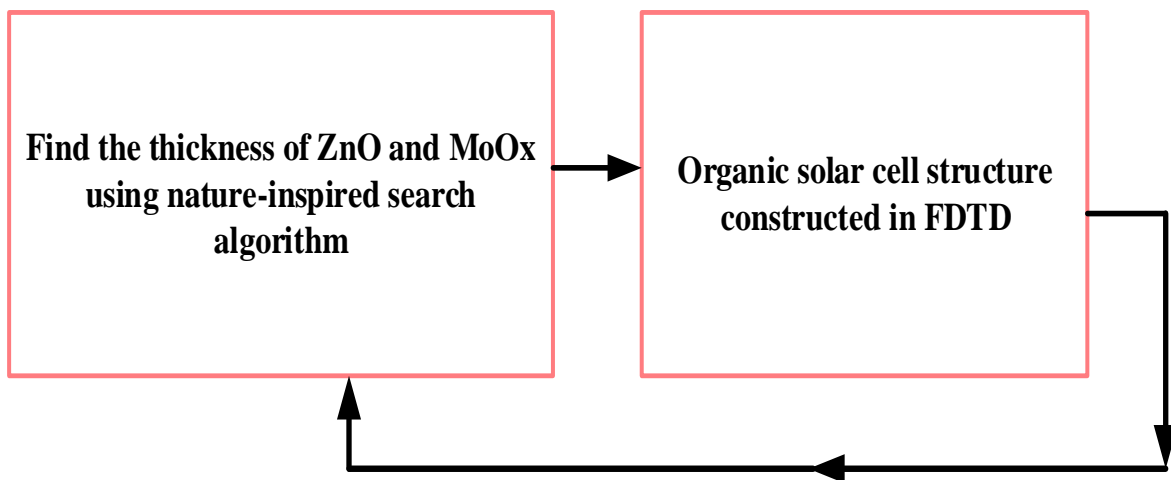


Figure 1 : Proposed methodology

### Solar cell structure

The structure of the multi-layer OSC used in this study is shown in Figure 1.

The structure comprises a 150 nm layer of indium tin oxide (ITO), as utilized in our prior investigation [11]. The aluminum (Al) layer's thickness was fixed at 100 nm, as light is fully reflected from the Al electrode at this thickness. Further increasing its thickness would not impact the results of our optical simulations. The active layer, consisting of poly (3-hexylthiophene) (P3HT): indene-C60 bisadduct (ICBA), was set at 200 nm due to its demonstrated efficiency in [12]. The charge transport layers, zinc oxide (ZnO) and molybdenum oxide (MoOx), serve as both charge carriers and optical spacer layers and

are adjustable parameters in our simulation. For a material to qualify as an optical spacer, it must possess refractive index properties that can modify the distribution of the light-induced electric field within the solar cell structure by varying its thickness. ZnO has previously been identified as a suitable optical spacer in [11]. While the ITO/poly (3,4-ethylenedioxythiophene):poly(styrenesulfonate) (PEDOT:PSS)/P3HT:phenyl-C61-butyric acid methyl ester (PCBM)/ZnO/Al structure is more commonly used in solar cells [13], PEDOT:PSS lacks the necessary refractive index to control the electric field distribution for the wavelengths under consideration. MoOx was identified as a suitable replacement for PEDOT:PSS as a hole transport layer in a study by Bohao et al. [14].

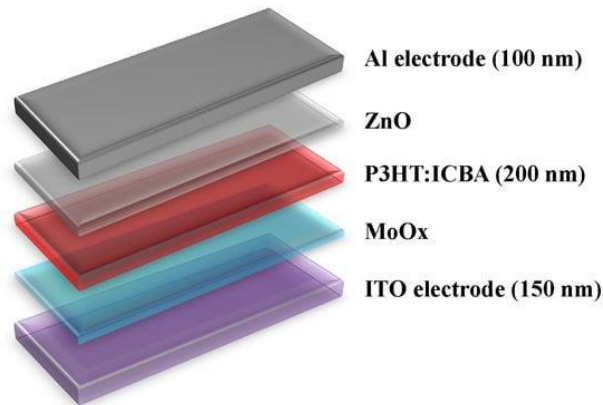


Figure 2: Organic solar cell structure [9]

**Result and discussion:**

At initially the motor is began to rotate in Constant speed by varying torque by SMC Controller. From 0-2 sec the motor will operate and rotate in 1500 RPM and settle downs to settled rpm. At that time the torque will have some fluctuations of +- 50 and it began to stable in a linear way by SMC Controller.

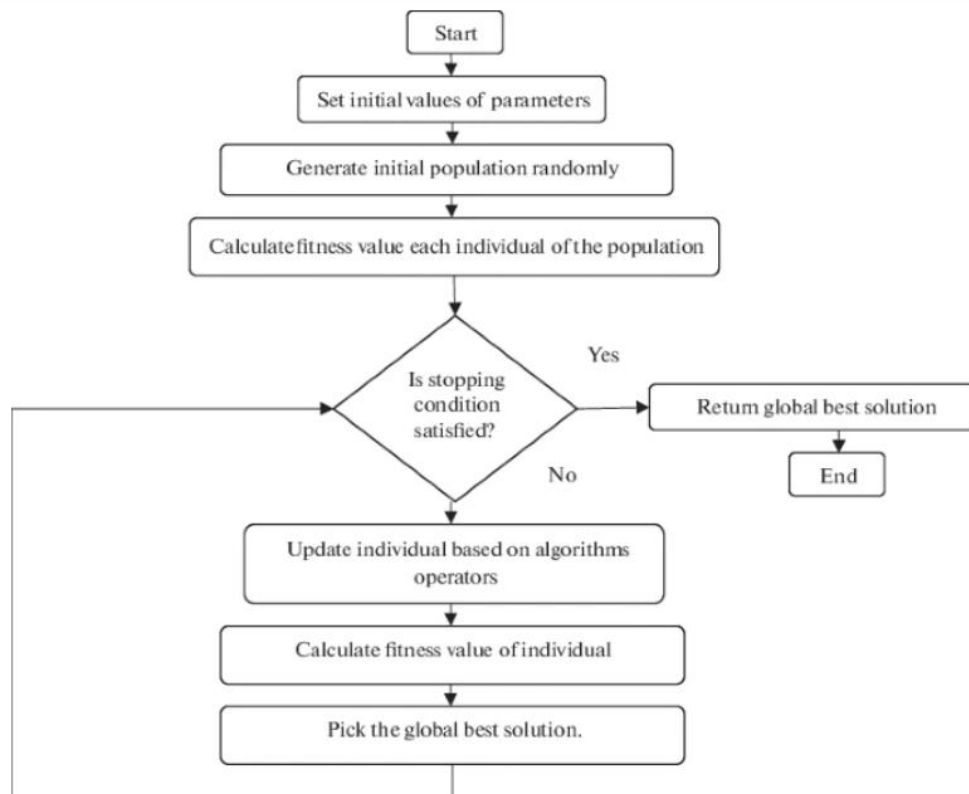


Figure 3 General Flowchart of Nature-Inspired Optimization Algorithms.

### Problem statement :

The main objective of this work is to determine the optimal thickness of the ZnO and MoOx optical spacer layers in a multilayer organic solar cell, as described in section 2.1, using nature-inspired search algorithms outlined in section 2.2. A search algorithm aims to find the best or optimal value of a search variable by minimizing or maximizing a fitness function, which depends on the problem being addressed. In this study, the thickness values obtained from the search algorithm are given as input into the FDTD system, where the organic solar cell is simulated to calculate the short-circuit current density ( $J_{sc}$ ), which serves as the fitness function. Finally, the problem statement addressed in this work is formulated as follows:

To find the thickness combination of ZnO and MoOx optical space layers via nature-inspired search algorithm that maximize  $J_{sc}$  output from the FDTD simulation.

### Result:

In this section, the simulation results are presented. The search space for the thickness of ZnO and MoOx are set in the range [0 30 nm] and [0 80 nm] respectively. The brute-force method can take large number of simulations to find the optimal thickness. For brute-force approach, the thickness of the ZnO layer was increased by 1 nm, ranging from 0 to 80 nm, whereas the MoOx layer underwent the same increment from 0 to 30 nm. For this search space, a total of 2511 simulations were conducted to determine the optimal thicknesses for the optical spacer layers, resulting in 24 nm for ZnO and 8 nm for MoOx. Therefore, computational cost and time taken by brute force method is expensive. The nature-inspired search algorithms can be applied so that less simulations are required to find the optimal thickness values. The comparative results of the five nature-inspired algorithms for the optimization process is shown in Figure 4. The figure shows the convergence of each algorithms for 100 iterations i.e. it depicts the number of simulation it took to find the optimal thickness values of ZnO and MoOx that produces the maximum current density ( $J_{sc}$ ), which is the goal of this simulation. It can be observed from this graph that TSA and PSO algorithms took less number of simulations for the optimization process. However, it can also be observed that all the nature-inspired search algorithms took lesser number of simulations as compared to brute-force method in finding the optimal thickness values of ZnO and MoOx optical space layers, which completes the man objective of this study. The simulation time taken by each algorithm is also given in Table 1.

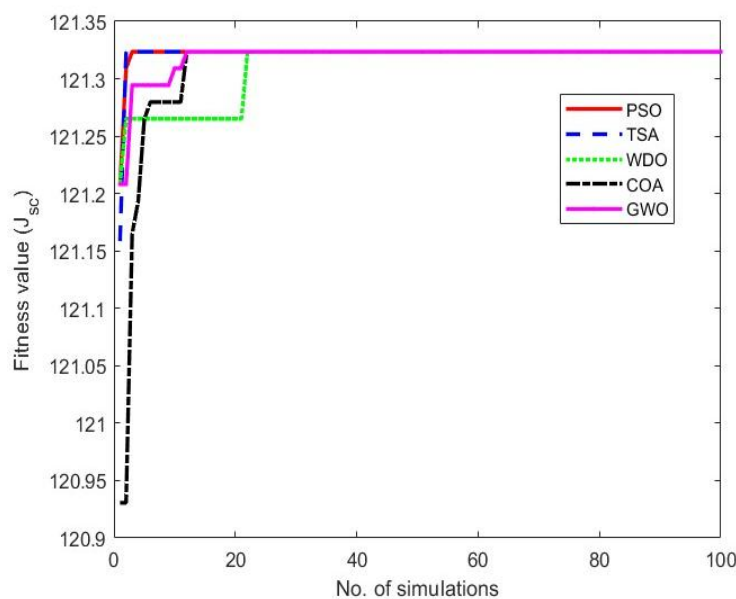


Figure 4: Comparative results in terms of convergence

Table 1: Time taken to complete the simulation

Sl. No.	Algorithm	Elapsed time (in seconds)
1	PSO	0.15
2	TSA	0.32
3	WDO	0.41
4	COA	0.60
5	GWO	0.58

### Conclusion:

In this paper, we have investigated the application of nature-inspired search algorithms for thickness optimization of a multilayer organic solar cell. A simulation study was carried out to find the optimal thickness of ZnO and MoO<sub>x</sub> optical space layer of the solar cell. The simulation results have demonstrated that nature-inspired search algorithms took lesser number of simulations to find the optimal thickness as compared to brute-force method. In future, the proposed technique can be applied to different solar cell structure to evaluate its effectiveness.

### References:

1. Ali O M Maka, Jamal M Alabid, Solar energy technology and its roles in sustainable development, *Clean Energy*, Volume 6, Issue 3, June 2022, Pages 476–483.
2. S. Akhil, S. Akash, Altaf Pasha, Bhakti Kulkarni, Mohammed Jalalah, Mabkhoot Alsaiani, Farid A. Harraz, R Geetha Balakrishna, “Review on perovskite silicon tandem solar cells: Status and prospects 2T, 3T and 4T for real world conditions”, *Materials & Design*, Vol. 211,2021,110138.
3. Mirnaziry, S.R., Shameli, M.A. & Yousefi, L., “Design and analysis of multi-layer silicon nanoparticle solar cells.”, *Sci Rep* 12, 13259 (2022).
4. Anjali Rai, Syed Sadique Anwer Askari, Mukul Kumar Das, Subindu Kumar, Efficiency enhancement of solar cells using multi-layer interdiffused InGaAs/ GaAs quantum dots: A numerical approach, *Micro and Nanostructures*, Volume 172, 2022, 207445.
5. Bhatti, K. A., Khan, M., Saleem, M., Alvi, F., Raza, R., & Rehman, S. U. (2019). Analysis of multilayer based TiO<sub>2</sub> and ZnO photoanodes for dye-sensitized solar cells. *Materials Research Express*, 6(7), 075902.
6. Solak EK, Irmak E. Advances in organic photovoltaic cells: a comprehensive review of materials, technologies, and performance. *RSC Adv.* 2023 Apr 19;13 (18):12244-12269.
7. Zhang, C., Tong, S. W., Jiang, C., Kang, E., Chan, D., & Zhu, C. (2008). Efficient multilayer organic solar cells using the optical interference peak. *Applied Physics Letters*, 93(4).
8. Andreani, L. C., Bozzola, A., Kowalczewski, P., Liscidini, M., & Redorici, L. (2018). Silicon solar cells: toward the efficiency limits. *Advances in Physics: X*, 4(1), 1548305.
9. Vincent P, Cunha Sergio G, Jang J, Kang IM, Park J, Kim H, Lee M, Bae J-H. Application of Genetic Algorithm for More Efficient Multi-Layer Thickness Optimization in Solar Cells. *Energies*. 2020; 13(7):1726.
10. Bayoumi ASA, El-Sehiemy RA, Badawy M, Elhosseini M, Aljohani M, Abaza A. Optimizing Multi-Layer Perovskite Solar Cell Dynamic Models with Hysteresis Consideration Using Artificial Rabbits Optimization. *Mathematics*. 2023; 11(24):4912.
11. Vincent, P.; Song, D.S.; Jung, J.H.; Kwon, J.H.; Kwon, H.B.; Kim, D.K.; Choe, E.; Kim, Y.R.; Kim, H.; Bae, J.H. Dependence of the hybrid solar cell efficiency on the thickness of ZnO nanoparticle optical spacer interlayer. *Mol. Cryst. Liq. Cryst.* 2017, 653, 254–259.

12. Vincent, P.; Shin, S.C.; Goo, J.S.; You, Y.J.; Cho, B.; Lee, S.; Lee, D.W.; Kwon, S.R.; Chung, K.B.; Lee, J.J.; et al. Indoor-type photovoltaics with organic solar cells through optimal design. *Dyes Pigment*. 2018, 159, 306–313.
13. Jouane, Y.; Colis, S.; Schmerber, G.; Kern, P.; Dini, A.; Heiser, T.; Chapuis, Y.A. Room temperature ZnO growth by rf magnetron sputtering on top of photoactive P3HT: PCBM for organic solar cells. *J. Mater. Chem*. 2011, 21, 1953–1958.
14. Li, B.; Ren, H.; Yuan, H.; Karim, A.; Gong, X. Room-Temperature, Solution-Processed MoO<sub>x</sub> Thin Film as a Hole Extraction Layer to Substitute PEDOT/PSS in Polymer Solar Cells. *ACS Photonics* 2014, 1, 87–90.
15. Zhongqiang Ma, Guohua Wu, Ponnuthurai Nagarathnam Suganthan, Aijuan Song, Qizhang Luo, Performance assessment and exhaustive listing of 500+ nature-inspired metaheuristic algorithms, *Swarm and Evolutionary Computation*, Volume 77, 2023,101248,

# Automatic Solar Classifier

Abdul Hadi C<sup>1</sup>, Adeb T<sup>2</sup>, Muhammed Harshad C<sup>3</sup>, Ansif Mohammed T<sup>4</sup>, Jithin Mohan<sup>5</sup>

<sup>1,2,3,4</sup>UG Student, Dept. Of EEE, MEA Engineering College, Perinthanna, Kerala, India.

<sup>5</sup> Assistant professor, Dept. Of EEE, MEA Engineering College, Perinthanna, Kerala, India.

Emails: <sup>1</sup>abdulhadi.caa@gmail.com, <sup>2</sup>adeebtmusthafa@gmail.com, <sup>3</sup>harshadmuhammed21@gmail.com, <sup>4</sup>[ansifmohammed124@gmail.com](mailto:ansifmohammed124@gmail.com) <sup>5</sup>[jithinmohan033@meae.edu.in](mailto:jithinmohan033@meae.edu.in)

**Abstract:** *This work introduces an innovative solution to address the issue of reduced efficiency in solar panels due to the accumulation of dust on their surfaces. The proposed system is an Arduino-based solar panel cleaning mechanism designed for cost-effectiveness, automation, and remote control. The three-step cleaning mechanism involves an exhaust fan functioning as an air blower, a wiper for dust removal, and a water splashing pipe for thorough cleaning. A DC motor powers the wiper, blower, and water pump, making the system efficient and practical for both rural and urban areas. Experimental results demonstrate the system's capability to operate with an impressive efficiency range of 87-96%, effectively tackling various types of contaminants such as sand and dirt. This novel cleaning approach presents a promising solution to enhance the performance and longevity of solar panels in diverse environmental conditions.*

**Keywords:** *Solar panel, Arduino nano, Bluetooth connectivity*

## Introduction:

In the pursuit of a sustainable environment, solar energy emerges as a pivotal player, offering an abundant, inexhaustible, and environmentally friendly energy source. Its direct applicability for electrical power generation across residential, commercial, and industrial sectors makes solar energy a compelling solution. Unlike conventional energy sources, solar power generation poses no threat to the environment or human health, emitting no harmful gases during the energy conversion process. Notably, the vast solar energy potential is exemplified by the fact that the total sunlight hitting the earth's surface in an hour and a half can meet the world's annual energy consumption, as indicated by the US Department of Energy. In the context of solar energy systems, photovoltaic (PV) solar panels play a crucial role by harnessing continuous solar energy to generate DC electricity. To optimize the energy output from PV systems, a maximum power point tracking (MPPT) method based on a fuzzy logic controller is introduced. Once solar panels are installed, the cost of fuel becomes negligible, offering an economically advantageous and sustainable energy solution. However, despite being a clean and renewable energy source, solar panels require regular maintenance to ensure optimal efficiency. The accumulation of dust particles on solar panels, primarily originating from urban and industrial activities, poses a significant challenge. Various dust particles, including SiO<sub>2</sub>, Al<sub>2</sub>O<sub>3</sub>, Fe<sub>2</sub>O<sub>3</sub>, CaMg(CO<sub>3</sub>)<sub>2</sub>, Ca(OH)<sub>2</sub>, CaO, and CaCO<sub>3</sub>, have been identified on the solar panel surface. This accumulation adversely affects the system's efficiency, with an estimated 50% reduction and a potential 15% power loss in dry areas. Recognizing the critical importance of maintaining a clean solar panel surface, this paper introduces an automatic solar panel cleaner. The proposed system, driven by an Arduino-based design, aims to address the challenges of dust accumulation efficiently, ensuring sustained high performance and longevity of solar energy systems in diverse environmental conditions. This proposed automatic cleaning system is not only geared towards improving the overall efficiency of solar panels but also stands out for its economic viability. By integrating these three cleaning steps, the system aims to provide a comprehensive and efficient solution to the challenges associated with dust accumulation on solar panels, contributing to the sustained performance and longevity of solar energy systems in various environmental contexts.

### System architecture:

The system consists of solar panel, rtc, bluetooth module, blower fan for blowing air, dc motor, water pump for spraying, arduino nano, motor drive, wiper for wiping panel.

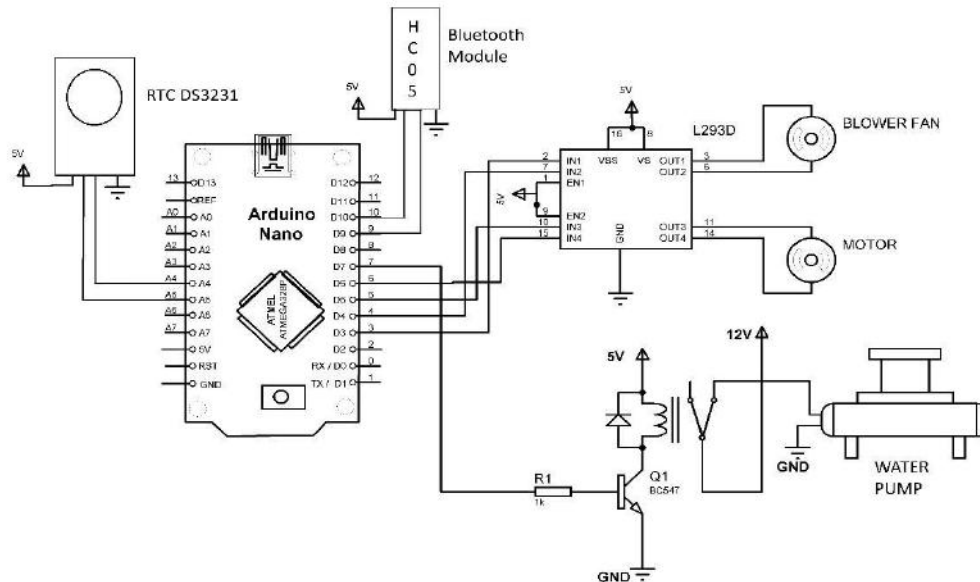


Fig 1. Automatic solar cleansifier circuit diagram

**Solar panel:** Solar panels are devices that convert sunlight into electricity through the photovoltaic effect. They are made up of individual solar cells, typically composed of silicon, which generate direct current (dc) electricity when exposed to sunlight. solar panels can be used to power various applications, from small calculators and lights to large-scale residential and commercial buildings. the efficiency of solar panels varies depending on factors such as the quality of the materials used, the angle and orientation of the panels, and environmental conditions. Solar energy is renewable and environmentally friendly, as it produces electricity without emitting greenhouse gases or other pollutants. Solar panels require minimal maintenance and have a lifespan of 25 years or more. The cost of solar panels has been decreasing steadily over the years, making solar energy increasingly competitive with traditional fossil fuels. Solar panels can be installed on rooftops, in solar farms, or integrated into building materials like solar roof tiles. Advances in technology, such as thin-film solar cells and concentrated solar power systems, continue to improve the efficiency.

**RTC:** The DS3231 is a highly accurate real-time clock (RTC) module manufactured by Maxim Integrated. It is widely used in electronic devices requiring precise timekeeping.

**Arduino Nano:** The arduino nano is a compact and versatile microcontroller board based on the atmega328p microcontroller, which is the same chip used in the popular arduino uno board

**Motor Drive:** he l293d is a popular integrated circuit (ic) commonly used in robotics and motor control applications. it is a dual h-bridge motor driver ic, which means it can control the direction and speed of two dc motors independently.

**Pump:** A water pump is a mechanical device used to move water from one place to another. it's a vital component in various applications, including residential, commercial, agricultural, industrial, and



environmental settings.

**Bluetooth Module:** The hc-05 bluetooth module is a simple bluetooth spp (serial port protocol) module that allows for the setup of a transparent wireless serial connection. its communication is via serial communication which makes an easy way to interface with the controller or pc.

### **Working :**

Solar panel cleaner system could work with three sequential mechanisms: air blowing, water spraying, and wiping with a wiper, operating consecutively every three days:

#### **1. Air Blowing Mechanism:**

On the first day of the cycle, the system activates the air blowing mechanism to remove loose debris, dust, and particles from the surface of the solar panels. Fans or compressed air nozzles positioned above the panels blow air across the surface, dislodging and blowing away any accumulated debris. This initial step prepares the panels for deeper cleaning by removing larger particles that could hinder the effectiveness of subsequent cleaning methods.

#### **2. Water Spraying Mechanism:**

On the second day of the cycle, the system initiates the water spraying mechanism to wash away remaining dirt and residues from the panels. Nozzles or sprinklers located above the panels spray water onto the surface, effectively rinsing and cleaning the panels. The water helps to dissolve and flush away stubborn contaminants, leaving the panels clean and ready for optimal sunlight absorption.

#### **3. Wiping with Wiper Mechanism:**

On the third day of the cycle, the system activates the wiper mechanism equipped with soft brushes or wiper blades to provide a final cleaning. The wiper mechanism traverses across the surface of the panels, gently wiping away any remaining dirt or streaks. This wiping action ensures a thorough and streak-free cleaning, maximizing the efficiency and performance of the solar panels.

#### **4. Control System:**

A central control unit or microcontroller manages the sequential operation of the cleaning mechanisms based on a predefined schedule. The control system coordinates the activation of each mechanism in sequence, ensuring that the cleaning process is thorough and efficient. Sensors may be incorporated to monitor environmental conditions and adjust the cleaning schedule as needed, for example, delaying cleaning during rainy or windy weather.

### **Result and discussion:**

The cleaning efficiency of the automatic solar cleaner was evaluated through three mechanisms: blowing air, water splashing, and wiping. Individually, blowing air effectively removed loose debris, while water splashing dislodged adhered dirt, and wiping provided a thorough clean. Combining blowing air with water splashing enhanced efficiency, and further adding wiping achieved the highest cleaning effectiveness. The synergy between these methods ensured a spotless finish by addressing different types of contaminants. Energy efficiency was considered, with blowing air being the most energy-efficient option, though overall energy consumption of the combined mechanism should be noted. Adaptability to various conditions and maintenance requirements were also assessed, highlighting the need for long-term functionality and cost-effectiveness. Future improvements could focus on optimizing each mechanism, integrating smart technology for real-time monitoring, and exploring alternative cleaning agents for challenging stains.

### **Conclusion:**

The proposed automatic solar panel cleaning system, constructed from easily accessible components, proves to be an economical and water-efficient solution. Through a three-step mechanism involving exhaust fans for air blowing, a solenoid valve for water flow, and a wiper for the final touch,

the system successfully removes dust without causing scratches, as evidenced by experimental tests. This design not only ensures the safety of the solar panels but also minimizes water wastage, making it an environmentally conscious choice. The system's capability to serve its intended purpose underscores its practicality and effectiveness in maintaining the optimal performance of solar panels. As a cost-effective and reliable solution, this cleaning system stands as a viable option for enhancing the efficiency and longevity of solar power installations

### References:

1. H. Hottel and B. Woertz,, "Performance of flat plate solar-heat collectors, "Trans.ASME (Am. Soc. Mech. Eng.); (United States), vol. 64, 1942.
2. Ali Omar Mohamed, Abdulazez Hasan, "Effect of Dust Accumulation on Performance of Photovoltaic Solar Modules in Sahara Environment" Journal of Basic and applied scientific Research, Volume 2, Issue11, Pages 11030-11036.
3. Shaharin A. Sulaiman ``Effects of Dust on the Performance of PV Panels` International Journal of Mechanical, Aerospace, Industrial, Mechatronics and Manufacturing Engineering Vol:5, 2011.
4. Satish patil, Mallaradhya H M (2016) design and implementation of microcontroller based automatic dust cleaning system for solar panel. international journal of engineering research and advanced technology (ijerat) issn: 2454-6135 special volume. 02 issue.01, may-2016
5. K. P. Amber *et al.*, "A self-cleaning device for pole mounted solar photovoltaic installations," Thermal Science, vol. 23, no. 2A, pp. 739- 49, 2019.
6. Syafaruddin, F. A. Samman, Muslimin, and S. Latief, "Design of automatic control for surface cleaning system of photovoltaic panel," ICIC Express Letters, Part B: Appl., vol. 8, no. 11, pp. 1457-64, 2017.
7. H. Kawamoto, "Electrostatic cleaning equipment for dust removal from soiled solar panels," J. of Electrostatics, vol. 98, pp. 11-16, 2019.
8. M. Mazumder *et al.*, "Characterization of electrodynamic screen performance for dust removal from solar panels and solar hydrogen generators," IEEE Trans. Ind. Appl., vol. 49, no. 4, pp. 1793-1800, 2013.
9. B. Parrott, P. C. Zanini, A. Shehri, K. Kotsovos, and I. Gereige, "Automated, robotic dry-cleaning of solar panels in Thuwal, Saudi Arabia using a silicone rubber brush," Solar Energy, vol. 171, pp. 526- 33, 2018.
10. S. Alagoz and Y. Apak, "Removal of spoiling materials from solar panel surfaces by applying surface acoustic waves," J. Cleaner Production, vol. 253, 2020, 119992.

# Dual Powered Smart Street Light with Fault Recognition

Adarsh Joseph<sup>1</sup>, Rojin Manuel<sup>2</sup>, Traies Rose Thomas Kurian<sup>3</sup>, Noyal Thomas<sup>4</sup>, Kanaka Xavier<sup>5</sup>

<sup>1,2,3,4</sup>UG Student, Dept of EEE, Albertian Institue Of Science And Technology, Kalamassery

<sup>5</sup>Associate Professor, Dept of EEE, Albertian Institue Of Science And Technology, Kalamassery

Email: <sup>1</sup>adarshj11@gmail.com, <sup>2</sup>rojinmanuel05@gmail.com, <sup>3</sup>traiesrose2002@gmail.com ,

<sup>4</sup>noyalt16@gmail.com, <sup>5</sup>kanakaxavier@aisat.ac.in

**Abstract:** *Street light automation is quite common these days, but generating the required energy for the streetlight from the speed breaker is latest trend in the technology. Therefore, the aim is to generate electric energy from the speed breaker, store it into a battery, and utilize the stored energy when required. To prove this concept practically, a prototype module is constructed with spring loaded type mechanical structure, which is aimed to generate energy whenever some force is applied to its surface. Entire system is designed, as automatic, human involvement is not required for switching on/off the light. Speed breaker is designed using electro-mechanical technology, and to generate electricity one small DC motor is used. This motor functions like dynamo and its shaft is coupled with mechanism through geared wheel.*

*Whenever the speed breaker is pressed, motor shaft will be rotated automatically, and the motor generates a maximum voltage of 12 V. Solar energy also plays a major role in our project. We know how impactful and efficient the solar energy is. By combining these two ways of power generation we can create more efficient and sustainable energy. The voltage generated by the motor is regulated and it is used to charge the battery, here a heavy-duty battery of 6V/4.5AH is used for long back-up time. The streetlight is designed with 20 high-glow cool LED's and it is powered through automatic trigger circuit designed with 555-timer chip. The streetlight will be energized automatically in the evening and it will be de-energized in the morning. LDR is used for sensing the natural light. As it is a prototype module, lower ratings of power devices are used, for real applications high power devices must be used.*

**Keywords:** speed breaker, fault recognition, solar, street light, power generation

## Introduction:

As the availability of conventional energy declines, there is need to find alternate energy sources. All most all the state electricity departments in our country, they are unable to supply the power according to the demand. The power produced by these companies is not even sufficient for domestic utilities; in such critical situation it is very difficult to divert the energy for other public needs. There by an alternative source must be discovered, many people propose for solar energy, but it is going to be a costliest affair, moreover availability of solar energy is poor particularly in rainy and winter seasons, as a result it is not dependable. Hence an alternative cheapest method must be determined for few applications; consequently, this project work has been taken up, which is aimed to generate electricity from speed breaker mechanism. Out of the many alternative energy resources, this technology described in this project report is the ultimate source of all known forms of energy. It is clear, safe, and free, does not pollute the environment and thus will be an extremely viable alternative in the days to come. As our road traffic is increasing day by day, and vehicles are running one after another continually at high ways as well as in the cities, the speed breaker mechanism generates nonstop energy, which can be stored and utilized to energize the street lights. Here the concept is to convert the mechanical energy in to electric energy.

To prototype module is constructed with low power rating electrical devices, this is aimed to prove

the concept practically. The entire system obtains energy from the battery; additional power source is not required. To charge the battery, the mechanism must be activated continuously. To activate the mechanism human efforts are required, because it is a prototype module and it cannot be used for real applications, therefore running vehicles over this mechanism is not possible. So for demo purpose, the battery can be charged through mains. To estimate the energy potential at particular place, where this kind of speed breaker mechanism is to be installed, detailed information about the traffic density must be collected properly, if nonstop traffic flow is expected, there this system can be used for efficient results. Utility of energy is also important; it should not be wasted because it is precious. Therefore, the produced energy can be utilized properly at that particular point by energizing a suitable streetlight arranged near the speed breaker.

**Problem statement:**

Comparing to the current scenario there are many defects in our street lighting system. Because of that many bad impacts are caused for our country. Let's go through some of the problems we are facing

**A. Inefficiency**

Current street lights we have in our country is very less efficient and most of them doesn't work properly. Lack of power supply and maintenance is the main reason for this. We see many reports about this in the newspapers and social medias. Current street lights often rely on outdated technology, such as incandescent or fluorescent bulbs, which are inefficient in terms of energy consumption. Additionally, many street lights lack smart technology for adaptive brightness control, resulting in unnecessary energy wastage during off-peak hours. Retrofitting existing infrastructure with energy-efficient LED lights and implementing smart lighting systems could significantly reduce energy consumption and maintenance costs. By implementing this project we can successfully overcome this problem forever.

**B. Energy sustainability**

Energy sustainability involves responsibly managing resources to meet present needs without compromising the ability of future generations to meet their own needs. This includes prioritizing renewable energy sources like solar, wind, and hydroelectric power, which have minimal environmental impact and are replenishable. Implementing energy-efficient technologies and practices across sectors is crucial for reducing carbon emissions and mitigating the impacts of climate change on our planet's ecosystems.

**C. Energy efficiency**

Implementing smart street lights powered by a combination of speed breaker-generated kinetic energy and solar energy can significantly reduce operational costs by minimizing reliance on grid electricity. These systems utilize renewable sources to generate electricity, reducing long-term energy expenses while also promoting sustainability. Additionally, the incorporation of smart technology allows for efficient fault detection and maintenance, further optimizing operational efficiency and minimizing downtime.

**D. Traffic safety**

Incorporating smart street lights powered by speed breaker-generated kinetic energy and solar energy can enhance traffic safety by ensuring consistent illumination even during power outages. These lights provide reliable visibility, reducing the risk of accidents and improving overall road safety, especially in areas prone to blackouts or low visibility conditions. Moreover, the smart technology integrated into these lights enables real-time monitoring of traffic patterns and road conditions, allowing for timely adjustments to optimize safety measures.

## Methodology:

The methodology for the dual powered street light with fault recognition;

### A. Principle of working:

The principle of the electric power generation using speed breaker mechanism is very simple. It is based on the same principle as in the case of electricity generation in case of hydroelectric power plant, thermal electric power plant, nuclear power plant, geothermal energy, wind energy, tidal energy etc. In all of the above power plant mechanical energy is converted into electrical energy [9]. In this setup also mechanical energy is converted into electrical power using a D.C. generator. The project is concerned with generation of electricity from speed breakers-like set up. The load acted upon the speed breaker - setup is there by transmitted to rack and pinion arrangements. Here the reciprocating motion of the speed-breaker is converted into rotary motion using the rack and pinion arrangement [6]. The axis of the pinion is coupled with the sprocket arrangement. The sprocket arrangement is made of two sprockets. One of larger size and the other of smaller size. Both the sprockets are connected by means of a chain which serves in transmitting power from the larger sprocket to the smaller sprocket[1].

As the power is transmitted from the larger sprocket to the smaller sprocket, the speed that is available at the larger sprocket is relatively multiplied at the rotation of the smaller sprocket. The axis of the smaller sprocket is coupled to a gear arrangement. Here we have two gears with different diameters. The gear wheel with the larger dimension is coupled to the axis of the smaller sprocket. Hence the speed that has been multiplied at the smaller sprocket wheel is passed on to this gear wheel of larger dimension. The smaller gear is coupled to the larger gear. So as the larger gear rotates at the multiplied speed of the smaller sprocket, the smaller gear following the larger gear still multiplies the speed to more intensity. Hence, although the speed due to the rotary motion achieved at the larger sprocket wheel is less, as the power is transmitted to gears, finally the speed is multiplied to a higher speed.

This speed which is sufficient to rotate the rotor of a generator is fed into to the rotor of a generator. The rotor which rotates within a static magnetic stator cuts the magnetic flux surrounding it, thus producing the electric motive force (emf). This generated emf is then sent to an inverter, where the generated emf is regulated. This regulated emf is now sent to the storage battery where it is stored during the day time. This current is then utilized in the night time for lighting purposes on the either sides of the road to a considerable distance.

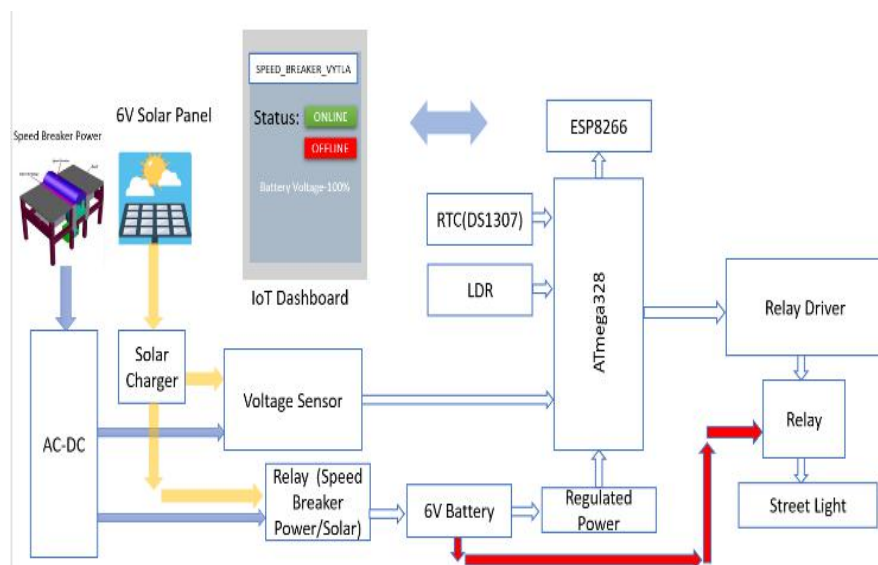


Fig 1: Block diagram of dual powered smart street light

## B. Speed breaker mechanism

The mechanical structure that contains four legs system is considered as motion converter, the mechanical motion created by the vehicle is converted into the electrical energy, there by it is called as motion converter. In general, any motion converter that generates electricity by applying some force will be constructed by implementing electro-mechanical techniques. In this regard here a simple spring loaded type mechanism is designed, whenever some force is applied manually to its surface, the mechanism will be pulled down by which the chain drive system rotates the motor shaft through its pinion. It works on the principle of simple physics i.e. in practical it works on the principle that when a moving vehicle passes through this set up, the kinetic energy of vehicle will cause roller to rotate which will further rotate transmission shaft and hence the generator armature (i.e. acting as prime mover to run generator). The electrical device used to generate electricity is a simple DC motor; this motor shaft is coupled with the moving mechanism. A small pinion with fewer teeth is synchronized with the chain, when the mechanism is pulled down, this motor rotates in clock wise, similarly when the mechanism is released, due to its spring action it moves to its home position. In this condition, the motor rotates in anti-clock wise. There by the motor rotates in both directions, is that when the vehicle moves over the inclined plates, the motor rotates in both directions and generates energy in the form of two peak levels. The mechanical structure is constructed with square type of steel pipes, the speed breaker mechanism is constructed with inclined plates, when the plates come down, and this in turn rotates a geared shaft loaded with recoil springs. The output of this shaft is coupled to a dynamo to convert kinetic energy into electricity. This the basic principle involved in it.

## C. Chain sprocket mechanism

The chain sprocket used mainly converts the input linear motion into rotational motion to the shaft. The rotation of shaft will act as an input for dc generator which will produce the desired electrical output. Chain and sprocket is useful for when the distance between shafts is relatively large compared to the desired size of the gearing. The sacrifice is typically strength as solid gear teeth are usually stronger than chains. The reason a bike uses a chain and sprocket is that the desired distance between shafts would be inconvenient for gear to gear meshing. Now one could consider a driveshaft like a car but it would be heavier, more awkward to package, and not gain anything relevant in terms of durability. And remember lighter is better for bicycles. So in short, chain and sprocket is the lightest transmission possible that would deliver durability that consumers demand. And that's to say nothing of Derailleur mass vs gearbox for multiple speeds.

Bicycles that use shaft drives, a type of rack-and-pinion gear mechanism, have too many disadvantages for mainstream adoption, but they have persisted in niche markets for over a hundred years, mostly through novelty appeal. For instance, the Sonoma D-drive pictured below is sold at Walmart as a commuter bike. Shaft drives never caught on like chain-and-sprocket designs for several reasons. The main problems are weight, higher cost, added complexity, more difficult maintenance, and lower mechanical efficiency. The deal-breaker is that every problem solved by a shaft drive can be solved with a chain case, except for the utter impossibility of looking cool while riding a bike with a chain case. In that regard, the shaft drive wins [7].

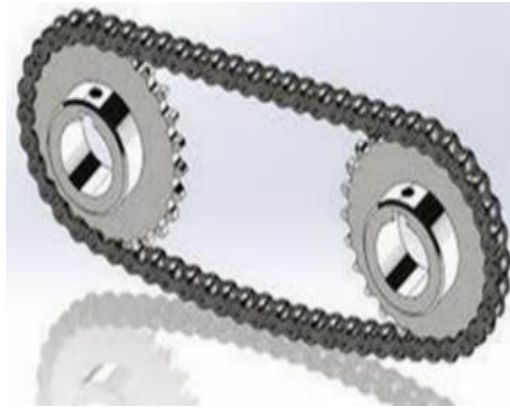


Fig 2: Chain and Sprocket

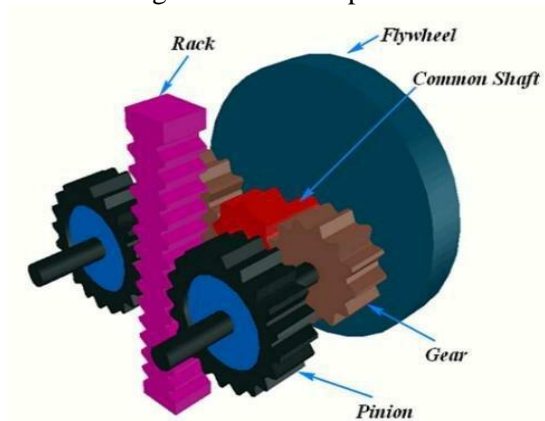


Fig 3: Gear and Sprocket

#### D. Spring coil mechanism

**Spring Coil Mechanism** A coil spring functions by storing energy in order to release it, absorb shock or maintain force between two surfaces. If you apply too much force, you can stretch a spring beyond its limit which will permanently distort the spring. The most common type of spring is the coil spring, which is made out of a long piece of metal that is wound around itself. Coil springs were in use in Roman times, evidence of this can be found in bronze Fibulae the clasps worn by Roman soldiers among others. These are quite commonly found in Roman archaeological digs. Coil springs can be either compression springs, tension springs or torsion springs, depending on how they are wound. A coil spring is a mechanical device which is typically used to store energy and subsequently release it, to absorb shock, or to maintain a force between contacting surfaces. They are made of an elastic material formed into the shape of a helix which returns to its natural length when unloaded. They are commonly used in mattresses, automotive suspensions, and residential plumbing. Coil springs come in a variety of sizes and shapes and can be used for a variety of applications. Small coil springs are often used in electronic devices, while larger ones are used in automobile suspensions. Coil springs can be made from various materials, including steel, brass, and bronze [6][8].

By following to this comprehensive methodology, the smart street light with fault recognition powered by speed breaker and solar energy can be implemented. Continuous refinement, informed by real-world feedback, becomes integral to the project's success and scalability. This iterative process allows for adjustments that enhance efficiency and address specific community needs, ultimately contributing to the long-term viability and positive impact of the initiative.

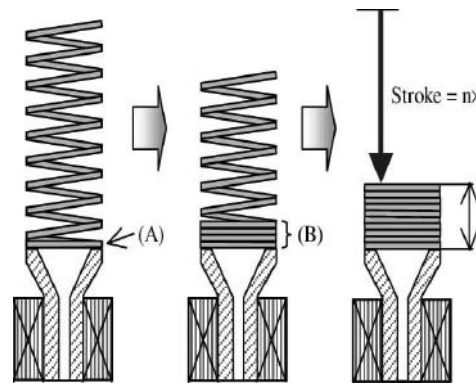


Fig 4: Spring Coil Mechanism

### Ault Recognition and Smart Street Lighting:

Fault recognition is a main part in our project. This automation helps in detecting the faults that happen in the system that will restrict the light to come out.

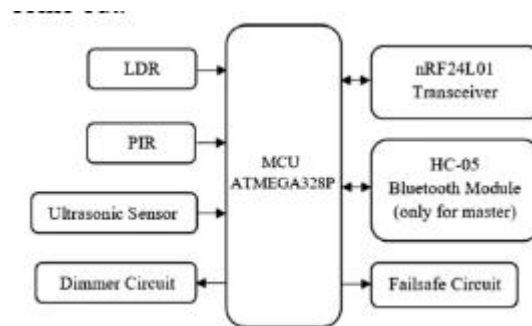


Fig 5: Block diagram for fault recognition and smart street lighting

#### A. Fault recognition

Fault recognition in street lights encompasses the monitoring of parameters like power consumption, light intensity, and operational status. Sensors or remote monitoring systems facilitate this continuous surveillance, ensuring prompt identification of deviations from expected values. Such anomalies serve as triggers for alerts or notifications, prompting swift maintenance or repair actions to uphold uninterrupted illumination and energy efficiency.

The use of sensors enables real-time data collection, allowing for proactive fault detection before issues escalate. By swiftly addressing faults, municipalities can minimize downtime and optimize energy consumption. Remote monitoring systems offer the convenience of centralized oversight, streamlining maintenance efforts across large urban areas. In essence, fault recognition systems play a pivotal role in maintaining reliable street lighting infrastructure. Through proactive monitoring and prompt responses to deviations, these systems contribute to enhanced safety, energy efficiency, and overall urban quality of life.

#### B. Smart street lighting:

Smart street lighting systems represent a transformative approach to urban lighting management, harnessing advanced technologies to enhance efficiency and functionality. These systems integrate sensors, wireless connectivity, and data analytics to enable intelligent control of street lights. By incorporating motion sensors and ambient light sensors, smart street lights can dynamically adjust brightness levels based on real-time traffic flow and natural lighting conditions, conserving energy and improving visibility while minimizing light pollution [2].

Moreover, remote monitoring and control capabilities allow for proactive maintenance, with system administrators promptly alerted to faults or malfunctions. This facilitates swift repairs, reducing



downtime and ensuring uninterrupted illumination throughout the city. Furthermore, the integration of environmental sensors provides valuable data on air quality and other factors, supporting urban planning initiatives and fostering healthier, more livable communities. Overall, smart street lighting systems offer a holistic approach to urban lighting management, promoting energy efficiency, safety, and sustainability in cities worldwide.

### Solar Power:

Solar street lights consist of a few key parts. The most important is the solar panel, which uses the photovoltaic effect to convert sunlight into electricity. This electricity then travels to a charge controller. The controller's job is to regulate the charging process and prevent the battery from overcharging, which can damage it. The electricity is stored in a rechargeable battery, typically a lithium-ion battery for its efficiency. Finally, at night, the stored energy from the battery powers the LED light source in the street lamp [10].

Solar street lights offer a number of advantages. They are completely reliant on solar power, meaning they don't require any connection to the electricity grid. This translates to significant cost savings on electricity bills in the long run. Additionally, solar street lights are low maintenance because they have no wires to bury or replace, and the LED lights themselves last for years. They also contribute to environmental benefits by relying on a clean and renewable energy source, reducing greenhouse gas emissions.

### Result and discussion:

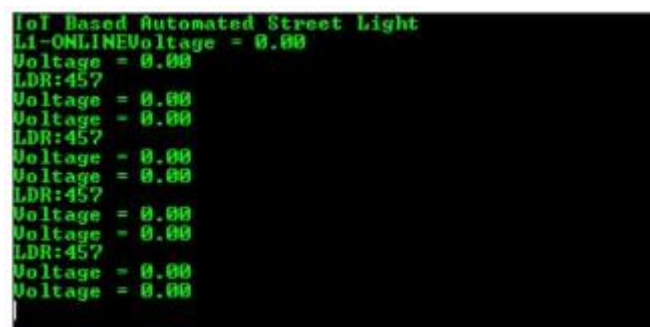
We utilized Proteus, a proprietary software suite crucial for electronic design automation. This tool is pivotal for electronic design engineers and technicians, aiding in the creation of schematics and electronic prints for manufacturing printed circuit boards [11]. Our project involved constructing a circuit diagram derived from the block diagram illustrated in Figure 1.

Through Proteus, we conducted simulations under three distinct conditions. These simulations aimed to test the functionality and performance of the circuit under varying parameters. Upon analysis of the results, we observed trends and discrepancies across the different conditions.

These findings provided insights into the circuit's behavior and its response to changing inputs. The simulations facilitated the identification of potential issues and optimizations, enhancing the overall design process. Leveraging Proteus for simulation allowed us to iteratively refine and validate the circuit design before physical implementation. Ultimately, this approach contributed to the development of a robust and optimized electronic system for our project. [12].

The conditions and results are given below.

I. When both solar and speed breaker is turned off



```
IoT Based Automated Street Light
Li-ONLINE Voltage = 0.00
Voltage = 0.00
LDR:457
Voltage = 0.00
Voltage = 0.00
LDR:457
Voltage = 0.00
Voltage = 0.00
LDR:457
Voltage = 0.00
Voltage = 0.00
LDR:457
Voltage = 0.00
Voltage = 0.00
```

Figure1 : Speed changes with respect

```

LDR:457
Voltage = 6.02
Voltage = 0.00
LDR:457
Voltage = 6.02
Voltage = 0.00
LDR:457
Voltage = 6.02
Voltage = 0.00
LDR:457
Voltage = 6.02
Voltage = 0.00
LDR:457
Voltage = 6.02
Voltage = 0.00

```

Figure 2: Result of condition II

Voltage when both speed breaker and solar is switched on

```

Speed Breaker -POWER ON
Voltage = 6.02
Voltage = 11.98
LDR:457
Speed Breaker -POWER ON
Voltage = 6.02
Voltage = 11.98
LDR:457
Speed Breaker -POWER ON
Voltage = 6.02
Voltage = 11.98
LDR:457
Speed Breaker -POWER ON
Voltage = 6.02
Voltage = 11.98

```

Figure 3: Result of condition III

### Calculation For Power Developed:

Let us consider that the mass of a vehicle moving over the speed breaker is 250 kg approximately. Let the height of the speed breaker on the road is 10 cm. We know that the work done is equal the product of force and distance. Here the force is equal to weight of the body; i.e. 2425.5 N. Distance travelled by the body means the height of the speed breaker. After getting the work done we have to find the output power. That is work done by 60 seconds. So we get the output power as 4.085 W for one pushing force. This is the power developed for 1 minute. Power developed for 1 hour is equal to 240.25 W and for 24 hours is equal to 5.866 kW. This much of energy is enough to burn 4 to 5 street lights.

### Novelty:

Integrating fault recognition technology into smart street lights represents a significant advancement in urban infrastructure management. By deploying a network of sensors within the street lights, the system gains the ability to continuously monitor their operational status. These sensors can detect various faults, ranging from electrical malfunctions to physical damages caused by accidents or environmental factors. Upon detecting a fault, the system promptly alerts maintenance teams through a centralized monitoring platform. This proactive notification system enables swift response and repair, minimizing downtime and ensuring consistent illumination along the streets. As a result, pedestrian safety is enhanced, and the overall functionality of the urban environment is improved.

Furthermore, the integration of speed breaker and solar energy harvesting mechanisms adds a layer of sustainability to the smart street light system. Speed breakers are equipped with kinetic energy harvesting technology, which converts the mechanical energy generated by passing vehicles into electrical power. This energy is then stored and utilized to supplement the electricity generated by solar panels during

periods of low sunlight or high energy demand. By harnessing renewable energy sources like solar and kinetic energy, the smart street light system reduces its dependence on conventional power grids. This not only decreases carbon emissions but also contributes to the resilience of the urban infrastructure by diversifying its energy sources. In addition to environmental benefits, this innovative approach offers economic advantages by lowering energy costs and reducing the frequency of maintenance interventions. Over time, the cumulative savings from reduced energy consumption and optimized maintenance operations contribute to the overall efficiency of municipal budgets [3].

Overall, the integration of fault recognition technology, coupled with energy harvesting from speed breakers and solar panels, represents a holistic and sustainable solution for urban lighting infrastructure. It not only enhances safety and efficiency but also aligns with the global imperative of mitigating climate change and fostering environmental stewardship in urban areas

### **Conclusion:**

This innovative concept falls under the purview of nonconventional energy resources, offering a promising alternative to traditional energy sources [4] spiral spring [5]. Among the various alternative energy resources, solar energy stands out as a dependable source, albeit at a considerable cost. Conversely, generating electricity from a speed breaker presents itself as a more economical alternative. The technology showcased here represents an incredibly inexpensive source of energy, surpassing many other known forms. In practical implementation, each speed breaker, depending on its size and traffic flow, has the potential to produce tens of kilowatts of power every day. This generated power can be effectively utilized for a myriad of applications. Given the objective of highways to facilitate the free flow of traffic without impediments, traditional speed breakers pose a challenge. However, in urban areas where traditional speed breakers are ubiquitous and road traffic is constantly increasing, the integration of this technology presents an opportune solution. By retrofitting existing speed breakers with this technology, all street lights within a particular city can be effectively energized, providing illumination while simultaneously harnessing renewable energy from the kinetic motion of vehicles.

### **References:**

1. Electricity generation using Power hump with automatic street light control” by Kuldeep Singh Chauhan, Ayushi Tomar, Dheeraj Kumar, Gaurav kumar, Journal of Engineering Sciences, Volume 14 issue 06, 2023
2. “Automatic Street Light Generation Through Speed Breakers” Ikalithkar Sridevi,2 Bedadam Nithish,3Mrs.Ch.Sarita , International Journal of Engineering and Technical Research ISSN:2321-0869, Special issue
3. Mukherjee Chakrabarti, 2005, “Fundamentals of renewable energy systems”, New Age international limited publishers, New Delhi, New Age International, 2014.
4. Sharma.P.C, 2003, “Non-conventional power plants”, Public printing service, New Delhi , Energy Procedia ,Volume 118, August 2017, Pages 104-109
5. Krishna, G.V., Srinivasarao, S., Sriharsha, P., Neerav, B.V., and Satyasai, G.E. (2019).” Modeling and Analysis of Flat Spiral Spring Based Speed Breaker Device for Generation of Electricity”.
6. Ijmer, J., and Mr., A.S. (2015). “Air Compression and Electricity Generation by Using Speed Breaker with Rack And Pinion Mechanism”.
7. Watts,G., “Effects of speed distribution on the Hormonoise model predictions”, Inter-noise Conference, Prague, 2004.
8. “Production of electricity by the method of road power generation”, IJAEEE, 2010 .
9. Deshpande, S., Kulkarni, B., and Joshi, A. (2016). “Electricity Generation Using Speed

Breaker”.

10. Bintu, MdFaiyad Bin et al. “Hybrid Power Generation using Speed Breaker.” 2022 International conference.
11. Satar, Mohamad Nasrul Abdul; Ishak, Dahaman (2011). "Application of Proteus VSM in modelling brushless DC motor drives". 2011 4th International Conference on Mechatronics (ICOM). pp. 1–7
12. Zhenwei, Han; Kefei, Song (2011). "Design of thermostat system based on Proteus simulation software". Proceedings of 2011 International Conference on Electronic & Mechanical Engineering and Information Technology. pp. 1901–1904

# Failure Modes and Effects Analysis of Power Transformer

<sup>1</sup> Abhijith A, <sup>2</sup> Prof. Valsa Basil

<sup>1</sup>UG student, Dept. of EEE, Marian Engineering College Thiruvananthapuram

<sup>2</sup>Assistant Professor, Dept. of EEE, Marian Engineering College Thiruvananthapuram

**Abstract:** *Failure Mode and Effects Analysis (FMEA) is a critical technique used to evaluate the reliability and enhance the design of power transformers. It involves identifying key failure modes, including insulation breakdown, winding faults, core faults, tank faults, and accessory faults, and understanding the causes and effects associated with each. FMEA helps prioritize these failure modes based on factors like severity, frequency, and detection. Preventive measures such as surge protection, temperature monitoring, and maintenance are recommended to address these issues. Additionally, FMEA plays a crucial role in determining the consequences of each failure mode on equipment performance, safety, and economics. It offers valuable insights for condition monitoring, predictive maintenance, and overall asset management, contributing to the design of more reliable and safer transformers.*

**Key Words:** *FMEA, Transformers.*

## Introduction:

Since the advent of electricity, human beings have been using Power transformers to transmit electrical power between generators and distribution networks. The major issue occurs when the Transformer fails or is rendered inoperable for extended periods of time. This is very undesirable since electricity plays a central role in almost all day to day activities of any average human being, without electricity it would not be easy to manage the proper upkeep of most facilities, infrastructures, functioning of factories, establishments and other institutions. The significance of power transformers in ensuring the efficiency and reliability of power transmission networks is undeniable. However, their elevated cost and inherent risk due to the substantial oil content and high voltage elements necessitate a meticulous approach to mitigate potential hazards, especially concerning fire and explosion in abnormal circumstances or technical failures. To address this, a strategic focus on planning and prioritizing efforts is crucial to enhance overall system reliability and reduce the risk of transformer failures. The initial phase of a comprehensive system reliability study often involves the implementation of the Failure Modes and Effects Analysis (FMEA), a vital method for risk assessment and management through meticulous failure analysis. FMEA serves as a qualitative analysis, encompassing a detailed listing of failure modes, potential causes for each failure, the effects of such failures, and their severity. Moreover, FMEA incorporates recommendations for corrective actions, contributing to a proactive strategy for risk mitigation [1].

Failure Mode and Effects Analysis (FMEA) stands as a critical methodology in ensuring the robustness and operational reliability of power transformers within energy transmission networks. The application of FMEA in the realm of power transformers involves a meticulous examination of potential failure modes, their causes, and the effects these failures could have on transformer functionality. By systematically dissecting various failure scenarios, FMEA provides a comprehensive understanding of the vulnerabilities inherent in transformer systems. Failure Mode and Effects Analysis (FMEA) stands as a cornerstone practice across industries, pivotal in pre-emptively identifying and addressing potential risks and failures within systems, processes, or products. Its significance stems from multifaceted advantages that profoundly impact organizational success. FMEA's primary role lies in risk prevention, meticulously uncovering potential failure modes, their origins, and potential impacts. Armed with this insight, organizations proactively institute measures to curtail risks, drastically reducing the likelihood of failures. Moreover, the early detection and resolution of potential issues during the design or planning phases translate into substantial cost savings, circumventing expensive rework or recalls that could arise during

later developmental stages. This cost-efficiency is magnified by FMEA's ability to fine-tune product or process quality systematically, instigating enhancements that bolster reliability and customer satisfaction, amplifying competitiveness in the market.

### Applications of FMEA :

Failure Mode and Effects Analysis (FMEA) encompasses various types tailored to specific applications and industries. In the context of power transformers and other systems, common types include:

1. Design FMEA (DFMEA): Focuses on assessing and mitigating potential failure modes during the design phase of a product or system. In power transformers, this involves evaluating design aspects to enhance reliability and prevent failures in their construction.[4]

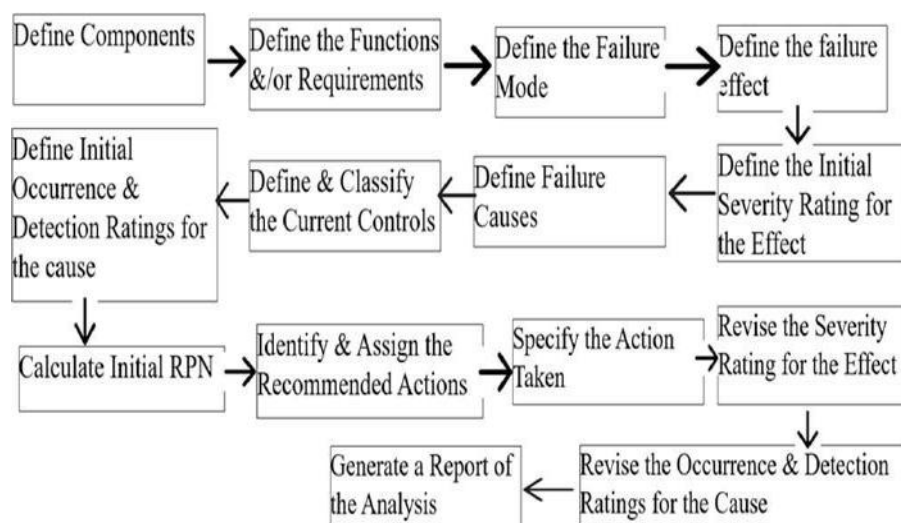


Fig. 1. Methodology of FMEA Block Diagram

2.Process FMEA (PFMEA): Concentrates on analyzing potential failure modes within manufacturing or operational processes. In power transformer manufacturing, PFMEA identifies and addresses process-related risks that could impact quality and reliability.[4]

3.System FMEA (SFMEA): Considers the overall system functionality, identifying potential failure modes that could occur due to interactions between various components or subsystems. In power transformers, SFMEA examines the entire system, including auxiliary systems and controls, to ensure overall reliability.[4]

4.Functional FMEA (FFMEA): Evaluates the potential failure modes based on specific functions or operations within a system. In power transformers, FFMEA focuses on critical functions like insulation, winding, and core operations to prevent failures impacting these functions.

5.Software FMEA (SW-FMEA): Addresses potential failure modes in software systems or applications. In the context of power systems, this could involve control software used in transformer monitoring and operations.

6.Hardware FMEA (HW-FMEA): Evaluates potential failure modes related to hardware components, including materials, electronic components, and physical structures. In power transformers, HW-FMEA might assess failure modes related to insulation materials or core components.

Each type of FMEA serves a specific purpose, aiding in the identification, assessment, and mitigation of potential failure modes across different stages of a product or system's life cycle, contributing to improved reliability and performance.

**FMEA Methodology :**

Artificial Intelligence The Failure Mode and Effects Analysis (FMEA) methodology follows a structured sequence of steps aimed at systematically identifying and mitigating potential failures in a system or process.

A) Comprehensive Component and Failure Mode Analysis.

1)Identifying the Components and Relationships:

In the context of a power transformer, the components might include the core, windings, insulation materials, cooling systems, tap changers, and various auxiliary devices. Matrix A, in this scenario, represents the relationships between these components and how they influence one another. For example, the windings’ integrity might influence the overall insulation effectiveness, while the core’s condition could impact cooling efficiency. This qualitative description helps understand how changes or failures in one component might affect others, forming a comprehensive view of the transformer’s interdependencies.

	U1	U2	U3	U4	
L1	1	0	0	1	Fig 1 : (load)component, Matrix A
L2	0	0	0	1	
L3	1	1	1	1	

	M01	M011	M012	M111	M0111	
M 01	0	1	1	0	0	Fig 2: Failure Modes Matrix , Matrix B
M 011	0	0	0	1	0	
M 012	0	0	0	0	1	
M 0111	0	0	0	0	1	
M01111	0	0	0	0	0	

Fig. 2. Matrices A and B

2)Identifying Failure Modes and Matrix Formation:

For a power transformer, failure modes might include insulation breakdown, winding faults like open circuits or short circuits, core issues such as mechanical damage, tank faults like leaks, and accessory failures in tap changers or cooling systems.[3] Using a coding system where the first two numbers represent components and subsequent numbers indicate affected failure modes, a matrix, let’s call it Matrix B, is formed. For instance, if 01 represents the core and 02 represents insulation breakdown, a cell in Matrix B could show how a core issue (01) might affect insulation breakdown (02) due to increased stresses. This matrix allows visualizing how component failures might propagate and affect other failure modes within the power transformer system.

**Severity, Occurance And Detection**

Severity

- 1 Category IV(Minor) primary function can be done but urgent repair is required.
- 2 Category III(Marginal) reduction in ability to primary function
- 3 Category II(Critical) causes a loss of primary function
- 4 Category I(Catastrophic) product becomes inoperative

Occurrence

- 1 Level E(Extremely Unlikely) A single failure mode probability of Occurrence is less than 0.001
- 2 Level D(Remote) A single failure mode probability is more than 0.001 but less than 0.01
- 3Level C(Occasional) A single failure mode probability is more than 0.01 but less than 0.10
- 4 Level B(Reasonably probable) Single failure mode probability is more than 0.10 but less than 0.20

5 Level A(Frequent) Single failure mode probability of occurrence is greater than 0.20

#### Detection

- 1.Level F- Good identification
- 2.Level E -Fair identification
- 3.Level D -Good detection and rough identification
4. Level C -Fair detection
5. Level B -Rough detection
6. Level A -Complementary test

#### **Risk Priority Numbering :**

Risk Priority Number (RPN) serves as a crucial tool in Failure Mode and Effects Analysis (FMEA), providing a quantifiable method to prioritize potential failure modes based on severity, occurrence, and detection ratings. Calculated by multiplying the severity, occurrence, and detection ratings assigned to each failure mode. The Risk Priority Number (RPN) in Failure Mode and Effects Analysis (FMEA) quantifies potential risks by multiplying Severity, Occurrence, and Detection ratings assigned to each failure mode RPN Calculation Formula:

$RPN = \text{Severity} \times \text{Occurrence} \times \text{Detection}$ .

Example Failure Mode: Failure Mode: Insulation Breakdown Ratings Assigned:

Severity: Category II (Critical) - Causes a loss of primary function.

Occurrence: Level C (Occasional) - Probability more than 0.01 but less than 0.10.

Detection: Level B (Rough Detection) - Detection capability is rough.

#### RPN Calculation:

$RPN = \text{Severity} \times \text{Occurrence} \times \text{Detection}$  Substituting the assigned ratings:

$RPN = \text{Category II} \times \text{Level C} \times \text{Level B}$  Assigning numerical values (these are arbitrary for this example):

Category II: Assigned a value of 3 • Level C: Assigned a value of 3

Level B: Assigned a value of 4 Calculating:  $RPN = 3 \times 3 \times 4 = 36$

Result: The RPN for the "Insulation Breakdown" failure mode in this example is 36. This value helps prioritize the failure modes within the FMEA, indicating the relative urgency of addressing this particular failure mode compared to others based on its Severity, Occurrence, and Detection characteristics.

#### **Findings:**

Advanced Sensor Technologies -The integration of advanced sensor technologies, particularly fiber optic sensing, holds immense potential for real-time monitoring within power transformers. Fiber optic sensors embedded within the transformer windings facilitate continuous monitoring of crucial parameters like strain, temperature, and gas concentrations. These sensors provide unparalleled accuracy and sensitivity, enabling precise detection and early warning of potential failure modes such as overheating, mechanical stress, or insulation degradation. The ability to capture these subtle changes in transformer conditions in real-time empowers proactive maintenance strategies, minimizing the risk of catastrophic failures and ensuring prolonged operational reliability

AI-Driven Predictive Analytics - The convergence of artificial intelligence (AI) and FMEA is poised to revolutionize predictive maintenance strategies for power transformers. AI algorithms, leveraging vast datasets from diverse sensors, historical records, and operational patterns, can discern intricate patterns and anomalies. By continuously analyzing this data, AI-powered systems can forecast potential failure modes with remarkable accuracy. These predictive insights enable utilities to proactively address emerging issues, optimizing maintenance schedules, and mitigating risks before they escalate[5]. This



sophisticated analysis not only enhances transformer reliability but also maximizes operational efficiency and minimizes unplanned downtime.

**Enhanced Diagnostic Tools-** The future of FMEA in power transformers involves the development of more sophisticated diagnostic tools and software. These tools would conduct comprehensive simulations and analyses, leveraging advanced computational models and simulations techniques. These advancements allow for more detailed evaluations of potential failure scenarios, providing deeper insights into transformer behaviour under various conditions. The predictive capability of these diagnostic tools aids in identifying vulnerabilities, estimating component lifespans, and optimizing maintenance schedules for proactive interventions, thereby ensuring optimal performance and reliability.

**Intelligent Maintenance Strategies -** The evolution of FMEA is steering towards intelligent maintenance strategies that align with smart grid technologies. The integration of FMEA insights with smart grid infrastructure enables real-time monitoring, control, and decision-making. This integration facilitates the implementation of adaptive maintenance schedules based on real-time performance data and predictive analytics. By focusing on critical areas prone to failure, utilities can optimize resource allocation, minimize downtime, and significantly enhance transformer reliability within the grid infrastructure.

**Continual Process Improvement -** The future of FMEA lies in continual refinement and improvement. By leveraging real-time operational data and learning from practical experiences, FMEA methodologies will continuously evolve to adapt to the evolving landscape of power transmission. Continuous feedback loops from maintenance actions and operational data will fuel ongoing improvements in analysis methodologies and preventive measures, ensuring the adaptability and effectiveness of FMEA in mitigating potential failure modes.

### **Conclusion:**

The essence of Failure Mode and Effects Analysis (FMEA) for power transformers lies in its pivotal role in preemptively identifying, mitigating, and preventing potential failure modes within these critical assets of the power grid. As an indispensable tool, FMEA not only enhances the operational reliability of power transformers but also contributes significantly to ensuring the stability and efficiency of the entire electrical infrastructure. By employing advanced sensor technologies, such as fiber optics for real-time monitoring, and integrating artificial intelligence for predictive analytics, the future of FMEA promises a paradigm shift in maintenance strategies[5]. This shift involves a transition from reactive to proactive measures, enabling utilities to anticipate potential failure modes and take preemptive actions. These advancements not only minimize the risk of catastrophic failures but also optimize resource allocation, thereby reducing downtime and enhancing overall operational efficiency. Furthermore, the continual evolution and refinement of FMEA methodologies, coupled with their integration with smart grid technologies, are driving the transformation of traditional maintenance approaches. This amalgamation empowers utilities with real-time insights, enabling adaptive maintenance strategies that focus on critical areas prone to failure, thereby ensuring a more robust and resilient power transmission network. In conclusion, the future of FMEA in power transformers embodies a proactive and adaptive approach, leveraging cutting-edge technologies, data-driven insights, and intelligent strategies. By fortifying transformers against potential vulnerabilities, FMEA stands as a cornerstone in safeguarding the reliability, resilience, and longevity of power grid assets, ensuring uninterrupted and efficient electricity supply for modern society's burgeoning energy needs.

### **References:**

1. Failure Modes and Effects Analysis (FMEA) for Power Transformers". By Mohsen Akbari, P. Khaz- aeeI. Sabetghadam and P. Karimifard.
2. Condition Monitoring of Power Transformer Using Failure Modes and Effects Analysis" ,By

Jaspreet Kaur ,Dr. Navneet Singh Bhangu

3. Model based FMEA for electronic products”. By Jingjing Cui, Yi Ren, Dezhen Yang, Shengkui Zeng
4. Deployment of an FMEA- Integrated Framework to Improve Operational Performance in Semiconductor Manufacturing: A Case Study”. By C F Liew,J Prakash , S Kamaruddin
5. Integration of Failure Modes and Effects Analysis (FMEA) in the Engineering Design Process.” By Hua- wei Wen
6. Evaluating Potential Failures of Power Transformer Using Failure Mode and Effects Analysis (FMEA)”By Jaspreet Kaur and Navneet Singh Bhangu
7. Failure Mode and Effect Analysis (FMEA) Implementation: A Literature Review” By Kapil Dev Sharma and Shobit Srivasthava.
8. Transformer Failure Analysis:Reasons and Methods”By Jaspreet Singh and Sanjeev Singh.
9. Comparative Study Of Quality Practices Between Japanese And Non-Japanese Based Electrical And Electronics Companies In Malaysia: a Survey “Md. Fauzi Bin Ahmad , Sha’iri Mohammed Yusof and Noordin Mohammed Yusof.
10. Application Of Fmea For Improvement In The Manufacturing Process Of Mobile Phones In a Factory Of The Industrial Pole Of Manaus” By Marcelo Oliveira Samuel BatistaDe’rcio Reis Gabriela Veroneze and Ra’issa Maciel.

# Efficient Dual Motor Power Train For Two-wheeled Electric-Cycle

Likhitha S Shenoi<sup>1</sup>, Salim C Shajahan<sup>2</sup>, Shoma Mani<sup>3</sup>

<sup>1,2</sup>UG student, Dept. of EEE, Mangalam College of Engineering, Ettumanoor, Kerala, India. <sup>3</sup>Assistant

<sup>3</sup>Assistant Professor, Dept. of EEE, Mangalam College of Engineering, Ettumanoor, Kerala, India

Email: <sup>1</sup> [likhithasshenoi@gmail.com](mailto:likhithasshenoi@gmail.com), <sup>2</sup> [salimchali321@gmail.com](mailto:salimchali321@gmail.com), <sup>3</sup> [shoma.mani@mangalam.in](mailto:shoma.mani@mangalam.in)

**Abstract:** *In this paper, as the market of two-wheeled Electric Vehicle is growing and it is to improve the efficiency of the electric power train. Most of the two-wheeled Electric Vehicles are either motor mounted in the wheel-hub or connected to the rear wheel through a transmission. In-wheel motor has a limited torque capacity whereas the other configuration the transmission reduces the system efficiency. So here this paper proposes a Dual-motor power-train topology which aims to combine the best of both configurations. To evaluate and compare the configurations, the energy consumption of the Single-motor and the Dual-motor topologies is calculated over a driving cycle. Here It is shown that Dual-motor topology is efficiently utilizes the available energy compared to Single-motor topology*

## Introduction:

India is the largest manufacturing country and market for two wheelers. This presents a great opportunity to have a greater impact on reducing emissions by replacing internal combustion engines in two-wheelers with electric power-trains. According to the unions of concerned scientists, the current cost of manufacturing a lithium-ion battery pack is around \$200/kwh. Improve system efficiency in electric vehicles. In this topology the in-wheel motors are connected to the front wheels. The chassis mounted engine is linked via a two-speed fixed gearbox. The main goal is to combine the two topologies to maximize battery usage. Bicycles have long been popular among people of all ages because they are lightweight, and require no maintenance or fuel costs. Cycling, like any other physical activity, contributes to health benefits. All normal bicycles are driven by people, so people tends to get tired and nervous when riding for long times. The advantage of the bicycle is that is combined with the additional engine power of the e-bike. An e-bike is an electric bicycle with an integrated electric motor that must be used for propulsion. A chassis-mounted motor is connected through a two-stage fixed transmission. The aim is to combine the best of the two topologies to maximize battery utilization. Unlike traditional trail usage, electric-assist modes enable users to reach higher speeds, cover longer distances, and transport more gear or equipment. These features can pose safety issues for hikers, conventional bicyclists, and horseback riders, who typically travel at slower speeds, cover shorter distances, and carry less equipment. This paper explores the development and implementation of an efficient dual motor power train for two-wheeled electric cycles. The dual motor configuration offers several advantages over traditional single motor systems, including improved torque distribution, better handling, and increased overall efficiency. By distributing the load between two motors, this approach can potentially reduce wear and tear on individual components, leading to a longer lifespan and lower maintenance costs. Our research focuses on the design, optimization, and testing of a dual motor powertrain system tailored for e-cycles. We aim to address key challenges such as energy management, motor synchronization, and control strategies to ensure a seamless and efficient riding experience. The findings of this study will provide valuable insights for manufacturers and designers in the e-cycle industry, contributing to the advancement of electric mobility solutions.

## Modeling And Simulation:

The model provides the charging and discharging curves based on the Shepherd's equations as given below.

Discharging

$$V_{batt} = E_0 - K \frac{Q}{Q - i t} - R i + A e^{-B t} - K \frac{Q}{Q - i^* t} \tag{1}$$

$$\text{Charging: } V_{batt} = E_0 - K \frac{Q}{Q - i t} - R i + A e^{-B t} - K \frac{Q}{Q - 0.1 Q i^*} \tag{2}$$

Where,  $V_{batt}$  = battery voltage (V)

$E_0$  = battery constant voltage (V)

$K$  = polarization constant (V/Ah) or polarization resistance ( $\Omega$ )

$Q$  = Battery capacity (Ah)  $i t = R i t =$  actual battery charge (Ah)

$A$  = exponential zone amplitude (V)

$B$  = exponential zone time constant inverse ( $\text{Ah}^{-1}$ )  $R$  = internal resistance ( $\Omega$ )

$i$  = battery current (A)

$i^*$  = filtered current (A)

By simulating the model with a delay block instead of the filter the ripple frequency was obtained and then the current filter was designed with the required time constant. The Lithium-ion (Li-ion) battery specifications: Voltage = 48V, Capacity = 6Ah.

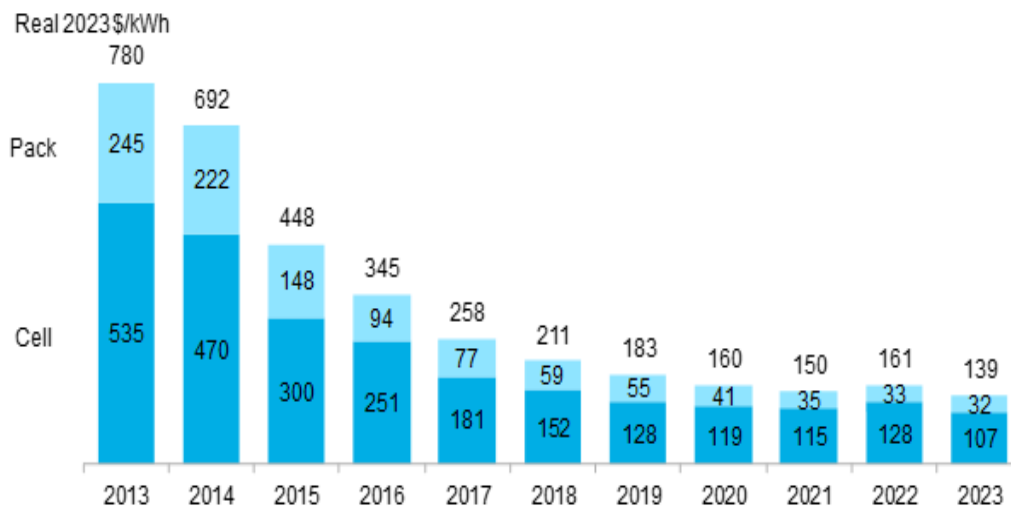


Fig: 1 Trend of battery manufacturing cost (Source: BloombergNEF)

**Vehicle Category & Specifications:**

$$F_{tractive} = [m a + 1/2 \rho C_d A V^2 + \mu m g + m g \sin \theta g]$$

When the vehicle is operating with wide open throttle (WOT), the vehicle starts accelerating and reaches the maximum speed of 80kmph in 48.2s.

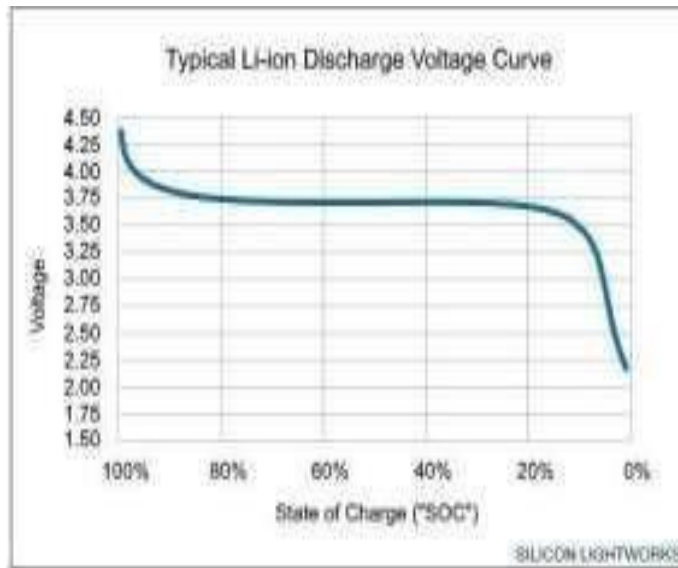


Fig: 2 Typical battery discharge curve

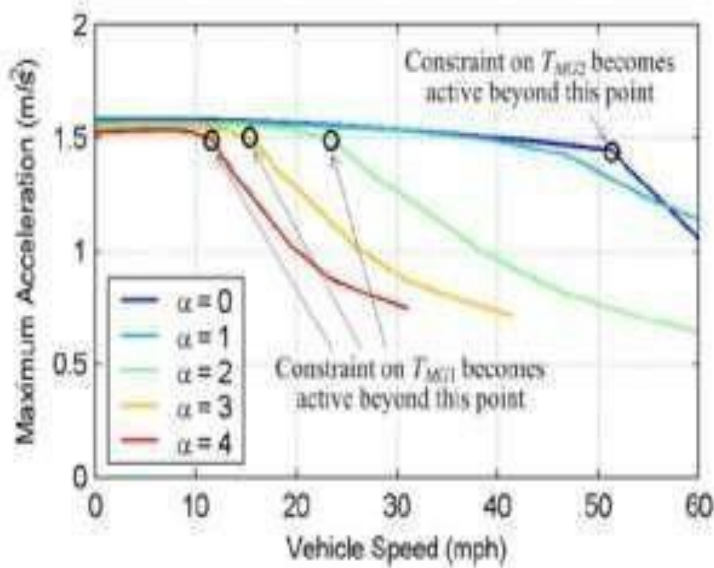


Fig 3: Speed trajectories under wide-open throttle acceleration from 0 to 60 MPH using different operation modes.

**Driving Cycle:**

The driving cycle chosen for this study is the abbreviated World Motorcycle Test Cycle (WMTC) as shown in the figure. The driving cycle has a maximum speed of 50 km/h and a driving time of 600 seconds. WMTC has an average speed of 23 km/h. The maximum and minimum acceleration are 1.72 m/s<sup>2</sup> and -1.92 m/s<sup>2</sup> respectively.

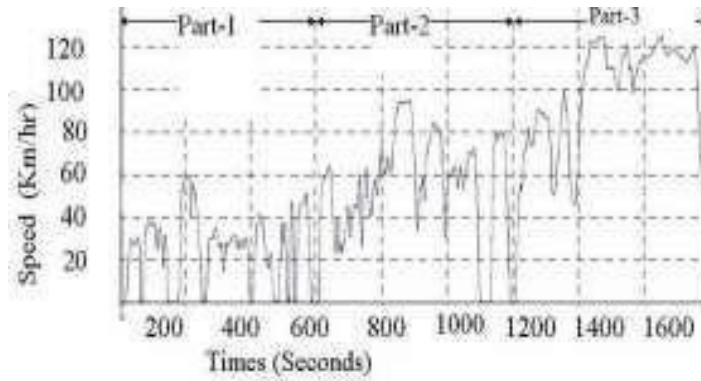


Fig 4.: WMTC

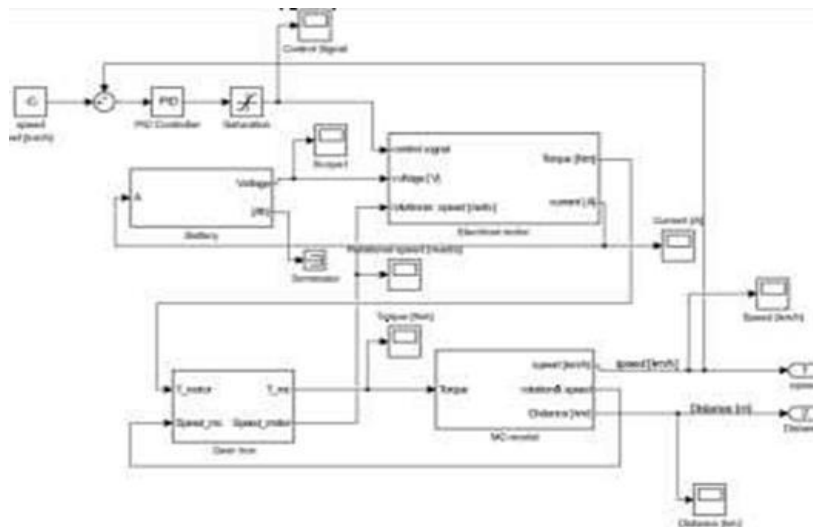


Fig 5: A Simulink model of an electric motorcycle

**Proposed Model:**

In this electric bi-cycle two motors and two batteries are added. Solar headlight. Rechargeable small generator (mini motor) by producing charge through rotating. The electric bi-cycle can be charged just by pedaling. Motor watt: 150 w, voltage: 24v. System level design of Human torque is combined in the mechanical realm with torque from the engine through gears. The double implementation of manpower has the positive effect of being able to achieve optimal cadence on all inclines while reducing overall efficiency. When implementing a serial hybrid approach, special attention should be paid to ensuring a natural driving experience and minimizing the perceived kinematic index. In this first system-level design phase, one more question must be answered. The question is whether the system should include regenerative braking. It should also be possible to operate the bike purely electrically, without the rider stepping on the pedals (e-bike) and without the rider having to use electricity all the time.

**Simulation Result:**

The software here is used MATLAB Simulation. The front motor has limited field weakening capability with maximum speed equal to 1.6 times the base speed. The base speed is selected to achieve maximum motor efficiency when vehicle speed is between 40- 60kmph. The rear motor has higher field weakening capability. The maximum speed is 2.8 times the base speed.

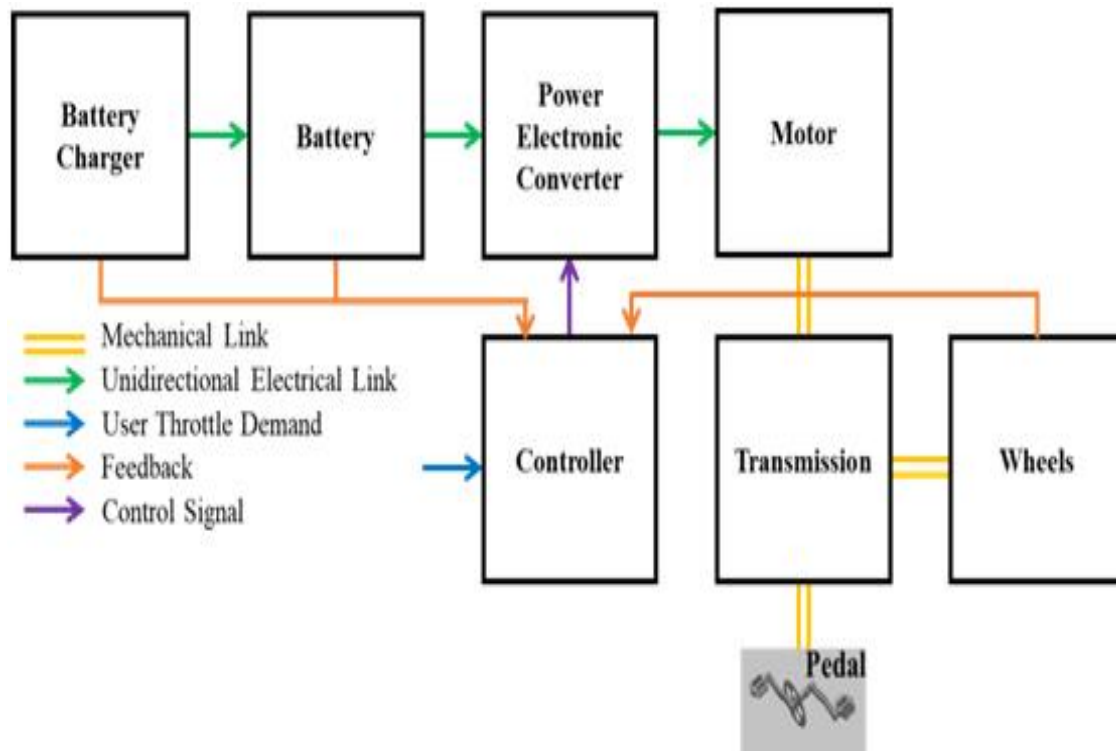


Fig 6: Basic block diagram of pedelic E-bike system

The base speed of the rear motor is selected to maximize motor efficiency when the vehicle speed is between 20- 40kmph. Also, it is connected to the rear wheel through a two stage fixed transmission with a gear ratio of 1:10. Similar to Single-motor topology, the efficiency of the gearbox is assumed to be 85% and remains constant over the speed range. The powertrain model is shown in Fig.4. The torque reference obtained from the PI controller is given to a torque distribution block which provide torque reference for front and rear motors. For both the motors, the torque-speed and efficiency maps which include inverter losses. Fig 6 shows the single motor power train for Two-Wheeled electric cycle is shown in the figure in the MATLAB software and when the simulation was run, the output wave form also shown below. So this is the existing model

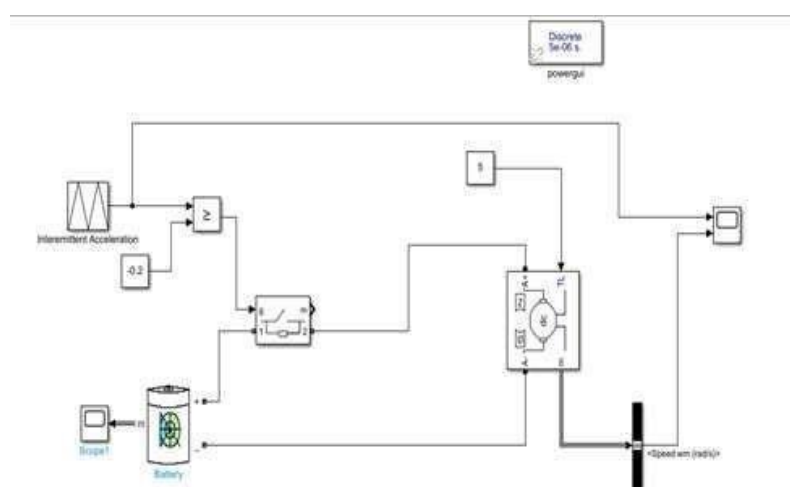


Fig 7.: Single motor simulation

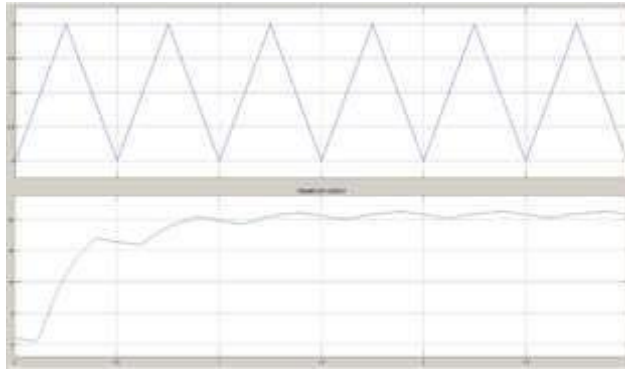


Fig 8: Single motor Wave form

**Proposed Modelling:**

Here in this diagram shows the dual motor power-train for Two Wheeled electric cycle is shown in by using MATLAB Simulation, the output waveform also shown. So this the dual motor in this we use two motors. If need we have to use two batteries also.

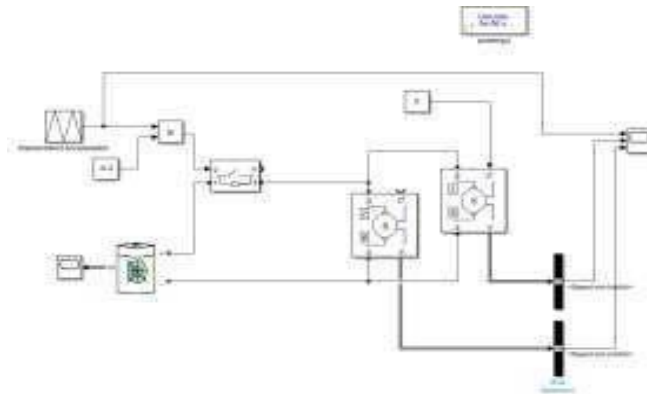


Fig 9: Dual motor Simulation

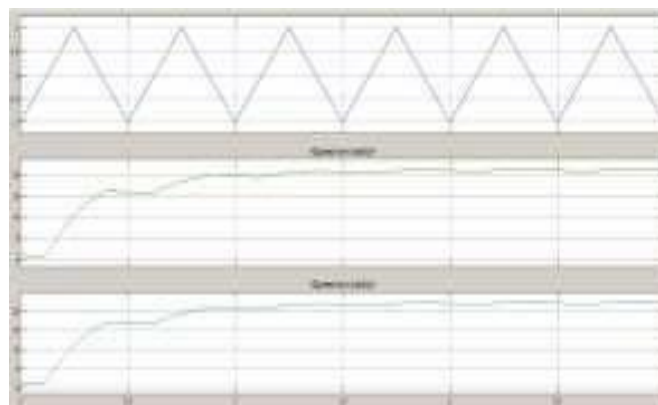


Fig 10: Output Waveform

**Conclusion:**

The basic e-bike system model is developed and simulated under two different slope. Performance tested for different assist levels provided under each case. It can be concluded from the results obtained that the system behaves close to a practical e-bike where the motor provides the extra torque to drive through slopes with lower pedal effort. It is also clear that higher the assistance the



current drawn from the battery will be more and hence with a single charge the distance that can be traveled will reduce with increased assistance. The motor control system developed in this model can be further improved to reduce third harmonic ripples by using SVPWM (Space vector PWM) instead of PWM. An additional cutoff limit is to be added for assistance start as in a practicable-bike. The energy consumption of the Dual-motor topology can further be optimized by limiting the maximum torque delivering capacity of the front motor. At the optimized point, the Dual-motor powertrain consumes 23.8% less energy compared to Single-motor powertrain.

### References:

1. Anchal Saxena Department of Electrical Engineering Indian Institute of Technology Bombay Mumbai, India [anchal05@gmail.com](mailto:anchal05@gmail.com) Saurabh P. Nikam Aproposdrive Technology Pvt. Ltd. Pune, India [saurabhnikamcoop@gmail.com](mailto:saurabhnikamcoop@gmail.com) B.G. Fernandes Department of Electrical Engineering Indian Institute of Technology Bombay Mumbai, India [bgf@ee.iitb.ac.in](mailto:bgf@ee.iitb.ac.in)
2. M.Ehsani, Y.Gao, S.E.Gay and A.Emadi, "Electric Vehicles" and "Electric Propulsion System", in Modern Electric, Hybrid Electric, and Fuel Cell Vehicles, Muhammad H. Rashid, USA: CRC press, 2004.
3. A.Muetze and Y.C.Tan, "Electric Bicycles", IEEE Industry Applications Magazine , vol.13, Issue.4, pp.12 - 21, July-Aug. 2007
4. C.Abagnale, M.Cardone, P.Iodice, S.Strano, M.Terzo , G.Vorraro , " Model-based control for an innovative power assisted bicycle", in 69th Conf. of the Italian Thermal Machines Engineering Association, Italy, 2015, pp.606-617.
5. Vladimir Kindl, Roman Pechanek, Martin Zavrel, Tomas Kavalir Faculty of Electrical Engineering, University of West Bohemia, Univerzitetni 26, 306 14 Plzen, Czech Republic, [vkindl@kev.zcu.cz](mailto:vkindl@kev.zcu.cz)
6. C.Abagnale, M.Cardone, P.Iodice, S.Strano, M.Terzo , G.Vorraro , " Model-based control for an innovative power assisted bicycle", in 69th Conf. of the Italian Thermal Machines Engineering Association, Italy, 2015, pp.606-617..

# An Intelligent Vacuum Based Grass Cutter for Agricultural Application

Aswin Aji<sup>1</sup>, Albin Thomas<sup>2</sup>, Jolly George<sup>3</sup>, Aiswarya Chandran<sup>4</sup>

<sup>1,2</sup>UG student, Dept. of EEE, Mangalam college of Engineering, Kottayam, India.

<sup>3,4</sup>Assistant Professor, Dept. of EEE, Mangalam college of Engineering, Kottayam, India.

Email: [1aswinaji2004@gmail.com](mailto:1aswinaji2004@gmail.com), [2albinthomas760@gmail.com](mailto:2albinthomas760@gmail.com), [3jollygeorge90@gmail.com](mailto:3jollygeorge90@gmail.com), [4aiswarya.chandran301@gmail.com](mailto:4aiswarya.chandran301@gmail.com)

**Abstract:** A robot's control system plays a critical role in its ability to assist humans with everyday tasks. Robotic technology for lawn maintenance has been done in an effort to reduce the possibility of potential risks while also taking time, money, and energy efficiency into account. But in certain situations, human supervision has not entirely replaced robotic assistance in work. Therefore, even if this lawn mower robot's application has been thoroughly researched, there are still areas that need to be developed to increase its effectiveness and performance. The lawn mower model has an inbuilt vacuum cleaner. Basically, the robot operates in two automatic modes based on the situation. With regard to the creation of the overall system, including the hardware and software components, microcontrollers play a significant role. It is designed to take commands in order to detect objects in its environment and steer the robot away from collisions. The battery powers the entire circuitry.

**Keywords-** Robotic technology, Bluetooth controlling, Microcontroller, Rechargeable battery, Motor drivers, Control system.

## Introduction:

Due of their efficacy in supporting people in cleaning applications, robotic cleaners have received significant interest in recent years in robotic research. Cleaning is the process of eliminating undesirable elements from a space or thing, such as dust, pathogens, and other contaminants. Cleaning takes place in a variety of settings and with a variety of techniques. One of the procedures that takes more time is the typical cleaning techniques used by humans. Vacuum cleaners were a huge advance in the cleaning procedure that came about many years ago. Our nation must maintain its cleanliness in order to attract foreign investment and give people better facilities. In many ways, intelligent machines will replace or improve human talents. Research into artificial intelligence research has spawned the fast-expanding field of expertise system. Vibration caused by the transit causes the iron ore to slide off the conveyor. Around the conveyor, the iron ore that has been dropped builds up. Recently, the dirt pile has been cleaned up using a Hoover car. This cleaning technique was known as Hoover work. The use of a hose linked to a Hoover car to remove and collect the dirt pile is known as Hoover work. However, the conveyor must be stopped in order to avoid having workers collide with falling iron ore while performing Hoover work. Steelworks productivity suffers as a result. Additionally, employees spend a lot of time vacuuming in a dusty environment. As a result, employees have health issues like Pneumoconiosis and shortness of breath. Due to these issues, a robot that performs Hoover work instead of humans must be created. An automated mapping system for the domestic environment as well as a method for cleaning the entire map's region were created.

## Objective:

To achieve this, you would need to carefully design the product with two separate modes of operation.

One mode would be for lawn mowing, and the other mode would be for vacuum cleaning. You would also need to ensure that the machine is able to perform both functions efficiently and effectively.

### Method:

This effort focuses on evaluating the usage of Ardo Pilot to accomplish total grass covering using an autonomous lawn mower prototype outfitted with an IMU and GPS. To the authors' knowledge, no prior research has been done to evaluate the viability of employing the navigation system. As in the case of the robotic lawn mower created in this work, control algorithms in Ardo Pilot are applied to a small-scale vehicle to completely cover a predefined area that requires less than 1 m resolution.

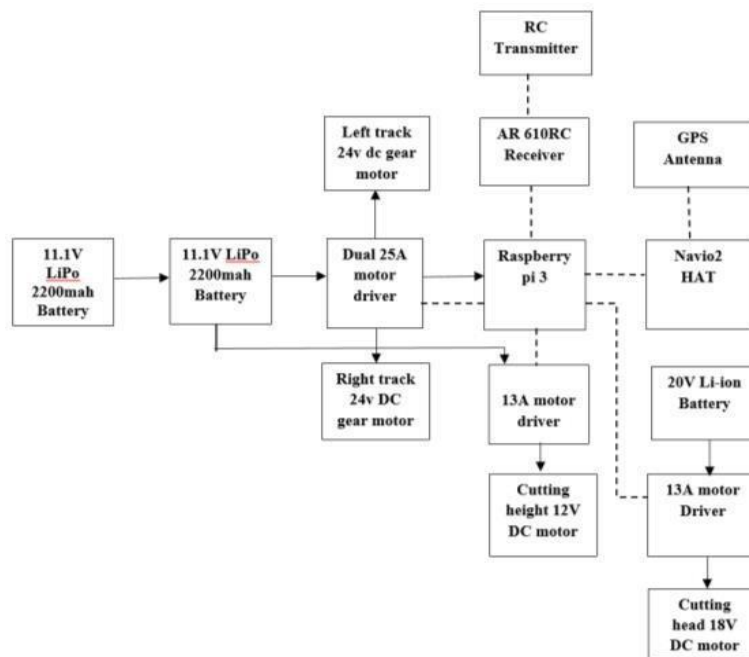


Figure 1: Autonomous Lawn Mower Block Diagram

### Overview of a lawn mover:

The goal of this research is to create a completely autonomous lawn mower that is suitable for usage by individuals with disabilities. The lawnmower may be programmed to operate independently over a predetermined area or it can be operated manually using a radio control (RC) transmitter, allowing the user to modify the grass cutting height, operate the mower motor at a chosen pace, and remotely control the lawn mower in any direction. The user may choose the area to be mowed and set the grid pattern the lawn mower will follow in autonomous mode. The lawnmower was put through field testing when the prototype was finished in order to confirm the general functioning and precision of the autonomous mission plan and to ascertain the overall runtime battery life. Results of the fully functional prototype demonstrate a successful autonomous operation.

### Overview of a vacuum cleaner:

There are issues with workers colliding with falling iron ore and experiencing health issues from dust inhalation when cleaning the dirt pile around the conveyor with a Hoover. Consequently, a robot that uses a Hoover car to perform the cleaning must be created of employees. Numerous studies on cleaning-related robots have talked about automation and cleaning effectiveness, including automatic mapping and coverage path planning. The effectiveness of cleaning and the automation of robots that can complete

the cleaning with a Hoover car are not discussed, though. It's important to avoid washing the same area more than once and leave uncleaned parts because doing so extends the cleaning process. As a result, in our research, we first the region where the hose suctions the dirt pile. Then, we put forth a technique for determining the best route that cuts down on cleaning time. We have created a control system that implements the ideal path. Finally, we performed a verification experiment under the assumption that the conveyor was next to an aisle. The suction-port position control system in the experiment verified that the coincidence rate with the ideal route was around 70%. In this block diagram, the robot body is the central component that carries the nozzle swing mechanism, which is responsible for controlling the movement of the suction port. The hose bending mechanism is also included to ensure that the bending reaction force of the hose is suppressed. The suction port positioning system is responsible for controlling the movement of the nozzle swing mechanism based on user inputs received through the user interface. The control and power system provides the necessary power and signals to operate the various components of the system. Overall, this system is designed to allow the cleaning robot to efficiently perform vacuum work in narrow spaces while being lightweight enough to be carried by a human.

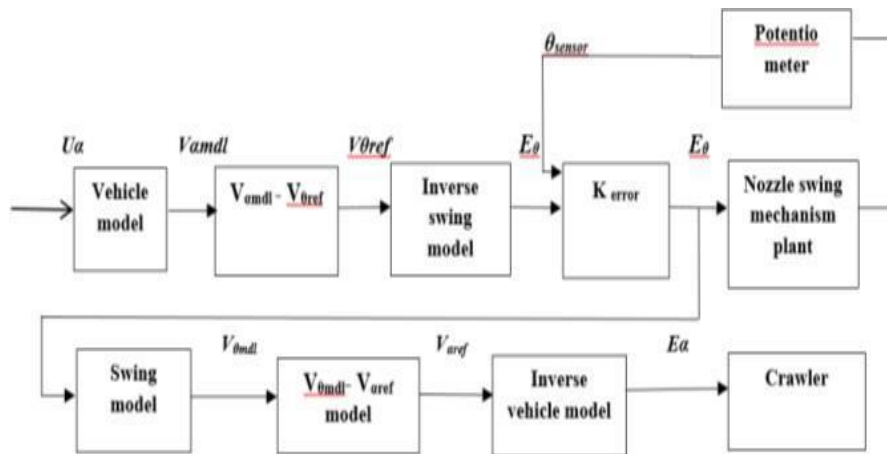


Figure 2. Block diagram of suction-port positioning system

**Block diagram of self-regulated lawn mower with vacuum cleaner:**

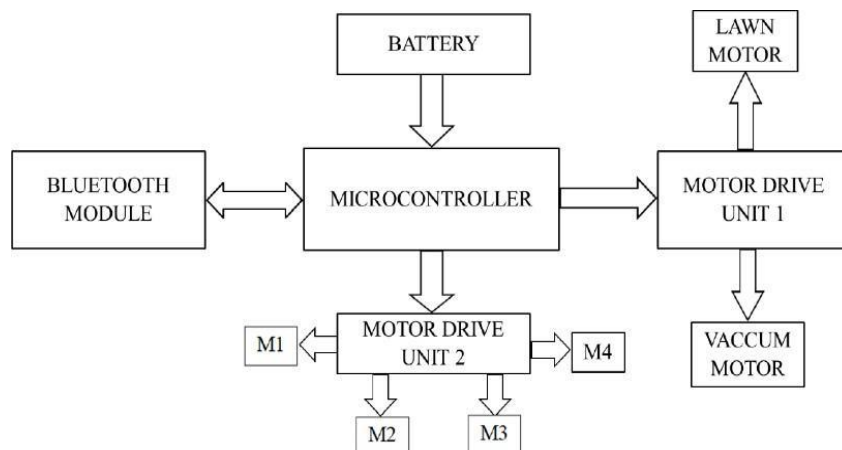


Figure 3: Block Diagram

In this block diagram, the 12V DC lithium-ion battery is the power source for all the components. The DC-to-DC converter is used to step down the voltage from 12V to 5V for the Arduino Uno. The Arduino Uno is the central component that controls the entire operation of the project, using the

Bluetooth module for communication with a control device. The motor driver is used to control the movement of the chassis motors, while the grass-cutting motor and vacuum motor are controlled directly by the Arduino Uno. Overall, this project uses a total of six DC motors, with four used for the movement of the chassis, one for cutting grass, and one for the vacuum. The microcontroller and Bluetooth module enable wireless control of the project, while the DC-to-DC converter ensures that the Arduino Uno is supplied with the correct voltage.

**Simulation results:**

Using the proteus software simulation program we get the results of these projects. The circuit diagram is connected as shown in the figure in the proteus software and when the Simulation was run, the motoras turned ON and the indication is shown in the figure.

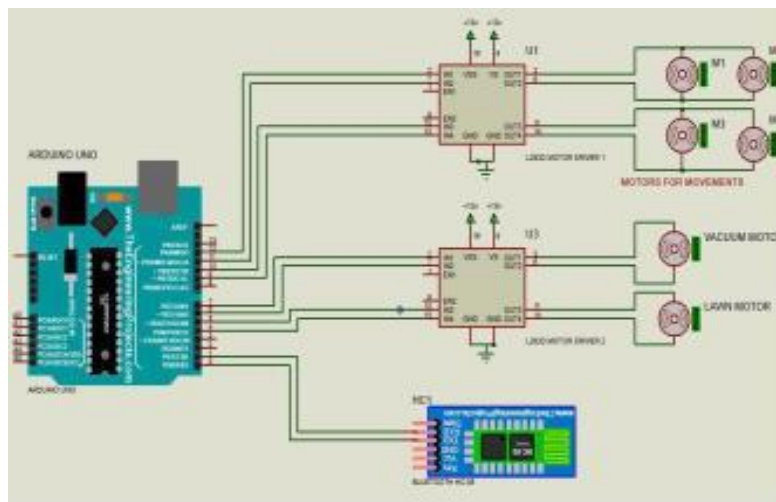


Figure 4: Simulation before run

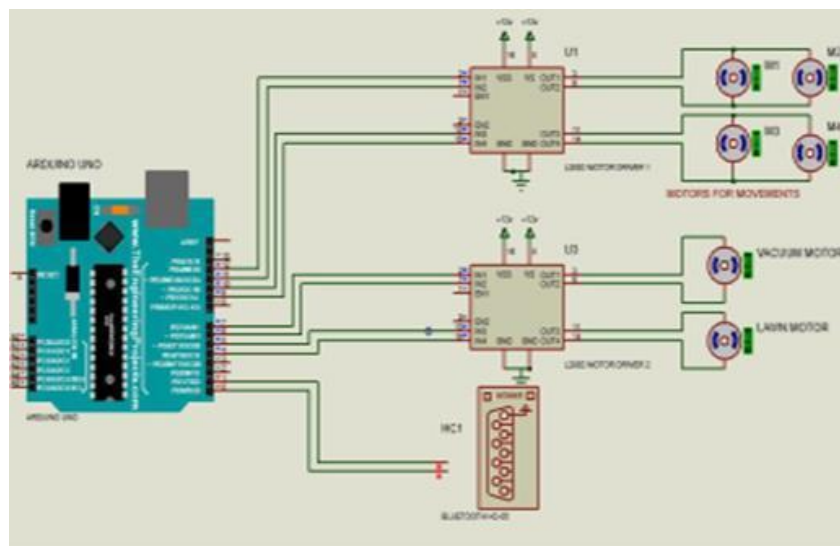


Figure 5 : Simulation after run

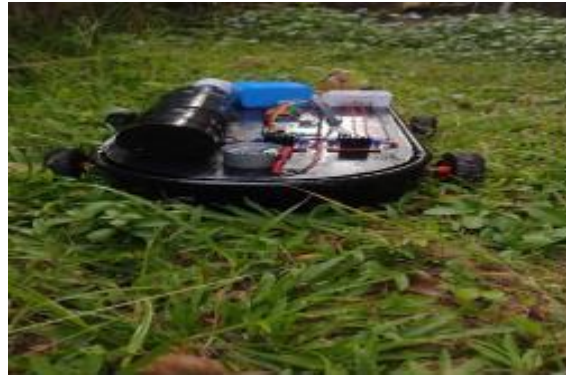


Fig 6: Working model

### Conclusion:

This project includes a summary of the issue information, project talks, and an evaluation of the current status in respect to ongoing and completed activities, a budget breakdown, and a timeframe comparison. The project's comprehensive study has highlighted two areas where projects could be improved the team should first get more knowledgeable about electrical theory and its applications. This would have given the team more time to identify the issue with the present monitoring circuitry and perhaps even create a fix. When we talk about upcoming projects or new developments for this project, we should pay more attention to precisely planning the timeline. The project's initial timetable was given.

### References:

- [1] Hyunjin Kim, Hyunjeong Lee, Stanley Chung, Changsu Kim, "User-Centered Approach to Path Planning of Cleaning Robots: Analyzing User's Cleaning Behavior" 2nd ACM 978- 1-59593-617 Pg no. 373-380, Vol 2, IEEE 2012.
- [2] Jesin James, Jesse Wilson, Jovna Jetto, Alna Thomas, Dhahabiya V K "Intelligent Track Cleaning Robot" 978-1- 5090-2396 Pg no.332- 337 vol 6 IEEE 2016.
- [3] Liang Yuming, Wen Ruchun, Zhang Zhenli, Zhu Junlin "Dynamic Coverage Path Planning and Obstacle Avoidance for Cleaning Robot Based on behaviour" 978- 1-4244-8039 vol7 IEEE 2011.
- [4] Seohyum Jeon, Minsu Jang, Daeha Lee, Chang- Eun Lee, Young-Jo Cho "Strategy for Cleaning Large Area With Multiple Robots" 978-1-4799- 1197 Pg no.652-654 vol 8 IEEE 2013.
- [5] Sang-Hyuk Park, Young-Ho Choi, Sang-Hoon Baek, Tae- Kyung Lee, Se-Young Oh" Feature Localization using Neural Networks for Cleaning Robots with Ultrasonic Sensors" Oct 17-20, pg no.449-453 vol 4 IEEE 2007.
- [6] XuMiao, Jaesung Lee,Bo-YeongKang, "Scalable Coverage Path planning for Cleaning Robots Using Rectangular Map Decomposition on Enviroment" vol 6, IEEE 2018.
- [7] Miao, J. Lee, and B. Kang, Scalable Coverage Path Planning for Cleaning Robots Using Rectangular Map Decomposition on Large Environments, IEEE Access, vol. 6, pp.38200 38215, July, 2018.
- [8] H. Liu, J. Ma, and W. Huang, Sensor-based complete coverage path planning in dynamic environment for cleaning robot, CAAI Transactions on Intelligence Technology, vol. 3, Issue: 1. March, 2018, pp. 6872.

# Efficiency Analysis of Gear Change Control Strategy of Clutchless Automatic Manual Transmission of an Electric Vehicle

Alsufiyan Nazim P N<sup>1</sup>, Lekshmi Nair J<sup>2</sup>, Preethi Sebastian<sup>3</sup>

<sup>1</sup>Embedded Software Engineer, Amara Raja Design Alpha Pvt Ltd, Ernakulam, India

<sup>2</sup> Assistant Professor, Department of Electrical Engineering, Mangalam College of Engineering, Kottayam, India

<sup>3</sup> Associate Professor, Department of Electrical Engineering, Mangalam College of Engineering, Kottayam, India

Email – <sup>1</sup> [alsufiyanazim5@gmail.com](mailto:alsufiyanazim5@gmail.com), <sup>2</sup> [lekshmi.j@mangalam.in](mailto:lekshmi.j@mangalam.in), <sup>3</sup> [preethy.sebastian@mangalam.in](mailto:preethy.sebastian@mangalam.in),

**Abstract:** Conventional automatic-manual transmission for vehicle powered by IC engine requires an electronically controlled clutch to isolate and engage the engine power for smooth gear changes because of the high inertia of the internal-combustion engine. This makes the system complicated and, therefore, more expensive. A Clutchless Automatic Manual Transmission (CLAMT) employed for electric vehicles is analysed in this paper. It has the benefits of high efficiency, low cost, and simple structure. To increase speed and make the speed controller useful for the CLAMT system, a synchronisation speed control technique based on the sliding-mode method is used. By utilizing the electronic control unit (ECU) of CLAMT system, it can achieve the smooth gear-shifting process, with regard to the efficiency of the drive train. The ECU, employs two 32-bit floating-point digital signal processors, TI TMS320LF2407 and TMS320F2801.

**Keywords:** CLAMT, Electric vehicle, ECU.

## Introduction:

Automatic transmissions (AT) were once regarded as a high-end alternative to manual gearboxes in the automotive industry because they provide automated gear shifting, saving the driver from having to manually shift into gear [1]. The benefit of an automatic gear schedule has become more significant, though, as energy efficiency of automobiles has been one of the primary goals of automobile manufacturers [2]. It is feasible to let the engine or powered motor operate in areas with low energy consumption by delegating the responsibility of choosing an appropriate gear for engine/powered motor operation from the driver to the gearbox. Pure electric vehicles have gained international attention as a result of advancements in power electronics technology and electric components. The driving motor of a pure electric car is typically equipped with a decelerator or a transmission device to increase the efficiency of an electric driving system while still meeting the standards of vehicle drivability [3]. It is inappropriate to utilise an AT or continuous-variable transmission (CVT) when building the EV because an AT suffers from significant power losses and a CVT can only be used for small-sized passenger cars at the moment [4]. Using a standard multispeed manual gearbox plus electric, pneumatic, or hydraulic power, the AMT can be deployed with ease.

## Materials:

Table 1.1 shows the specification of Gear Ratio in MT Gearbox. Due to the high inertia of the ICE, conventional AMT for ICE-powered vehicles requires an electronic controlled clutch to separate and engage engine power for smooth gear changes. This adds complexity to the system and raises costs. This paper proposes an AMT system for electric vehicles (EVs) without the clutch apparatus. Shift quality is one of the most important factors in transmission control. Shift quality is determined by torque hole and

shifting time. When the transmission gear is disengaged and the drive shaft gear advances toward the target gear, a torque hole occurs. The torque hole reduces the vehicle's ability to shift gears smoothly and comfortably. To increase the quality of the shift, it is crucial to minimise these speed disparities and complete the gear shift as quickly as possible.

Table 1 Specification of Gear Ratio in MT Gearbox

<b>Gear level</b>	<b>Gear ratio (driving: driven)</b>
1 <sup>st</sup>	12: 43
2 <sup>nd</sup>	18:43
3 <sup>rd</sup>	24:33
4 <sup>th</sup>	35:36
5 <sup>th</sup>	38:34
Final	16:82

The viability, optimization, and control method of applying CLAMT to electric vehicle drive trains are discussed based on the motor drive system characteristics and the overall requirements of the vehicle. The synchronisation at gear shifting is always ensured through the speed regulation of the driving motor (based on driving conditions). Additionally, it makes it possible to minimise shifting time and reduce shift holes. The shift quality and driving comfort are enhanced as a result.

In this paper, a Clutchless Automatic Manual Transmission (CLAMT) is adopted and designed in this work. It has the benefits of high efficiency, low cost, and simple structure. This article's goal is to discuss the CLAMT's gear-change control technique. This includes identifying model parameters, controlling speed synchronisation during gear engagement, and controlling the motion of the gear-change actuation mechanism. The results from theoretical analysis, modelling, and experimental verification show that the suggested control approach can manufacture smoothly shifting gears, and the viability of CLAMT is confirmed.

### **Method:**

The objective of the paper is to design a gear-change control technique for a clutchless automatic-manual transmission and the identification of the model parameters, control of the synchronization speed during gear engagement, and motion control of the gear-change actuator mechanism. The block diagram of the Clutchless Automatic Manual Transmission ECU is shown in Figure 2.

The ECU consists of the 32-bit floating-point digital signal processors, TI TMS320LF2407 and TMS320F2801, is employed to implement the gear-shifting control strategy and the servo control of the BLDC machine. The operation of the drivetrain is separated into two different states: the internal synchronized state (during the period when the gear is disengaged) and the power-outputting state (after gear engagement). During vehicle driving, the drivetrain operates in the power-outputting state and the output power torque of motor is adjusted according to the driver's pedal signal.



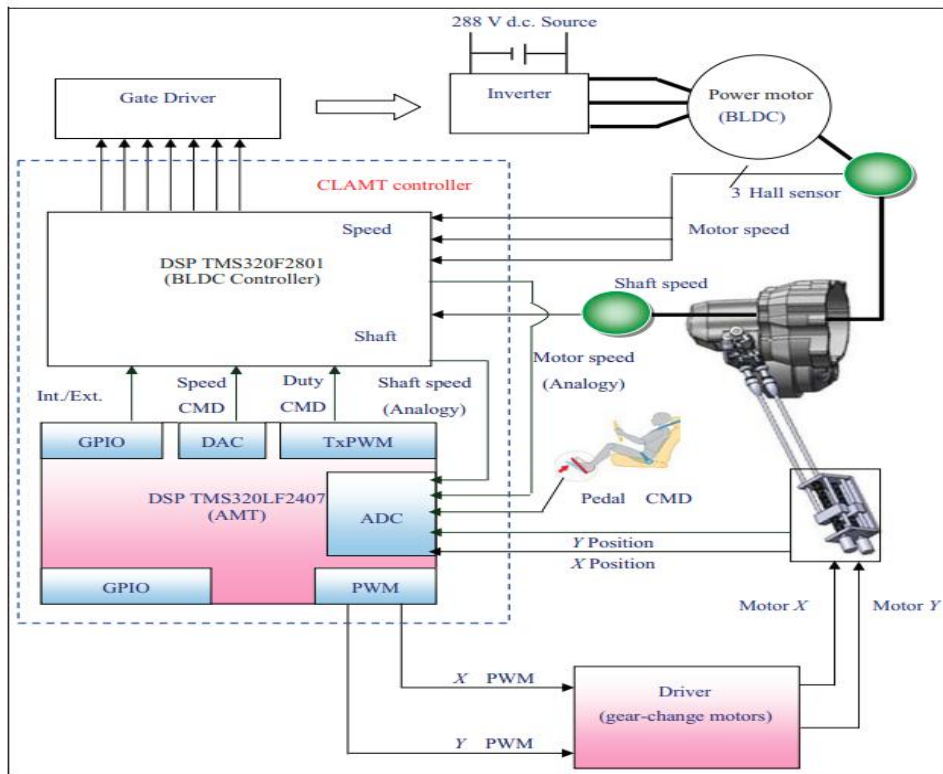


Figure 2. Clutchless Automatic Manual Transmission ECU

When the driver persistently accelerates or decelerates, the operation of the drivetrain is transferred from the power-outputting state to the internal synchronized state in order to execute the gear-change process. The digital signal processor (DSP) of the AMT is responsible for determining the most appropriate gear position according to the vehicle speed and the driver’s pedal signal and for calculating each target value (including the powered motor speed and torque commands and a movement sequence for the gear-change actuators).

**Analysis:**

The DSP of the BLDC controller receives the input signal information from the DSP of the AMT and decides whether to execute either speed control for gear engagement (in the internal synchronized state) or torque output control (in the power-outputting state). The hardware model set up is shown in Figure 3.

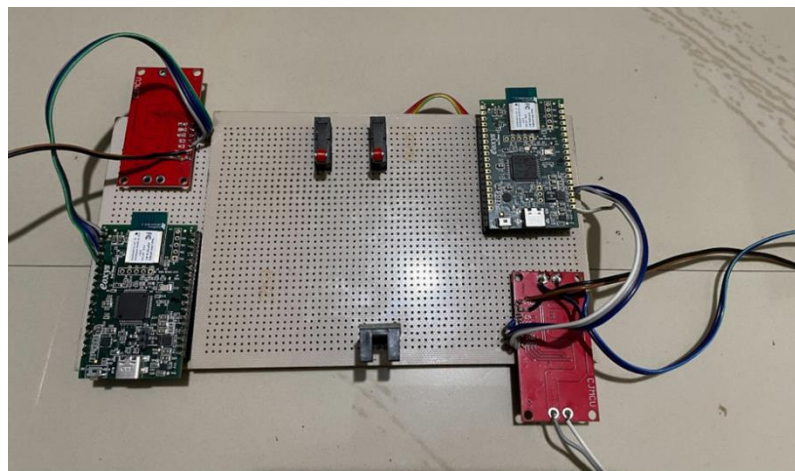


Figure 3 Circuit diagram of proposed model

**Result:**

The CLAMT system's gear-change operation, which is broken down into gear disengagement, gear selection, speed synchronization, and gear engagement, is the same as for traditional MT systems. The durations of mechanical operation and electronic synchronization together make up the overall amount of time needed for a gear shift. The gear change mechanism design, the gear-change motors' time constant, and the mechanical synchronizer's operation time during gear engagement dictate the mechanical operation time interval. The efficiency of the synchronization speed controller and the power motor's time constant dictate the expense time for electronic synchronization. In order to simulate a vehicle being driven on a road, the experimental apparatus was made to perform sequential upshifting and downshifting in accordance with a gradual increase and a gradual decrease, respectively, in the pedal signal. This was done to test the viability of the proposed gear-shifting control strategy of the CLAMT in practical applications. As shown in Figure 4, fixed PID gains are used, notably during the gear upshift from fourth to fifth gear, causing the traditional controller to demonstrate poor coordination of synchronization even though it could follow the appropriate speed command during the internal synchronized state.

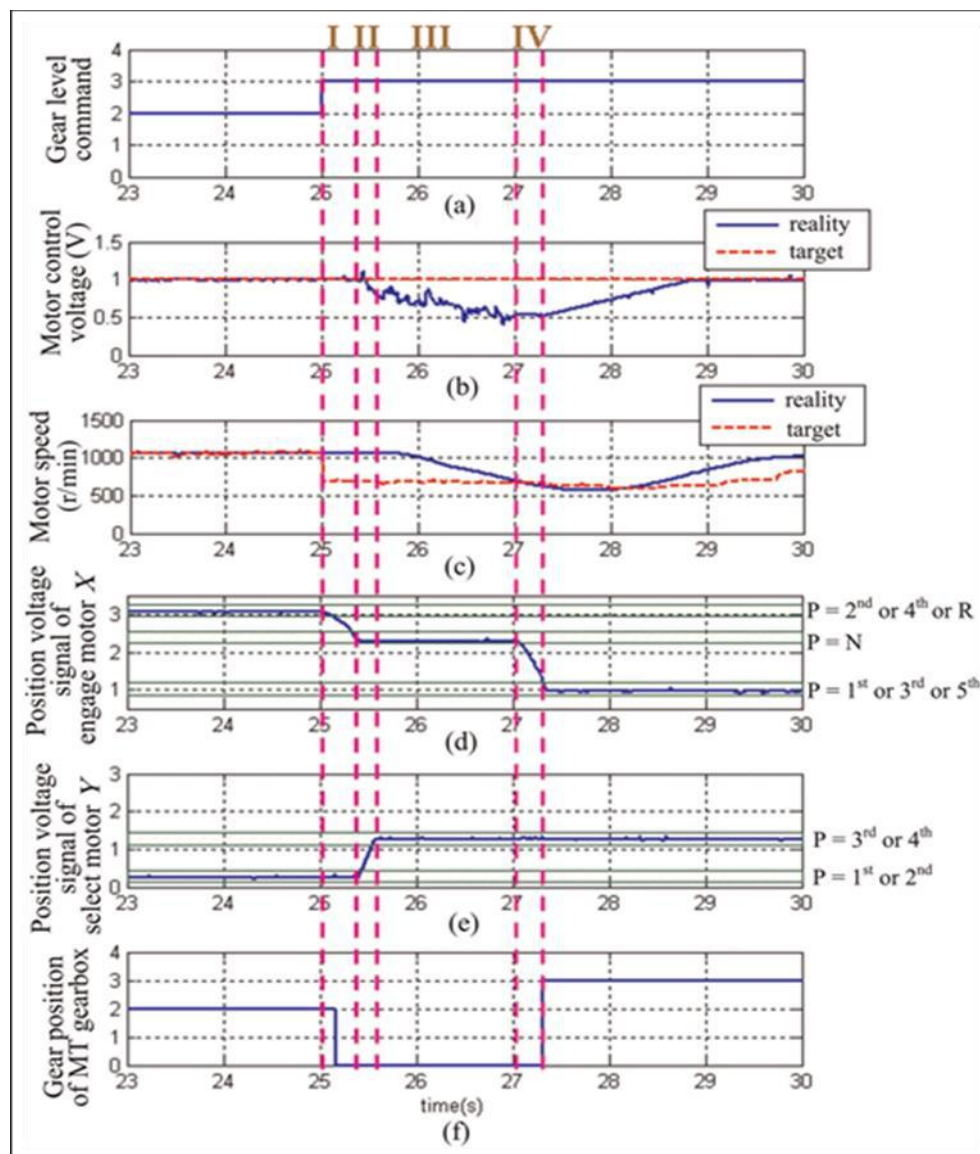


Figure 4. Analysis of gear shifting procedure

**Conclusion:**

Due to the gear-shifting quality directly related to the driving comfort of the vehicle, it is significant to reduce the gap of torque interruption by means of shortening the gear-change time. By accelerating the gear-changing process, it is possible decrease the torque interruption gap and increase gear-shifting quality, which is directly tied to how comfortable the car is to drive. This paper examines the practicality of a CLAMT utilized in an EV and develops a gear change control mechanism for the CLAMT in order to perform the gear-shifting operation quickly and smoothly. By utilizing the electrical control unit of CLAMT system, it can achieve the smooth gear-shifting process, with regard to the efficiency of the drive train.

**References:**

1. Yu C.H and Tseng C, (2013). Research on gear-change control technology for the clutchless automatic-manual transmission of an electric vehicle. Proceedings of the Institution of Mechanical Engineers, Part D: Journal of Automobile Engineering, 227(10),1446-1458.
2. Yang T, Nong Z, Shilei Z and Paul D, W, (2020). Model and gear shifting control of a novel two-speed transmission for battery electric vehicles. Mechanism and Machine Theory, 152(2).
3. Huang W, J, Jianfeng H, Chengliang Y and Lifang W, (2020). "Optimal Speed Regulation Control of the Hybrid Dual Clutch Transmission Shift Process" World Electric Vehicle Journal 11(1).
4. X. Zhang, C, Li, D. Kum and H. Peng, (2020). Configuration Analysis of Power-Split Hybrid Vehicles with a Single Planetary Gear. IEEE Transactions on Vehicular Technology, 61(8)3544-3552.
5. Xi Jun, Xiong Gand Zhang Y, (2008), Application of automatic manual transmission technology in pure electric bus", Proc. IEEE Vehicle Power and Propulsion Conference, Harbin, 1-4.

# Maximizing Voltage Gain and Efficiency In BLDC Motor Driven Electric Vehicle Through Sepic Converter Integration

Anu Lal B<sup>1</sup>, Shwetha Saji<sup>2</sup>, Ojes O<sup>3</sup>, Althaf Hassan<sup>4</sup>

<sup>1,2,3,4</sup>UG student, Dept. of EEE, Sree Buddha College of Engineering, Pattoor

**Abstract:** *Electric vehicles (EVs) have gained significant attention as a sustainable alternative to traditional combustion engine vehicles. At the heart of these vehicles lies the Brushless DC (BLDC) motor, serving as the primary propulsion system. BLDC motors offer a multitude of advantages that make them well-suited for EV applications. Efficiency and voltage gain are the pivotal factors in the performance of Brushless DC (BLDC) motor-driven Electric Vehicle (EV) systems. This paper proposes the integration of a SEPIC Converter to optimize these aspects. By enhancing the voltage gain and efficiency concurrently, the proposed integration offers a comprehensive solution to address the challenges faced in contemporary EV propulsion systems. The study also investigates the operational principles of the SEPIC Converter and compares it with other DC-DC converters within the context of BLDC motor-driven EV systems, emphasizing its potential to maximize energy conversion and utilization. The study also explores the usage of various other converters in the context of BLDC motor. Through theoretical analysis and simulation studies, the efficacy of the integrated system is demonstrated, showcasing significant improvements in both voltage gain and overall system efficiency. Potential applications of this integration are discussed, highlighting its relevance in advancing the performance standards of EV propulsion technologies.*

## Introduction:

The transition towards electric transportation has gained significant traction due to its potential to mitigate environmental issues and reduce reliance on fossil fuels. In this context, Electric Vehicles (EVs) utilizing Brushless DC (BLDC) motors have emerged as promising contenders against conventional internal combustion engine vehicles. The efficiency and effectiveness of BLDC motor-driven EV systems hinge upon the careful optimization of voltage gain and overall efficiency. This optimization is pivotal as it directly influences critical factors such as extending the driving range, enhancing energy utilization, and ultimately improving the performance of the entire system. By maximizing voltage gain and efficiency, EVs can operate more efficiently, utilize energy resources more effectively, and deliver a superior driving experience to consumers. Thus, the quest to optimize voltage gain and efficiency in BLDC motor-driven EV systems is central to advancing the sustainability and practicality of electric transportation. Brushless DC (BLDC) motors are recognized for their exceptional efficiency, which minimizes energy loss and consequently extends the driving range of electric vehicles [1, 2]. This efficiency is pivotal in addressing concerns related to range anxiety and enhancing the overall sustainability of electric transportation. Moreover, BLDC motors offer precise speed control, enabling smooth acceleration and deceleration processes. This accuracy in speed control not only enhances the driving experience but also contributes to energy optimization and battery longevity. Additionally, the compact size and lightweight nature of BLDC motors make them highly versatile and adaptable to various vehicle chassis designs [3, 4].

With both step-up and step-down capabilities. This flexibility makes it well-suited for the varied operating conditions encountered in EVs. The SEPIC converter's primary function is to regulate voltage levels while maximizing energy conversion efficiency. In the context of BLDC motor-driven EV systems, this capability is particularly valuable. By precisely controlling voltage levels, the SEPIC converter ensures that the BLDC motor receives the required voltage for optimal performance, regardless of

fluctuations in the input voltage from the battery or power source. This regulation contributes to stable and efficient operation, enhancing the overall performance of the EV system. The integration of the SEPIC converter into Electric Vehicle (EV) systems powered by Brushless DC (BLDC) motors. The objective is to maximize both voltage gain and efficiency within these systems. This integration is crucial for enhancing the overall performance and effectiveness of EV propulsion. Additionally, the study involves conducting a comparative analysis with other types of DC-DC converters commonly used in EV applications. This comparative analysis aims to evaluate the suitability of various converter topologies for EV systems, considering factors such as efficiency, voltage regulation, reliability, and cost-effectiveness. Ultimately, the research aims to contribute to the advancement of power electronics technologies in electric propulsion. Identifying the most effective converter topology for EV applications can inform the development of more efficient and sustainable transportation solutions, driving innovation in the design and implementation of power electronics systems for electric vehicles, ultimately benefiting the automotive industry and society as a whole.

The contributions of this paper are listed as follows:

- Integrating the SEPIC converter into BLDC motor-driven Electric Vehicle (EV) systems to enhance voltage gain and efficiency.
- Comparative analysis between SEPIC converters and other DC-DC converters within the context of BLDC motors.
- Implementation of SEPIC converter within BLDC motor-driven EV systems to optimise energy conversions, crucial for maximizing driving range and overall system performance.

### Methodology:

The proposed system mainly focuses on designing and implementing a SEPIC converter for a BLDC controlled electric vehicle. The purpose of this system is to enhance the efficiency and overall gain of the system thereby optimising energy conversions which are crucial for EV applications. The system mainly comprises of a single phase AC supply which is then rectified using a full bridge rectifier. The rectified output is passed onto the SEPIC converter whose working is based on the input signals from the controller. The SEPIC converter is controlled by a PI controller, which guarantees consistent and efficient voltage boosting. The three-phase VSI receives the enhanced output after that. To manage the speed of the BLDC motor, an additional PI controller controls the output of the VSI. The input of the controller is the voltage generated from the back emf of the BLDC Motor. Sensorless control of BLDC motor is used in this system for improved accuracy and cost effectiveness. By analyzing motor parameters and electrical signals, develop models for estimating torque output under various operating conditions.

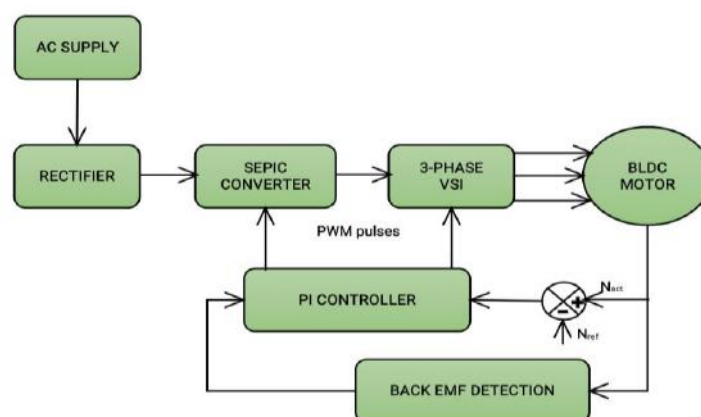


Figure 1 : Block Diagram

The proportional term of the PI controller adjusts the control input based on the current error between

the desired back EMF value (setpoint) and the actual measured back EMF value. If the measured back EMF deviates from the desired value, the proportional term applies a correction that is proportional to the magnitude of the error. This component ensures that the controller responds quickly to sudden changes in the back EMF, providing immediate corrective action to bring the system closer to the desired setpoint. The integral term of the PI controller takes into account the cumulative sum of past errors over time. It continuously integrates the error signal, amplifying the corrective action if the error persists over time. This component helps address any steady-state errors that may arise due to factors such as system friction, nonlinearities, or external disturbances. By gradually adjusting the control input based on the accumulated error, the integral term ensures that the system eventually reaches and maintains the desired back EMF value, even in the presence of persistent disturbances or inaccuracies in the system.

### Proposed System Modeling:

A DC rectifier is an electrical device used to convert alternating current (AC) into direct current (DC). Its primary function is to rectify the flow of current, ensuring that electricity flows consistently in one direction. This process is crucial in numerous applications where DC power is required, such as in electronic devices, industrial machinery, and power transmission systems.

The most common type of DC rectifier is the diode rectifier, which utilizes semiconductor diodes to allow current flow in one direction while blocking it in the opposite direction. When AC voltage is applied to the input of a diode rectifier, the diodes alternate between conducting and blocking current flow, effectively converting the AC waveform into a pulsating DC waveform. This pulsating DC is then smoothed using capacitors or filters to produce a more stable DC output. DC rectifiers are essential components in various electrical systems, including power supplies for electronics, battery charging systems, and renewable energy systems such as solar panels and wind turbines. They play a vital role in ensuring efficient and reliable power conversion, enabling the operation of countless devices and equipment that rely on DC power. In summary, DC rectifiers are critical devices that play a fundamental role in converting alternating current into direct current for a wide range of applications. By rectifying the flow of current, these devices enable the efficient and reliable operation of electronic devices, industrial machinery, and renewable energy systems, contributing to the advancement of technology and modern infrastructure.

### Sepic Converter:

The study of power amplification systems has focused on enhancing the static gain of single and multiphase amplified DC to DC converters. Fig. 2 adapts an electromagnetic amplification approach using a Sepic converter. The SEPIC converter benefits from the computations of the capacitor C and diode D. A number of the operational characteristics of the superior Sepic converter are altered by the potential enhancement.

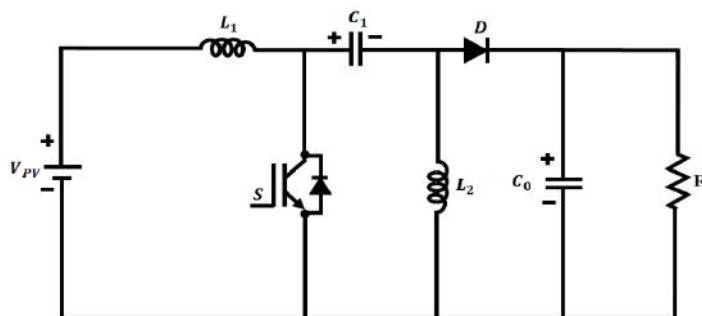


Fig 2 SEPIC Converter



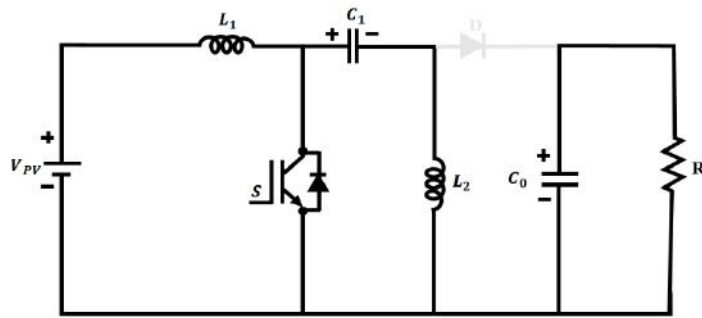


Fig 3. Mode 1

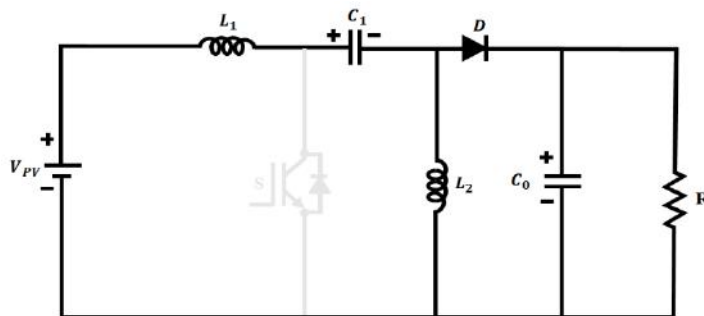


Fig 4. Mode 1

Mode 1: In mode 1 of operation, the switch is closed, causing the inductor  $L_1$  to charge from the source voltage ( $V_{L1} = V_{pv}$ ). Concurrently, considering the current direction, inductor  $L_2$  charges through capacitor  $C_1$  ( $V_{L2} = V_{c1} = V_{pv}$ ). Until the filter capacitors  $C_1$  and  $C_0$  are depleted, no steady-state current passes through them. In Fig.3 there is high capacitance in  $C_1$  and  $C_0$  results in the disappearance of input and output voltage ripple in the Sepic converter. This process ensures efficient energy transfer and minimizes voltage fluctuations, enhancing overall converter performance.

Mode 2: In mode 2, with the switch in the off position, inductor currents  $I_{L1}$  and  $I_{L2}$  charge capacitors  $C_1$  and  $C_0$  respectively, and the load. According to Kirchhoff's voltage law, the average voltage equation across inductors  $L_1$ ,  $L_2$ , capacitor  $C_1$ , and source  $V_{pv}$  is  $-V_{pv} + V_{L1} + V_{c1} - V_{L2} = 0$ . In steady state, the average voltage across inductors is assumed to be zero due to constant energy storage. In Fig.4, when  $V_{L1}$  and  $V_{L2}$  are zero,  $V_{c1}$  equals  $V_{pv}$ , leading to  $V_{L1} = -V_o$ . During transient states, the equation becomes  $-V_{pv} + V_{L1} + V_{c1} - V_{L2} = 0$ . This analysis enables understanding of voltage dynamics across components, aiding in efficient system operation.

The PI controller regulates speed or by comparing desired values with feedback from back EMF sensing. It calculates error as the difference between these signals and adjusts the SEPIC converter's duty cycle using proportional and integral actions. Proportional adjustment scales with error magnitude, while integral adjustment integrates error over time to eliminate steady-state error, improving response to load changes. The controller's output modulates the converter's duty cycle, regulating the BLDC motor's speed or torque. The first step in the PI control process is to calculate the error. In this case, the error is the difference between the desired speed (set point) and the estimated speed based on BEMF feedback. The control signal is used to adjust the motor's voltage or current, typically through pulse-width modulation (PWM) control. The PWM duty cycle is adjusted based on the controller's output. A higher duty cycle increases motor power, while a lower duty cycle decreases it. The motor's actual speed is monitored through Motor feedback. The controller continuously adjusts the control signal to minimize the speed error and maintain the motor at the desired speed.

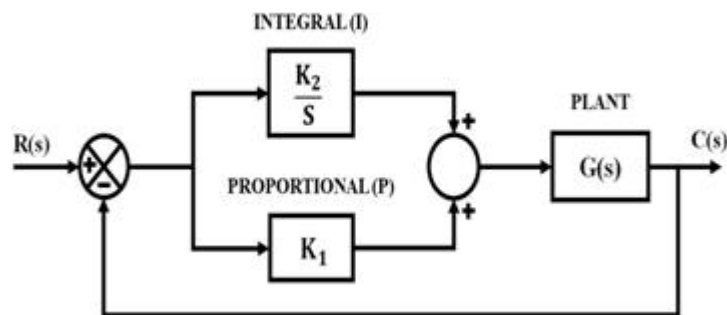


Fig 5 PI Control

**Three Phase VSI:**

A 3-phase Voltage Source Inverter (VSI) is a key component in controlling Brushless DC (BLDC) motors. The 3-phase Voltage Source Inverter (VSI) serves as a critical element in the conversion process from DC to AC power, utilizing pulse width modulation (PWM) techniques to finely regulate the output voltage. This alternating current is subsequently directed towards Brushless DC (BLDC) motors, affording precise manipulation of both speed and torque parameters. The upper and lower switches' On and Off states dictate the output voltages. Modulation techniques commonly entail converting three-phase quantities into two-phase equivalents, achieved through either stationary frames or synchronously rotating frames.

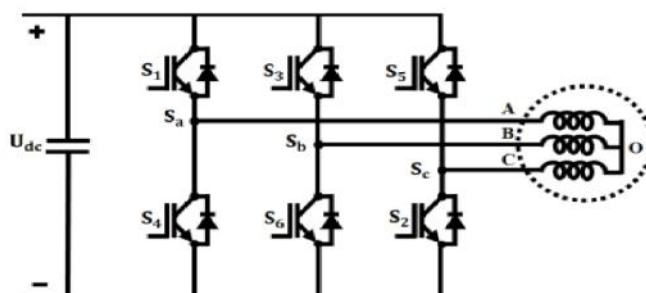


Fig 6 Voltage Source Inverter

**BLDC Motor:**

In a three-phase BLDC motor, there are three separate sets of windings arranged around the stator. These windings generate the rotating magnetic field necessary for the motor's operation. The rotor, which contains permanent magnets, interacts with this magnetic field to produce motion. Due to the presence of these permanent magnets, the effects of rotor-induced currents are minimal, and therefore, damper windings, which are typically used to mitigate these currents, are not included in the model of the motor.

$$\begin{bmatrix} V_a \\ V_b \\ V_c \end{bmatrix} = \begin{bmatrix} R_a & 0 & 0 \\ 0 & R_b & 0 \\ 0 & 0 & R_c \end{bmatrix} \begin{bmatrix} i_a \\ i_b \\ i_c \end{bmatrix} + p \begin{bmatrix} L_a & L_{ba} & L_{ca} \\ L_{ba} & L_b & L_{cb} \\ L_{ca} & L_{cb} & L_c \end{bmatrix} \begin{bmatrix} i_a \\ i_b \\ i_c \end{bmatrix} + \begin{bmatrix} e_a \\ e_b \\ e_c \end{bmatrix} \tag{1}$$

It has been determined that the stator resistance of each winding is equal. Assuming further that the rotor reluctances remain constant across angles.



$$\therefore i_a + i_b + i_c = 0(2)$$

$$\begin{bmatrix} e_a \\ e_b \\ e_c \end{bmatrix} = \omega_m \lambda_m \begin{bmatrix} f_{as}(\theta_r) \\ f_{bs}(\theta_r) \\ f_{cs}(\theta_r) \end{bmatrix} (3)$$

$$T_e = \frac{1}{\omega_m} * (e_a i_a + e_b i_b + e_c i_c) (4)$$

The three-phase generates relatively little torque and is more efficient. Despite certain expense issues, the three phase gives incredibly good control accuracy.

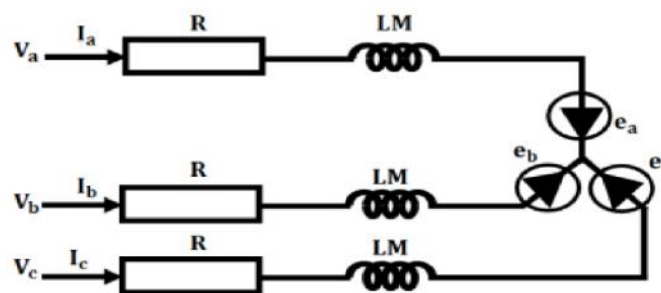


Fig 7 Brushless DC Motor

**Findings:**

The efficiency comparison of the converters: Boost, Buck Boost, Cuk, Sepic are depicted in Fig.8. It is found that Sepic converter has the highest efficiency of 93% compared to the other converters with 85.5%, 90% and 91.5% respectively.

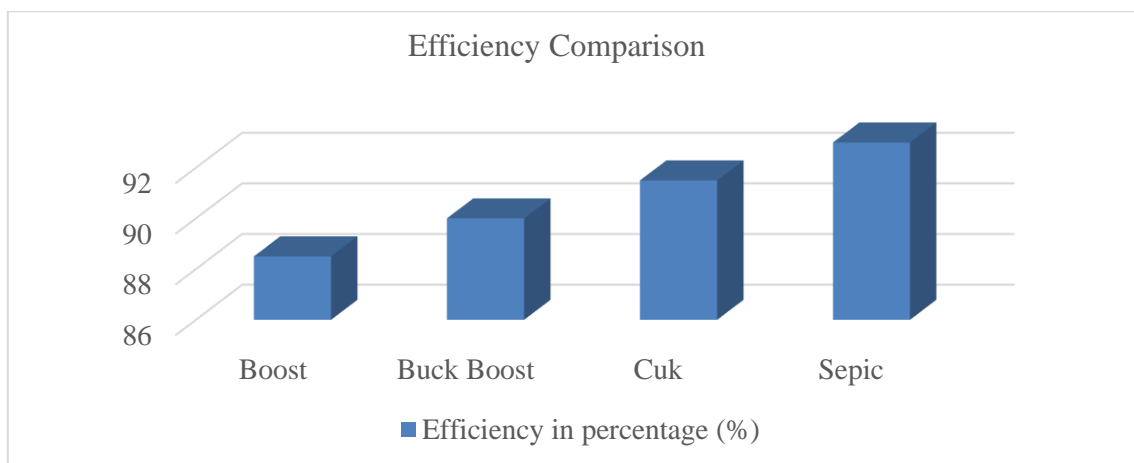


Fig 8 Efficiency comparison Between the Converters

The voltage gains of the different converters Boost, Buck Boost, Cuk and Sepic are depicted in Fig. 9. The voltage gain of sepic converter is found to be 1:8 whereas the other converters have a voltage gain of 1:3, 1:5, 1:6 respectively.

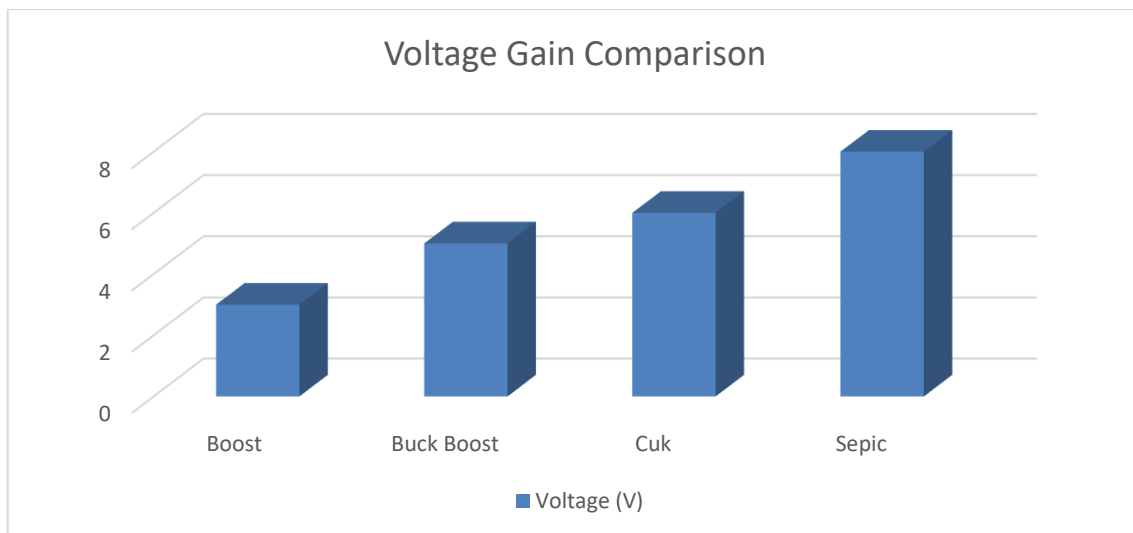


Fig 9 Voltage gain comparison Between the Converters

**Result and Discussion:**

The planned task has been replicated in MATLAB Simulink and the subsequent delineation of output waveform is provided below:

The Sepic converter voltage waveform shows efficient voltage boosting of 420V with faster settling time in Fig.10.

Table 1: Parameter Specifications of SEPIC Converter

Parameters	Values
R	10Ω
L1	1mH
L2	1mH
C1	4.8μF
C2	4.8μF
C3	1100μF

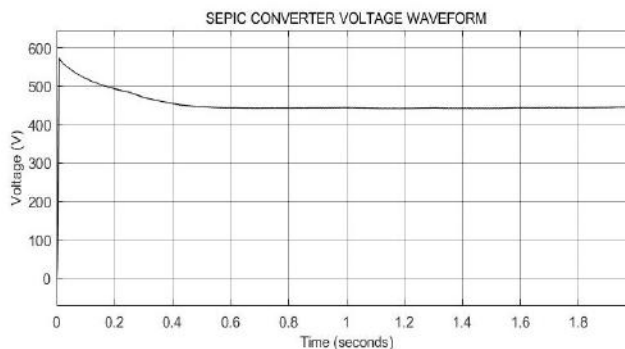


Fig.10: Sepic Converter Voltage Waveform

The torque waveform of the BLDC motor depicted in Fig 11 remains steady at 4 N-M, exhibiting minimal torque fluctuations.

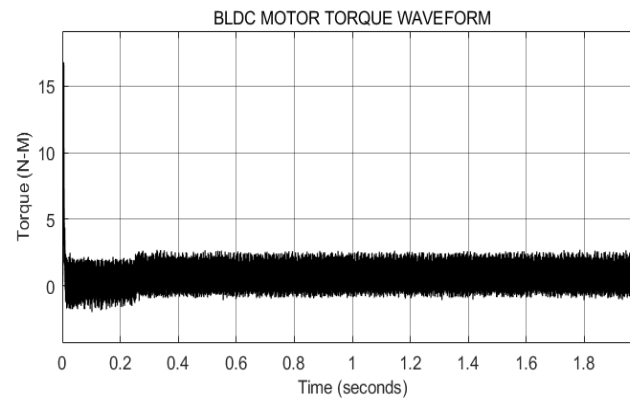


Fig.11: BLDC Motor Torque Waveform

### Conclusion:

The proposed system represents a holistic approach to addressing key challenges in electric vehicle (EV) applications, with a primary focus on enhancing efficiency and overall system gain through the implementation of a SEPIC converter and sensorless control of a Brushless DC (BLDC) motor. Electric vehicles continue to gain traction as a sustainable transportation solution, but their widespread adoption hinges on improving energy efficiency and optimizing power management systems. The integration of advanced power electronics and control techniques, as demonstrated in this system, plays a crucial role in achieving these objectives.

Furthermore, the implementation of sensorless control for the BLDC motor offers several advantages, including improved accuracy, cost-effectiveness, and reduced complexity. By analyzing motor parameters and electrical signals, the system develops models for estimating torque output under various operating conditions, enabling precise control of motor speed and torque without the need for cumbersome sensors. This approach not only simplifies the motor control system but also enhances reliability and reduces maintenance requirements, contributing to the overall cost-effectiveness and sustainability of EV applications.

Key to the performance of the system is the utilization of Proportional-Integral (PI) controllers for regulating both the SEPIC converter and the BLDC motor. The PI controller for the SEPIC converter ensures consistent and efficient voltage boosting, while the PI controller for the BLDC motor facilitates precise speed control based on the back electromotive force (EMF) generated by the motor. By dynamically adjusting control inputs in response to deviations between desired and measured values, the PI controllers optimize system performance and ensure stable operation under varying load conditions.

In conclusion, the incorporation of the SEPIC converter stands out as a pivotal aspect of the proposed system, offering exceptional versatility and efficiency in voltage regulation within the electric vehicle architecture. With a remarkable conversion efficiency of 93% and a substantial voltage gain of 1:8V, the SEPIC converter serves as the linchpin for optimizing energy conversions and power management within the system. By efficiently converting the rectified AC input voltage into a higher DC voltage suitable for driving the BLDC motor, the SEPIC converter minimizes energy losses and maximizes overall system efficiency. Its ability to seamlessly adjust voltage levels while providing galvanic isolation ensures robust and reliable operation across a wide range of operating conditions.

Moreover, the SEPIC converter's compact size, high efficiency, and low component count make it an ideal choice for electric vehicle applications where space, weight, and energy efficiency are paramount considerations.

**References:**

1. Liu, Jia, Zhitao Liu, and Hongye Su. "Passivity-based PI control for receiver side of dynamic wireless charging system in electric vehicles." *IEEE Transactions on Industrial Electronics*, Vol. 69, no. 1. pp. 783-794, 2021.
2. Serra, F. M., G. L. Magaldi, Walter Gil-González, and Oscar Montoya. "Passivity-Based PI Controller of a Buck Converter for Output Voltage Regulation". In *2020 IEEE ANDESCON*, pp. 1-6. IEEE, 2020.
3. Gil-Gonzalez, Walter, Oscar Danilo Montoya, and Alejandro Garces. "Direct power control for VSC-HVDC systems: An application of the global tracking passivity-based PI approach." *International Journal of Electrical Power & Energy Systems*, Vol. 110, pp. 588-597, 2019.
4. Wang, Jin-Liang, and Lin-Hao Zhao. "PD and PI control for passivity and synchronization of coupled neural networks with multi-weights." *IEEE Transactions on Network Science and Engineering*. Vol.8, no. 1. pp. 790-802, 2021.
5. Borja, Pablo, Romeo Ortega, and Jacquélien MA Scherpen. "New results on stabilization of port-Hamiltonian systems via PID passivity-based control." *IEEE Transactions on Automatic Control*, Vol: 66, no. 2, pp.625-636, 2020.
7. Bobtsov, Alexey, Romeo Ortega, Nikolay Nikolaev, and Wei He. "A globally stable practically implementable PI passivity-based controller for switched power converters." *International Journal of Adaptive Control and Signal Processing*, Vol. 35, no. 11. pp. 2.

# Novel Single Phase Cuk Derived Bridgeless PFC Converter For On Board EV Charger with Alternate DC Source and Reduced Number of Components

Kavyasree A<sup>1</sup>, Dr ReshmaGopi R<sup>2</sup>

<sup>1</sup>PG Student, Dept of EEE, Mangalam College of Engineering, Ettumanoor, India

<sup>2</sup>Associate Professor, Dept of EEE, Mangalam College of Engineering, Ettumanoor, India  
Email -<sup>1</sup>kavyasre3231@gmail.com, <sup>2</sup>reshma.gopi@mangalam.in

**Abstract:** *This article proposes a novel single-phase bridgeless-derived power factor corrected (PFC) converter with reduced component count for on-board EV charging application. The unique feature of this proposal is to design and operate the output inductor of the converter in discontinuous current mode for the complete power range to attain PFC naturally at ac mains, thereby not requiring the input voltage and input current sensing, which reduces the converter cost, and improves the power density as well as converter robustness to high-frequency noise. Through ingenious circuit design and component optimization, the converter achieves a notable reduction in the overall component count, contributing to cost efficiency and compact design. The converter control is very simple in operation and easy in implementation with only a single sensor-based voltage control loop. The semiconductor components voltage stress of the proposed power converter is lower when compared to the traditional converter. It also contains an alternate dc source from fuel cell. This research signifies a significant leap forward in the field of EV charging technology. The reduced component count enhances reliability, reduces costs, and contributes to the development of more sustainable and efficient electric transportation.*

**Keywords:** *On-Board Charging, Electric Vehicle (EV), Power Factor Correction (PFC), Bridgeless-Derived Converter, Component Optimization, Efficiency, Sustainable Transportation.*

## Introduction:

Battery powered EVs help in building a cleaner and quieter ecosystem together with operating and transportation cost reduction. These technologies fall in the domain of interest of government and automakers thereby, these are aided by several government-based development program. In 2019, there were 5.6 million EVs on road, but current market research indicates that during 2040 and 2050, the roads will have more than 1 billion EVs. These EVs run on high-voltage battery packs of 400 V level. Thus, a battery charger is required to recharge the power source of the EV. Two types of battery chargers are currently available in market: On-board charger and off-board chargers. The chargers basically convert variable ac input voltage to the required level of dc voltage and current. A Power Factor Corrected (PFC) converter at supply front end is necessary for an on-board battery charger to meet the harmonic limits set by the standards. A typical battery charger consists of ac filter at the input followed by an ac/dc boost PFC converter with dc-link bus capacitors connecting the isolated dc/dc converter to the PFC converter. Finally, a dc output filter is connected at the end. Numerous topologies are proposed for on-board EV charging applications. The two-stage configurations consist of an active PFC converter in the first stage which is followed by an isolated dc/dc converter. The two-stage topologies have the advantage of easy implementation, but the major demerits are higher component count, high cost, and relatively low efficiency due to the processing of total power in two conversion stages. Therefore, the single-stage configurations are reported. The single-stage structures are usually formed utilizing an

uncontrolled diode bridge rectifier and a dc/dc converter. The input diode bridge rectifier high conduction loss requires a different solution that is elimination of the diode bridge rectifier which is known as bridgeless (BL) topologies. Even though, the reported BL topologies solve the issue of diode bridge, they still have the same components count as conventional ones. Therefore, a novel BL Cuk-derived bridgeless PFC converter for on board EV charger with alternate DC source and lower number of components with a simple control scheme has been proposed in this project. Instead of two stage topologies with higher number of components, the proposed system having only single stage structure with reduced number of components. The existing system need input current and voltage sensing for PFC correction, but the proposed system is simple to operate, easy to implement and effective in achieving PFC with simple control and simple sensor only.

**Method:**

This project aims to propose a novel single-phase bridgeless Cuk-derived PFC converter with minimum number of components for on-board EV charging application. The unique feature of this proposal is the DCM operation of the output inductor for the complete converter power range to attain PFC naturally at ac mains without the need of traditional input voltage and input current sensors. The proposed system can also be works on an alternate DC source as well. The proposed single-phase BL Cuk-based PFC power converter is represented in Fig 1. It consists of a bidirectional switch, two output diodes, one inductor at input, one inductor at output, and three capacitors in total. The total number of components required for the proposed power converter implementation is eight which is two less in count when compared to the traditional Cuk converter where the required number of components is ten for converter realization. The two power switches are connected back-to-back to provide the bidirectional blocking capability and they are driven by the common gate signal which means they are turned ON and OFF at the sametime.

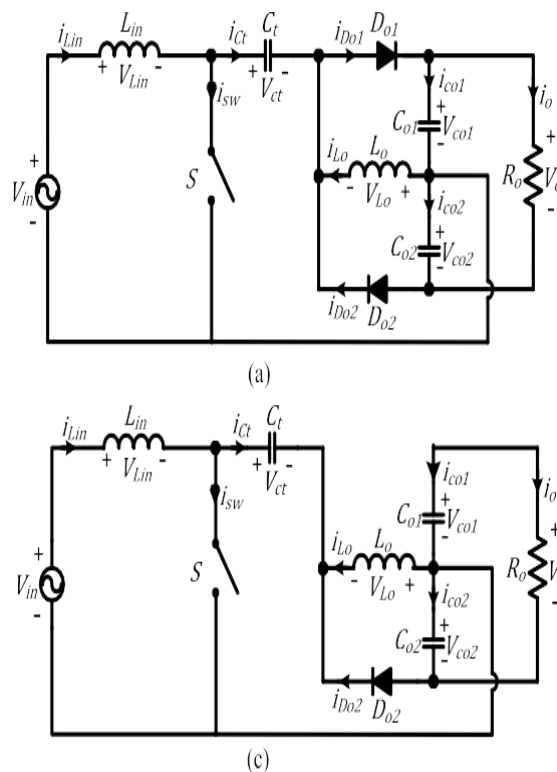


Fig 1. Circuit Diagram of the proposed converter

The configuration of the proposed power circuit during positive and negative half-cycles is represented

in Fig. During positive half-cycle, the output diode “Do1” is active, whereas the output diode “Do2” is active during negative half-cycle. It is worth noting that either the switch or only one diode will be in current conduction path for the entire power converter operation. Hence, it lessens the conduction losses, and additionally, makes the power converter thermal management easy. The other key feature of the proposed power converter is the lower voltage stress ( $V_m + V_o$ ) of these semiconductor devices in comparison to the conventional Cuk converter voltage stress ( $V_m + V_o$ ), and as a result the switching losses are decremented, and the converter operating efficiency is boosted. The inductor at output in the power converter is designed to operate in discontinuous current conduction mode for the entire power converter range of power to achieve natural PFC at the ac input side. The power converter voltage at output is controlled by employing a simple voltage control loop, and it is represented in Fig. Thereby, the power converter requires only a voltage sensor at output, which reduces the cost of the battery charger, increments its robustness, and reliability. It is to be noted that for a specific output voltage and output power, the power converter works with constant duty cycle as the duty cycle is only dependent on the error between the reference and measured voltages.

**Analysis:**

This section describes the detailed steady-state analysis of the proposed power converter for a complete switching cycle. Due to the symmetric operation of the proposed converter during positive and negative half-cycles, the power converter analysis is discussed for positive half-cycle only. The key waveforms of the proposed power converter during positive half-cycle for a complete switching cycle with discontinuous output inductor current are represented in Fig. In the proposed Cuk-derived power converter, the current discontinuity in output diode defines the discontinuous current operation. Three modes of operations are observed in total in a single switching cycle. The converter operation description is as follows.

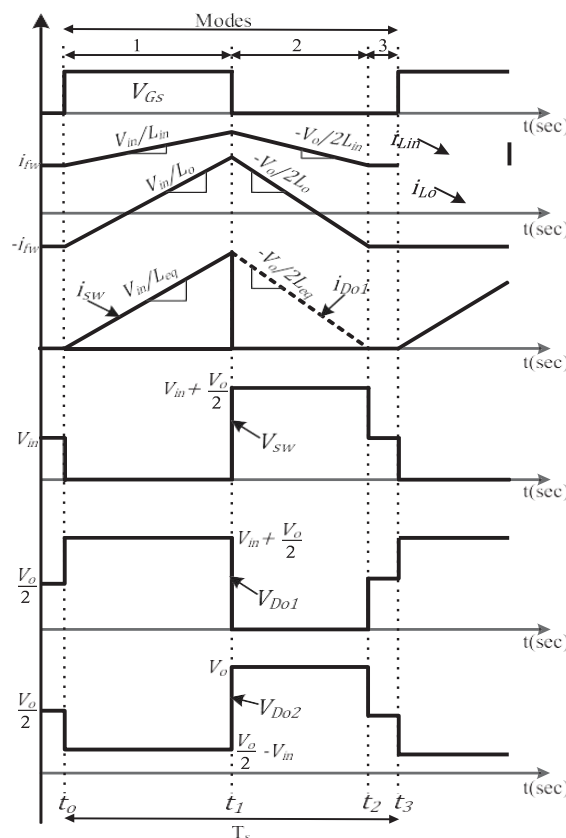


Fig 2. Output waveforms of the proposed power converter

**Mode Of Operation:**

**Mode-1 ( $t_0 - t_1$ ):**

The switch “S” is active in this mode, and the output diodes are inactive. Prior to entering this mode, the current at input “ $i_{Lin}$ ” is freewheeling in the loop created by “ $V_{in}$ ,” “ $L_{in}$ ,” “ $C_t$ ,” and “ $L_o$ ,” and it is shown as “ $ifw$ ”. The equivalent circuit of the power converter for this mode is represented. The inductor at input “ $L_{in}$ ” stores the energy from source supply “ $V_{in}$ ,” and the inductor at output “ $L_o$ ” stores the energy from transfer capacitor “ $C_t$ ” having a slope of “ $V_{in} / L_{in}$ ” and “ $V_{in}/L_o$ ,” respectively:

$$i_{Lin} = ifw + V_{in}/L_{in} * t \tag{1}$$

$$i_{Lo} = - ifw + V_{in}/L_o * t. \tag{2}$$

**Mode-2 ( $t_1 - t_2$ ):**

The switch “S” is inactive in this mode and the diode at output “ $D_{o1}$ ” is active. Before entering this mode, the inductor at input and the inductor at output currents have reached to their maximum values. When the switch “S” is inactive, the entire switch current has been taken over by the diode at output “ $D_{o1}$ ,”. The equivalent circuit of the power converter for this mode is presented. The inductor at input and the inductor at output demagnetize by giving the energy stored to the output load, while the capacitor at output “ $C_{o1}$ ,” and the transfer capacitor “ $C_t$ ” is getting charged:

$$i_{Lin} = ifw + V_{in}/L_{in} * DT_s - V_o/2L_{in} * t \tag{3}$$

$$i_{Lo} = - ifw + V_{in}/L_o * DT_s - V_o/2L_o * t \tag{4}$$

where  $DT_s = t_{on}$  is the switch active period. This mode comes to an end when the current through the diode at output “ $D_{o1}$ ” becomes zero, that implies.

$$i_{Lin} + i_{Lo} = 0. \tag{5}$$

Solving (5), Gives

$$D1T_s = 2V_{in}/V_o * DT_s \tag{6}$$

where  $D1T_s$  represents the mode-2 time period.

**Mode-3 ( $t_2 - t_3$ ):**

The equivalent circuit of the power converter for this mode is depicted in Fig 3 . All the switches are in inactive state, and the output capacitors supply to the load.

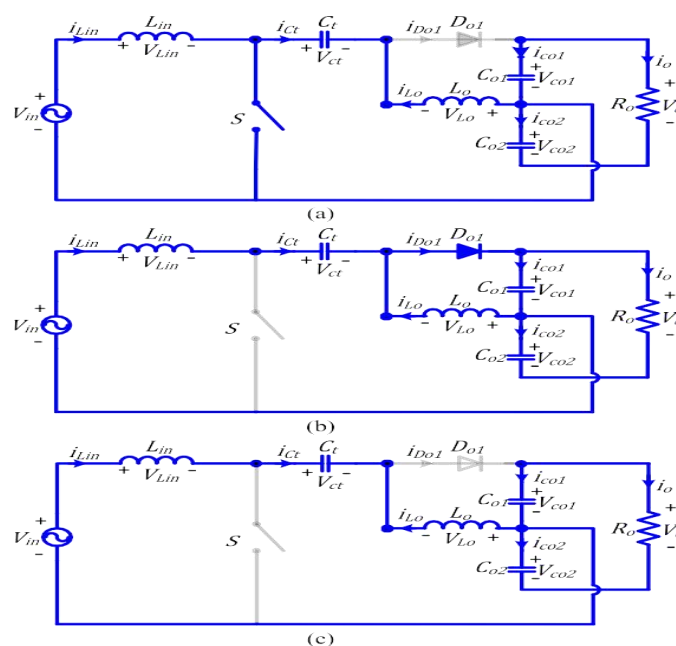


Fig 3 Circuit of the Power Converter in Mode 3



**Discontinuous Current Operation Condition**

The power converter discontinuous current operation is confirmed,

When  $DT_s + D1T_s \leq T_s$

$$D \leq M/M + 2 \sin \omega t \quad (8)$$

Where  $V_{in} = V_m \sin \omega t$  and  $M = V_o/V_m$

In the equation given above, the minimum duty cycle occurs when  $\sin \omega t = 1$ , which implies  $\omega t = \pi/2$ . Hence, the condition for power converter discontinuous current operation is

$$D \leq M/M + 2 \quad (9)$$

From (9), the voltage conversion ratio critical value for a specific duty cycle can be defined, and is shown as

$$M_{cr} \geq 2D/1 - D \quad (10)$$

Where  $M_{cr}$  defines the critical voltage conversion ratio. From the configuration of power converter, it can be seen that the power converter voltage at output must be higher than twice of the maximum voltage at input to reverse bias the diodes at output. Therefore, for the converter to operate as required, the voltage gain of the power converter must be

$$M \geq M_{cr} \geq 2. \quad (11)$$

**Average Output Current:**

The power converter average current at output in an entire switching cycle is same as the diode at the output “ $D_o1$ ” average current. Due to the triangular shape of the current which flows through the output diode, and its average value can be calculated using

$$i_{D_o1, avg} = i_{D_o1, pk} D1T_s/2T_s \quad (12)$$

where  $i_{D_o1, pk} = V_{in}/L_{eq} * DT_s$  is the maximum value of diode at output “ $D_o1$ ” current, and  $L_{eq} = L_{in}L_o/L_{in} + L_o$ . Solving (12), we get

$$i_{D_o1, avg} = V_m 2D^2 T_s / 4L_{eq} V_o * \sin 2\omega t. \quad (13)$$

Now, integrating the equation above for a half-line period, the power converter average current at output for a line period is derived, and given as

$$I_{D_o1, avg} = V_m 2D^2 T_s / 4L_{eq} V_o \quad (14)$$

**Converter Passive Components Design**

Peak current ripple of input inductor “ $\Delta i_{Lin}$ ” is given by

$$\Delta i_{Lin} = V_m / L_{in} * DT_s \quad (15)$$

$$L_{in} = V_m / \Delta i_{Lin} * DT_s. \quad (16)$$

The inductor at output “ $L_o$ ” is given as

$$L_o = L_{in} L_{eq} / L_{in} - L_{eq} \quad (17)$$

The “ $Leq$ ” value is derived from (9) and (14), and is given as

$$Leq \leq \frac{V_m^2 V_o^2 T_s^4}{P_o (V_o + 2V_m)^2} \quad (18)$$

where  $P_o$  is nominal load power.

By assuming  $C_{o1} = C_{o2} = C_o$ , the low-frequency voltage ripple at output is given as

$$\Delta V_{o,ripple} = \frac{1}{C_o} * (\int i_{Co1} dt + \int i_{Co2} dt) \quad (19)$$

$$\Delta V_{o,ripple} = \frac{1}{C_o} * \int (i_{D_{o1,avg}} - 2i_o)$$

$$dt = \frac{2i_o}{\omega C_o} \quad (20)$$

$$C_o = \frac{2i_o}{\omega \Delta V_{o,ripple}}. \quad (21)$$

The transfer capacitor “ $C_t$ ” design is critical as it has high influence on the input current quality and the value should be determined in a way such that low-frequency oscillations are not developed with inductors at output and input.

**Table1:** Input Specifications

PARAMETER	VALUE
Input voltage	120V
Output voltage	400V
Output power	1Kw
Output voltage ripple	2%
Input current ripple	8%
Switching frequency	50 kHz
Line frequency	60kHz

**Table 2:** Design Parameters

PARAMETER	VALUE
Max duty cycle	0.541
Input inductor	1.5Mh
Output inductor	29 microfarad
Transfer capacitor	2.3 microfarad
Output capacitor	1.66 millifarad

## Results:

The converter in Fig. 1(a) has been modeled and simulated in PSIM 11. The input specifications and the design results are given in Tables I and II, respectively. For the acquirement of necessary system response, a proportional integral (PI) controller ( $K_i/s + K_p$ ) is deployed which is sufficient owing to the reason that the plant transfer function is a single pole system. The controller tuning is completed using MATLAB Siso tool having phase margin (PM) of 60° and bandwidth with a value less than 754 rad/s.

Damping of 60% and 10% overshoot corresponds to a PM of 60°. The transfer function as obtained is given in (28). The value of  $k_p(= 0.0062)$  and  $k_i(= 0.28286)$  can be derived. The system’s capability to track the reference dc with no steady-state error can be understood from the open-loop transfer function given in which for lower frequencies has a gain of infinity. Further, the source voltage and load change disturbance robustness are confirmed. The Hall-effect sensor LV25-P is employed to sense the output voltage. The designed controller is implemented in real-time by programming the TI-DSP-TMS320F28335 to generate the PWM signals for the gate of the MOSFETs of the power converter which is basically done by comparing the sensed voltage to a reference voltage and the resultant error is given as input to the PI controller which gives out the duty cycle and is the input to saturation block. The output of the saturation block is compared to a Sawtooth waveform of 50 kHz. As a result, the PWM signals of the power MOSFETs are generated. To restrict the power converter to enter CCM as well as for overload protection, a limiter is placed:

$$G(s) = Vo(s)/D(s) = 1030/ 0.133s + 1 \tag{27}$$

$$H(s) = 0.28286s + 0.0062 \tag{28}$$

The unity power factor operation of the converter at full load is shown, Simulation diagram, output voltage and current from AC supply source and output voltage and current from fuel cell and also capacitor simulations results are shown below.

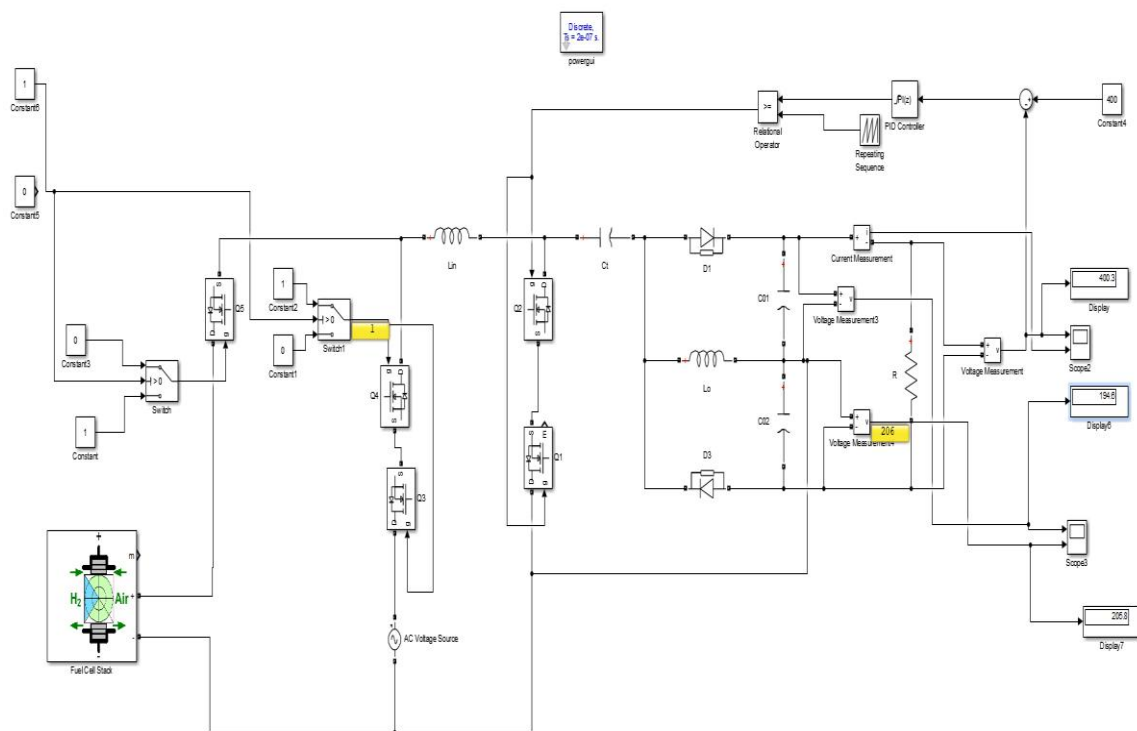


Fig 4 Simulation of Circuit

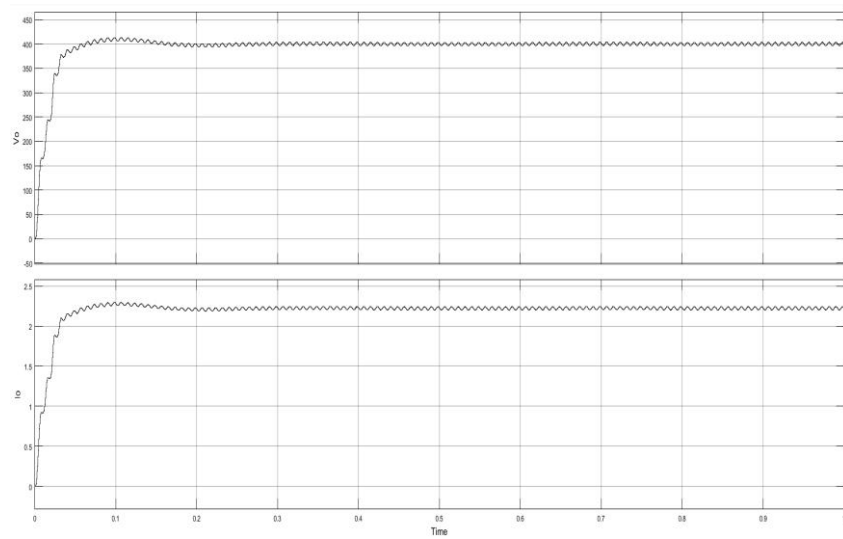


Fig 5 Output voltage and current from ac supply source

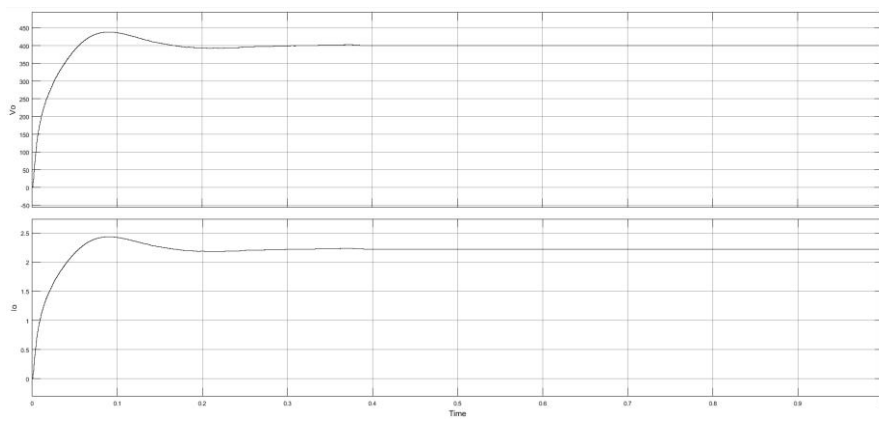


Fig 6 Output voltages and current from fuel cell

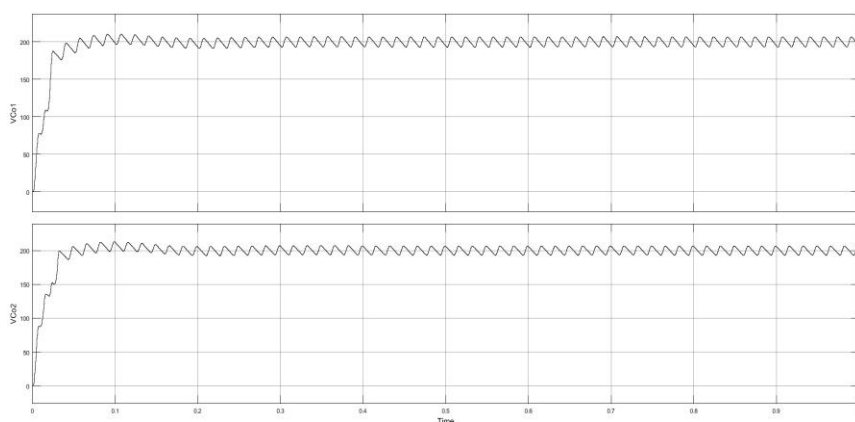


Fig 7 Capacitor Output

**Conclusion:**

An single-sensor-based BL single-phase Cuk-derived PFC converter with lower component count as on-board G2V charger is proposed and analyzed in this article. The proposed power converter inductor at output is designed to work in discontinuous current conduction mode for the entire range of power to acquire PFC naturally at the ac input side, and thereby, the sensor necessity lessens which reduces the cost of operation of the power converter augments the robustness of the converter towards high-frequency noise and offers high density. The proposed single-phase Cuk-derived power converter has decreased components voltage stress relative to the traditional Cuk PFC power converter, which results in reduction of the r4cv f components switching losses and the overall power converter efficiency is boosted. Additionally, for the complete converter operation range, only one semiconductor device is in current conduction path. Hence, lessening the power converter losses due to conduction, and ensures easy thermal management. The simplicity of topology, effectiveness of the control, and practicality of the solution are the major key merits. This article presents a brief description of several BL Cuk-based topologies. The power converter steady-state analysis over single switching cycle is detailed along with the derivation of design expressions. The small-signal modeling and design of closed-loop controller for the proposed Cuk-based PFC converter is elaborated as well. The Cuk-based power converter control-to-output transfer function is derived. A systematic procedure for voltage loop design is provided. The PI controller parameter's selection is described. The proposed power converter analysis and design are validated with simulation results from PSIM 11.

**References:**

1. J. G. Pinto, V. Monteiro, H. Gonçalves, and J. L. Afonso, "Onboard reconfigurable battery charger for electric vehicles with traction-toauxiliary mode," *IEEE Trans. Veh. Technol.*, vol. 63, no. 3, pp. 1104–1116, Mar. 2014, doi: 10.1109/TVT.2013.2283531.
2. H. V. Nguyen and D. Lee, "Advanced single-phase onboard chargers with small DC-link capacitors," in *Proc. IEEE Int. Power Electron. Appl. Conf. Expo.*, 2018, pp. 1–6.
3. R. Kushwaha and B. Singh, "Interleaved landsman converter fed EV battery charger with power factor correction," in *Proc. IEEE 8th PowerIndia Int. Conf.*, 2018, pp. 1–6.
4. A. Emadi, M. Ehsani, and J. M. Miller, *Vehicular Electric Powersystems: Land, Sea, Air, and Space Vehicles*. New York, NY, USA: Marcel Dekker, 2003.
5. C. C. Chan and K. T. Chau, "An overview of power electronics in electric vehicles," *IEEE Trans. Ind. Electron.*, vol. 44, no. 1, pp. 3–13, Feb. 1997, doi: 10.1109/41.557493.
6. K. Yoo, K. Kim, and J. Lee, "Single- and three-phase PHEV onboard battery charger using small link capacitor," *IEEE Trans. Ind. Electron.*, vol. 60, no. 8, pp. 3136–3144, Aug. 2013.
7. A. Y. Saber and G. K. Venayagamoorthy, "Plug-in vehicles and renewable energy sources for cost and emission reductions," *IEEE Trans. Ind. Electron.*, vol. 58, no. 4, pp. 1229–1238, Apr. 2011, doi: 10.1109/TIE.2010.2047828.
8. A. Hajimiragha, C. A. Canizares, M. W. Fowler, and A. Elkamel, "Optimal transition to plug-in hybrid electric vehicles in Ontario, Canada, considering the electricity-grid limitations," *IEEE Trans. Ind. Electron.*, vol. 57, no. 2, pp. 690–701, Feb. 2010, doi: 10.1109/TIE.2009.2025711.
9. Y. Lee, A. Khaligh, and A. Emadi, "Advanced integrated bidirectional AC/DC and DC/DC converter for plug-in hybrid electric vehicles," *IEEE Trans. Veh. Technol.*, vol. 58, no. 8, pp. 3970–3980, Oct. 2009, doi: 10.1109/TVT.2009.2028070.
10. A. Dixit, K. Pande, S. Gangavarapu, and A. K. Rathore, "DCM based bridgeless PFC converter for EV charging application," *IEEE J. Emerg. Sel. Topics Ind. Electron.*, vol. 1, no. 1, pp. 57–66, Jul. 2020, doi: 10.1109/JESTIE.2020.2999595.
11. "Innovation outlook: Smart charging for electric vehicles," *International Renewable Energy*

Agency, Abu Dhabi, UAE, 2019. [Online]. Available: [https://www.irena.org//media/Files/IRENA/Agency/Publication/2019/May/IRENA\\_Innovation\\_Outlook\\_EV\\_smart\\_charging\\_2019.pdf](https://www.irena.org//media/Files/IRENA/Agency/Publication/2019/May/IRENA_Innovation_Outlook_EV_smart_charging_2019.pdf)

12. “Asia-Pacific electric three-wheeler market (2013–2023),” Research And- Markets.com, para. 1, Oct. 2018. [Online]. Available: <https://www.researchandmarkets.com/research/l4k8s8/asiapacific?w=4>

13. S. Gangavarapu, A. K. Rathore, S. K. Mishra, and R. K. Singh, “Analysis and design of a single-phase bridgeless Cuk-based PFC converter as on-board charger with reduced number of components and losses,” in Proc. IEEE Transp. Electrific. Conf., 2019, pp. 1–6, doi: 10.1109/ITEC-India48457.2019.ITECINDIA2019-194.

14. H. Li, S. Wang, Z. Zhang, J. Tang, X. Ren, and Q. Chen, “A SiC bidirectional LLC on-board charger\*,” in Proc. IEEE Appl. Power Electron.Conf. Expo., 2019, pp. 3353–3360

# DC-DC Converter with Single Input and Dual Output for Electric Vehicle

Ms. Aadhiya Majeed<sup>1</sup>, Ms. Aparna Pradeep<sup>2</sup>, Dr. Honey Baby<sup>3</sup>, Mr. Arun Chandrakumar K<sup>4</sup>

<sup>1</sup>PG Student, Department of EEE, Mangalam College of Engineering

<sup>2</sup>PG Student, Department of EEE, Mangalam College of Engineering

<sup>3</sup>Associate Professor, Department of EEE, Mangalam College of Engineering<sup>3</sup>

<sup>4</sup>Assistant Professor, Department of EEE, Mangalam College of Engineering<sup>4</sup>

Email - <sup>1</sup>[\\_aadhiyamajeed555@gmail.com](mailto:_aadhiyamajeed555@gmail.com), <sup>2</sup>[aparnapradeep93@gmail.com](mailto:aparnapradeep93@gmail.com),

<sup>3</sup>[honey.baby@mangalam.in](mailto:honey.baby@mangalam.in), <sup>4</sup>[arun.chandrakumar@mangalam.in](mailto:arun.chandrakumar@mangalam.in)

**Abstract:** *Multiport converters are important for applications involving electric vehicles (EVs). The only converter that can be utilized for both the production and consumption is the DC-DC converter. The converters can be multi input or multi output in different configurations. The majority of single input multi output (SIMO) converters generate outputs with limitations on the duty ratio and inductor charging. One ongoing challenge in the design of SIMO converters is the cross regulation issue. In order to successfully avoid cross regulation while controlling the loads, this study presents a DC-DC converter with single input dual output (SIDO), which provides independent outputs without affecting the other loads during operation. Because there are fewer components in the proposed converter, the circuit is simple and cost-effective. The usefulness of an auxiliary power module for EV application is analysed using simulation results.*

**Key Words:** *Single Input Multi Output Converters.*

# A Comparative Study of the Recent High Gain Boost Converters Topology for Renewable Energy Applications

Ms. Nivya P S<sup>1</sup>, Mrs. Aiswarya Chandran<sup>2</sup>

<sup>1</sup>PG Student, Department of EEE, Mangalam College of Engineering

<sup>2</sup>Assistant Professor, Department of EEE, Mangalam College of Engineering

Email - <sup>1</sup>[nivyasr37@gmail.com](mailto:nivyasr37@gmail.com), <sup>2</sup>[aiswarya.chandran@mangalam.in](mailto:aiswarya.chandran@mangalam.in)

**Abstract:** *Maximizing energy from renewable sources requires power electronics. High gain converters are where most power electronics advances take place. By generating enough power output, high gain DC-DC converters help renewable energy sources (RES) like fuel cells and photovoltaics meet high load demands. The many high-gain DC-DC converter topologies are examined and discussed in this paper. These consist of non-isolated, non-coupled inductor-based high gain DC to DC converters, non-isolated quadratic DC-DC boost converters, and switching the inductor and capacitor divider network-based high gain boost converters. Through a combination of study, simulation, and topology comparison, the optimal topology for a photovoltaic system was developed. The voltage gain and component count are examples of performance parameters.*

**Key Words:** *Renewable Energy Sources, DC-DC Converters*



# Ai Based PLL for Grid Synchronization

Dilshad P<sup>1</sup>, Faheem Irshad M T<sup>2</sup>, Mr. Gaisoon Jafer<sup>3</sup>, Murshid K P<sup>4</sup>, Riyas P<sup>5</sup>, Jithin Raj V<sup>6</sup>  
<sup>1,2,2,3,4,5</sup>UG student, dept. of EEE, MEA Engineering College, Perinthalmanna, Kerala, India  
<sup>6</sup>Assistant Professor, dept. of EEE, MEA Engineering College, Perinthalmanna, Kerala, India  
Email -, <sup>1</sup>[20gee11@meaec.edu.in](mailto:20gee11@meaec.edu.in), <sup>2</sup>[faheemirshadmt@gmail.com](mailto:faheemirshadmt@gmail.com), <sup>3</sup>[20nee07@meaec.edu.in](mailto:20nee07@meaec.edu.in),  
<sup>5</sup>[murshidkmpd@gmail.com](mailto:murshidkmpd@gmail.com), <sup>6</sup>[riyasp@meaec.edu.in](mailto:riyasp@meaec.edu.in), <sup>1</sup>[21mlee05@meaec.edu.in](mailto:21mlee05@meaec.edu.in)

**Abstract:** *In the realm of power systems, achieving accurate grid synchronization is paramount for ensuring efficient and stable operation. Traditional Phase-Locked Loops (PLLs) have long been utilized for this purpose, relying on predefined algorithms that may struggle with dynamic and non-linear grid conditions. The concept behind an AI-based Phase-Locked Loop (PLL) involves the utilization of a beetle swarm optimization algorithm to design and tune the parameters of a PI controller, enabling adaptive and optimized grid synchronization. PLL structure typically consists of a phase detector (PD), loop filter (LF), and voltage control oscillator (VCO). Design and tuning of proportional-integral (PI) controller-based LF is a challenging task under distorted grid voltage conditions. Traditional PLLs often rely on fixed parameters or manually tuned controllers, which may struggle to adapt to dynamic grid conditions. By harnessing the collective intelligence of beetle swarms, the BSO offers a nature-inspired optimization technique capable of efficiently fine-tuning PI controller parameters. The proposed AI-based PLL framework combines the adaptive learning capabilities of the BSA with the robustness and flexibility of AI algorithms, such as neural networks, to dynamically adjust PI controller parameters in response to changing grid dynamics. This synergistic approach aims to optimize PLL performance in real time, ensuring accurate grid synchronization under varying operating conditions. This abstract sheds light on the innovative fusion of AI and swarm intelligence techniques for enhancing grid synchronization through PLLs. By leveraging the innate behaviors of beetles and the computational power of AI, this approach holds the potential to revolutionize power system control, enabling smarter and more adaptive grid operations in the future.*

**Key Words:** *PLL, Grid synchronization, Beetle swarm optimization, PI controller.*

# Grid - Tied Solar Panel Companion Inverter

Mr. Nivedh Johnson<sup>1</sup>, Mr. Manu M Venu<sup>2</sup> Ms. Jolly George<sup>3</sup>,

<sup>1,2</sup>UG Student, Department of EEE, Mangalam college of engineering

<sup>3</sup>Assistant Professor, Department of EEE, Mangalam college of engineering

Email: [nivedhjohanson@outlook.com](mailto:nivedhjohanson@outlook.com), [manumvenu@ieee.org](mailto:manumvenu@ieee.org), [jolly.george@mangalam.in](mailto:jolly.george@mangalam.in)

*Abstract: A Solar panel companion inverter (SPCI) is a single-stage DC-AC power converter, installed behind each solar panel and is topologically similar to a cascaded H-Bridge inverter. Six solar panels and their corresponding SPCIs are taken into consideration. Each H-Bridge consists of four power electronics devices preferably Metal Oxide Semiconductor Field Effect Transistors (MOSFETs), one DC link capacitor, and a parasitic power supply harvesting energy from the solar panel itself. DC voltage output of a photo-voltaic solar panel is converted to quasi-square wave voltages with variable pulse width, which when aggregated realize a superior quality multilevel waveform that can be directly interfaced with the power grid. A Maximum Power Point Tracking (MPPT) using the control algorithm extracts the maximum power at the panel level. In the initial step, six DC inputs are provided to six H-Bridges and a 13-level output voltage is obtained. A general study on a Phase Locked Loop (PLL) is also going to be conducted as the control of grid-connected inverters needs the phase information of the source. Closed loop current control of the SPCI needs to be done and the regulation of the grid current to be studied.*

*Key Words: Photovoltaic Inverter, Cascaded H-bridge Inverter, Multilevel Inverter, Control Strategies, Photo Voltaic Power Conversion, Maximum Power Point Tracking, MPPT*

# Power Quality Enhancement in Electrical System by Incorporating Renewable Energy Resources With UPQC

Ms. Aparna Pradeep<sup>1</sup>, Ms. Aadhiya Majeed<sup>2</sup>, Dr. Honey Baby<sup>3</sup>

<sup>1,2</sup>PG Student, Department of EEE, Mangalam college of engineering

<sup>3</sup>Associate Professor, Department of EEE, Mangalam college of engineering

Email - <sup>1</sup>[aparnapradeep93@gmail.com](mailto:aparnapradeep93@gmail.com), <sup>2</sup>[aadhiyamajeed555@gmail.com](mailto:aadhiyamajeed555@gmail.com), <sup>3</sup>[honey.baby@mangalam.in](mailto:honey.baby@mangalam.in)

**Abstract:** *The integration of renewable energy resources, such as solar into the electrical grid presents challenges related to power quality due to their intermittent nature. This speculative approach suggests a solution for enhancing power quality by incorporating Flexible AC Transmission System (FACTS) devices like Unified Power Quality Conditioner (UPQC) into the system which can eliminate numerous power quality events comprises voltage sags, swells, harmonics, and power factor correction and integrating with RES, the consistency and permanency of the grid can be significantly improved. It discusses the principles of operation, benefits and challenges associated with the integration of RES and FACT devices like UPQC for power quality enhancement. Through simulation studies and real-world examples, the proposed approach is demonstrated in modern power systems aiming for high quality and reliable while embracing renewable energy.*

**Key Words:** *Renewable Energy System, FACTS, Power Quality, Unified Power Quality Conditioner.*

# Third Eye for Blind

Mr. Mohamad sha K<sup>1</sup>, Mr. Anandeshwer E R<sup>2</sup>, Mr. Justin Peter<sup>3</sup>, Ms. Alishya Philip<sup>4</sup>,  
Dr. Reshma Gopi R<sup>5</sup>

<sup>1,2,3,4</sup>UG Student, Department of EEE, Mangalam college of engineering

<sup>5</sup>Associate Professor, Department of EEE, Mangalam college of engineering

Email: <sup>1</sup>[muhammadshah803@gmail.com](mailto:muhammadshah803@gmail.com), <sup>2</sup>[anandeshwer1234@gmail.com](mailto:anandeshwer1234@gmail.com), <sup>3</sup>[justinpeter@gmail.com](mailto:justinpeter@gmail.com),  
<sup>4</sup>[alishyaphilip2019@gmail.com](mailto:alishyaphilip2019@gmail.com), <sup>5</sup>[reshma.gopi@mangalam.in](mailto:reshma.gopi@mangalam.in)

**Abstract:** *Over the last few decades, the development in the field of navigation and routing devices has become a hindering task for the researchers to develop smart and intelligent guiding mechanism at indoor and outdoor locations for blind and visually impaired people (BVIPs). The existing research need to be analysed from a historical perception including early research on the first electronic travel aids to the use of modern artificial vision models for the navigation of BVIPs. Diverse approaches such as: e-cane or guide dog, infrared-based cane, laser-based walker and many others are proposed for the navigation of BVIPs. But most of these techniques have limitations such as: infrared and ultrasonic based assistance has short range capacities for object detection. While laser-based assistance can harm other people if it directly hit them on their eyes or any other part of the body. These trade-offs are critical to bring this technology in practice. to systematically assess, analyse, and identify the primary studies in this specialized field and provide an overview of the trends and empirical evidence in the proposed field. This systematic research work is performed by defining a set of relevant keywords, formulating four research questions, defining selection criteria for the articles, and synthesizing the empirical evidence in this area. Our pool of studies include 191 most relevant articles to the proposed field reported between 2011 and 2020 (a portion of 2020 is included). This systematic mapping will help the researchers, engineers, and practitioners to make more authentic decisions for finding gaps in the available navigation assistants and suggest a new and enhanced smart assistant application accordingly to ensure safety and accurate guidance of the BVIPs. This research work has several implications in particular the impact of reducing fatalities and major injuries of BVIPs.*

**Key Words:** *Navigation, Travel aids, Assistive Technology, Blind and Visually impaired*

# **INTER-DISCIPLINARY PAPER**

# A Study On The Enhancement Of Electrochemical Performance Of Copper Tin Sulphide ( $\text{Cu}_3\text{SnS}_4$ ) Annealed At Different Temperatures.

Anju Sebastian<sup>1</sup>, , Deepthi V<sup>1</sup>, Anandhan A Saj<sup>2</sup>, B Vidhya\*<sup>1,2</sup>, V Maheskumar<sup>3</sup>

<sup>1</sup>Department of Applied Physics, Karunya Institute of Technology and Sciences, Coimbatore, 641114, India

<sup>2</sup>Centre for Nanoscience and Genomics, Karunya Institute of Technology and Sciences, Coimbatore, 641 114, India

<sup>3</sup>Department of Environmental Engineering, Kyungpook National University, 80 Daehak-ro, Buk-gu, Daegu-41566, Republic of Korea

[vidhya@karunya.edu](mailto:vidhya@karunya.edu)

**Abstract:** Copper Tin Sulphide electrocatalyst have been successfully synthesised via ball milling and subsequently annealed at different temperatures of 200 °C, 300°C, and 400°C. The structural and morphological properties of  $\text{Cu}_3\text{SnS}_4$  are investigated by XRD, SEM, EDAX and TEM. The results disclosed that the annealing temperature contributes widely in the structure formation and the electrochemical performances of  $\text{Cu}_3\text{SnS}_4$ . It also revealed that the sample annealed at 400°C shows better hydrogen evolution with lower resistance and higher stability when compared with samples annealed at other temperatures. The overpotential of the 400 °C annealed  $\text{Cu}_3\text{SnS}_4$  is 302mV at the current density of 10 mA cm<sup>-2</sup> and the tafel slope is 65 mV dec<sup>-1</sup>. An increase in the double layer capacitance ( $C_{dl}$ ) value with temperature proves the improvement in the electron transfer efficiency.

**Keywords:**  $\text{Cu}_3\text{SnS}_4$ , Ball milling, Electrocatalyst, HER.

## 1. Introduction:

Copper Tin Sulphide, a semiconducting material has gained a considerable attention due its attractive ability as an electrocatalytic, photocatalytic and photothermal properties[1]. CTS is explored owing to its multifunctional ability. CTS is a p-type semiconductor with a narrow bandgap range from 0.9 eV to 1.5 eV and an enhanced carrier transport property[2]. It is a polymorphic material and the bandgap varies according to the different polymorphs. The natural availability, comparatively low toxicity, easily tuneable morphology and stability of this material makes it a suitable candidate as an electrocatalyst in Hydrogen evolution reaction [3].

The two prominently used methods to produce clean hydrogen energy are photochemical water splitting and electrochemical water splitting in which the latter is preferred in common due to the high efficiency levels reported. Electrochemical Hydrogen evolution reaction (HER) neither consumes nor produce pollutant wastes of any kind. Platinum is the most common electrocatalyst in the market with extraordinary results such as low overpotential and tafel slope during the electrolysis of water. But the scarcity of the metal and high price makes it difficult for commercial use. Hence there is a need to search for an active catalyst which is cheap and abundantly available in nature. Based on our previous reports CTS has proved to give better results both as an electrocatalyst and photocatalyst [4][5][6][7][8].

Synthesising the nanoparticles via ball-milling helps in producing new metal surfaces, increasing the surface area, forming new nanostructures and microstructures and initiating the formation of defects[9]. The electrocatalytic studies conducted by Fariba Jaleel et.al on Ni nanoparticles prepared via ball milling showed high HER activity which is owed to the formation active sites[10]. Yuewei Li et.al synthesised  $\text{MoS}_2$  via a combination of ball milling and liquid phase exfoliation (LPE) where the

former was used to improve the active sites and surface area. It exhibited a high HER activity with 284mV overpotential at 10 mA/cm<sup>2</sup>[11]. Jack .P. Hughes et.al worked on enhancing the efficiency of Fe<sub>3</sub>P synthesised via ball milling. It was proved that the ball milling reduced the average particle size and hence helped in tuning HER kinetics[12].

Research shows that annealing temperature is one of the key factors for improving the electrochemical performance of the nanoparticles. Change in structural properties like the smaller particle size, improved crystallinity, surface area and dispersity during annealing improves the activation rate, specific charge density, reaction reversibility, lower electrochemical impedance, cycle stability resulting in a better inhibiting effect for HER of the materials[13]. Jie Zhang et.al synthesised nanoporous active tungsten foil for HER, where they observed the annealing of the samples exhibited superior electrocatalytic activity due to their nanoporous structure and large specific surface area[14]. Olalekan C et.al synthesised CTS in two different ratios and temperatures to study their electrochemical properties. Different phases of CTS resulted in different electrochemical properties which confirms that change in temperature influences the HER properties of a material[15]. High temperature annealing (above 500°C) of CTS deteriorates the structural properties of the material due to the evaporation of tin and sulphur atoms or the decomposition of CTS due to high temperature[16].

In continuation to our work on Cu<sub>3</sub>SnS<sub>4</sub> prepared by ball milling in this work we report the change in structural, morphological and electrochemical properties of ball milled CTS annealed at different temperatures. Ball milling generally reduces the crystalline size and induces defects in the prepared materials ref. Annealing aids in improving the crystallinity and hence the properties of materials.

## 2. Experimental:

Cu<sub>3</sub>SnS<sub>4</sub> is prepared by ball milling followed by annealing at different temperatures (200 °C, 300 °C, 400 °C). The synthesis includes 3 mmol of granular copper, 1 mmol tin, and 4 mmol sulphur that were added to the planetary ball mill (Fritch premium line P-7) where the milling was done. The starting materials were initially put to a zirconia grinding jar with zirconia balls and ball to powder ratio was maintained as 1:5. The entire process was done at the rotation speed of 800 rpm for 60 hours. The powder was then annealed for 3hrs at temperatures 200°C, 300°C and 400°C using a furnace.

XRD studies were carried out using Shimadzu X-600, Japan instrument with Cu K $\alpha$  ( $k = 1.5416 \text{ \AA}$ ) X-ray source. SEM images were used for the morphological analysis and the instrument used was JEOL 6390, Japan. Electrocatalytic studies were done on CHI 660 D electrochemical workstation (CH Instruments, USA) in a three electrode cell. The catalyst solution was prepared using 0.01 gm of catalyst in 1ml ethanol and 0.1 ml nafion solution. The solution was ultrasonicated for 45 minutes and then coated on the Glassy carbon working electrode. Platinum and Ag/AgCl electrode were used as the counter electrodes and reference electrode respectively. The electrodes were dipped in an acidic electrolyte (0.5 M H<sub>2</sub>SO<sub>4</sub>) which was nitrogenized for 30 minutes prior to the experiments. Cyclic voltammetry and Electrochemical Impedance studies were carried out.

## 3. Results And Discussions:

### 3.1 Structural Analysis

The structural properties of the CTS samples prepared and annealed at different temperatures were studied using X-ray diffraction analysis. The XRD patterns of CTS, CTS/200, CTS/300, CTS/400 are shown in the Fig. 1. The observed diffraction peaks are well in agreement with the JCPDS no :33-0501 which confirms the formation of CTS and the tetragonal structure of the all the prepared samples. The major peaks identified at 28.66, 32.72, 47.78, 56.45 are attributed to (112), (020), (024), (312) hkl planes of CTS. No secondary peaks were observed which confirms that there is no incomplete

conversion of the precursors used hence no impurities and the end product is pure. The acute peaks after annealing at different temperatures confirms that the materials were well crystallized [17]. The peaks also confirm the formation of the compound before annealing and no phase change is observed after annealing. With the increase in annealing temperature, the high intensity peaks became sharper and narrow, which indicated an improved crystallization of the powder. The calculated values show a constant increase in the crystalline size which supports the observations. The average crystalline size ( $D$ ) of the samples are calculated for high intensity peaks using Debye-Scherrer formula,

$$D = k\lambda/\beta\cos\theta$$

Where,  $k$  is a constant for shape factor (0.94),  $\lambda$  is the wavelength of X-ray ( $1.541 \text{ \AA}$ ),  $\beta$  is the FWHM value of the diffraction peak in radians and  $\theta$  is the Bragg angle. The structural parameters calculated are given in the Table. 1. The crystalline size ranges from 10nm to 20nm with the increase in annealing temperature. This change could be due to the coalescence of the particles as a result of solid-state diffusion where free energy of the system is reduced by the decrease in surface area of the nanoparticles [18]. With the increase in annealing temperature decrease in average dislocation density and microstrain is observed which could be due to the atomic motion during the heat treatment confirming the quality of the prepared samples [19].

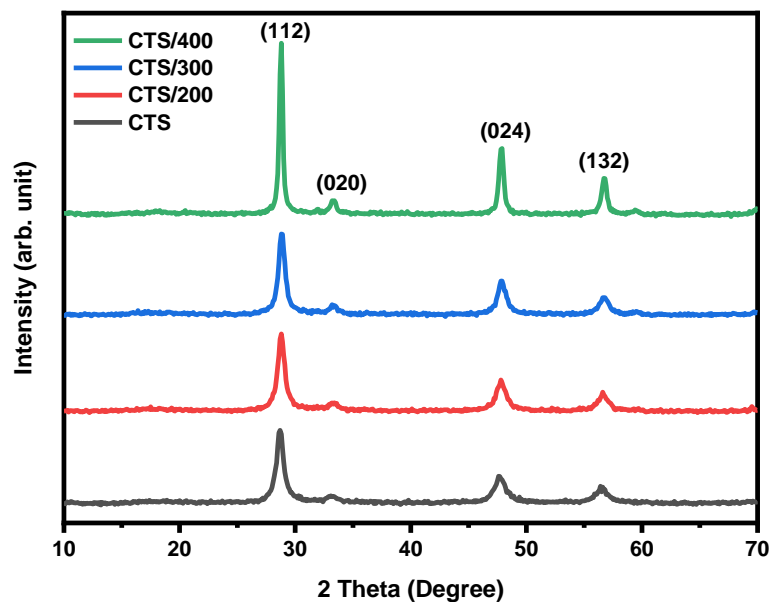


Fig.1: XRD spectra of CTS, CTS/200, CTS/300, CTS/400.

Table 1: Structural parameters of CTS, CTS/200, CTS/300, CTS/400.

Samples	Average crystalline size, $D$ (nm)	Average dislocation density, $d$ ( $\text{nm}^{-2}$ )	Average microstrain, $\mu$ ( $\text{m}^{-1}$ )	Observed $a$ and $c$ ( $\text{\AA}$ )
CTS	10	11	3.71	$a=5.38, c=10.79$
CTS/200	10	11	3.73	$a=5.37, c=10.79$
CTS/300	11	8	3.22	$a=5.37, c=10.79$
CTS/400	20	3	1.87	$a=5.37, c=10.79$



### 3.2 Morphological Studies

The morphological studies of the samples were performed using SEM. The SEM images of CTS, CTS/200, CTS/300, CTS/400 at the magnification range of 10,000 is shown in the Fig.2. Though the increase in the temperature doesn't show noticeable change in the shape, agglomeration of the small particles resulting in the formation of more number of bigger particles is evident with the increase in annealing temperature[20]. Also these results go hand in hand with the XRD analysis where the CTS/400 was proved to have better crystallinity. EDAX spectra are used to determine the composition of the elements in samples. It also helps to find the presence of impurities if any. The EDAX analysis and their weight percentage shows the co-existence of Cu, Sn and S [Fig.4(a),(b)], confirming the purity of CTS.

TEM and HRTEM analysis were carried out in order to have a deeper insight on the morphological characteristics of CTS/400. Strong aggregation of the synthesised nanoparticles are clear in the TEM image. The lattice fringes 0.25 nm, 0.20 nm of the sample were calculated from the HRTEM image and matched with the corresponding (020), (213) hkl values from the JCPDS no :33-0501. It confirms the formation of tetragonal structure in CTS/400.

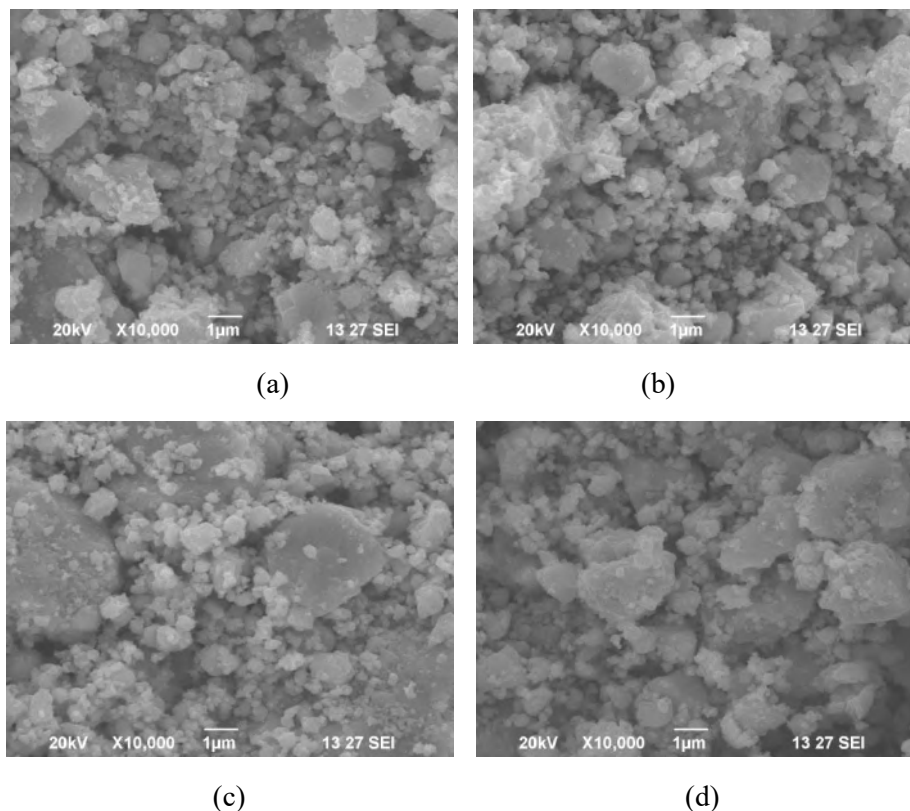


Fig.2: SEM images of CTS.(a) CTS, (b) CTS/200, (c) CTS/300, (d) CTS/400

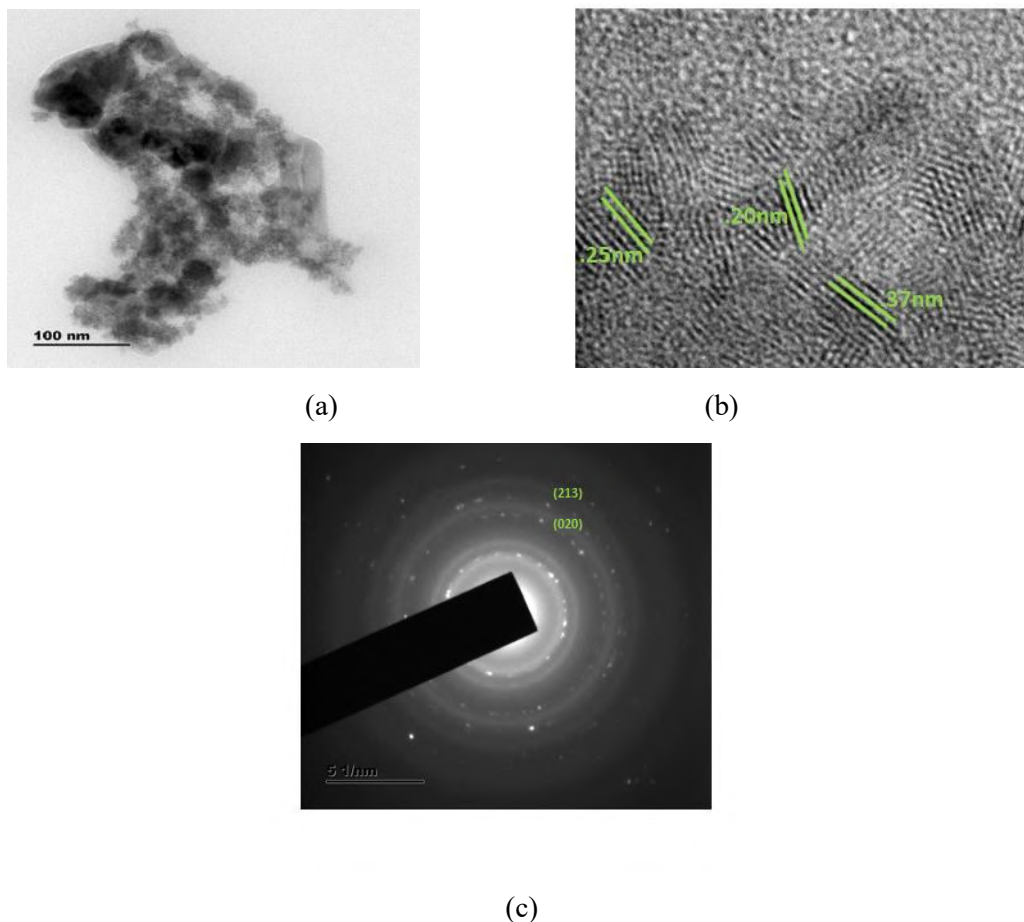
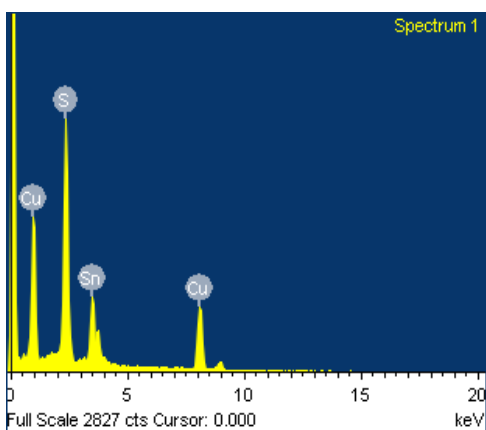


Fig. 3 (a) TEM image of the CTS/400, (b) HRTEM image of CTS/400, (d) The corresponding SAED pattern of CTS/400



COMPOSITIONAL ANALYSIS	
$Cu_3SnS_4$	Atomic %
CTS	45:13:42
CTS/200	51:13:36
CTS/300	53:13:34

(a) (b)

Fig.4: (a) EDAX spectra, (b) Composition of CTS/400

### 3.3 Optical Properties

The band positions of CTS were determined experimentally by Mott-Schottky plot (Fig.5(a)). The slopes are negative which indicates that all the CTS materials before and after annealing are p-type

in nature. The theoretical bandgap and energy structure of the samples were calculated by considering Tauc plot from the obtained UV-Vis-NIR diffused reflectance spectra datas (Fig.5(b)).The bandgap of the CTS was calculated by using Kubelka Munk function which are 1.62 eV,1.49 eV,1.62 eV,1.47eV for CTS, CTS/200, CTS/300, CTS/400 respectively.The valence band and conduction band positions were also derived which was then compared with the oxidation reduction potential of water(1.23eV and 0.0 eV) (Fig.5(c)). eV).The resulted VB and CB positions are 1.05eV,1.09eV,1.03eV,1.10eV and 0.53eV,0.4eV,0.59eV,0.37eV respectively for CTS, CTS/200, CTS/300, CTS/400.This proves that CTS can be investigated as a catalyst for HER.

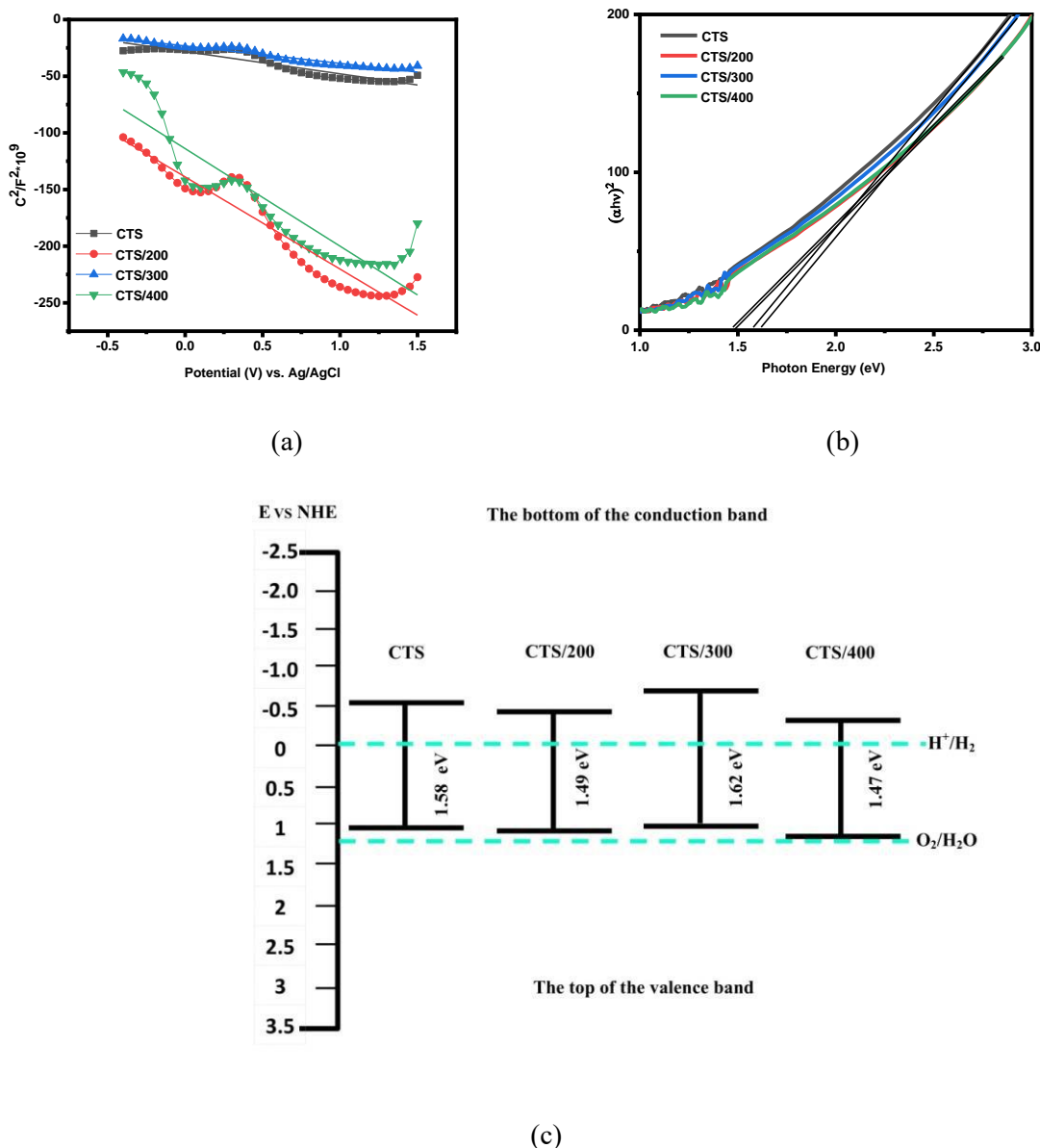


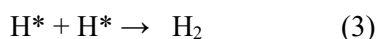
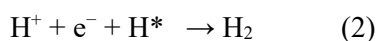
Fig.5: (a) Mott-Schottky plots of CTS,CTS/200,CTS/300,CTS/400 sample at a fixed frequency of 1000 Hz; (b)Calculated bandgap of CTS,CTS/200,CTS/300,CTS/400 (c) Schematic diagram of band structures of CTS,CTS/200,CTS/300,CTS/400.

### 3.4 Electrocatalytic Hydrogen Evolution Studies

The electrochemical characteristics of the  $\text{Cu}_3\text{SnS}_4$  samples were studied using a three electrode system in an acidic electrolyte. The use of acidic electrolyte has been proved to improve the efficiency and decrease the energy consumption[21]. The glassy carbon electrodes coated with the catalysts were activated by running CV scans. The kinetic efficiency of the samples were studied using Linear Sweep

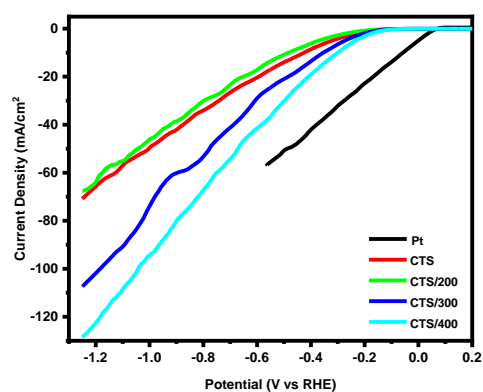
Voltammetry at the scan rate of  $5 \text{ mVs}^{-1}$  [Fig. 6(a)]. CTS, CTS/200, CTS/300, CTS/400 and Pt needs an overpotential of 422 mV, 487 mV, 357mV, 302mV and 87mV respectively to reach the current density of  $10 \text{ mA cm}^{-2}$ . The polarisation study shows the superior electrocatalytic activity of the CTS/400 sample with the lowest overpotential compared to other CTS samples. It also shows a pattern of initial dropping of the catalytic activity of CTS when annealed at  $200^\circ\text{C}$  which could also be inferred from the current density values. This could be due to the poor desorption of hydrogen atoms generated at the surface of the catalyst [22]. The current density values of CTS, CTS/200, CTS/300, CTS/400 are  $70.76 \text{ mA cm}^{-2}$ ,  $67.52 \text{ mA cm}^{-2}$ ,  $107.17 \text{ mA cm}^{-2}$ ,  $128.68 \text{ mA cm}^{-2}$  respectively.

In HER the rate determining step (rds) defines the electrocatalytic properties of the catalyst. Tafel slopes of the samples were studied from their corresponding CV curve in order to study the catalytic mechanism [Fig. 6(b)]. Obtained slopes of CTS, CTS/200, CTS/300, CTS/400 are 105, 118, 81 and  $65 \text{ mV dec}^{-1}$ . CTS/400 with the lowest value of tafel slope proves to be the one with highest catalytic activity and faster kinetics which means the fast increase in the hydrogen generation rate is observed with the applied overpotential. The classic theory suggests that HER in an acidic media happens in two main steps. Volmer reaction, the first step includes the electrochemical reduction of  $\text{H}^+$  (eq.1). The second reaction could either be the Heyrovsky reaction where an ion and atom reacts (eq.2) or Tafel reaction where two atoms combines (eq.3). The reported tafel slope values of all the samples confirms the domination of Volmer step in the reaction.

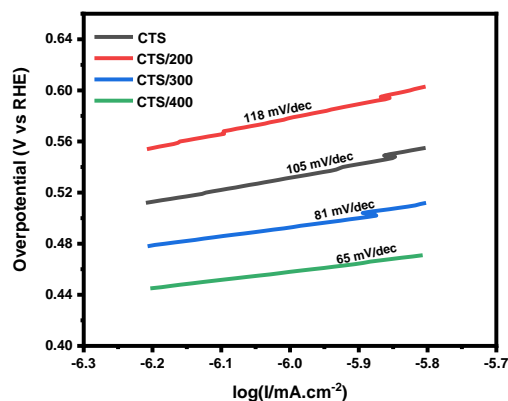


The electrochemical active surface area (ECSA) of the samples was studied to explain the enhancement in the HER activity. The CV test was done with a potential window ranges from 0.25V to 0.55V using different scan rates of 10, 20, 30, 40 and 50 mV/s. The double layer capacitance value ( $C_{dl}$ ) for the CTS/400 ( $40.6 \text{ mF cm}^{-2}$ ) [Fig. 6(d)] is much higher than that of the CTS ( $15.95 \text{ mF cm}^{-2}$ ) [Fig. 6(c)] which is not annealed. This proves that the annealing temperature affects the electron transfer efficiency. The effect of annealing on the charge transfer kinetics on the CTS catalysts was studied using electrochemical impedance studies. Comparing the semicircle formed in the Nyquist plot the resistance produced during the transfer of electron from electrode surface is explained. From the graph [Fig. 6(e)] it is visible that the sample annealed at 400 degree has the smallest semicircle and hence low resistance. The resistance values are  $18.96\Omega$ ,  $16.07\Omega$ ,  $12.12\Omega$  and  $10.5\Omega$  for CTS, CTS/200, CTS/300, CTS/400 respectively. This improvement in the electron transfer could be owed to the increase in number of active sites, conductivity and the surface area of electrodes [22]. The partialness of the semicircle in the impedance graph can be attributed to the non-uniformity and roughness of the material [23]. Randles circuit of CTS/400 has been plotted using “eis analyser” and is included in the Fig. 6(e).  $R_1$  and  $R_2$  represent the resistance of solids (connecting cables, the internal resistance of the probe etc.) and the electrolyte respectively, C is the capacitance, CPE the constant phase element and W the Warburg impedance.

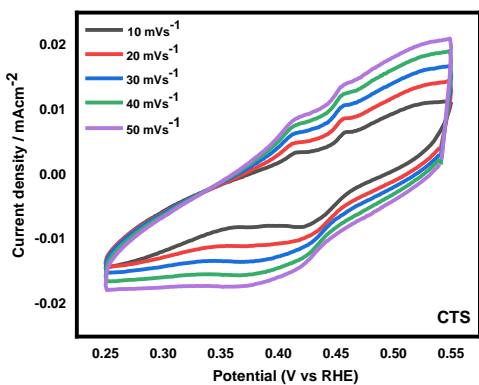
The stability in addition to excellent electrochemical performance is a non-avoidable factor when it comes to the definition of an electrocatalyst. The stability of CTS/400 which showed superior activity was obtained by conducting 1000 cycles of CV [Fig. 6(f)]. The polarisation curves before and after 1000 cycles are shown in the figure which shows a very slight shift after 1000 cycles. This indicates the good HER stability of CTS/400.



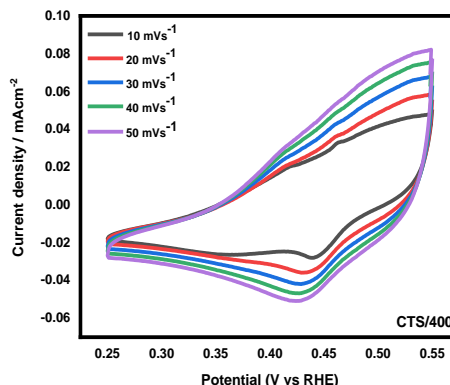
(a)



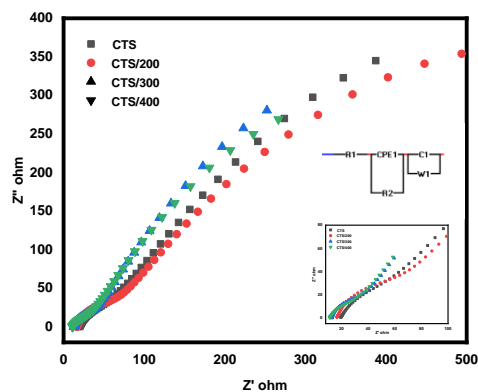
(b)



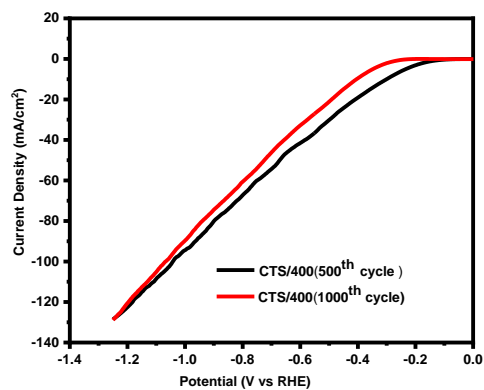
(c)



(d)



(e)



(f)

Fig. 6(a) Polarization curve for CTS,CTS/200,CTS/300,CTS/400 , (b) The corresponding tafel slope CTS,CTS/200,CTS/300,CTS/400 , (c,d) CV of CTS and CTS/400 with different potential scanning rates (10,20,30,40 and 50mV/s) , (e) The impedance spectra of CTS,CTS/200,CTS/300,CTS/400 , (f) The polarization curve for 500 and 1000 cycles for CTS/400

#### 4. Conclusion

In this work CTS, CTS/200, CTS/300, CTS/400 nanoparticles were synthesised successfully using ball milling. A detailed study was carried out to explore the influence of annealing on the structural, morphological and electrochemical properties of the materials. The results revealed the excellent performance of  $\text{Cu}_3\text{SnS}_4$  when annealed at  $400^\circ\text{C}$ . There was no change in the phase or presence of impurities after the annealing process in the samples whereas there was noticeable improvement in the crystalline properties. Annealing helps in increasing the number of active sites, electron transfer and the conductivity of the materials which in turn boosted Electrochemical HER performance of the CTS/400.

#### Acknowledgements:

The authors are thankful to the Centre for Nanoscience and Genomics, Karunya Institute of Technology and Sciences, for providing the central research facilities. We would also like to thank the Department of Science and Technology, New Delhi, India, (DAE- BRNS Project no. 34/32/1221/2012) for providing the electrochemical workstation facility. One of the authors Ms. Anju Sebastian is thankful for the Evangeline Dhinakaran Doctoral Fellowship provided by Karunya Institute of Technology and Sciences, for her PhD programme.

#### Compliance with ethical standards

The authors declare that they have no conflicts of interest.

#### Reference:

- [1] A. Sebastian, V. Maheskumar, N. Bhuvanesh, B. Vidhya, R. Nandhakumar, and Z. Jiang, "Photocatalytic performance of  $\text{Cu}_3\text{SnS}_4$  (CTS)/reduced graphene oxide (rGO) composite prepared via ball milling and solvothermal approach," *J. Mater. Sci. Mater. Electron.*, vol. 4, 2020, doi: 10.1007/s10854-020-04654-3.
- [2] K. Lohani, E. Isotta, N. Ataollahi, C. Fanciulli, A. Chiappini, and P. Scardi, "Ultra-low thermal conductivity and improved thermoelectric performance in disordered nanostructured copper tin sulphide ( $\text{Cu}_2\text{SnS}_3$ , CTS)," *J. Alloys Compd.*, vol. 830, 2020, doi: 10.1016/j.jallcom.2020.154604.
- [3] V. Maheskumar, T. Selvaraju, and B. Vidhya, "Influence of solvent in solvothermal synthesis of  $\text{Cu}_3\text{SnS}_4$ : Morphology and band gap dependant electrocatalytic hydrogen evolution reaction and photocatalytic dye degradation," *Int. J. Hydrogen Energy*, vol. 43, no. 51, pp. 22861–22873, 2018, doi: 10.1016/j.ijhydene.2018.09.072.
- [4] V. Maheskumar, P. Gnanaprakasam, T. Selvaraju, and B. Vidhya, "Comparative studies on the electrocatalytic hydrogen evolution property of  $\text{Cu}_2\text{SnS}_3$  and  $\text{Cu}_4\text{SnS}_4$  ternary alloys prepared by solvothermal method," *Int. J. Hydrogen Energy*, vol. 43, no. 8, pp. 3967–3975, 2018, doi: 10.1016/j.ijhydene.2017.07.194.
- [5] V. Maheskumar, P. Gnanaprakasam, T. Selvaraju, and B. Vidhya, "Investigation on the electrocatalytic activity of hierarchical flower like architected  $\text{Cu}_3\text{SnS}_4$  for hydrogen evolution reaction," *J. Electroanal. Chem.*, vol. 826, pp. 38–45, 2018, doi: 10.1016/j.jelechem.2018.07.027.
- [6] V. Maheskumar and B. Vidhya, "Investigation on the morphology and photocatalytic activity of  $\text{Cu}_3\text{SnS}_4$  synthesized by ball milling and solvothermal method," *J. Photochem. Photobiol. A*

- Chem.*, vol. 356, pp. 521–529, 2018, doi: 10.1016/j.jphotochem.2017.12.026.
- [7] V. Maheskumar, I. Sheebha, B. Vidhya, J. P. Deebasree, T. Selvaraju, and S. Akash, “Enhanced electrocatalytic and photocatalytic activity of ball milled copper tin sulphide by incorporating GO and rGO,” *Appl. Surf. Sci.*, vol. 484, no. December 2018, pp. 265–275, 2019, doi: 10.1016/j.apsusc.2019.03.241.
- [8] H. D. Shelke, A. C. Lokhande, J. H. Ki, and C. D. Lokhande, “Effect of Copper Content on Structural, Morphological, Optical and Photoelectrochemical Properties of SILAR Deposited Cu<sub>3</sub>SnS<sub>4</sub> Thin Films,” *ES Mater. Manuf.*, 2020, doi: 10.30919/esmm5f922.
- [9] K. Alsabawi, E. M. A. Gray, and C. J. Webb, “The effect of ball-milling gas environment on the sorption kinetics of MgH<sub>2</sub> with/without additives for hydrogen storage,” *Int. J. Hydrogen Energy*, vol. 44, no. 5, pp. 2976–2980, 2019, doi: 10.1016/j.ijhydene.2018.12.026.
- [10] F. Jalili, M. Zhiani, and S. Kamali, “Preparation and evaluation of a new hybrid support based on exfoliation of graphite by ball milling for Ni nanoparticles in hydrogen evolution reaction,” *Int. J. Hydrogen Energy*, pp. 21187–21195, 2018, doi: 10.1016/j.ijhydene.2018.09.202.
- [11] Y. Li, X. Yin, X. Huang, X. Liu, and W. Wu, “Efficient and scalable preparation of MoS<sub>2</sub> nanosheet/carbon nanotube composites for hydrogen evolution reaction,” *Int. J. Hydrogen Energy*, vol. 45, no. 33, pp. 16489–16499, 2020, doi: 10.1016/j.ijhydene.2020.04.085.
- [12] J. P. Hughes, S. Rowley-Neale, and C. Banks, “Enhancing the efficiency of the hydrogen evolution reaction utilising Fe<sub>3</sub>P bulk modified screen-printed electrodes via the application of a magnetic field,” *RSC Adv.*, vol. 11, no. 14, pp. 8073–8079, 2021, doi: 10.1039/d0ra10150h.
- [13] F. Li *et al.*, “Influence of annealing temperature on the structure and electrochemical performance of the Fe<sub>3</sub>O<sub>4</sub> anode material for alkaline secondary batteries,” *Electrochim. Acta*, vol. 178, pp. 34–44, 2015, doi: 10.1016/j.electacta.2015.07.106.
- [14] J. Zhang, Y. Huang, Z. Wang, and Y. Liu, “Preparation of a nanoporous active tungsten foil by two-step anodizing and deoxidized annealing for hydrogen evolution reaction,” *Nanotechnology*, vol. 30, no. 1, 2019, doi: 10.1088/1361-6528/aae7a7.
- [15] O. C. Olatunde and D. C. Onwudiwe, *Copper-based ternary metal sulfide nanocrystals embedded in graphene oxide as photocatalyst in water treatment*. Elsevier Inc., 2020.
- [16] Q. Chen *et al.*, “Study on the photovoltaic property of Cu<sub>4</sub>SnS<sub>4</sub> synthesized by mechanochemical process,” *Optik (Stuttg.)*, vol. 125, no. 13, pp. 3217–3220, 2014, doi: 10.1016/j.ijleo.2013.12.023.
- [17] B. Zhao, S. Li, M. Che, and L. Zhu, “Synthesis of Cu<sub>3</sub>SnS<sub>4</sub> nanoparticles with a novel structure as low-cost counter electrode in dye-sensitized solar cell,” *Int. J. Electrochem. Sci.*, vol. 11, no. 8, pp. 6514–6522, 2016, doi: 10.20964/2016.08.29.
- [18] A. Jafari, S. Farjami Shayesteh, M. Salouti, and K. Boustani, “Effect of annealing temperature on magnetic phase transition in Fe<sub>3</sub>O<sub>4</sub> nanoparticles,” *J. Magn. Magn. Mater.*, vol. 379, pp. 305–312, 2015, doi: 10.1016/j.jmmm.2014.12.050.
- [19] R. Sathyamoorthy, C. Sharmila, K. Natarajan, and S. Velumani, “Influence of annealing on structural and optical properties of Zn<sub>3</sub>P<sub>2</sub> thin films,” *Mater. Charact.*, vol. 58, no. 8-9 SPEC. ISS., pp. 745–749, 2007, doi: 10.1016/j.matchar.2006.11.015.

- [20] A. Jafari, S. Pilban Jahromi, K. Boustani, B. T. Goh, and N. M. Huang, “Evolution of structural and magnetic properties of nickel oxide nanoparticles: Influence of annealing ambient and temperature,” *J. Magn. Magn. Mater.*, vol. 469, pp. 383–390, 2019, doi: 10.1016/j.jmmm.2018.08.005.
- [21] Q. Chen, Y. Zhang, D. Zhang, and Y. Yang, “Ag and N co-doped TiO<sub>2</sub> nanostructured photocatalyst for printing and dyeing wastewater,” *J. Water Process Eng.*, vol. 16, pp. 14–20, 2017, doi: 10.1016/j.jwpe.2016.11.007.
- [22] Z. Khajehsaeidi, P. Sangpour, and A. Ghaffarinejad, “A novel co-electrodeposited Co/MoSe<sub>2</sub>/reduced graphene oxide nanocomposite as electrocatalyst for hydrogen evolution,” *Int. J. Hydrogen Energy*, vol. 44, no. 36, pp. 19816–19826, 2019, doi: 10.1016/j.ijhydene.2019.05.161.
- [23] C. M. Brett, “Electrochemical Impedance Spectroscopy in the Characterisation and Application of Modified Electrodes for Electrochemical Sensors and Biosensors,” doi: <https://doi.org/10.3390/molecules27051497>.